Development of Novel Small-Size Peptides as Putative Therapeutic Drugs

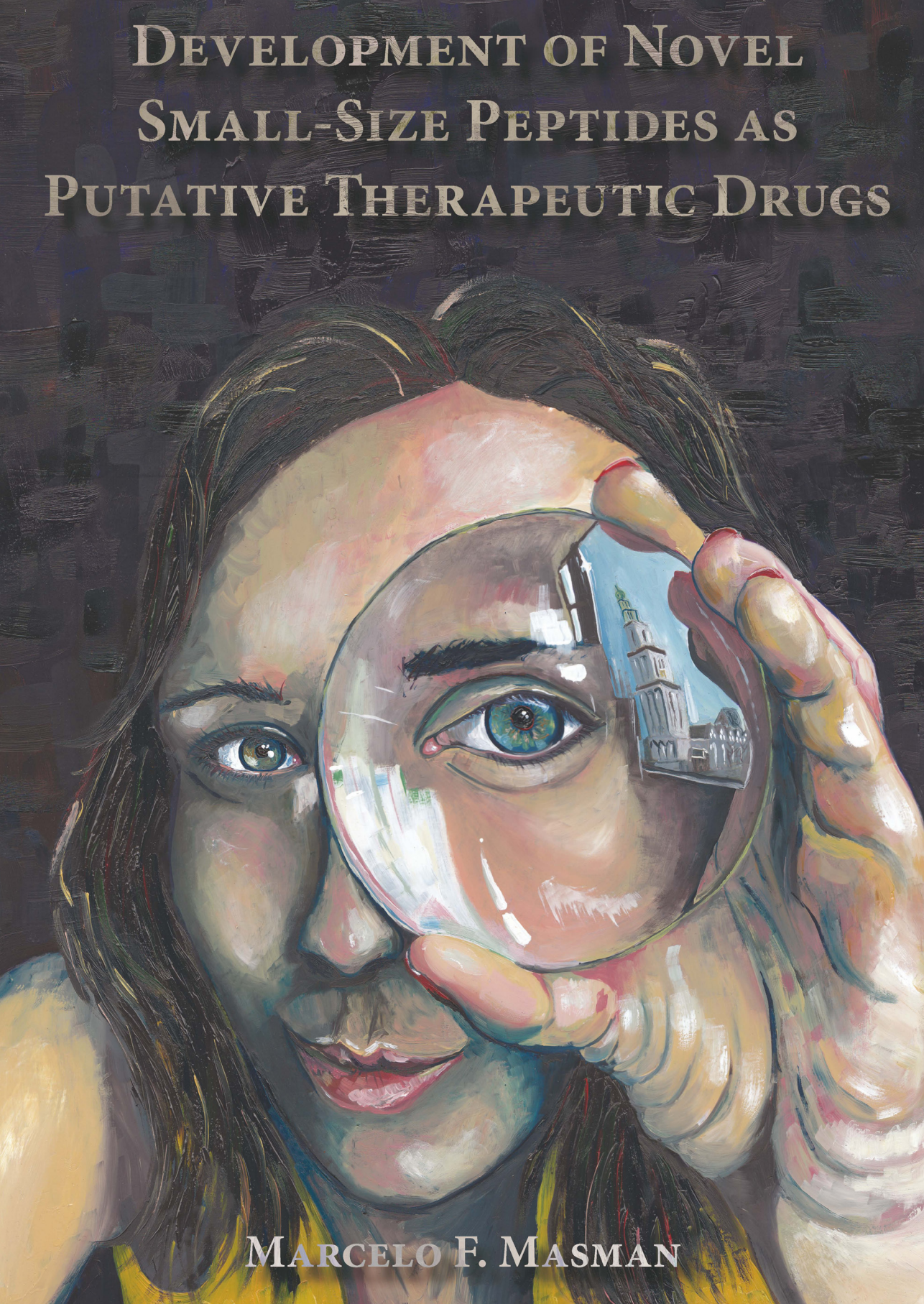

Marcelo F. Masman

2010

Development of Novel Small-Size Peptides as Putative Therapeutic Drugs

M. F. Masman

The studies reported in this thesis were carried out partially at the Universidad Nacional de San Luis (UNSL), Argentina and the Rijksuniversiteit Groningen (RuG), The Netherlands as a cooperation fellowship between this two Universities. The printing out of this thesis was financially supported by the Faculty of Mathematics and Natural Sciences, RuG and the School of Behavioral and Cognitive Neurosciences (BCN). BCN have organized the educational program of the candidate during his stay in Groningen.

ISBN: 978-90-367-4418-8 (printed version)

ISBN: 978-90-367-4419-5 (digital version)

Cover design and lay-out by M.F. Masman.

Cover illustration: "Magnifying Groningen" by M.F. Masman, oil on paper (320x450 mm).

Printed in the Netherlands by Print Partners Ipskamp, Enschede.

An electronic version in Adobe® portable document format (PDF) is available on the internet at:

http://dissertations.ub.rug.nl/faculties/science/2010/m.f.masman/

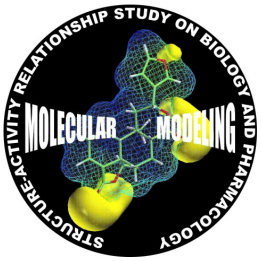

RIJKSUNIVERSITEIT GRONINGEN

Development of novel small-size peptides as putative therapeutic drugs

Proefschrift

ter verkrijging van het doctoraat in de
Wiskunde en Natuurwetenschappen
aan de Rijksuniversiteit Groningen
op gezag van de
Rector Magnificus, dr. F. Zwarts,
in het openbaar te verdedigen op
maandag 5 juli 2010
om 13.15 uur

door

Marcelo Fabricio Masman
geboren op 12 januari 1979
te Mendoza, Argentinië

Promotores:	Prof. dr. P.G.M. Luiten Prof. dr. R.D. Enriz Prof. dr. S.J. Marrink Prof. dr. U.L.M. Eisel
Beoordelingscommissie:	Prof. dr. H.H. Kampinga Prof. dr. K.L. Leenders Prof. dr. A.E. Mark

Se puede vivir una larga vida sin aprender nada.
Se puede durar sobre la tierra sin agregar ni cambiar una pincelada del paisaje.
Se puede simplemente no estar muerto sin estar tampoco vivo.
Basta con no amar nunca a nada, a nadie.
Es la única receta infalible para no sufrir.
Yo aposté mi vida a todo lo contrario y hacía mucho tiempo que había dejado de importarme si lo perdido era más que lo ganado.
Creía que ya estábamos a mano el mundo y yo, ahora que ninguno de los dos respetaba demasiado al otro.
Pero un día comprendí que todavía podía hacer algo para estar completamente vivo antes de estar definitivamente muerto.
Entonces... me puse en movimiento

[Jose, Caballos Salvajes, Argentinean film directed by Marcelo Piñeyro – 1995]

a Kiko y a mi amada Alma

PREFACE

Computational medicinal chemistry is a rapidly growing field of modern science. Mathematics and computational sciences have long played a dominant role in our understanding of physics, chemistry, and other life sciences. However, the wholesale application of computational methods in medicine, more specifically in drug design, is relatively recent. Currently, the intriguing questions of molecular interactions, conformational molecular behavior, protein folding, cell signaling, cell movement, genomics, ecology, infectious diseases, and diseases development are being successfully tackled with and analyzed using mathematical and computational methods.

This thesis is based upon studies conducted during the period between March 2005 and August 2009 at the Molecular Modeling group (2005-2007), Universidad Nacional de San Luis, Argentina, and at the Molecular Neurobiology group (2007-2009), Rijksuniversiteit Groningen, The Netherlands. These studies have been funded by the Consejo Nacional de Investigaciones Científicas y Técnicas (CONICET), Argentina and by the Rijksuniversiteit Groningen, The Netherlands. The thesis consists of a total of eight chapters, five of which correspond to papers published in various international journals, and the material for yet another chapter is in preparation to be submitted for publication. These chapters cover various aspects of computational medicinal chemistry applied to peptide compounds with potentials to become a drug. The majority of these papers are written jointly with other scientists, some of whom are more theoretical chemists than biologists, while some are more biologists that theoretical chemists. In the first chapter, however, I have given a general introduction to peptides in medicinal chemistry and a survey of the new technological/scientific approaches. Thus, CHAPTER 1 has been written in such a way that it is relatively easy to read for any person who possesses a minimum scientific knowledge. This is also valid for CHAPTER 8, General discussion & future perspectives.

Besides my profound scientific background, I am deeply interested in several forms of art, among these however, visual art, especially painting is the form that allows me to express myself as an artist. My affinity for art and my scientific education give me a creative and analytical approach to life that I wanted to reflect in this thesis. Therefore, parallel to the hard scientific content presented in this thesis, I have decided on a more personal form of presentation, introducing each chapter with a painting. Thus, my relation to creative work can also be presented with the help of artistic suggestions in harmony with scientific content. The creation of these paintings, including the cover painting, has been based on selected key words, the inspirational words, related to the research topic of each chapter. Far from making a literal interpretation of the inspirational words, these painting are a collection of life-experiences collected during my stay in Groningen. All these art works have been made "*alla prima*" (Italian for "*at once*"), which is a style of painting where, instead of building colors up with layers or glazing over an underpainting, the whole painting is completed while the paint is still wet. The charm of *alla prima* is that it retains the fresh and spontaneous feelings that come as one paints. It seems to me the most intuitive way to paint.

This thesis is my ultimate attempt to harmonically conjugate art and science into a personal project. Of course, no such project can be free from errors and incompleteness, which with time and more hard work can be improved in a near future. ▪

M.F. Masman, 5th May 2010, Groningen.

"Every portrait that is painted with feeling is a portrait of the artist, not of the sitter"

O. Wilde

CONTENTS

"Bitter-sweetly and paradoxically, the disappointment of a left hand allows the right hand to come"
(M.F. M.)

01

"My left hand"

oil on paper (320x450 mm)
M.F. Masman 2010

Chapter 1

General introduction:

Peptides as a promising source of therapeutic agents

Marcelo F. Masman

1.1 A short history of peptide drug design. Benefits and drawbacks

Although the important role that peptides and proteins play in almost all biological processes was already known by 20th's century scientists, its far fetching consequences were not fully understood nor appreciated by most organic and medicinal chemists at that time. This was partly due to the still limited knowledge of synthetic amino acids, peptides and peptidomimetic compounds. The lack of appreciation of the stereo-structural and conformational properties of amino acids as building blocks of peptides and proteins was probably another reason. However, this has changed considerably thanks to the scientific progress of the 20th century. One of the most likely reasons for this to happen was the increasing need to produce peptides on a larger scale to study their characteristics. This became more urgent after the discovery of many new compounds of this kind with extremely important biochemical activities, such as peptide hormones, neurotransmitters, enzymes, cytokines, growth factors, adhesion proteins, glycoproteins, receptors, antigenic sites, antibodies, structural proteins, oncogenes, ion channels and so on. In parallel major progress in peptide synthesis at the end of the 20th century (in fact at the end of 1980s) served as a stimulus to create and use large peptide libraries. The solid-phase method of peptide chemistry initiated by Merrifield introduced a tremendous step forward in the synthesis of peptides (Merrifield 1986; Merrifield 1963). The subsequent development of multiple peptide synthesis by Geysen and colleagues (Geysen 1985; Geysen et al. 1984; Geysen et al. 1987), and the "*tea bag method*" by Houghten and coworkers (Houghten 1985) have clearly changed the perspectives in the potential use of these compounds in the medicinal chemistry field.

Nowadays, at the beginning of the 21st century, we may be on the brink of a therapeutic revolution partly as a result of the accelerated advance of complex computational techniques on the medicinal chemistry field. The use of peptides as therapeutic drugs has rapidly grown over the last decades, and this trend is likely to be continued due to our burgeoning knowledge on the activity-structure relationship. It is now well known that peptides regulate most physiological processes, acting at some sites as endocrine or paracrine signals and at others as neurotransmitters or growth factors. Peptides are already being used therapeutically in such diverse areas as neurology, endocrinology and haematology (Edwards et al. 1999).

One of the fist problems that medicinal chemists face in the process of peptide drug discovery is the fact that most peptides cannot be administered orally since they are rapidly broken down by gastrointestinal enzymes, thus requiring subcutaneous or intravenous application. Therefore, great efforts are focused on alternative routes of delivery of this type of drugs, including inhalation, buccal, intranasal and transdermal routes, as well as novel delivery systems such as the use of protective liposomes. An exciting future area of drug research relate to peptides for treatment of brain disorders (Fulop et al. 2004; Granic et al. 2009; Hetenyi et al. 2002b; Juhasz et al. 2009; Permanne et al. 2002; Soto et al. 1996; Soto et al. 1998; Tjernberg et al. 1997; Tjernberg et al. 1996). Peptidergic drugs for combatting brain diseases are subject to dual problems of localized targeted delivery, and the blood-brain barrier (BBB) that prevent peptide compounds from gaining ready access to the required site of action, although some solutions are appearing at the horizon of peptide chemistry. Additional clinical value is created with the development of rational drug design and specific synthetic modification of the peptide molecular structure in order to endow the analog ideally with only one specific activity. This way new peptides or peptidomimetic compounds can express the desired specific biological property. Moreover, by following such rational approaches and designs the resistance of the peptide to enzymatic break-down can be increased. The most frequently applied approach to render a peptide resistant to enzymatic attack has been by replacement or modification of chemical functional groups, such as *N*- and *C*-terminal groups, disulfide bond, *N*-alkylation, *N*-arylation, etc. The nature of these changes is usually such that the hydrophobicity of the peptide is enhanced, and as a result the compounds may permeate into the cell instead of remaining in the extracellular system, or may be transported over the BBB membranes. However, it is important to realize that if these agents cannot be broken down *in vivo* due to an extreme resistance to enzymatic attack and accumulate intracellularly, their clinical application may cause undesirable consequences in patients. Generally speaking however, chemical modifications on the peptide molecular structure based on conformational considerations, rather than on an empirical or intuitive approach, in principle should lead to analogs with the required properties and biological activity.

Nevertheless, peptides thus far have not played a major commercial role as therapeutic agents, at least not at industrial levels, with certain exceptions such as insulin and adrenocorticotropic hormone (ACTH). However, this situation may rapidly change as more and more naturally occurring or synthetic low molecular weight peptides with interesting biological activities are being discovered or designed.

Attractive examples of rational design of potential peptidergic drugs are the neurohypophyseal hormones (Kotelchuck et al. 1972; Marks and Walter 1972; Pliska et al. 1967; Urry and Walter 1971; Walter et al. 1972; Walter et al. 1971; Walter and Shlank 1971; Walter et al. 1974), captopril and derivatives (Atkinson and Robertson 1979; Bull et al. 1985; Ondetti et al. 1979; Patchett et al. 1980; Wyvratt and Patchett 1985), antifungal peptides (Carotenuto et al. 2007; Cutuli et al. 2000; Grieco et al. 2003; Grieco et al. 2005; Masman et al. 2009b; Masman et al. 2006; Masman et al. 2008), anti amyloid peptides or so-called "β-sheet breakers" (Fulop et al. 2004; Granic et al. 2009; Hetenyi et al. 2002b; Juhasz et al. 2009; Soto et al. 1996; Soto et al. 1998; Tjernberg et al. 1997; Tjernberg et al. 1996), amongst others. In the case of neurohypophyseal hormones their proposed preferred conformations (Urry and Walter 1971; Walter et al. 1972) suggest that substitutions of amino-acid residues in the corners of the 3-turns of the hormones (positions 3, 4, 7, and 8, which are not primarily involved in the intramolecular stabilization of the peptide backbone and, therefore, are available for intermolecular interactions)

would lead to analogs with a selectively modified activity profile. By these modifications certain activities will be enhanced while others will be diminished or even abolished in these compounds (Walter et al. 1971; Walter and Shlank 1971; Walter et al. 1974). This example is given to illustrate the importance of knowing and understanding the conformational behavior as well as the structural intricacies of a potential peptide drug. It is at this stage where computational chemistry shows its invaluable help in the field of the medicinal chemistry.

Peptides, as many other drugs, act by binding to specific cell surface receptors. The perfect therapeutic agent would be a small-molecular-mass chemical compound that mimics the natural receptor ligand, cheap to manufacture, stable at normal storage conditions, with known pharmacokinetic and pharmacodynamics, and reach the site of action after an easy and non-invasive e.g. oral administration. However, receptors are large protein complexes with many potential binding sites, whereas peptides have a complex secondary and tertiary structure, both of which determine the peptide's specificity as well as its sensitivity. As a consequence of the complex requirements of peptide drugs, the production of successful peptidomimetics using chemical libraries is largely unsuccessful. Therefore, large part of the design of peptide drugs still relies on the native peptide for therapeutic purposes, as will be addressed in further chapters of this thesis.

It is well-known that the discovery of new lead structures is one of the principal bottlenecks in medicinal chemistry. In this sense peptides could be an interesting source of new structures for further developments. Because of the aforementioned one may ask: why peptides? Peptides constitute a class of organic molecules that interact with, essentially, all the rest of the known chemical world: peptides can control, catalyze and modulate most biological processes and are highly compatible with and generally nontoxic to living systems. In addition, synthetic peptide chemistry is perhaps the most recent highly developed domain of biological chemistry, with high-yield stereospecific synthetic methodologies.

The list of peptides as potential therapeutic drugs is huge and space limitations do not permit to discuss them all. It is beyond the scope of this chapter to focus on peptide therapies such as luteinizing-hormone-releasing hormone (LHRH), growth hormone, arginine vasopressin or the very interesting peptide, cyclosporine (Borel 1989a, b; Borel et al. 1989; Lee et al. 1990). Instead, we will shortly address some exciting areas of research as well as recent developments in the use of more established peptide therapies.

Historically, it is well known that insulin was the first peptide to be isolated and administered therapeutically, and is still the most commonly prescribed peptide. However, it is needed yet to find novel analogues and chemical mimics, as well as new methods of administration. Manipulation of the insulin molecule has allowed the development of shorter-acting insulin analogs e.g. Lispro insulin which can be rapidly absorbed, readily dissociates into insulin monomers, and produces plasma levels that more closely mimic the normal postprandial insulin profile. Thus, Lispro can be injected immediately prior to a meal, unlike conventional short-acting insulin analogs that should be injected half an hour earlier (Puttagunta and Toth 1998).

Peptide antibiotics have been under investigation for a number of years. Currently one family of antibiotic peptides is been distributed, the polymyxins, namely; polymyxin B and colistin (polymyxin E). Colistin is occasionally given by injection to treat *Pseudomonas aeruginosa* in patients with cystic fibrosis, though more frequently aerosol preparations have been used (Diot et al. 1997). Polymyxin B is just used as a topical preparation for local eye and ear infections. Both antibiotics are prescribable for local skin

infections. Several classes of other antibiotic peptides including defensins, protegrins, magainins, tachyplesins, cecropins, mutacins and clavanins are under investigation. The inability of present non-peptide antibiotics to kill certain bacteria, make it likely that antibiotic peptides will form an important part of our fight to defeat multi-drug resistance in the twenty-first century.

At the neurological level, especially in the central nervous system (CNS), there have been described more than 100 peptides acting as neurotransmitters, neuromodulators and growth hormones. Amongst them, it is worthy to mention the angiotensins, neuromedin B, gastrin releasing peptide, bradisin, calcitonin, β-endorphin, Leu-encephalin, Met-encephalin, endothelins, gastrin, neuropeptide Y, oxitocine, somatostatin, substance P, vasopressin, glucagon, etc. In the field of medicinal chemistry, there are numerous examples of drugs that were developed on the basis of peptide structures. Amongst the best known examples we should mention the encephalin and endorphins mimicking drugs, agonists of cholecystokinin, agonists and inhibitors of angiotensin-converting enzyme (ACE), etc. The better known peptide neurotransmitters are, without any doubt, the encephalins and the endorphins. Thus, the synthesis of peptidomimetic analogues with a better agonist activity, higher stability and potentially orally administrated is one of the most explored subjects in medicinal chemistry.

Another well-known example is the development of captropril and the anti-hypertensive drugs acting on angiotensin-converting enzyme (or ACE, dipeptidyl carboxi-peptidase I). In 1965, Ferreira reported that a mixture of peptides of the venom of the South American pit viper *Bothops jararaca* potentiated the action of bradykinin by inhibition of some bradykininase activity (Ferreira and Rocha e Silva 1965). Bakhle and coworkers subsequently showed that these peptides also inhibited the conversion of angitensin I to angiotensin II (Bakhle et al. 1969). Thus, nine active peptides were isolated from this venom; the structure of a pentapeptide (Pyr-Lys-Trp-Ala-Pro, where Pyr stands for *L*-pyroglutamate) was identified (Ferreira et al. 1970a). This peptide was shown to inhibit the conversion of angitensin I to II and bradykinin degradation *in vitro* (Ferreira et al. 1970b) and *in vivo* (Stewart et al. 1971). The structures of six more related peptides were determined by Ondetti and coworkers (Ondetti et al. 1971). Some of these peptides have shown a significant *in vivo* potency and were effective in lowering blood pressure. Although none of these peptides were effective when administrated orally, they laid the foundation for the design of orally active ACE inhibitors nowadays worldwide used.

From the above mentioned finding it appears that peptides are an excellent new source to obtain novel drugs. However, we must be aware that there are also serious limitations with respect to the use of peptides as new drugs. In terms of drug bioavailability, stability, pharmacokinetics and pharmacodynamics, most peptides are as bad as proteins, and in general do not make good drugs unless modifications have been performed on their structures. It is clear that in general peptides possess significant limitations to be used directly as drugs; however many of these peptides are excellent starting structures to develop new drugs with novel and specific mechanisms of action and therefore developing new effective and safer therapeutic agents.

Without any doubt, the knowledge gained over the last decades regarding electronic molecular structure, as well as conformational behavior of peptide compounds is one of the fundamental factors that have allowed peptides to be, nowadays, an important source of new potential therapeutic agents with a wide variety of biological activity. This knowledge of the conformational/electronic structure would not be accessible without the great support of computational techniques to molecular modeling.

1.2 Molecular Modeling: A Powerful Tool To Study Peptides

The key to successfully analyzing the complex relationship between structure and function of peptides requires data and information from both experimental and computational technologies and the integration of fundamental principles from a range of disciplines like for example molecular pharmacology, physical chemistry, computational chemistry, medicinal chemistry and molecular biology amongst others. All in all, modern medicinal chemistry has become an extremely multidisciplinary field in which chemistry, pharmacology, biomedical science, medicine and theoretical physical-chemistry has to be integrated.

The ultimate goal of the medicinal chemist is to discover by rational design a molecule which will produce a desired biological activity without producing undesirable collateral effects. In this sense it must be noted that although the present available techniques of molecular modeling have allowed more "rational" and planned researches with respect to those developed in the last century, they are still far from perfect. One may be forced to seek compromises in view of the complexity of the biological system and individual variations. On a more positive note, however, molecular modeling studies using theoretical calculations can be used to select peptides having high probability of success as useful drugs after an adequate chemical modification. Since the number of peptides and peptide mimetics to choose from synthetic or natural sources is astronomically large, any methodology which increases the odds of success is greatly welcomed. Molecular modeling; a powerful tool to study peptides.

One of the first references of the use of molecular modeling in drug design is from 1955 (Marshall 1996). Since then, computational techniques have initiated a revolution in drug design. Researchers use computational techniques to model the therapeutic target in order to determine the essential characteristics that the new drug must possess. These characteristics are known as a pharmacofore. Once a pharmacofore is determined and defined, we may proceed on one of two routes. Part of this process may involve performing quantitative structure-activity relationship (QSAR) analysis on a given set of data. Also, based on the pharmacophore, one may "invent" potential compounds that may perform the required function. Calculations of these "virtual compounds" can be produced, and "virtual tests" can be run to assess its suitability before an expensive, and sometimes difficult, synthesis attempt is made. Once the candidate compound has been determined, molecular modeling can help to determine which ones are the most promising compounds. Virtual experiments are cheaper, faster and safer than real experiments, and data can help us eliminate compounds that will not successfully perform the required task.

In spite of the technological advances, the key information that permits rational approaches to drug design is knowledge of the etiology of a given disease, or at least of the biochemical process which is disturbed. The genetic revolution had added a major new dimension to the role of computational chemistry in the medicinal chemistry field. The search for key targets in genes offers computational medicinal chemists the opportunity to fight many diseases at their bio-molecular source. Thus, the so-called structure-based drug design (SBDD) describes the design of the therapeutic agent (ligand) based on the structure of the target or receptor molecule. In SBDD, the modeler seeks a molecule to complement the active site of a 3D structured molecular target, which is typically determined from X-ray, nuclear magnetic resonance (NMR), or protein homology modeling studies. Once the 3D structure of a receptor protein's active site is known, modelers use that knowledge to find or design a corresponding ligand, the potential new drug.

The active site must be characterized to determine the location of the major functional groups, which are typically hydrophobic and hydrogen bonding sites. Once the geometry and functional features of the active site are known, modelers look for the "inverse" shape and feature to describe the ligand's complementary structure.

Modern simulation methods enable to study the properties of larger and more complex systems than before. Dynamics simulations provide a tremendous amount of information that is not available from a static approach of the system. For example, a protein might "open up" to reveal an apparently inaccessible active cleft that enables a ligand or potential drug candidate to bind. Simulating the movements and conformational behaviors of molecules reveals a deep understanding of intermolecular interactions and the motions responsible for controlling biological and chemical activity. While the traditional lock and key model for protein-ligand docking is useful as a first approximation for ligand interaction, highly accurate docking requires the consideration of conformational changes on the ligand and/or the receptor. In addition, solvent effects may play a crucial role in the binding of ligands (Suvire et al. 2001; Zamora et al. 2003).

In today's medicinal chemistry laboratory, modeling and simulation methods are an integral part of developing drugs that optimally bind to receptor with great selectivity and improved efficacy. Having an accurate picture of what happens at the molecular level includes an understanding of how atoms move. By incorporating simulations into the drug design process, it is possible not only help to optimize the potency of existing lead compounds, but *de novo* drug design.

The exponential increase in power and software availability that has occurred with molecular modeling in just the past 20 years is very promising. Faster computers with superior graphics capabilities will become more inexpensive, and molecular modeling software packages will be more user friendly. It is clear that the role of computational simulation in drug discovery analyzing 3D structures of targets gives an unprecedented insight into the conformational behavior and mechanics of drug binding and biological activity that can be available for almost any scientist.

The goal of determining the stereoelectronic feature of a peptide from its constituent amino acid sequence stems from the universal acceptance that the activity of a peptide is a direct consequence of its folded or unfolded molecular configuration and its physicochemical properties. The capability of describing and understanding the structure-activity relationship of peptides is essential to obtain successful results. Nevertheless, the conformational study of peptides is extremely complex due to the structural diversity that they posses, not only in terms of chemical functionality, but also in terms of conformational space research. Each peptide building block, namely amino acids, has mainly two conformational spaces to be taken into account: the backbone (φ-ψ Ramachandran space) and the side-chain groups (χ space), both of which have a considerable high conformational flexibility (FIGURE 1.1). Hence, a simple hexapeptide not only has its unique chemical structure but also has hundreds or even tens of thousands of available conformations at physiological temperature. In fact, it is well established that not only one but several of this possible conformational structure can trigger the activation signal in a given biological system, depending on the surrounding environment (solvent, temperature, pressure, pH, salt strength, concentration, etc) as well as on the molecular interactions with the corresponding receptor molecule.

Once the biologically relevant structure of a given peptide is obtained it is necessary to carry out an electronic study which has to be done at the highest level of theory possible, in

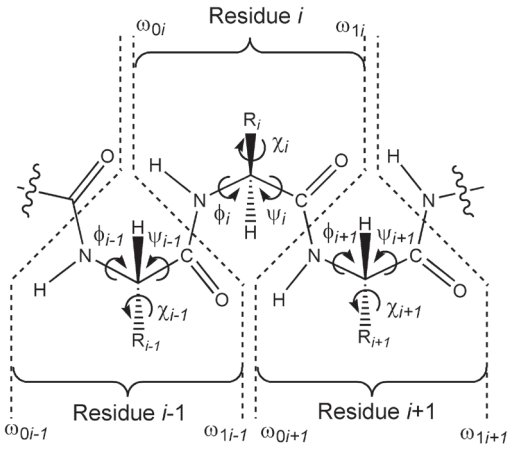

Figure 1.1: Schematic representation of an *L*-amino acid containing peptide. The ω dihedral angles represent the torsion of the peptide linkage itself. All ω dihedral angles are represented in their trans ($\omega \approx 180^{o}$) configuration. The main dihedral angles that define the peptide backbone (φ and ψ) are also shown. R stands for the side chain moiety which can include multiple χ dihedral angles depending on the nature of the residue, e.g.: the side chain of the residue Arg has 5 χ torsions while the side chain of a residue Gly does not possess this type of dihedral angle.

order to have the optimal description of its electronic distribution. Of course, to achieve this goal it is mandatory to use quantum mechanics approaches. Knowledge of the stereoelectronic attributes and properties of peptides will contribute significantly to the elucidation of the molecular mechanism involved in the biological activity. Molecular Electrostatic Potentials (MEPs), which are the visualization of the molecular electrostatic fields, offer an informative description of the capacity of peptides to generate stereoelectrostatic forces. MEPs have been shown to provide reliable information, both on the interaction sites of molecules with point charges and on the comparative reactivity of those sites (Murray and Politzer 1998; Naray-Szabo and Ferenczy 1995; Politzer and Truhlar 1981). More positive potentials reflect nucleus predominance, while less positive values represent rearrangements of electronic charges and lone pairs of electrons. The fundamental application of this study is the analysis of non-covalent interactions (Politzer and Truhlar 1981) mainly by investigating the electronic distribution in the molecule. Thus, this methodology was used to evaluate the electronic distribution around the molecular surface for peptides reported in this thesis.

It is clear that an astronomical increase of computing power will become available in the foreseeable future. A retrospective and prospective view about the developments of softwares and hardwares from 1950 to 2050 was previously reported showing the amazing increase in the computer capabilities (Chasse et al. 2001). Furthermore, it becomes clear that such an unprecedented increase in computing capability will make it possible to produce more accurate theoretical results than can be measured experimentally at a substantially lower cost. It was estimated that this will occur around 2020 (Enriz 2005).

In the present thesis, the studies on synthesis, bioassays and molecular modeling of small-size peptides have been directed towards two problems that are of great interest in today's medicinal chemistry; (*i*) the search of new peptides with antifungal activities and (*ii*) the development of novel anti-amyloid peptides with potential therapeutic properties for the treatment of Alzheimer's disease. Hereinafter, a brief description, as well as the importance and necessity of the above mentioned study goals is given.

1.3 The need for new antifungal drugs

Fungal infections have continued to be a major medical problem during the past two decades especially involving immunocompromised patients (Georgopapadakou and Tkacz 1995; McNeil et al. 2001; Pfaller and Diekema 2007; Walsh et al. 2004). Invasive fungal infections, as well as dermatomycoses produced by fungal organisms with even low virulence can be life-threatening (Nagiec et al. 1997) for patients such as neonates, cancer patients receiving chemotherapy, organ transplant patients, and burn patients, apart from those with acquired immu-

nodeficiency syndrome (AIDS). Other risk factors include corticosteroid and antibiotic treatments, diabetes, lesions of epidermis and dermis, malnutrition, neutropenia and surgery (Walsh et al. 2004). Many fungal infections are caused by opportunistic pathogens that may be endogenous (*Candida* infections) or acquired from the environment (*Cryptococcus* and/or *Aspergillus* infections). Patients with significant immunosuppression frequently develop *Candida* esophaguitis. *Criptococcosis*, caused by the encapsulated yeast *Cryptococcus neoformans*, which has been the leading cause of fungal mortality among HIV-infected patients. This organism has predilection for the central nervous system and leads to severe, life-threatening meningitis. In addition, an increasing number of normal individuals, including children in third-world nations that suffer deficient sanitation and education, have fungal infections, specially those involving the skin and mucosal surfaces (Ablordeppey et al. 1999; Freixa et al. 1998).

Although it appears that many drugs are available for the treatment of systemic and superficial mycoses, there are in fact only a limited number of efficacious antifungal drugs (Walsh et al. 2004). Many of the drugs currently available have undesirable effects or are very toxic (e.g.: amphotericin B); are fungistatic and not fungicidal (e.g.: azoles), or can lead to the development of resistance as in flucytocine (also called 5-fluorocytosine or 5-FC) (White et al. 1998). Amphotericine B, developed in the late 50's, still remains a widely used antifungal drug, most recently gaining renewed life through lipid based formulations. According to Polak ideal drugs to cure fungal infections have not been discovered yet (Polak 1999). Certain conditions are required for a compound to be a good antifungal agent: it must be fungicidal rather than fungistatic and have a good broad spectrum of activity, a minimum emergence of resistant strains, and a selective mechanism of action. In addition, the agent should have minor toxic side effects and good availability (Ablordeppey et al. 1999; Polak 1999; Zacchino et al. 2003). In the meantime, resistance to currently available antifungal agents continues to grow (Bartroli et al. 1998a). Although combination therapy has emerged as a good alternative to bypass these disadvantages (Bartroli et al. 1998b; Polak 1999), there is a real need for a next generation of safer and more potent antifungal agents (Bartroli et al. 1998b; Walsh et al. 2004). This event resulted in the identification of novel molecules, which could result useful for a future development.

In the course of a screening program for new and selective antifungal compounds, the molecular modeling group of the National University of San Luis, Argentina has previously reported the antifungal activity of different compounds obtained from natural (Bisogno et al. 2007; Freile et al. 2003; Zacchino et al. 1999; Zacchino et al. 1997; Zacchino et al. 1998) and synthetic (Giannini et al. 2004; Karolyhazy et al. 2003; Kouznetsov et al. 2000; Kouznetsov et al. 2008; Lopez et al. 2001; Sortino et al. 2007; Suvire et al. 2006; Vargas M et al. 2003; Villagra et al. 2003) sources. Among them a series of 4-aryl-or 4-alkyl-N-arylamino-1-butenes ("homoallylamines") and related tetrahydroquinolines and quinolines (Kouznetsov et al. 2000; Vargas M et al. 2003) display a range of antifungal properties against dermatophytes, fungi that produce most of the dermatomycoses in humans. This study was extended introducing a new series of 4-N-arylamino-1-butenes containing the pyridinyl or quinolinyl moieties at C4 and other structurally related compounds (Kouznetsov et al. 2008). Regarding their mode of action, active compounds showed *in vitro* inhibitory activities against (1,3) β-*D*-Glucan-synthase and mainly against chitin-synthase, enzymes that catalyze the synthesis of major fungal cell wall polymers (Kouznetsov et al. 2008; Sortino et al. 2007; Suvire et al. 2006). Since fungal but not mammalian cells possess a cell wall, these structures appeared as promising leads for the development of selective antifungal compounds. Other classes of structure possessing interesting potential as antifungal agents are the peptides. Some of the most relevant antecedents about these compounds are discussed in the next section.

1.4 Cationic peptides acting as antifungal compounds

With an understanding of the pivotal role that cationic host defense (antimicrobial) peptides play in preventing infections by microbial pathogens in many organisms, it has been proposed that these peptides might form the foundation for a new class of clinically useful antimicrobials. To date, more than 700 peptides (in virtually all species of life) have been described that not only kill pathogenic microorganisms, including Gram-positive and Gram-negative bacteria, viruses, protozoa and fungi, but also play a central role in recruiting and promoting elements of the innate immune system (Bowdish and Hancock 2005; Brown and Hancock 2006; Hancock 2001; Hancock 1997). This enormous peptide diversity is achieved through several structural classes, whereby all peptides, regardless of class, share a net positive charge and approximately 50 % hydrophobic residues, which confers the ability to fold into amphiphilic conformation upon interaction with membranes (Zasloff 2002). Although, it was in the early 80's when the use of amphipathic structures from the structural analyses of complement toxins was settled as a non-enzymatic way of cell membrane disruption (Bhakdi et al. 1983; Bhakdi and Tranum Jensen 1983), its mechanisms of action, at the molecular level, was not fully understood by then.

A major motivation for therapeutic peptide use is their diverse potential application: they can be used as single antifungal, in combination with other antifungals for a synergistic effect, or as immunomodulatory and/or endotoxin-neutralizing compounds (Powers and Hancock 2003). Although the potency of these amtimicrobial peptides against the more susceptible pathogens is normally not as strong as certain conventional antifungals, one of their major strengths is their ability to kill multi-drug-resistant fungi at similar concentrations.

Some natural peptides have been recently reported as antifungal compounds; they showed to inhibition of a broad spectrum of pathogens and microorganisms (Bulet and Stöcklin 2005; Hancock et al. 1995; Hancock and Lehrer 1998; Lee et al. 2003). It has been reported that a group of cationic antimicrobial peptides are major players in the innate immune response. These peptides are very ancient elements of the immune response of all species of life, and the induction pathways for these compounds in vertebrates, insects and plants (Boman et al. 1993; Ganz and Lehrer 1995; Hoffmann et al. 1999; Zasloff 1992) are highly conserved. Furthermore, it is becoming increasingly apparent that cationic antimicrobial peptides have many potential roles in inflammatory responses, which represent an orchestration of the mechanisms of innate immunity.

Small cationic peptides are abundant in nature and have been described as "nature´s antibiotics" or "cationic antimicrobial peptides" (Hancock 2001; Hancock and Patrzykat 2002). These peptides are 12-50 amino acids long with a net positive charge of +2 or +9, which is due to an excess of basic arginine and lysine residues, and approximately 50% hydrophobic amino acids (Hancock 2001). These molecules are also folded in three dimensions so that they have both a hydrophobic face comprising non-polar amino acid side-chains, and a hydrophilic face of polar and positively charged residues: these molecules are amphipathic. Despite these two similarities these compounds vary considerably in length, amino acid sequence, and secondary structure. The different spatial orderings include small β-sheets stabilized by disulphide bridges, amphipathic α-helices and, less commonly, extended and loop structures.

In this thesis two families of peptides with antifungal properties have been studied: (*i*) peptides that are structurally related of the α-MSH hormone (CHAPTERS 2, 3) and (*ii*) pepdides analogues of Penetratin, a cell penetrating peptides (CPP) of 16 amino acid long (CHAPTER 4).

1.5 Alzheimer disease, the phantom threat

Alzheimer's disease (AD) is a complex multifactorial neurodegenerative syndrome characterized by the patient's memory loss and impairment of cognitive abilities. This devastating disease affects more than 37 million people worldwide and, as a consequence of the worlds aging population, the prevalence of AD is expected to increase in an exponential fashion within decades (Blennow et al. 2006; Melnikova 2007; Pratico and Delanty 2000). AD is the most studied amyloid-based disease, whose main hallmarks are characterized by pathological high levels of brain lesions (senile plaques) and neurofibrillary tangles in dead and dying neurons, and also by abnormally elevated numbers of amyloid deposits in the walls of cerebral blood vessels (Haass and Selkoe 2007; Holtzman and Mobley 1991).

This degenerative brain syndrome was described by first time by the German neurologist and psychiatrist Alois Alzheimer in 1906. A. Alzheimer was a specialist of neuropathology who by observation of *postmortem* human brain tissue described the possible hallmarks of a degenerative syndrome which leads to a progressive decline in memory with concomitant abatement of thinking, comprehension and learning capabilities (Citron 2004). Thus, Alzheimer is credited with identifying the first published case of *"pre-senile dementia"*, which the influential E. Kraepelin would later name as Alzheimer's disease. AD accounts for most cases of dementia that are diagnosed after the age of 60 (Verdon et al. 2007; WHO-WebSite 2009). Numerous hypotheses have been put forward to explain the etiology of AD but for the vast majority of AD patients the cause of this disease remains unknown. However the best known and acknowledged hypothesis is the so-called amyloid hypothesis (figure 1.2). This hypothesis is based on the fact that the major component of senile plaques is a small peptide of 39-43 amino acids called β-amyloid (Aβ). $A\beta_{40}$ is the most prevalent species, while $A\beta_{42}$ is the more toxic one; other lengths are rare. Aβ is produced through endoproteolysis of the amyloid precursor protein (APP) which was first cloned and characterized in the late eighties (Muller-Hill and Beyreuther 1989). During the pathogenesis of AD the equilibrium of Aβ generation and Aβ clearance is disturbed, which eventually leads to elevated Aβ levels, increased Aβ aggregation and impaired memory function (Citron 2004; Wasling et al. 2009). Due to the above described processes AD is at least at the molecular level, a protein/peptide misfolding disease. For several years it was believed that the fibrillar final product, namely the plaques itself, of the amyloid-cascade was the main responsible element of the neuronal toxicity of Aβ aggregates. Recent evidence however for the involvement of soluble, non-fibrillar Aβ in AD has been gathered through four distinct experimental approaches that utilize (*i*) synthetic Aβ peptides; (*ii*) cell culture systems in which APP is over-expressed; (*iii*) APP transgenic mice; and (*iv*) human CSF and *postmortem* brain. In the case of human brain, it has long been recognized that amyloid plaque number does not correlate well with severity of dementia (Dickson et al. 1995; Katzman 1986; Terry et al. 1991); indeed this has been frequently cited as a critical flaw in the amyloid cascade hypothesis.

By using aqueous buffer free of detergents or chaotropes, Kuo et al. isolated a range of non-fibrillar forms of Aβ from both AD and control human brain (Kuo et al. 1996), with the major contribution coming from low-*n* oligomers ranging from dimers to octamers (up to *ca.* 100 kDa oligomers). In a complementary study, McLean and colleagues extracted samples of frontal cortex and putamen in PBS and after centrifugation and western blot analysis of the supernates from AD brain, the presence of variable proportions of monomeric, dimeric and trimeric Aβ species was revealed (McLean et al. 1999). Moreover, it was demonstrated that synthetic Aβ peptides are toxic to hippocampal and cortical neurons, both *in vitro* and *in vivo* (Busciglio et al. 1992;

Deshpande et al. 2006; Hartley et al. 1999; Hoshi et al. 2003; Lambert et al. 1998; Pike et al. 1991). Despite the above mentioned, it is important to be aware of the fact that Aβ is a natural biological product and is present in the brain and cerebrospinal fluid (CSF) of normal humans throughout life (Haass et al. 1992b; Ida et al. 1996; Seubert et al. 1992; Vigo-Pelfrey et al. 1993; Walsh et al. 2000) and just the mere presence of this product in brain does not necessarily lead to AD. Further evidence supporting soluble forms of Aβ as the principal mediators of neuronal toxic challenge comes from a report using PDAPP mice in which Aβ-mediated deficits of memory were reversed by a single intraperitoneal injection of an anti-Aβ antibody (Dodart et al. 2002). Using another well-characterized APP transgenic mouse model, Tg2576, Lesne and colleagues searched for the appearance of an Aβ species that coincided with the first observed changes in spatial memory (Lesne et al. 2006). It has been previously documented that the same Tg2576 mice show impaired performance in a hippocampal dependent contextual fear conditioning assay, decreased spine density in the dentate gyrus, and impairment of long-term potentiation (LTP) at ages long before the first apparent detection of Aβ dodecamer (Dineley et al. 2002; Jacobsen et al. 2006; Lesne et al. 2006). Thus, while the appearance of dodecamer correlates with the impairment of spatial memory in Tg2576 mice, it does not correlate with changes in other forms of memory, nor does it correlate with changes in synaptic form and function. Therefore, it seems likely that other lower-*n* oligomers may be responsible for the observed effects. We address the conformational behavior of low-*n* oligomers (specifically tri- and penta- $A\beta_{42}$ aggregates) in aqueous solution in CHAPTER 5 by using an *in silico* approach.

Expressing overt fear of dementia in the later phase of life, the dark humour about Alzheimer's disease, making so-called fun when someone starts to forget facts of daily life or mild signs of loss of decorum, signs of late onset depression, leads me to use a term like "*the phantom threat*" for this devastating human disease. When considering the current statistics on prospective projections of AD in our societies it is only logical that one feels certain threat by the possibility of becoming a victim of this disease, especially due to the very silent and almost asymptomatic beginning of it. Obviously, one of the first questions I would like to address is: which are the therapeutic possibilities that exist currently to deal with this threat? And what are the possibilities to design a new putative drug to fight against the phantom threat?

1.6 ACETYLCHOLINESTERASE INHIBITORS, THE FIRST GENERATION OF PROMISING THERAPEUTICS AGENTS

In the beginning of the '80s, biochemical and neuropathological evidences revealed the implications of the degeneration of basal forebrain, acetylcholinergic neurons in AD (Bartus 2000; Bartus et al. 1982), which became the basis of the so-called "*cholinergic hypothesis*". According to this hypothesis, the deterioration of cholinergic neurons in the basal forebrain and the associated loss of cholinergic neurotransmission in the cerebral cortex and other areas, significantly contribute to the neurodegeneration in AD (Bartus et al. 1982). Since acetylcholine in the forebrain was long known to be essential to memory function and attention, the so-called "*cholinergic hypothesis*" of AD held that cholinergic dysfunction in AD patients causes cognitive decline and that dementia therefore might be mitigated by the augmentation of acetylcholine activity in brain. The most logical therapeutic objective was to boost the levels of the transmitter, acetylcholine, by inhibiting its catabolic enzyme, acetylcholinesterase. Historically, acetylcholinesterase inhibitors were the first group of drugs marketed for AD treatment. Nowadays, several acetylcholinesterase inhibitors

are marketed and investigated for the treatment of mild-to-moderate dementia (Silvestri 2009). They have been demonstrated to mildly improve, relative to placebo, various cognitive and functional capacities (Scarpini and Cogiamanian 2003; Scarpini et al. 2003), and there is evidence that they may slow down the pathogenesis of AD (Hashimoto et al. 2005). Furthermore, a new drug called memantine, an inhibitor of the ionotropic receptor NMDA sensitive to the neurotransmitter glutamate, was recently approved for use in moderate-to-severe dementia (Koch et al. 2005). However, due to the severe damage that multiple neuronal systems undergo in AD, the benefits of agents that selectively target the activity of certain neurotransmitters offer poor and only temporary improvements. The limitations of the current generation of AD therapies led to recent reports not encouraging drugs like donepezil, rivastigmine, galantamine or memantine for the treatment of dementia (Kmietowicz 2005a, b; Mayor 2006). Even though, the improvements are modest and mainly acting at the symptomatic level of the disease, these drugs offered, and still do, hope to patients and their families. Nevertheless, they must eventually face the reality that the drugs cannot halt the unyieldingly severe deterioration of the patient's mental capacities. Fortunately, several extensive research programs on the fundamental molecule based pathogenesis of AD reveal promising new strategies for arresting the disease.

1.7 Targeting the amyloid hypothesis, a new generation of therapeutics agents

The amyloid cascade hypothesis was proposed in 1991 by John Hardy and David Allsop. This hypothesis states that the deranged metabolism of APP is the initiating event in AD pathogenesis, subsequently leading to the aggregation of Aβ, specifically $A\beta_{42}$, since Aβ was identified in the 80's as the main component of amyloid plaques (Glenner 1980a, b; Glenner and Wong 1984). Formation of neuritic plaques would then give rise to further pathological events, including the disruption of synaptic connections, which would lead to a reduction in neurotransmitters, death of tangle-bearing neurons and finally dementia (Hardy and Allsop 1991). As it was discussed in section 1.5, at the beginning it was believed that the fibrillar final product, namely the plaques itself, of the amyloid cascade was the main element responsible of the neuronal toxicity of Aβ. Nevertheless, recent evidence convincingly shows the involvement of soluble Aβ aggregates (see section 1.5 of this thesis). Thus, this hypothesis serves different points where the disease can be, at least in part, arrested at the very beginning of the molecular trigger events (figure 1.2).

Five major points of interference are easily seen on the pathway of this hypothesis; (*i*) blocking the Aβ production, (*ii*) preventing the self-assembly of Aβ monomers (aggregation), (*iii*) promoting the Aβ catabolism, (*iv*) stimulating the Aβ clearance and (*v*) blocking the cytotoxicity of multimeric Aβ aggregates. A brief description of each of the above mentioned points now will be given.

1.7.1 *Blocking the Aβ production*. This approach aims to decrease the biological production of Aβ by controlling the cleavage of the APP. APP is usually cleaved within the Aβ sequence by the enzyme α-secretase, which splits Aβ, leading the non-amyloidogenic pathway (figure 1.3A). Alternatively, this protein can be also cleaved by the enzyme β-secretase (β-amyloid cleaving enzyme, or BACE) and γ-secretase at the Aβ *N*- and *C*-termini, respectively, thus yielding monomeric Aβ (figure 1.3B). These Aβ monomers may then aggregate and form neurotoxic products. This amyloidogenic pathway is the core of the amyloid cascade (figure 1.2). Therefore, the main targets of this approach are obviously the cleavage enzymes α-, β-, and γ-secretases. Most pharmacological efforts to reduce the production of Aβ have been directed towards inhibiting β- or γ-secretase by the action of peptide and non-peptide inhibitors (Black et al. 2005; Brunkan and Goate 2005; Eriksen et al. 2003; Kornacker et al. 2005;

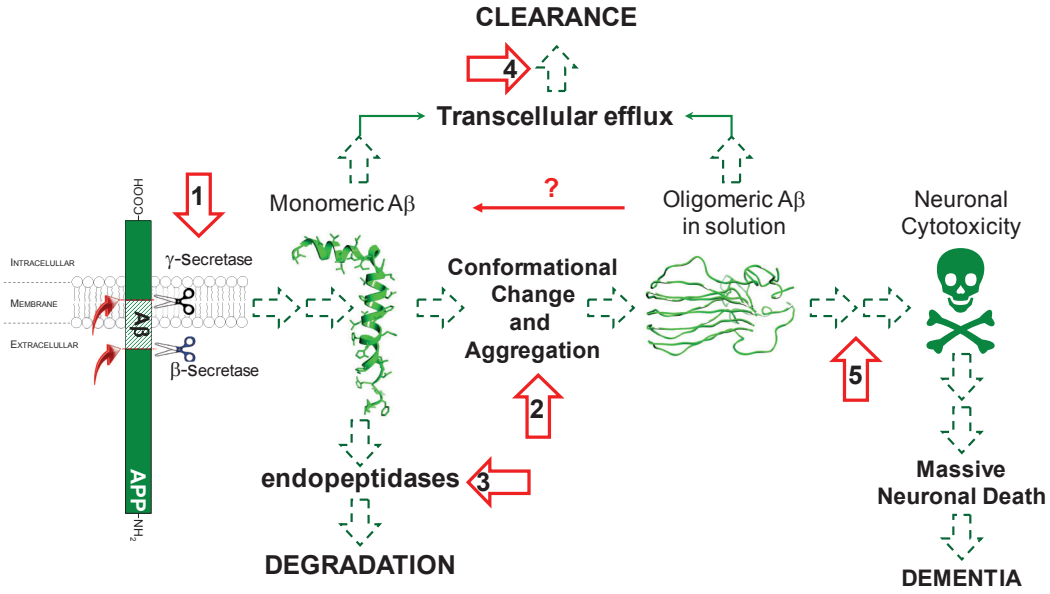

Figure 1.2: Schematic representation of the amyloid hypothesis. Five major points of interference are shown on the pathway of this hypothesis; (**1**) blocking the Aβ production (section 1.7.1), (**2**) preventing the self-assembly of Aβ monomers (aggregation, section 1.7.2), (**3**) promoting the Aβ catabolism (section 1.7.3), (**4**) stimulating the Aβ clearance (section 1.7.4) and (**5**) blocking the cytotoxicity of multimeric Aβ aggregates (section 1.7.5).

Lanz et al. 2005; Maiorini et al. 2002; Pollack and Lewis 2005; Silvestri 2009; Singer et al. 2005). Even though blocking the γ-secretase complex lowers Aβ formation in experimental systems, this can also play an important role in the receptor/signalling system of the protein Notch. The reduction of Notch activity could interfere with important cellular proliferation and differentiation pathways (Pollack and Lewis 2005). Reducing Aβ production by enhancing α-secretase cleavage also is a plausible, yet complex, strategy (Lichtenthaler and Haass 2004), and there is evidence that statins, which might reduce the risk of AD, partly act in this manner (Parvathy et al. 2004).

1.7.2 *Preventing the self-assembly of Aβ monomers*. This strategy aims to interfere with the aggregation of Aβ into oligomeric and/or fibrillar assemblies (Mason et al. 2003). Several attempts to design a drug with these properties have been devoted to this aspect of the pathogenesis e.g.: Tramiprosate (Alzhemed™) which recently reached phase III clinical trials (Aisen 2005). Although it is a theoretically very appealing tactic, impeding protein–protein interactions can be extremely difficult pharmacologically (Walker and LeVine Iii 2002). On the other hand, it is very important to mention that there is a need of interrupting the Aβ self-assembly process very early in the cascade, since inhibiting just the fibril formation conceivably could cause the accumulation of prefibrillar soluble oligomers and thereby could exacerbate neurocytotoxicity.

1.7.3 *Promoting the Aβ catabolism*. As many other peptides, Aβ can be broken down by endopeptidases, notably neprilysin and insulin-degrading enzyme (IDE) (Tanzi et al. 2004). There is evidence that by increasing the activity of these enzymes in APP-transgenic mice reduces brain Aβ levels and senile plaque load (Leissring et al. 2003). However, it is important to be mindful that selective up-regulation of enzymatic activity can be dangerously problematic, since other substrates might be adversely affected. Therefore, to interfere the enzymatic liberation of Aβ remains a more attractive approach.

1.7.4 *Stimulating the Aβ clearance*. This is a very ambitious and auspicious strategy for halting AD pathogenesis. Either immunologically (Billings et al.

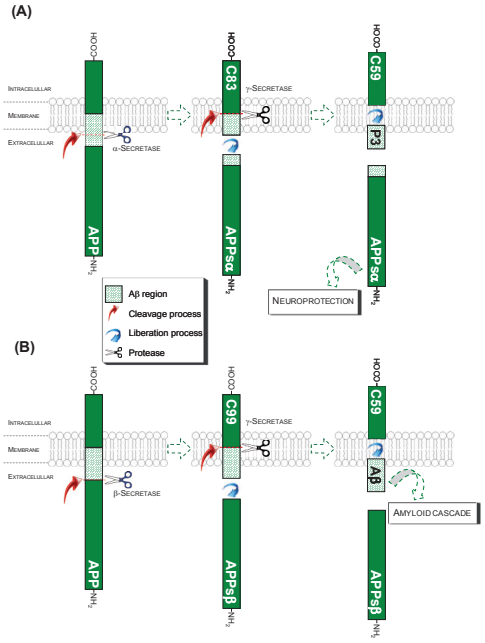

Figure 1.3: Schematic representation APP and its metabolites biochemical pathways relevant to Alzheimer's disease (not drawn to scale). The non-amyloidogenic (A) and the amyloidogenic (B) biochemical pathways are depicted. In pathway A, α-secretase cleaves in the middle of the Aβ region to release a large soluble APP fragment, α-APPs. The *C*-terminal C83 peptide is metabolized to p3 and C59 (APP intracellular domain) by γ-secretase. In pathway B, β-secretase releases a large soluble fragment, β-APPs. The *C*-terminal C99 peptide is then metabolized to Aβ and C59 by γ-secretase. β-Secretase inhibitors block the formation of β-APPs and C99; γ-secretase inhibitors block the formation of p3, Aβ and C59.

2005; Gilman et al. 2005; Hock et al. 2003) or by enhancing the transcellular efflux (Cirrito et al. 2005; Lam et al. 2001; Vogelgesang et al. 2004; Zerbinatti and Bu 2005) of Aβ out of the brain, this approach has shown some promising results. However, some adverse events, particularly aseptic meningoencephalitis, have hindered the clinical application of Aβ-immunotherapy in AD (Orgogozo et al. 2003a), but the effectiveness of immunisation in preclinical models justifies the current intensity of research on this matter. Nevertheless, this approach should be undertaken cautiously.

1.7.5 *Blocking the cytotoxicity of multimeric Aβ aggregates*. The biochemical pathways of how Aβ multimers aggregate exert their neurocytotoxic effects remains uncertain, and thus several hypothesis have been proposed. Two plausible possibilities have drawn mayor attention; (*i*) abnormal interactions of globular oligomers with cellular elements (Demuro et al. 2005) and (*ii*) the formation of membrane pores that act as anomalous ion channels (Quist et al. 2005). Thus, selective Aβ-channel-blocking agents could be useful for a future AD therapy if Aβ pores are proven to form in membranes of degeneration-prone cells. On the other hand, for instance, if a drug can be designed with the property of binding Aβ oligomers and by this mean to inactive their cytotoxicity properties, this drug should be able to bind selectively Aβ and specifically soluble low-*n* Aβ oligomers. This last opens an attractive field of opportunities to design peptidergic drugs based on the natural sequence of Aβ.

I would like to remark that so far none of the above mentioned strategies have led to more than promising treatments of AD, either by reducing the symptomatic implications or by slowing down the course of the disease. The definitive cure of this phantom threat seems to be as phantasmagoric as the disease itself.

1.8 Aβ-toxicity offsetting peptides

Due to the great incidence that AD has over the human aging population, there is an evident need of therapeutic agents that could at least significantly delay the progressive course of the disease (Hardy and Selkoe 2002; Wolfe 2002). Currently, several research groups attempt to develop therapies that aim at reducing Aβ production, enhancing its clearance and/or preventing or retarding the amyloidogenesis processes, as it was briefly discussed in section 1.7 of this thesis. Particularly appealing is the use of peptides or peptidomimetic molecules derived from the same Aβ sequence (Granic et al. 2009; Soto et al. 1998; Tjernberg et al. 1996; Wolfe 2002). Promising putative treatments may be those designed to inhibit steps that *precede* Aβ peptide aggregation, by

blocking production of the toxic soluble Aβ oligomers in the first place, or by reversing, somehow, the toxic effect of these oligomers. In fact, some short peptide derivatives from Aβ peptide have already been reported to specifically interact with Aβ and cause interferences in its neurotoxic effects. Leu-Pro-Phe-Phe-Asp (Soto et al. 1996; Soto et al. 1998), Lys-Leu-Val-Phe-Phe (Hetenyi et al. 2002b; Tjernberg et al. 1997; Tjernberg et al. 1996), Arg-Ile-Ile-Gly-Leu-NH_2 (Fulop et al. 2004) and Leu-Pro-Tyr-Phe-Asp-NH_2 (Datki et al. 2003; Datki et al. 2004; Granic et al. 2009; Juhasz et al. 2009; Szegedi et al. 2005) are some of the promising starting points to develop potential drugs that can somehow reverse the devastating impact of Aβ aggregates. Specifically, the case of Leu-Pro-Tyr-Phe-Asp-NH_2 is addressed in CHAPTER 6. In order to increase the anti-amyloidogenic properties of these peptides, some groups have recently explored a new strategy consisting of the introduction of *N*-methyl amino acids in these sequences (Cruz et al. 2005; Gordon and Meredith 2003; Gordon et al. 2001; Gordon et al. 2002). *N*-Methyl amino acids have been used in several systems to control or prevent the aggregation of β-sheet and β-strand peptides (Chitnumsub et al. 1999; Clark et al. 1998; Doig 1997; Hughes et al. 2000; Nesloney and Kelly 1996; Rajarathnam et al. 1994). The main goal is to block the hydrogen bond network that stabilizes the β-sheet amyloid structure and hopefully inhibit the formation of toxic oligomers and/or amyloid aggregates. A series of *N*-Methyl amino acids containing peptides has been described in CHAPTER 7.

I would like to propose the use of the term Aβ-Toxicity Offsetting Peptides (Aβ-TOP), since to our opinion some of the peptides mentioned in this section have been erroneously named as β-sheet breaker peptides. The term β-sheet breaker peptides was introduced firstly by C. Soto and coworkers (Soto et al. 1998), thus this term was widely used for almost all peptides derived of the Aβ sequence as a generic term. Some studies using CD spectrometry studies have been carried out on some of these so-called β-sheet breaker peptides (Datki et al. 2004; Hetenyi et al. 2002a; Hetenyi et al. 2002b; Laczko et al. 2008) but none of them so far have demonstrated proof at the molecular level of the β-sheet breaking properties of these peptides. Thus, we propose the use of this novel term based on the fact that this peptides, somehow, can protect neuron cells from the toxicity of Aβ, even though the mechanisms of how Aβ oligomers exert their toxicity are not yet clear and fully understood.

1.9 Scope of this thesis

Finally, I would like to spend a few words on the principal scope of this interdisciplinary thesis topic. It must be pointed out that we are looking not for another potential peptide drug, which can be made relatively easily, or even a more or less sophisticated potential peptidergic drug requiring a more laborious synthesis. In any case, we are not aiming to find a panacean compound, which might be a definite cure for a given disease. For many chronic diseases, like the two conditions that are the focus of this thesis, we need a totally new form of therapy, as penicillin, beta-blockers or H2-antagonists were in their time. Of course, everybody is looking for, and hoping to obtain these "*panacean drugs*". We have to remain realistic and we have to be content with only a partial approach to these ideal drugs, at least for the time being. Our aim is therefore more modest. Thus, we would like to place the minimum requirement to be able to generate a series of compounds that will provide the necessary guidelines to set out the route to a better understanding of the molecular bases of a given disease, in this case; fungal infections and Alzheimer's disease, by the useful approach of molecular modeling combined with techniques of molecular biology techniques. The question is: how do we generate this sort of compounds?

Structure based drug design (SBDD) provides a way to escape from molecular roulette, and this promising strategy represents a new chemotherapeutic revolution; however, at the moment there is no strategy (even the most rational one) totally free from serendipity.

On the other hand there are many sources where we can look for new structures to obtain new potential candidates to convert to leader compounds. It appears that the study of peptide structures as a starting point is a promising source in order to obtain such "leader structures".

In this thesis the results of synthesis, bioassays and molecular modeling on small-size peptides are presented. The structures obtained displayed potential applications on two burning topics in medicinal chemistry (*i*) the developing of new structures possessing antifungal activity and (*ii*) the development of new peptides displaying effective activity against Aβ toxicity. In these studies both theoretical and experimental tools have been used.

A brief description of what the reader will find in the following chapters of this multidisciplinary thesis is given here. Chapters 2 and 3 address the antifungal properties of peptides related to the sequence of the α-MSH. In chapter 2 the synthesis, *in vitro* evaluation and conformational study of the tetrapeptide His-Phe-Arg-Trp-NH_2 and related derivatives acting as antifungal agents, specifically against *Cryptococcus neoformans,* are reported. Chapter 3 discusses the implications in the antifungal properties of the octapeptide His-Phe-Lys-Trp-Gly-Arg-Phe-Val-NH_2 based on the conformational and electronic study, as well as the synthesis and *in vitro* evaluation. Chapter 4 presents also the synthesis, *in vivo* evaluation, conformational and electronic investigations of a series of cell penetrating peptides of 16 amino acid residues named penetratin and their derivatives.

Chapter 5 explores the contributions of the different structural elements of the trimeric and pentameric full-length $A\beta_{42}$ aggregates in solution to their stability and conformational dynamics. In chapter 6 the neuroprotective properties of the pentapeptide Leu-Pro-Tyr-Phe-Asp-NH_2 *in vitro*, as well as its memory preserving capacity against $A\beta_{42}$-induced learning deficits *in vivo* is investigated. Also, a conformational study and docking experiments were used to reveal part of the putative its mechanism of action. Finally, chapter 7 presents a novel *N*-Methyl amino acid containing peptide with anti-Aβ toxicity properties Ac-Lys-(Me)Ile-Ile-(Me)Gly-Leu-NH_2. A complete *in silico* design, as well as its *in vitro* neuroprotective properties and memory preserving capacity against $A\beta_{42}$-induced learning deficits *in vivo* are reported. ▪

"Ojalá pudiera haber reducirdo la rigidez de tus manos,
haberte conocido mejor, haberme sabido quien soy"
(M.F.M.)

02

"Kiko"

oil on paper (320x450 mm)

M.F. Masman 2010

Chapter 2

C2

Synthesis & conformational analysis of his-phe-arg-trp-NH_2 & analogues with antifungal properties

Marcelo F. Masman, Ana M. Rodríguez, Laura Svetaz, Susana A. Zacchino, Csaba Somlai, Imre G. Csizmadia, Botond Penke & Ricardo D. Enriz

Bioorganic and Medicinal Chemistry (2006) 14, 7604-7614

Abstract

The synthesis, *in vitro* evaluation and conformational study of His-Phe-Arg-Trp-NH_2 and related derivatives acting as antifungal agents are reported. Among them, His-Phe-Arg-Trp-NH_2 and His-Tyr-Arg-Trp-NH_2 exhibited antifungal activity against *Cryptococcus neoformans*. Antifungal activity of these compounds appears to be closely related to the α-MSH effect. A conformational and electronic study allows us to propose a biologically relevant conformation for these tetrapeptides acting as antifungal agents. In addition, these theoretical calculations permit us to determine the minimal structural requirements to produce the antifungal response and may provide a guide for the design of compounds with this biological activity.

2.1 Introduction

In the early 1980s, it was believed that virtually any fungal infection could be successfully treated with the wide range of available antifungal agents. Nevertheless, this belief was soon proved to be false (Garber 2001). The continuing increase in the incidence of fungal infections together with the gradual rise in resistance mainly to azoles in the last two decades highlighted the need to search novel compounds not tested previously in antifungal assays (Fromtling 1999; Kontoyiannis et al. 2003; Polak 1999; Zacchino et al. 2003). This event resulted in the identification of novel molecules of diverse structures, which could prove useful for a future development. Among them, some natural peptides have been recently reported as antifungal compounds. They showed to inhibit a broad spectrum of pathogens and microorganisms (Bulet and Stöcklin 2005; Hancock et al. 1995; Hancock and Lehrer 1998; Lee et al. 2003) and possess a very important characteristic, since they do not usually induce bacterial resistance (Hancock 1997). Regarding their structural features, they are cationic, but differing considerably in other characteristics such as size and presence of disulfide bonds and structural motifs (Epand et al. 1995; Epand and Vogel 1999).

Most of these peptides are believed to exert their antimicrobial activities either forming multimeric pores in the lipid bilayer of the cell membranes(Hancock 1997), or interacting with DNA or RNA after penetration into the cell (Boman et al. 1993; Cabiaux et al. 1994; Park et al. 1998). Nevertheless, α-melanocyte stimulating hormone (α-MSH) and its *C*-terminal tripeptide Lys-Pro-Val, which showed antimicrobial activity against two representative pathogens: *Staphylococcus aureus* and *Candida albicans* (Cutuli et al. 2000), appear to act through a mechanism substantially different from that of other natural antimicrobial peptides. Previous research suggests that the candidacidal effect of α-MSH is linked to the cAMP production in *C. albicans* and the adenylyl cyclase inhibitor ddAdo partly reversed the candidacidal effect of the peptide (Cutuli et al. 2000; Grieco et al. 2003; Grieco et al. 2005). It was suggested by Eberle and Schwyzer that α-MSH might have two message sequences, the first active sequence centered around the central tetrapeptide His-Phe-Arg-Trp and the second active site centered around the *C*-terminal tripeptide Ac-Lys-Pro-Val-NH_2 (Eberle et al. 1975; Eberle and Schwyzer 1975, 1976). Thus, we focussed our attention on both sequences in order to evaluate their potential antifungal effects.

As part of our ongoing program aimed at identifying novel antifungal agents, we have reported several natural and synthetic compounds (Freile et al. 2003; Giannini et al. 2004; Karolyhazy et al. 2003; Lopez et al. 2005; Lopez et al. 2001; Suvire et al. 2006; Urbina et al. 2000; Vargas M et al. 2003; Zacchino et al. 1999; Zacchino et al. 1997) exhibiting antifungal activities against different human pathogenic fungi. However, peptide structures had not been tested during this program until now. In the present study we report the design, synthesis and antifungal activity of novel small-size peptides: fifteen tripeptides structurally related to Lys-Pro-Val (the 11-13 sequence of α-MSH) and thirteen tetrapeptides structurally related to His-Phe-Arg-Trp (the 6-9 sequence of α-MSH). We tested these peptides against various human pathogenic strains including yeasts, filamentous as well as dermatophyte fungi. In addition, a conformational and electronic study on the most representative peptides reported here was carried out in order to determine a possible biologically relevant conformation for these compounds acting as antifungal agents. Thus, one of the goals of this study was to identify a topographical and/or substructural template, which may be the starting structure for the design of new antifungal compounds.

2.2 Results and discussion

2.2.1 Chemistry

Peptides **1-28** were prepared by manually solid-phase synthesis on a *p*-methylbenzhydrylamine resin (1 g MBHA, 0.39 mmol/g) and Merrifield resin (1 g, 1%, 200-400 mesh) with standard methodology using Boc-strategy. The peptides were cleaved from the resin with simultaneous side chain deprotection by acidolysis with anhydrous hydrogen fluoride containing 2% anisole, 8% dimethyl sulfide and indole. Details of the synthesis are given in Section 2.4.1 (Synthetic methods)

2.2.2 Antifungal activity

To carry out the antifungal evaluation, concentrations of peptides up to 250 μg/ml were incorporated to growth media following the guidelines of the National Committee of Clinical and Laboratory Standards for yeasts (Pfaller 2002a) and for filamentous fungi (Pfaller 2002b). Compounds producing no inhibition of fungal growth at 250 μg/ml level were considered inactive.

In a first step we focussed our attention on the activity of the sequence Ac-Lys-Pro-Val-NH_2 (peptide **1**, scheme 2.1), which has been reported as relevant for both receptor activation (Hruby et al. 1987) and antimicrobial activity (Cutuli et al. 2000). However, this tripeptide did not show any antifungal activity to the concentrations reported here against any of the strains of the fungal panel (yeasts: *Saccharomyces cerevisiae* and *Cryptococcus neoformans*; hialohyphomycetes: *Aspergillus flavus, A. niger and A. fumigatus*; dermatophytes: *Microsporum gypseum*, *Trichophyton rubrum* and *Trichophyton mentagrophytes*). It should be noted that compound **1** has been previously reported as antifungal against a strain of *C. albicans* (Cutuli et al. 2000). However, compound **1** was inactive against all the fungi tested here. Next, fourteen tripeptides with different residues (peptides **2-15**) were tested against the panel of opportunistic pathogenic fungi. It can be observed that none of these tripeptides showed antifungal activity against hialohyphomycetes or dermatophytes yeasts. It should be noted that peptide **6** was inactive against all the fungi tested here. This result is in agreement with those previously reported for peptide **6,** by Grieco et al. who reported only 2.7 % of inhibition of *C. albicans* for this tripeptide (Grieco et al. 2005).

Ac-Lys-Pro-Val-NH_2	(**1**)	His-Phe-Arg-Trp-NH_2	(**16**)
Ac-Lys-Pro-Val-OH	(**2**)	His-Tyr-Arg-Trp-NH_2	(**17**)
Lys-Pro-Val-NH_2	(**3**)	His-Phe-Lys-Trp-NH_2	(**18**)
Lys-Pro-Val-OH	(**4**)	His-Tyr-Lys-Trp-NH_2	(**19**)
Ac-Lys-Phe-Val-NH_2	(**5**)	His-Phe-D-Arg-Trp-NH_2	(**20**)
Lys-Phe-Val-NH_2	(**6**)	His-D-Phe-Arg-Trp-NH_2	(**21**)
Lys-Phe-Val-OH	(**7**)	His-D-Phe-Lys-Trp-NH_2	(**22**)
Ac-Arg-Pro-Val-NH_2	(**8**)	Ac-His-Phe-Arg-Trp-NH_2	(**23**)
Arg-Pro-Val-NH_2	(**9**)	Ac-His-Tyr-Arg-Trp-NH_2	(**24**)
Arg-Pro-Val-OH	(**10**)	Ac-His-Phe-Lys-Trp-NH_2	(**25**)
Ac-His-Pro-Val-NH_2	(**11**)	Ac-His-Tyr-Lys-Trp-NH_2	(**26**)
Ac-Lys-Gly-Ala-NH_2	(**12**)	Ac-Trp-Arg-Phe-His-NH_2	(**27**)
Ac-Lys-Gly-Gly-NH_2	(**13**)	For-His-Phe-Arg-Trp-NH_2	(**28**)
Ac-Lys-Ala-Ala-NH_2	(**14**)		
Ac-Val-Pro-Lys-NH_2	(**15**)		

Scheme 2.1: Sequence of the peptides studied in chapter 2.

In a second step of our study we focused on the tetrapeptide His-Phe-Arg-Trp-NH_2 (**16**), which is common to all melanocortin peptides and is important for binding to the known melanocortin receptors (Hruby et al. 1987). A very interesting result was that this tetrapeptide displayed a moderate but significant antifungal activity against *C. neoformans* (table 2.1) as well as against dermatophyte fungi (MICs values of 125, 250 and 250 μg/ml against *T. mentagrophytes*, *M. gypseum* and *T. rubrum*, respectively). Peptide **16** was the only peptide reported here showing antifungal activity against dermatophytes.

The next step consisted in testing twelve tetrapeptides structurally related to peptide **16** (peptides **17-28**), in which different replacements in the His-Phe-Arg-Trp-NH_2 sequence were performed to determine the contribution of each amino acid to the antifungal activity. None of these tetrapeptides displayed significant effect against *C. albicans, Saccharomyces cerevisiae, Aspergillus*

Table 2.1: Antifungal activity (MIC) of tetrapeptide His-Phe-Arg-Trp-NH_2 and derivatives against Cryptococcus Neoformans ATCC 32264

Peptide	Structure	MIC (μg/ml)
16	His-Phe-Arg-Trp-NH_2	125
17	His-Tyr-Arg-Trp-NH_2	125
18	His-Phe-Lys-Trp-NH_2	250
19	His-Tyr-Lys-Trp-NH_2	250
20	His-Phe-D-Arg-Trp-NH_2	250
21	His-D-Phe-Arg-Trp-NH_2	250
22	His-D-Phe-Lys-Trp-NH_2	250
23	Ac-His-Phe-Arg-Trp-NH_2	>250
24	Ac-His-Tyr-Arg-Trp-NH_2	>250
25	Ac-His-Phe-Lys-Trp-NH_2	>250
26	Ac-His-Tyr-Lys-Trp-NH_2	>250
27	Ac-Trp-Arg-Phe-His-NH_2	>250
28	For-His-Phe-Arg-Trp-NH_2	>250
	Standard drugs	
Amphotericin B		0.25
Ketoconazole		0.25

spp. and dermatophytes. However, six of these tetrapeptides (compounds **17-22)** displayed antifungal activity only against *Cryptococcus neoformans* (table 2.1). This is an important finding because cryptococcosis remains an important life-threatening complication for immunocompromised hosts and new compounds acting against this fungus are actually welcome (Polak 1999).

From the structure-activity analysis of the active peptides, it appears that the position of His and Trp-NH_2 in the amino acid sequence is essential for such activity, whereas the position of Phe and Arg are not. Replacement of the Phe residue in position 2 by Tyr (**16** → **17**) was possible without any loss of activity. Replacing Arg in position 3 by Lys was tolerated but with loss of activity (compare **16** with **18**). Peptide **19** showed that the replacement of the two central residues was tolerated but with loss of activity. An identical result was obtained replacing Arg with *D*-Arg (compare **16** with **20**). Our results indicate that replacement of Phe by Tyr gives a peptide as potent as the starting structure, whereas replacing Phe by its isomer *D*-Phe gives an active tetrapeptide but with loss of activity (compare **16** with **21** and **22**). In addition, all the acetylated (peptides **23**-**27**) and formylated (**28**) derivatives were inactive compounds.

In order to better understand the above experimental results and to establish some basis to obtain more active compounds, we performed a conformational and electronic study on the most representative peptides reported here, using theoretical calculations.

2.2.3 Conformational and electronic study of His-Phe-Arg-Trp-NH_2 and analogues

Linear peptides are highly flexible and therefore the determination of the biologically relevant conformations is not an easy task. It is necessary to perform an exhaustive conformational analysis for these structures. Therefore, eight tetrapeptides (**16-19** and **23-26**) were selected for energy calculations.

Table 2.2: Selected conformational search and clustering results for peptides **16-19** and **23-26** optimized at the EDMC/SRFOPT/ECCEP/3 level of theory

	Generated[a]				Accepted[b]				# F[c]	# $F_{0.20\%}$[d]	% P[e]
Pep	**Elec.**	**Ran.**	**Ther.**	**Total**	**Elec.**	**Ran.**	**Ther.**	**Total**			
16	3808	57095	80	60983	576	4359	65	5000	442	55	86.76
17	4592	65724	125	70441	651	4240	109	5000	436	51	87.84
18	4602	73490	235	78327	653	4168	179	5000	512	66	86.12
19	5403	78159	225	83787	747	4074	179	5000	449	37	87.72
23	6158	94316	340	100814	536	4199	265	5000	715	45	79.64
24	6517	91519	247	98283	743	4078	179	5000	623	59	82.22
25	7514	102050	499	110063	448	4190	362	5000	786	49	78.82
26	7104	95865	382	103351	518	4206	276	5000	659	51	81.94

[a] Number of conformations generated electrostatically, randomly and thermally during the conformational search.
[b] Number of conformations accepted from those generated electrostatically, randomly and thermally during the conformational search.
[c] **#F**: Total number of conformational families as result of the clustering run.
[d] **# $F_{0.20\%}$**: Number of conformational families with populations above 0.20%
[e] **% P**: Sum of the per cent relative population of **# $F_{0.20\%}$**

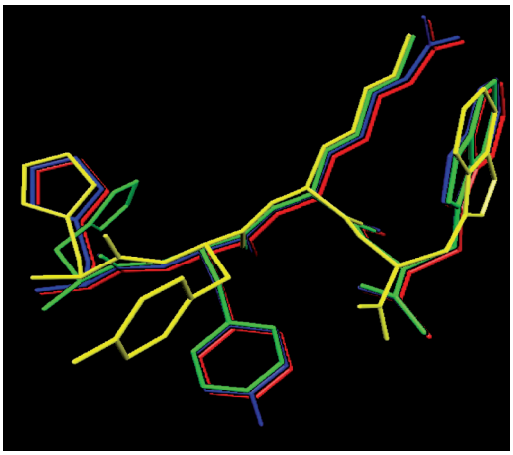

Figure 2.1: Stereoview of overlapping of conformer 1 for peptide **16** (red), conformer 1 for analogue **17** (bleu), conformer 19 for analogue **18** (green) and conformer 19 for analogue **19** (yellow). All hydrogens are omitted for clarity.

Theoretical calculations were carried out as described in section 2.4.4 Computational methods. These results are summarized in table 2.2 and tables 2.1S-2.8S (available in appendix A as supplementary material). Calculations yielded a large set of conformational families for each peptide studied. The total number of conformations generated for each peptide varied between 60983 and 110063, and the number of those accepted was 5000 for all the cases. In the clustering procedure, an R.M.S.D (Root Mean Square Deviation) of 0.75 Å and a ΔE of 20 kcal mol^{-1} were used. The number of families after clustering varied between 435 and 789. The total number of families accepted with a relative population higher than 0.20 % varied between 37 and 66. Their populations sum up to *ca* 80% of all conformations for each case (see table 2.2)

All low-energy conformers of tetrapeptides studied here were then compared to each other. The comparison involved the spatial arrangements, relative energy and populations. It was found that all the active tetrapeptides **16**-**19** possess similar low-energy conformers. Figure 2.1 shows a spatial view of most populates and energetically preferred conformations of compounds **16** and **17**. These conformations have been overlapped with conformation number 19 obtained for compounds **18** and **19** (tables 2.1S-2.8S in appendix A). The conformers shown in figure 2.1 are very close to one another considering the values of the dihedral angles for their backbones as well as comparing the dihedral angles defining the mutual spatial arrangement of side chains.

It is worth mentioning that the families 19 are not the preferred forms for peptides **18** and **19**, which possess 1.62 and 2.13 kcal mol^{-1} above their respective global minimum, and also they are not the most populated forms. In other words, compounds **18** and **19** can adopt a very similar spatial ordering to those obtained for peptides **16** and **17** but this is not possible without some energetic cost. Figure 2.2 gives a spatial view of the preferred conformations obtained for compounds **16**, **18** and **19**. It is clear that there is not a complete conformational overlapping between these conformers. In this case, a good fit among the two first amino acids (His-Phe in peptides **16** and **18** and His-Tyr in peptide **19**) was obtained, but there is not a good overlapping between the two last amino acids (Arg-Trp for **16** and Lys-Trp in peptides **18** and **19**). Interesting enough, com-

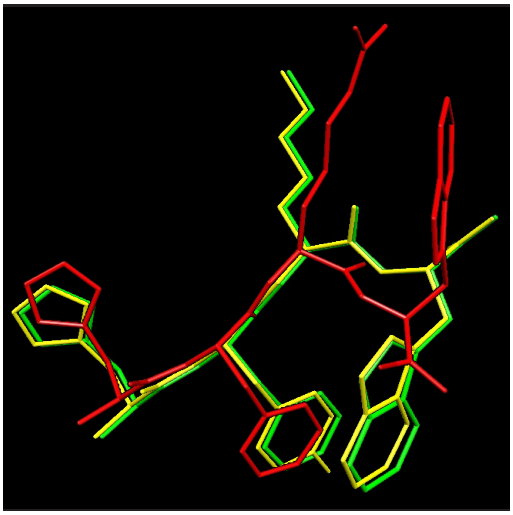

Figure 2.2: Stereoview of overlapping of conformer 1 for peptide **16** (red), conformer 1 for analogue **18** (green) and conformer 2 for analogue **19** (yellow). All hydrogens are omitted for clarity.

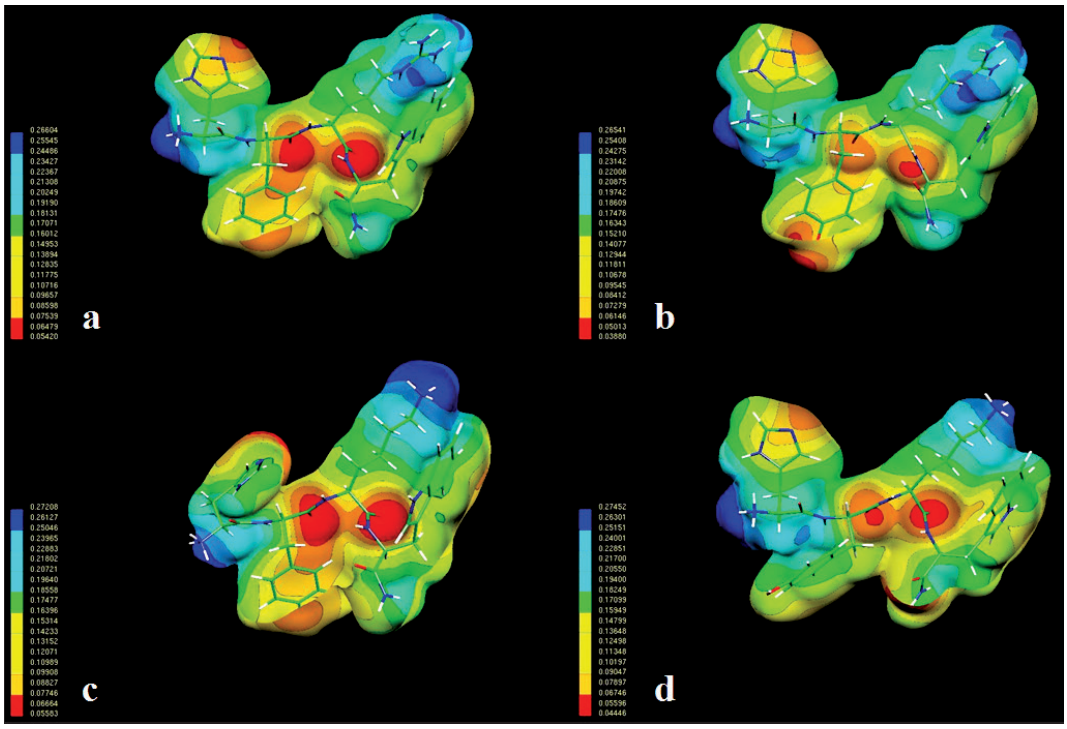

Figure 2.3: Electrostatic potential-encoded electron density surfaces of peptides **16** (**a**), **17** (**b**), **18** (**c**) and **19** (**d**). The surfaces were generated with Gaussian 03 after RHF/6-31G(d) single-point calculations. The coloring represents electrostatic potential with red indicating the strongest attraction to a positive point charge and blue indicating the strongest repulsion.

pounds **18** and **19** displayed half of the antifungal activity in comparison with compounds **16** and **17**. Thus, our results let us speculate that the different antifungal effect could be explained by this conformational difference.

Molecular recognition and the converse concept of specificity (Sarai 1989) are explained in mechanistic and reductionistic terms by a stereo-electronic "complementarity" between the ligand and the receptor (North 1989). In this context it is obvious that the knowledge of the stereo-electronic attributes and properties of His-Phe-Arg-Trp-NH_2 and its analogues will contribute significantly to the elucidation of the mechanism of action at the molecular level or at least, to determine a possible pharmacophoric pattern for these compounds acting as antifungal compounds. The intermolecular forces that contribute to both affinity and specificity can be schematically classified as hydrophobic and electrostatic ones. Therefore, Molecular Electrostatic Potentials (MEPs) are of particular value because they permit the visualization and assessment of the capacity of a molecule to interact electrostatically with a putative binding site (Carrupt et al. 1991; Greeling et al. 1996; Politzer and Truhlar 1981). MEPs can be interpreted in terms of a stereoelectronic pharmacophore condensing all available information on the electrostatic forces underlying affinity and specificity.

Once the low-energy conformations for the most active tetrapeptides reported here were obtained and in an attempt to find the potentially reactive sites for the ligands, we evaluated the electronic aspects of the molecules using MEPs. Figure 2.3 shows the MEPs obtained for compounds **16**-**19**. These results account for the general characteristics of the electronic behavior of active tetrapeptides reported here. The general pattern is similar for all of the active systems. The

MEPs exhibit clear minimum values (deep red zones) in the vicinity of the lone pair of nitrogen atom of His and near the carbonyl groups of the backbone. There are positive regions near the Arg residue (peptides **16** and **17)** or Lys residue (peptides **18** and **19)** and at the amino terminal group. Also three clear hydrophobic zones might be appreciated near the aromatic rings of His, Phe (or Tyr) and Trp.

All the acetylated derivatives tested here were inactive compounds. FIGURE 2.4b shows the spatial view obtained for the preferred conformation of peptide **23**. This conformer displays a very different spatial ordering with respect to the preferred conformation obtained for compound **16** (FIGURE 2.4a). While for active compounds, a partially extended (β-strand) conformation for the backbone is the preferred form, for peptide **23** the preferred form for the backbone is a folded conformation which is stabilized through hydrogen bonds. The interaction shown in FIGURE 2.4b is a bifurcated hydrogen bond between the carbonyl system of the acetyl group and the guanidine group of Arg residue.

This stabilizing interaction might be better appreciated in FIGURE 2.5. The different electronic distributions obtained for the acetylated peptides with respect to those attained for compounds **16**-**19** might be well appreciated com-

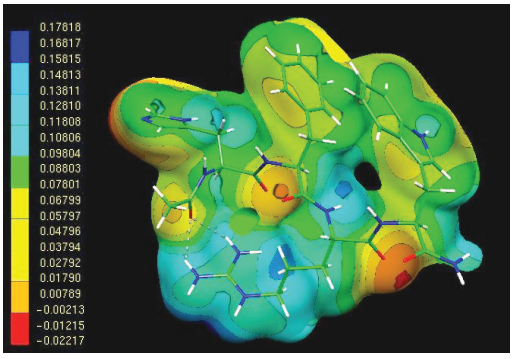

FIGURE 2.5: Electrostatic potential-encoded electron density surface of peptide **23**. The surface was generate with Gaussian 03 after RHF/6-31G(d) single-point calculation. The color-coded is shown at the left.

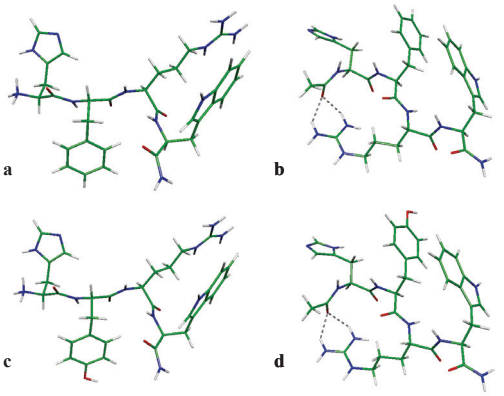

FIGURE 2.4: Spatial view of the preferred conformations obtained for peptides **16** (**a**), **23** (**b**), **17** (**c**) and **24** (**d**) using EDMC calculations. The hydrogen bonds are denoted by dotted lines.

paring FIGURES 2.3 with 2.5. All the acetylated and formylated derivatives (peptides **24**-**28**) displayed a conformational behavior closely related to that obtained for compound **23**. FIGURES 2.4c and d give a comparative spatial view between the preferred conformations of peptide **17** and its acetylated derivative (compound **24)**. On the basis of our results, we can conclude that the lack of antifungal activity of these acetylated peptides could be explained at least in part, by their different conformational and electronic behaviors.

It is worthwhile to compare the biologically active conformation for the backbone of the His-Phe-Arg-Trp-NH_2 proposed in this study to that previously reported for the same sequence from proton NMR studies in aqueous solution (Sugg et al. 1986). Sugg et al. reported that the observed topology was consistent with non hydrogen-bonded β-like structure (φ=139° and ψ=135° for *L*-amino acids) as the predominant solution conformation. This conformation is closely related to those obtained for the different conformers of the active peptides reported here. In FIGURE 2.6 we overlapped the conformation reported by Sugg et al. (in white) with three representative conformations obtained for peptide **16.** In the case of conformer 11 (FIGURE 2.6a) a complete overlap, not only with the backbone but also with the vici-

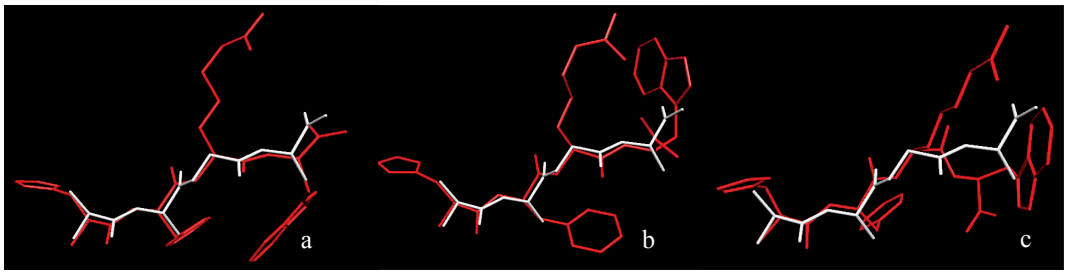

Figure 2.6: Overlapped stereoviews of the backbone conformation from Sugg et al in white and various conformations for compound **16** in red: (**a**) conformer 11, (**b**) conformer 5 and (**c**) conformer 1. All hydrogens are omitted for clarity.

nal side-chains was obtained. For conformers 5 and 1 (figure 2.6b and c) although there is not a complete fit, the resemblance is still apparent.

At this stage of our study, some general trends might be established: (*i*) the smallest fragments with measurable antifungal activity were His-Phe-Arg-Trp-NH_2 and its derivatives **17**-**22**. It has been shown that the minimal sequence possessing α-MSH-like activity is the central tetrapeptide His^6-Phe^7-Arg^8-Trp^9 (Hruby et al. 1987). This "core" sequence was suggested to be the "message" fragment for α-MSH, the rest of the molecule being regarded as the "address" sequence (Otsyka and Inouye 1964).

(*ii*) For the α-MSH activity, the importance of His^6 was demonstrated by the fact that Ac-α-$MSH_{7\text{-}10}$-NH_2 lacked measurable activity. Trp^9 was also critical for biological activity as demonstrated by the lack of biological activity of Ac-α-$MSH_{6\text{-}8}$. Our results suggest that the presence of His and Trp-NH_2 sequence appears to be a structural requirement for the antifungal activity as well. In contrast, our results indicate that Phe and Arg could be replaced.

(*iii*) A. Catania's group suggested that the antimicrobial effects of α-MSH are exerted through a unique mechanism different from that of other natural antimicrobial peptides (Cutuli et al. 2000; Grieco et al. 2003; Grieco et al. 2005). They suggested that the candidacidal effect of α-MSH is linked to the cAMP-inducing activity. Our results may be regarded as an additional support for that hypothesis.

(*iv*) It is interesting that the tetrapeptides **16**-**22**, being the smallest fragment with antifungal activity, contains three aromatic residues. In this regard, aromatic amino acids are common in the active site of many hormones and are often considered critical for biological activity (Sabesan and Harper 1983). Thus, our conformational and electronic study indicates that a predominant β-conformation without internal stabilizing hydrogen bond could be the "biologically relevant conformation" for these compounds.

2.3 Conclusions

We synthesized small-size peptides (tri and tetrapeptides) with different residues and tested their antifungal activity. Among the compounds tested, His-Phe-Arg-Trp-NH_2 and analogues displayed antifungal activities mainly against *Cryptococcus neoformans*. The antifungal activity of these compounds appears to be closely related to the α-MSH effect. These results are in a complete agreement with those previously reported by Grieco et al. against *Candida albicans* (Cutuli et al. 2000; Grieco et al. 2003; Grieco et al. 2005).

A detailed conformational and electronic study supported by theoretical calculations helped us to identify a possible "biologically relevant conformation" and understand the minimal structural requirements for the antifungal actions

of tetrapeptides reported here. Our results are very encouraging in that they show a great potential of His-Phe-Arg-Trp-NH_2 and analogues as a truly novel class of antifungal compounds particularly against the yeast *Cryptococcus neoformans*.

Although it is desirable to develop compounds having a broad spectrum of activity, it is also important to bear in mind that long treatments of fungal infections with the same broad spectrum antifungal agent may lead to a high resistance to the available antifungal agents (Ghannoum and Rice 1999). Thus, one of the strategies for overcoming this problem is the treatment of fungal infections with the appropriate narrow spectrum agent when the ethological agent is known (Didomenico 1999). The selective antifungal activity reported in this paper for peptides **16-22** (and among them for compounds **16** and **17** in particular) opens an interesting field of research, which deals with the discovery and further development of new antifungal peptides useful for treating cryptococcosis, an important life-threatening infection for immuno-compromised hosts.

2.4 Experimental section

2.4.1 Synthetic methods

Solid phase synthesis of the peptides (His-Phe-Arg-Trp-NH_2, His-*D*-Phe-Arg-Trp-NH_2, His-Tyr-Arg-Trp-NH_2, His-Phe-Lys-Trp-NH_2, His-*D*-Phe-Lys-Trp-NH_2, His-Tyr-Lys-Trp-NH_2, His-Phe-*D*-Arg-Trp-NH_2, His-*D*-Phe-*D*-Arg-Trp-NH_2, His-Phe-*D*-Lys-Trp-NH_2, Arg-Pro-Val-NH_2, Lys-Phe-Val-NH_2, Lys-Pro-Val-NH_2, Ac-Arg-Pro-Val-NH_2, Ac-Lys-Phe-Val-NH_2, Ac-Val-Pro-Lys-NH_2, Ac-His-Pro-Val-NH_2, Ac-Lys-Pro-Val-NH_2, Ac-Lys-Gly-Gly-NH_2, Ac-Lys-Gly-Ala-NH_2, Ac-Lys-Ala-Gly-NH_2, Ac-His-Phe-Arg-Trp-NH_2, For-His-Phe-Arg-Trp-NH_2, Ac-Trp-Arg-Phe-His-NH_2, Ac-His-Tyr-Arg-Trp-NH_2, Ac-His-Phe-Lys-Trp-NH_2, Ac-His-Tyr-Lys-Trp-NH_2, Lys-Pro-Val-OH, Arg-Pro-Val-OH, Lys-Phe-Val-OH, Ac-Lys-Pro-Val-OH) were carried out manually on a p-methylbenzhydrylamine resin (1 g MBHA, 0.39 mmol/g) and Merrifield resin (1 g, 1%, 200-400 mesh), respectively with standard methodology using Boc-strategy. Side chain protecting groups were as follows: Arg(Tos), His(Tos), Lys(2Cl-Z), Tyr(2Br-Z). All protected amino acids were coupled in CH_2Cl_2 (5 ml) using DCC (2.5 equiv.) and HOBt (2.5 equiv.) until completion (3 h) judged by Kaiser ninhydrin test. After coupling of the appropriate amino acid, Boc deprotection was effected by use of TFA/CH_2Cl_2 (1:1, 5 ml)) for 5 min first then repeated for 25 min. Following neutralization with 10% TEA/CH_2Cl_2 three times (5-5 ml of each), the synthetic cycle was repeated to assemble the resin-bond protected peptide. The peptides were cleaved from the resin with simultaneous side chain deprotection by acidolysis with anhydrous hydrogen fluoride (5 ml) containing 2% anisole, 8% dimethyl sulfide and indole at 5°C for 45 min. The crude peptides were dissolved in aqueous acetic acid and lyophilized. Preparative and analytical HPLC of the crude and the purified peptides were performed on an LKB Bromma apparatus (for preparative HPLC, column: Lichrosorb RP C18, 7 µm, 250x16 mm; gradient elution: 30-100%, 70 min; mobile phase: 80% acetonitrile, 0.1% TFA; flow rate: 4 ml/min, 220 nm, for analytical HPLC, column: Phenomenex Luna 5C18, 250x4.6 mm; mobile phase: 80% acetonitrile, 0.1% TFA; flow rate: 1.2 ml/min, 220 nm). ESI-MS: Finnigan TSQ 7000 (TABLE 2.3).

2.4.2 Microorganisms and media

For the antifungal evaluation, strains from the American Type Culture Collection (ATCC), Rockville, MD, USA and CEREMIC (C), Centro de Referencia Micológica, Facultad de Ciencias Bioquímicas y Farmacéuticas, Suipacha 531-(2000)-Rosario, Argentina were used: *Candida albicans* ATCC 10231, *Saccharomyces cerevisiae* ATCC 9763, *Cryptococcus neoformans* ATCC 32264, *Aspergillus flavus* ATCC 9170,

Table 2.3: HPLC data of the synthesized peptides

Pep.	Sequence	Retention factor (min)	Gradient elution (%)
1.	His-Phe-Arg-Trp-NH_2	12.912	5-60 (20 min)
2.	His-D-Phe-Arg-Trp-NH_2	6.510	20-50 (15 min)
3.	Lys-Pro-Val-NH_2	9.962	0-25 (15 min)
4.	His-Phe-Lys-Trp-NH_2	8.048	20-50 (15 min)
5.	His-Tyr-Arg-Trp-NH_2	6.523	20-50 (20 min)
6.	Arg-Pro-Val-NH_2	5.552	5-50 (20 min)
7.	Lys-Phe-Val-NH2	10.570	5-50 (20 min)
8.	His-Phe-D-Lys-Trp-NH_2	8.343	10-70 (20 min)
9.	His-D-Phe-D-Arg-Trp-NH_2	9.598	10-70 (20 min)
10.	His-Phe-D-Arg-Trp-NH_2	9.079	10-70 (20 min)
11.	His-Tyr-Lys-Trp-NH_2	9.004	10-70 (20 min)
12.	His-D-Phe-Lys-Trp-NH_2	6.068	20-50 (15 min)
13.	Ac-Lys-Gly-Gly-NH_2	7.434	5-80 (20 min)
14.	For-His-Phe-Arg-Trp-NH_2	12.750	10-45 (15 min)
15.	Ac-Lys-Phe-Val-NH_2	11.878	5-80 (25 min)
16.	Ac-Lys-Gly-Ala-NH_2	5.674	0-30 (10 min)
17.	Ac-Lys-Pro-Val-OH	8.311	10-45 (15 min)
18.	Ac-Lys-Pro-Val-NH_2	8.153	5-25 (10 min)
19.	Ac-His-Tyr-Lys-Trp-NH_2	8.919	15-45 (15 min)
20.	Ac-His-Phe-Lys-Trp-NH_2	12.703	5-80 (25 min)
21.	Ac-His-Pro-Val-NH_2	6.533	10-35 (10 min)
22.	Ac-Val-Pro-Lys-NH_2	8.364	5-35 (10 min)
23.	Ac-Trp-Arg-Phe-His-NH_2	11.770	5-80 (20 min)
24.	Ac-His-Tyr-Arg-Trp-NH_2	7.297	20-50 (10 min)
25.	Ac-His-Phe-Arg-Trp-NH_2	8.785	20-50 (10 min)
26.	Ac-Arg-Pro-Val-NH_2	8.781	5-80 (25 min)
27.	Ac-Lys-Ala-Ala-NH_2	6.235	0-40 (20 min)
28.	Lys-Pro-Val-OH	8.945	0-30 (15 min)
29.	Arg-Pro-Val-OH	9.254	5-20 (15 min)
30.	Lys-Phe-Val-OH	11.109	5-50 (20 min)

Aspergillus fumigatus ATCC 26934, *Aspergillus niger* ATCC 9029 and *Trichophyton mentagrophytes* ATCC 9972, *Trichophyton rubrum* C 113, *Microsporum gypseum* C 115.

Strains were grown on Sabouraud-chloramphenicol agar slants for 48 h at 30 oC, maintained on slopes of Sabouraud-dextrose agar (SDA, Oxoid) and subcultured every 15 days to prevent pleomorphic transformations. Inocula of cell or spore suspensions were obtained according to reported procedures and adjusted to 105 cells/spores with colony forming units (CFU) /mL (Wright et al. 1983).

2.4.3 Antifungal susceptibility testing

Minimal Inhibitory Concentration (MIC) of each compound was determined by using broth microdilution techniques according to the guidelines of the National Committee for Clinical Laboratory Standards for yeasts (M27-A2) (Pfaller 2002a) and for filamentous fungi (M38-A).(Pfaller 2002b) MIC values were determined in RPMI-1640 (Sigma, St Louis, Mo, USA) buffered to pH 7.0 with MOPS. The starting inocula were 1x103 to 5x103 CFU/ml. Microtiter trays were incubated at 35 oC for yeasts and hialohyphomycetes and at 28-30 oC for dermatophyte strains in a moist, dark chamber, and MICs were visually recorded at 48 h for yeasts, and at a time according to the control fungus growth, for the rest of fungi.

For the assay, stock solutions of peptides were two-fold diluted with RPMI 250-1 μg/ml (final volume = 100 μl) and a final DMSO concentration ≤ 1%. A volume of 100 μl of inoculum suspension was added to each well with the exception of the sterility control where sterile water was added to the well instead. MIC was defined as the minimum inhibitory concentration of pure compound which resulted in total inhibition of the fungal growth. Ketoconazole, Terbinafine and Amphotericin B were used as positive controls.

2.4.4 Computational methods

2.4.4.1 EDMC calculations

The conformational space of each peptide was explored using the method previously employed by Liwo et al. that included the Electrostatically Driven Monte Carlo (EDMC) method (Liwo et al. 1996b; Ripoll and Scheraga 1988, 1990). Conformational energy was evaluated using the ECEPP/3 force field (Némethy et al. 1992). This force field employs rigid valence geometry. Hydration energy was evaluated using a hydration-shell model with a solvent sphere radius of 1.4 Å and atomic hydration parameters that have been optimized using nonpeptide data (SRFOPT) (Vila et al. 1991; Williams et al. 1992). In this model in addition to a sum of electrostatic, non-bonding, hydrogen-bond and torsional energy terms, the total conformational energy includes terms accounting for loop closing and peptide solvation. The conformation with minimized

energy was subsequently perturbed by changing its torsional φ and ψ angles using the Monte Carlo method (Li and Scheraga 1987). Piela's algorithm (Piela and Scheraga 1987), which was also applied at this stage, greatly improves the acceptance coefficient. In this algorithm φ and ψ angles are changed in a manner which allows the corresponding peptide group to find the most proper orientation in the electrostatic field of the rest of the peptide chain. The energy of the new conformation is minimized, compared to the previous one and may be accepted or discarded on the basis of energy and/or geometry. If the new energy-minimized conformation is similar in shape and in energy to the starting conformation, it is discarded. Otherwise, the energy of the new conformation is compared to the energy of the parent conformation. If the new energy is lower, the new conformation is accepted unconditionally, otherwise the Metropolis criterion (Metropolis et al. 1953) is applied in order to accept or reject the new conformation. If the new conformation is accepted, it replaces the starting one; otherwise another perturbation of the parent conformation is tried. A temperature jump may be included if the perturbation is not successful for an arbitrarily chosen number of iterations. The process is iterated, until a sufficient number of conformations has been accepted. Sidor et al. has described this procedure in a very detailed fashion (Sidor et al. 1999).

In order to explore the conformational space extensively, we carried out 10 different runs, each of them with a different random number, for each peptide studied. Since the EDMC procedure uses random numbers, there is a need to initialize the random number generator by providing an integer. Therefore, we collected a total of 5000 accepted conformations for each peptide studied. Each EDMC run was terminated after 500 energy-minimized conformations had been accepted. The parameters controlling the runs were the following: a temperature of 298.15 K was used for the simulations. A temperature jump of 50000 K was used; the maximum number of allowed repetitions of the same minimum was 50; the maximum number of electrostatically-predicted conformations per iteration was 400; the maximum number of random-generated conformations per iteration was 100; the fraction of random/electrostically-predicted conformations was 0.30; the maximum number of steps at one increased temperature was 20; and the maximum number of rejected conformations until a temperature jump is executed was 100. Only trans peptide bonds (ω ≈ 180°) were considered.

The ensemble of obtained conformations was then clustered into families using the program ANALYZE (Meadows et al. 1994b; Post et al. 1990; Scheraga et al. 1983), which applies the minimal-tree clustering algorithm for separation, using all heavy atoms, energy threshold of 20 kcal mol^{-1} and R.M.S.D. of 0.75 Å as separation criteria. This procedure allows for substantial reduction of the number of conformations and eliminates repetitions.

2.4.4.2 Molecular electrostatic potentials

The electronic study of the peptides was carried out using Molecular Electrostatic Potentials (MEPs). MEPs have shown to provide reliable information, both on the interaction sites of molecules with point charges and on the comparative reactivities of these sites (Carrupt et al. 1991; Greeling et al. 1996; Politzer and Truhlar 1981). These MEPs were calculated using RHF/6-31G(d) wave function from the Gaussian 03 program (Frisch et al. 2003). EDMC coordinates were imported to generate the wave functions; thus, RHF/6-31G(d) single-point calculations were performed from Gaussian 03 program. All MEPs graphical presentations were created using Molekel (Flükiger et al. 2000). ▪

Acknowledgements

This work is part of the Hungarian-Argentine Intergovernmental S & T Cooperation Programme. This research was supported by grants from Universidad Nacional de San Luis and grants to S.A.Z. and R.D.E. (Agencia de Promoción Científica y Tecnológica de la Argentina PICT R 260) and it is part of the Iberoamerican Project X.7 PIBEAFUN (Search and development of new antifungal part of the Iberoamerican Program of Science and Technology for the Development (CYTED). R.D. Enriz is a member of the CONICET (Argentina) staff. The authors thank É.Menyhárth and I. Nógrádi for the technical assistance of peptide synthesis, as well as for the support of OTKA TS049817 and RET 08/2004 grants.

"Il pleut, c'est malheureux. Il pleut depuis ce matin. Il veut s'emparer de mon être sans paraitre malhonnête. Il pleut dans ces gouttes de pluie mes doutes s'enfuient je ne m'ennuie plus. Il pleut, mais ce n'est pas la pluie qui occupe mes nuits"
(E. Simon)

03

"The opportunist"

oil on paper (320x450 mm)

M.F. Masman 2010

Chapter 3

Structure-antifungal activity relationship of His-Phe-Arg-Trp-Gly-Lys-Pro-Val-NH_2 & analogues

Marcelo F. Masman, Csaba Somlai, Francisco M. Garibotto, Ana M. Rodríguez, Agustina de la Iglesia, Susana A. Zacchino, Botond Penke & Ricardo D. Enriz

Bioorganic and Medicinal Chemistry (2008) 16:4347-4358.

Abstract

The synthesis, *in vitro* evaluation and conformational study of His-Phe-Arg-Trp-Gly-Lys-Pro-Val-NH_2 and analogues acting as antifungal agents are reported. Among them, His-Phe-Lys-Trp-Gly-Arg-Phe-Val-NH_2 exhibited remarkable antifungal activity against *Cryptococcus neoformans*, *Candida albicans* and Candida tropicalis. A conformational and electronic study allows us to propose a biologically relevant conformation for these octapeptides acting as antifungal agents. In addition, these theoretical calculations allow us to determine the minimal structural requirements to produce the antifungal response and can provide a guide for the design of compounds with this biological activity. Antifungal activity of these compounds appears to be closely related to the α-MSH effect.

3.1 Introduction

The prevalence of systemic and dermal fungal infections has significantly increased during the past two decades and remains an important cause of great morbi-mortality of immunocompromised patients (Vicente et al. 2003). In a recent study, McNeil et al. found a dramatic increase in mortality from 1980 to 1997 due to mycoses originated in multiple causes which were mainly associated with *Candida*, *Aspergillus* and *Cryptococcus* spp. Infections (McNeil et al. 2001). Added to these fungal spp., new emerging fungal pathogens appear every year as the cause of morbidity and life-threatening infections in the immunocompromised hosts (Pfaller and Diekema 2007; Walsh et al. 2004).

Although different antifungal agents are available for the treatment of fungal infections, some of them have undesirable side effects, are ineffective against new or re-emerging fungi or develop resistance mainly due to the broad use of antifungal agents (Pfaller and Diekema 2004). As a consequence, there is an urgent need of a next generation of new antifungal agents, which may overcome the above disadvantages.

Natural and synthetic peptides have gained attention as potential new antifungal agents (Epand and Vogel 1999; Maloy and Kari 1995; Tossi et al. 2000; Weinberg et al. 1998). They have shown to inhibit a broad spectrum of pathogens and microorganisms (Bulet and Stöcklin 2005; Hancock et al. 1995; Hancock and Lehrer 1998) and possess the important characteristic that they do not usually induce bacterial or fungal resistance (Hancock 1997). Most of these peptides are believed to exert their antimicrobial activities either forming multimeric pores in the lipid bilayer of the cell membranes (Hancock 1997), or interacting with DNA or RNA after penetration into the cell (Boman et al. 1993; Cabiaux et al. 1994; Park et al. 1998). In contrast, α-melanocyte stimulating hormone (α-MSH) and its *C*-terminal tripeptide Lys-Pro-Val, which showed antimicrobial activity against the two representative pathogens *Staphylococcus aureus* and *Candida albicans* (Cutuli et al. 2000), appear to act through a mechanism substantially different from that of other natural antimicrobial peptides.

Catania et al. have reported the antifungal activity of several peptides (Carotenuto et al. 2007; Cutuli et al. 2000; Grieco et al. 2003; Grieco et al. 2005). They have indicated that the antimicrobial effects of α-MSH are exerted through a unique mechanism different from that of other natural peptides, suggesting that the candidacidal effect of these compounds is linked to the cAMP-inducing activity. As part of our ongoing program aimed at identifying novel antifungal compounds (Kouznetsov et al. 2000; Suvire et al. 2006; Vargas M et al. 2003), we have recently reported the synthesis and antifungal properties of His-Phe-Arg-Trp-NH_2 and structurally related tetrapeptides (Masman et al. 2006). In this paper, we report the synthesis and conformational analysis of His^6-Phe^7-Arg^8-Trp^9-Gly^{10}-Lys^{11}-Pro^{12}-Val^{13}-NH_2 (**1**), which is the 6-13 sequence of α-MSH and structurally related octapeptides with antifungal properties. The aim of our work is to develop more potent antifungal peptides and to understand the conformational features that enhance potency and selectivity and their relation to the amino acid sequence. For this purpose, ten new analogues with single or double replacements within the α-MSH(6-13) sequence were designed, prepared and tested (peptides **2-11** in TABLE 3.1).

For the α-MSH activity, the importance of the presence of His^6 has been previously demonstrated by the fact that Ac-α-MSH_{7-10}-NH_2 lacked measurable activity (Hruby et al. 1987). Trp^9 was also critical for activity as demonstrated by the lack of biological activity of Ac-α-MSH_{6-8}-NH_2 (Hruby et al. 1987). Recently, we reported that the presence of His^6 and Trp^9 residues appears to be a structural requirement for the antifungal activity as well. In contrast, our results indicated that Tyr

and Lys could replace Phe[7] and Arg[8], respectively. It is well known that the receptor binding and transducing properties of melanocortins depend on separate structural and conformational characteristics (Eberle 1988). For example, Phe[7] plays a key role in receptor binding whereas Lys[11] and Pro[12] are more important for receptor stimulation (Eberle 1988). Thus, the positions 7, 8, 11 and 12 were systematically mutated in the series presented here. The resulting peptides were tested against three human pathogenic strains (*C. albicans, C. neoformans* and *C. tropicalis*). In addition, an exhaustive conformational and electronic study on all the peptides reported here was carried out in order to determine a possible biologically relevant conformation for these compounds acting as antifungal agents. To determine the relative importance of some amino acid residues in the α-MSH(6-13) sequence to produce antifungal activity, systematic replacement at the *N*- and *C*- terminus (6-9 and 11-13 sequences) were undertaken. Parallel conformational and electronic study explored the stereoelectronic aspects of this series.

3.2 Results and discussion

The principal goal was to find α-MSH analogues with greater antifungal activity and to reach a better understanding of the peptide structure-antifungal relationship through design, synthesis and testing of novel octapeptide analogues in which several modifications were made. As starting structure, we chose the sequence α-MSH(6-13), His-Phe-Arg-Trp-Gly-Lys-Pro-Val-NH_2, which contains the invariant "core" sequence His-Phe-Arg-Trp (6-9), common to all melanocortin receptors (Hruby et al. 1987), and the sequence Lys-Pro-Val (11-13), which has been reported to be relevant to antimicrobial activity (Cutuli et al. 2000). Previously, we tested the antifungal activity of tetrapeptide His-Phe-Arg-Trp-NH_2 and Lys-Pro-Val-NH_2 against a panel of pathogenic fungi (Masman et al. 2006). Lys-Pro-Val-NH_2 did not show antifungal activity; in contrast, the tetrapeptide His-Phe-Arg-Trp displayed a moderated but significant antifungal effect, in particular against *C. neoformans* (Masman et al. 2006). To better characterize the structure-antifungal activity relationship of octapeptides **1-11** reported here, the present research explored influences of amino acid substitutions on its antifungal activity.

3.2.1 Antifungal activity

To carry out the antifungal evaluation, concentrations of peptides at 100 and 200 μM were incorporated to growth media according with the Experimental Section. Compounds producing no inhibition of fungal growth at 200 μM level were considered inactive.

In a first step of our study, we focused our attention on the *C*-terminal extreme (α-MSH(11-13) sequence), synthesizing and evaluating compounds **1-4**. Our results showed that octapeptide **1** did not inhibit *C. albicans* up to a concentration = 200 μM (table 3.1). This result is in contrast to that of Grieco et al. who reported that peptide **1** possessed a moderate inhibitory activity against *C. albicans* (59.4 %) at 100 μM (Grieco et al. 2005). Peptide **1** did not inhibit *C. tropicalis* either, but showed a low inhibitory effect against *C. neoformans* (24 %) at 200 μM. The replacement of Pro[12] by Phe in peptide **2** produced an enhancement of the antifungal activity against all fungi tested mainly at 200 μM. These results were in agreement with those of Grieco et al. who reported a higher inhibitory effect for peptide **2** in comparison to peptide **1** against *C. albicans* (Grieco et al. 2005). The replacement of Pro[12] of peptide **1** by Tyr in peptide **3** gave a higher enhancement of activity (compare **3** with **2** and **1**) only against *C. neoformans*. We then replaced Lys[11] in **2** by Arg obtaining peptide **4** which displayed an enhancement of the antifungal activity at 200 μM in the three fungi tested.

Table 3.1: Antifungal activity (% inhibition = mean ± SD) of peptides against *Cryptococcus neoformans* ATCC 32264, *Candida albicans* ATCC 10231 and Candida tropicalis C 131 2000.

Pep.	Sequence	*C. neoformans*		*C. albicans*		*C. tropicalis*	
		200 μM	100 μM	200 μM	100 μM	200 μM	100 μM
1	His-Phe-Arg-Trp-Gly-Lys-**Pro**-Val-NH_2	24 ± 5	9 ± 2	0	0	0	0
2	His-Phe-Arg-Trp-Gly-Lys-**Phe**-Val-NH_2	77 ± 30	15 ± 3	61 ± 23	5 ± 2	19 ± 10	9 ± 3
3	His-Phe-Arg-Trp-Gly-Lys-**Tyr**-Val-NH_2	99 ± 1	58 ± 1	43 ± 10	0	21 ± 10	0
4	His-Phe-Arg-Trp-Gly-**Arg**-**Phe**-Val-NH_2	94 ± 6	72 ± 7	80 ± 0.6	1 ± 0.2	64 ± 12	1 ± 3
5	His-Phe-**Lys**-Trp-Gly-Lys-**Phe**-Val-NH_2	97 ± 3	38 ± 6	72 ± 8	0	22 ± 5	0
6	His-Phe-**Lys**-Trp-Gly-**Arg**-**Phe**-Val-NH_2	97 ± 4	98 ± 3	100 ± 0.4	80 ± 1	92 ± 4	58 ± 6
7	His-Phe-**Lys**-Trp-Gly-Lys-**Tyr**-Val-NH_2	83 ± 20	50 ± 6	15 ± 12	0	0	0
8	His-**Tyr**-**Lys**-Trp-Gly-**Arg**-**Phe**-Val-NH_2	89 ± 5	47 ± 4	11 ± 3	0	23 ± 8	0
9	His-**Tyr**-**Lys**-Trp-Gly-Lys-**Tyr**-Val-NH_2	63 ± 15	42 ± 1	0	0	3 ± 3	0
10	His-**Tyr**-**Lys**-Trp-Gly-Lys-**Phe**-Val-NH_2	41 ± 10	25 ± 1	0	0	1 ± 2	0
11	His-**Tyr**-Arg-Trp-Gly-Lys-**Phe**-Val-NH_2	35 ± 10	21 ± 7	10 ± 6	0	1 ± 3	0
Amphotericin B		100	100	100	100	100	100

In a second step of our study, we focused our efforts on the introduction of modifications in the sequence α-MSH(6-9). Replacement of Arg^8 by Lys in **2** and **4** gave peptides **5** and **6,** respectively. This change produced a significant enhancement ($p < 0.01$) of antifungal activity, from 15% (peptide **2**) to 38% (peptide **5**) and from 72% (peptide **4**) to 98% (peptide **6**) of inhibition at 100 μM against *C. neoformans*. The same trend was observed for compounds **5** and **6** when tested against *C. albicans* and *C. tropicalis*. It is interesting to emphasize that peptide **6** was the most active peptide in this series, showing a significant antifungal activity against all the fungi tested, including *C. albicans*. Next, we replace Tyr by Phe^{12} in peptide **5** obtaining peptide **7**. Although peptide **7** displayed a similar activity against *C. neoformans* to that of **5** and **6** at 200 μM, its inhibitory effect against this yeast at 100 μM, as well as its activity against *C. albicans* and *C. tropicalis* was markedly lower. Peptides **8-11** were obtained replacing Phe^7 by Tyr in peptides **6, 7, 5** and **2,** respectively. In general these peptides displayed a lower inhibitory effect with respect to their congeners, in particular peptides **10** and **11**, which displayed only a marginal effect.

In order to better understand the above experimental results, we performed an exhaustive conformational and electronic study of all the peptides reported here using theoretical calculations. These results are presented in the next section and might be useful to perform a structure-activity relationship on this series.

3.2.2 Conformational Study

Linear peptides are highly flexible and therefore, to determine the biologically relevant conformations is not an easy task. It is necessary to perform an exhaustive conformational analysis for these structures to obtain a good perspective about their conformational intricacies. Thus, a conformational study on all peptides reported here was carried out using EDMC calculations (Ripoll and Scheraga 1988, 1990). Theoretical calculations were carried out as described in calculation methods section. These results are summarized in table 3.2 and tables 3.1S-3.11S (shown in appendix A).

Calculations yielded a large set of conformational families for each peptide studied. The total number of conformations generated for each peptide varied between 94082 and 110569, and the number of those accepted was 5000 for all cases. In the clustering procedure, a RMSD (Route Mean Square Deviation) of 0.75 Å and a ΔE of 30 kcal mol^{-1} were used. The number of families after clustering varied between 221 and 366. The total number of families accepted with a relative

population higher of 0.20 % varied between 8 and 20. Their populations summed up to ca 90% of all conformations in each case (see TABLE 3.2).

Our results indicate that these peptides are highly flexible, showing equilibrium of statistical-coil (Vila et al. 2002) structures. All low-energy conformers of octapeptides studied here were then compared to each other. The comparison involved the spatial arrangements, relative energy and populations.

The preferred fully-folded form with 42 % of population (global minimum) obtained for peptide **1** is comparable to the conformation reported by Caratenuto et al. from RMN spectroscopic data (Carotenuto et al. 2007). The torsional angles obtained for the fragment Arg^{8}-Trp^{9}-Gly^{10}-Lys^{11}-Pro^{12} are the following: φ_8= -65 (-67 ± 5), ψ_8= -41 (-41 ± 3); φ_9= -89 (-76 ± 3), ψ_9= -29 (-26 ± 2); φ_{10}= 94 (-84 ± 5), ψ_{10}= 39 (-1 ± 15); φ_{11}= -63 (-67 ± 13), ψ_{11}= -58 (-46 ± 6); φ_{12}= -68, ψ_{12}= -19 (-3 ± 45). The experimental data are given in brackets. As can be observed, there is a very good correlation between the theoretical and experimental dihedral angles for Arg^{8}, Trp^{9}, Lys^{11} and Pro^{12}. Nevertheless, the values obtained for Gly^{10} are quite shifted. Whereas from the theoretical calculations it appears that this residue adopts a bend structure, the experimental results suggest a turn form. However, it must be pointed out that Gly is a very flexible residue as was previously highlighted by Carotenuto et al. and therefore this difference is not unexpected.

It was found that the active octapeptides **2-9** possess low-energy conformers which were similar to each other. They showed mainly two preferred conformations considering the relative energy and population. These were a fully-folded conformation and a partially extended form (see FIGURE 3.1). The fully-folded conformation displayed a turn along 7-10 residues, a bend at residue 11 and the rest of the residues (6, 12 and 13) in a non-stable structure (FIGURE 3.1a). The partially extended conformation showed an extended form encompassing the first three residues, a turn along 9-12 residues and the last residue in a non stable structure (FIGURE 3.1b). In addition, peptides **7**, **8** and **9** displayed an α-helix conformation with a relatively relevant population. In general, the relative populations obtained for the fully-folded and partially extended forms were in equilibrium, giving at least 50 % of the whole population.

TABLE 3.2: Selected conformational search and clustering results for peptides **1-11** optimized at the EDMC/SRFOPT/ECCEP/3 level of theory.

Pep.	Generated[a]				Accepted[b]				# F[c]	# $F_{0.20\%}$[d]	% P[e]
	Elec.	Ran.	Ther.	Total	Elec.	Ran.	Ther.	Total			
1	7051	95871	237	103159	650	4158	192	5000	271	15	92.16
2	6450	88021	181	94652	501	4356	143	5000	254	20	92.86
3	7165	96921	258	104344	552	4246	202	5000	221	8	92.48
4	7277	96253	275	103805	622	4169	209	5000	298	16	91.38
5	6372	87496	214	94082	565	4266	169	5000	252	13	93.06
6	6525	87475	208	94208	468	4378	154	5000	272	14	92.08
7	7437	101014	267	108718	628	4164	208	5000	274	16	92.00
8	7419	100395	317	108131	500	4261	239	5000	305	13	91.52
9	7032	96579	258	103869	553	4284	163	5000	227	12	93.84
10	7547	102709	313	110569	530	4218	252	5000	366	20	88.74
11	6752	92559	227	99538	571	4247	182	5000	283	16	92.60

[a] Number of conformations generated electrostatically, randomly and thermally during the conformational search.
[b] Number of conformations accepted from those generated electrostatically, randomly and thermally during the conformational search.
[c] **#F**: Total number of conformational families as result of the clustering run.
[d] **# $F_{0.20\%}$**: Number of conformational families with populations above 0.20%
[e] **% P**: Sum of the per cent relative population of **# $F_{0.20\%}$**

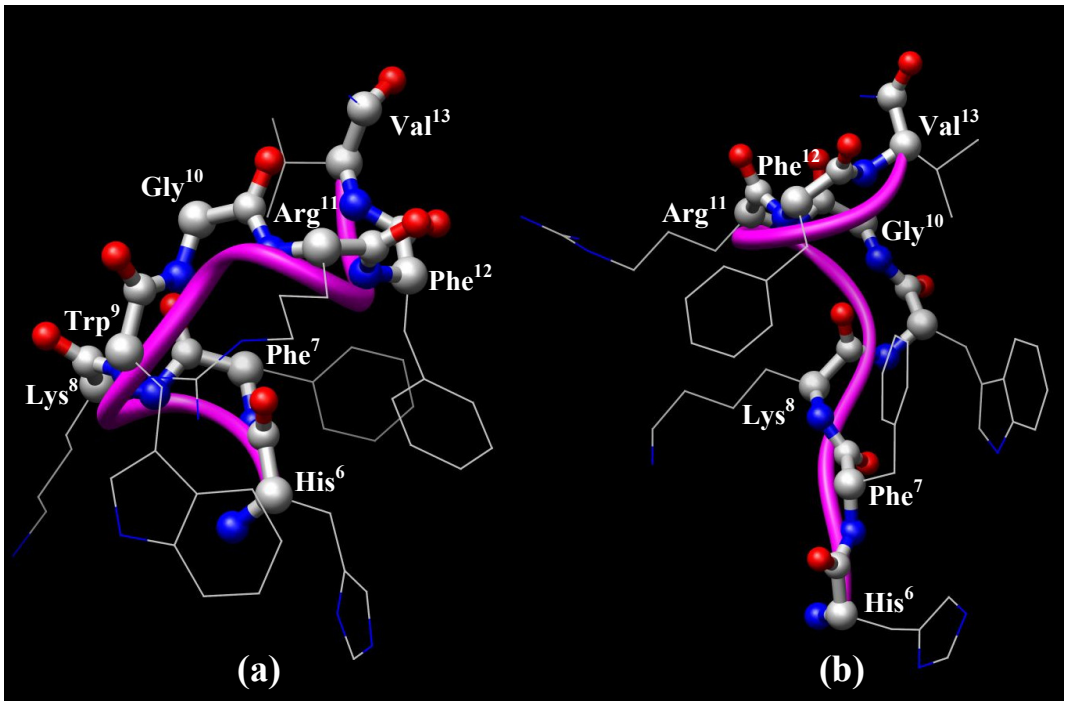

Figure 3.1: Spatial view of the preferred forms obtained for peptide **6**: (**a**) fully-folded conformation and (**b**) partially extended conformation. The backbones are shown as balls and sticks whereas the side chains are shown as wire representations. All hydrogens are omitted for clarity.

It is interesting to note that peptide **5,** which was one of the most active peptides in this series, displayed the partially extended conformation as the highly preferred form with a 65 % of the whole population. In contrast, peptides **1**, **10** and **11,** which were inactive or displayed only marginal activity, did not adopt the partially extended conformation among the preferred forms. These peptides displayed the fully-folded form as the highly preferred conformation, and a mixture between bend and coil conformations, as the second preferred form (see % of population in TABLES 3.1S, 3.10S and 3.11S in APPENDIX A). Thus, our results permit us speculate that the low antifungal activity obtained for peptides **1**, **10** and **11** could be explained at least in part by this conformational difference. Interestingly enough, in the fully-folded conformations, a stabilizing π-stacking interaction between the aromatic residue at 7 position (Phe^{7} or Tyr^{7}) and the other aromatic residue located at 12 position (Phe^{12} or Tyr^{12}) was observed.

Molecular recognition and the converse concept of specificity (Sarai 1989) are explained in mechanistic and reductionistic terms by a stereoelectronic "complementarity" between the ligand and the receptor (North 1989). In this context, it is obvious that the knowledge of the stereoelectronic attributes and properties of octapeptides and its analogues will contribute significantly to the elucidation of a possible pharmacophoric patron for these compounds acting as antifungal compounds. Once the low-energy conformations for the octapeptides reported here were obtained and, in an attempt to find the potentially reactive sites for the ligands, we evaluated the electronic aspects of the molecules under study using Molecular Electrostatic Potentials (MEP) (Politzer and Truhlar 1981).

3.2.3. MOLECULAR ELECTROSTATIC POTENTIALS

MEP are of particular value because they allow the visualization and assessment of the capacity of a molecule to interact electrostatically with a putative binding site (Murray and Politzer

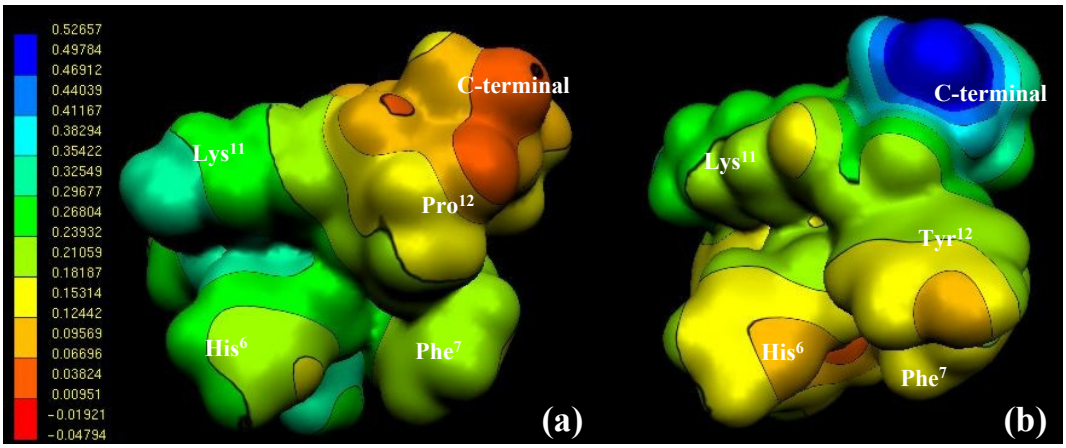

Figure 3.2: Electrostatic potential-encoded electron density surfaces of peptides **1** (**a**) and **3** (**b**). The surfaces were generated with Gaussian 03 using RB3LYP/6-31G(d,p) single point calculations. The coloring represents electrostatic potential with red indicating the strongest attraction to a positive point charge and blue indicating the strongest repulsion. The electrostatic potential is the energy of interaction of the positive point charge with the nuclei and electrons of a molecule. It provides a representative measure of overall molecular charge distribution. The color-coded is shown on the left.

1998; Naray-Szabo and Ferenczy 1995; Politzer and Truhlar 1981). MEP can be interpreted in terms of a stereoelectronic pharmacophore condensing all available information on the electrostatic forces underlying affinity and specificity. Figure 3.2 gives the MEP obtained for compounds **1** and **3**, showing the *C*-terminal portion of these peptides. The different electronic behavior obtained for this moiety of peptide **1** with respect to **3** and the rest of the octapeptides reported here can be appreciated in this figure. Note that the electrostatic potentials near to the *C*-terminal portion of **1** are markedly more negative than those obtained for peptide **3.** Thus, there is not only a different conformational behavior between peptide **1** and the rest of peptides but also a clear different electronic distribution due to the replacement of an aromatic residue (Phe or Tyr) by Pro^{12}. The different conformational and electronic behavior observed for **1** could explain the lack of antifungal effect observed for this peptide. Figure 3.3 gives the MEP obtained for peptides **5, 9** and **10** showing, in this case, a spatial view of the stabilizing π-stacking interaction between the aromatic residues located at positions 7 and 12. The π-stacking interaction between Phe^7 and Phe^{12} in peptide **5** (figure 3.3a) displays both aromatic residues in a parallel orientation and it is located far away in comparison to the similar interaction observed in peptides **9** and **10** (figure 3.3b and c, respectively). It should be noted that the π-stacking interactions involving Tyr residues (either at positions 7 or 12) adopted a perpendicular orientation between the aromatic residues and also displayed a nearby spatial position. These results suggest that π-stacking interactions involving Tyr residues appear to be stronger than those in which only Phe residues participate. The preference for fully-folded structures observed for peptides **3, 7-11** may be, in principle, related to the stronger stabilizing π-stacking interaction present in these structures. It appears that the replacement of Phe^7 or Phe^{12} by Tyr could be the responsible of such difference. It is interesting to note that the most active peptides (**4**, **5** and **6**) possessing preferred partially extended forms, do not have Tyr in their respective sequence.

3.2.4. Structure antifungal activity relationships

In a previous paper we demonstrated that the smallest fragment with measurable antifungal activity was His^6-Phe^7-Arg^8-Trp^9-NH_2 and some of its derivatives (Masman et al. 2006). It has been shown that the minimal sequence possess-

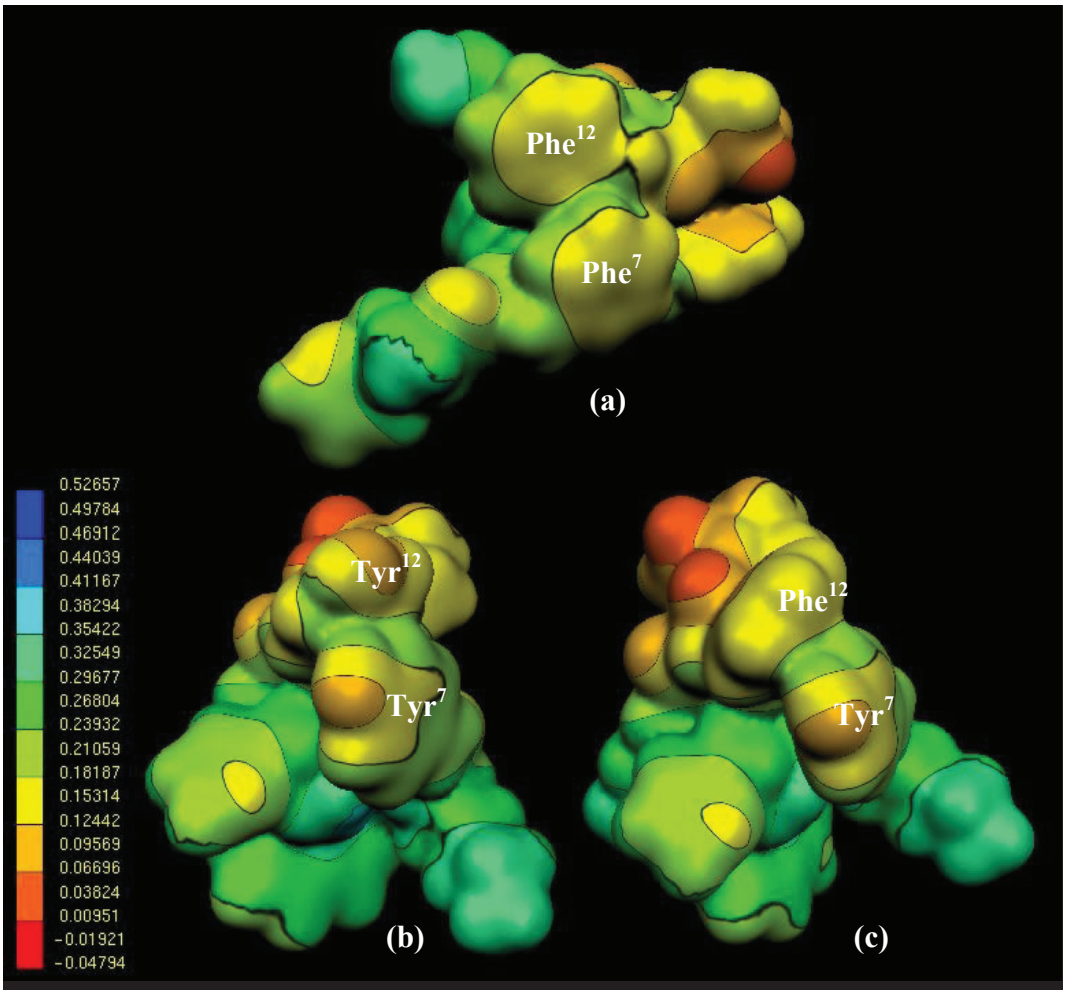

Figure 3.3: Electrostatic potential-encoded electron density surfaces of peptides **5** (**a**), **9** (**b**) and **10** (**c**). The color-coded is shown on the left.

ing α-MSH-like activity is the central tetrapeptide His-Phe-Arg-Trp (Hruby et al. 1987). This "core" sequence was suggested to be the "message" fragment for α-MSH, the rest of the molecule being regarded as the "address" sequence (Otsyka and Inouye 1964).

Keeping in mind that peptides 2-9 can be considered active, whereas peptides 1, 10 and 11 have reduced inhibitory effect, it is noteworthy that the partially extended conformations as preferred forms were only present in active analogues whereas fully-folded conformations were present both in active and inactive peptides. This suggests that the partially extended conformations could be operative in the recognition process between these peptides and their receptor. Figure 3.4 shows a spatial view of the most populated and energetically preferred conformation of peptide 5. This conformation has been overlapped with the partially extended conformations of the rest of the active peptides 2-4 and 6-9. The conformers shown in figure 3.4 are very close to each other considering the values of the dihedral angles obtained for their backbones of the *N*-terminal portion (residues 6-9). From the analysis of figure 3.4, it is clear that there is not a complete conformational overlapping between these conformers. However, all the active peptide adopted

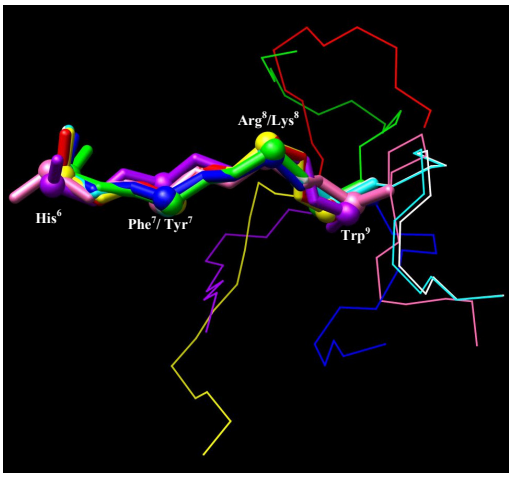

Figure 3.4: Stereoview of the overlapping of peptides 2-9 partially extended conformers. The backbone "core" 6-9 sequence is shown in sticks indicating each alpha carbon with spheres, the rest of the backbone structures are shown in wire representations. Peptide **2** is shown in red, **3** (blue), **4** (white), **5** (pink), **6** (cyan), **7** (yellow), **8** (green) and **9** (purple). All hydrogens and side chains are omitted for clarity.

a very similar spatial ordering for the "core" 6-9 sequence. A good fit among the four first amino acids was obtained, but there was not a good overlapping between the last four amino acids (residues 10-13). Thus, the backbone conformations of *C*-terminal tripeptide for the partially extended forms do not appear to be essential for the general spatial organization of these octapeptides. This situation might be well appreciated in FIGURE 3.4. In contrast, our results indicate that in the fully-folded forms of these peptides, the spatial ordering adopted by the *C*-terminal tripeptide (11-13 sequence) in particular the aromatic amino acid Phe^{12} or Tyr^{12} could play a determinant role for the whole conformation of the octapeptide making a stabilizing π-stacking interaction. These results are in good agreement with our previous ones postulating a partially extended conformation as the biologically relevant form for His-Phe-Arg-Trp-NH_2 and derivatives. Interestingly, the acetylation of the same peptides led to inactive compounds possessing a highly preferred fully-folded conformation (Masman et al. 2006).

Besides, these results agree fairly well with those previously reported by Sugg et al. postulating a partially extended conformation for the His-Phe-Arg-Trp "core" sequence as the biologically active α-MSH conformation (Sugg et al. 1986). Thus, it is worthwhile to compare the "biologically active conformation" proposed in this study for the backbone of the His-Phe-Arg-Trp-NH_2 portion, with that previously reported for the same sequence from proton NMR studies in aqueous solution. Sugg et al. reported that the observed topology was consistent with a non hydrogen-bonded β-like structure (φ = -139° and ψ = 135° for *L*-amino acids) as the predominant conformation in solution (Sugg et al. 1986). This conformation is closely related to those obtained for the "core portion" (6-9 sequence) of the different conformers of the active peptides. In FIGURE 3.5, we overlapped the conformation reported by Sugg et al. (in orange) with the partially extended conformations obtained for all the active peptides.

Grieco et al. suggested that the antimicrobial effects of α-MSH could be exerted through a unique mechanism different from that of other natural antimicrobial peptides (Grieco et al. 2003; Grieco et al. 2005). They suggested that the candi-

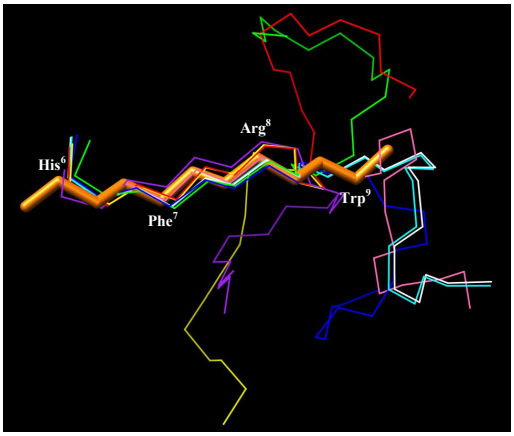

Figure 3.5: Stereoview of the overlapping of the backbone "core" 6-9 sequence conformation determined by Sugg and coworkers (Sugg et al. 1986) in orange sticks, and the partially extended backbone conformers of peptides **2-9** in wire representations. Peptide **2** is shown in red, **3** (blue), **4** (white), **5** (pink), **6** (cyan), **7** (yellow), **8** (green) and **9** (purple). All hydrogens and side chains are omitted for clarity.

dacidal effect of α-MSH is linked to the cAMP-inducing activity. On the basis of our results, it appears that there is some parallelism between the α-MSH and antifungal effects; however, it should be noted that there are interesting differences as well. Previous structure-activity studies on the α-MSH(11-13) sequence disclosed the significance of Pro^{12} to the anti-inflammatory influence of the tripeptide. Indeed, substitution of Pro^{12} with its *D*-isomer abolished the anti-inflammatory effect (Hiltz et al. 1991). Subsequently, researches on *C*-terminally modified analogues of α-MSH confirmed the important role of Pro^{12} for binding and activity at the MC1 receptor (Peng et al. 1997). In contrast, our results indicate that the presence of Pro^{12} is not relevant for the antifungal activity. Replacement of Pro^{12} by Phe or Tyr gives a clear enhancement of inhibitory effect. A striking difference can be observed between the roles of Pro^{12} of these peptides when acting as anti-inflammatory or antifungal compounds. On the other hand, the "core" 6-9 sequence (His-Phe-Arg-Trp) of melanocortins has long been considered essential for melanocortin receptor recognition and activation (Holder and Haskell-Luevano 2004). Alanine replacement studies in B16 melanoma cells showed that when each amino acid in the 6-9 sequence was replaced by alanine there was a substantial decrease in receptor recognition and activation by α-MSH (Sahm 1994). Our results indicate that the "core" 6-9 sequence, or a very similar structure, is also a structural requirement to produce the antifungal activity.

Carotenuto et al. hypothesized that the *N*-terminal portion (7-10) is responsible for receptor activation while the *C*-terminal moiety (10-13) works only enforcing the binding to the receptor through positive interactions with an auxiliary-binding site, for the candidacidal activity (Carotenuto et al. 2007). Our results are in a relatively good agreement with such hypothesis. It is clear that the fully-folded conformations, stabilized by p-stacking interactions, do not show an adequate spatial ordering for the hypothetical receptor possessing two binding sites. On one hand, they cannot reach the adequate distances for both interactions and, on the other hand, the intramolecular interactions could affect the binding of the *N*-terminal portion proposed as the responsible for the receptor activation. A similar explanation could be applied for the inactive acetylated derivatives previously reported (Masman et al. 2006). The fact that His-Phe-Arg-Trp-NH_2 is the smallest fragment with significant antifungal activity could be an additional support to consider the *N*-terminal portion as the responsible for receptor activation. However, caution is required for such speculations in particular because we are hypothesizing on a still unknown receptor. Although the actual existence of melanocortin receptors in yeasts has not been established, our results showing the effects of amino acid substitutions on critical portions, suggest that the presence of such receptors or more probably a structurally related receptor is highly plausible.

3.3 Conclusions

We designed and synthesized eleven α-MSH octapeptide analogues with different residues in the core and in the *C*-terminal sequences and tested their antifungal activity. Among compounds tested, His-Phe-Lys-Trp-Gly-Arg-Phe-Val-NH_2 (**6**) displayed the best antifungal activity against *C. neoformans*, *C. albicans* and *C. tropicalis*. Other octapeptide analogues reported here displayed moderate but still significant antifungal effects against *C. neoformans*.

A detailed conformational and electronic study supported by theoretical calculations helped us to identify a possible "biologically relevant conformation" and also understand the minimal structural requirements for the antifungal actions of octapeptides reported here. Our

results are very encouraging since they show a great potential of His-Phe-Lys-Trp-Gly-Lys-Phe-Val-NH_2 and derivatives as a truly novel class of antifungal compounds particularly against the yeast *C. neoformans*.

The general picture emerging from our results is that there is some parallelism between the recognition process for the α-MSH receptor and the hypothetical receptor involved in the antifungal response. However, in this regard it is interesting to note that there are also structural differences between the respective ligands, suggesting some structural difference between the α-MSH receptor and the putative yeast's receptor.

3.4 Experimental section

3.4.1 Synthetic methods

Solid phase synthesis of the peptides was carried out manually on a *p*-methylbenzhydrylamine resin (1 g MBHA, 0.39 mmol/g) with standard methodology using Boc-strategy. Side chain protecting groups were as follows: Arg(Tos), His(Tos), Lys(2Cl-Z), Tyr(2Br-Z). All protected amino acids were coupled in CH_2Cl_2 (5 ml) using DCC (2.5 equiv.) and HOBt (2.5 equiv.) until completion (3 h) judged by Kaiser ninhydrin test (Kaiser et al. 1970). After coupling of the appropriate amino acid, Boc-deprotection was effected by using of TFA/CH_2Cl_2 (1:1, 5 ml)) for 5 min first then repeated for 25 min. Following neutralization with 10% TEA/CH_2Cl_2 three times (5-5 ml of each), the synthetic cycle was repeated to assemble the resin-bond protected peptide. The peptides were cleaved from the resin with simultaneous side chain deprotection by acidolysis with anhydrous hydrogen fluoride (5 ml) containing 2% anisole, 8% dimethyl sulfide and indole at 5°C for 45 min. The crude peptides were dissolved in aqueous acetic acid and lyophilized. Preparative and analytical HPLC of the crude and the purified peptides were performed on an LKB Bromma apparatus (for preparative HPLC, column: Lichrosorb RP C18, 7 µm, 250x16 mm; gradient elution: 30-100%, 70 min; mobile phase: 80% acetonitrile, 0.1% TFA; flow rate: 4 ml/min, 220 nm, for analytical HPLC, column: Phenomenex Luna 5C18(2), 250x4.6 mm; mobile phase: 80% acetonitrile, 0.1% TFA; flow rate: 1.2 ml/min, 220 nm). ESI-MS: Finnigan TSQ 7000 (Table 3.3).

3.4.2 Microorganisms and media

Candida spp. *and Cryptococcus* sp. from the American Type Culture Collection (ATCC, Rockville, MD, USA) were used. The panel included *Candida albicans* 10231, *Candida tropicalis* C 131 and *Cryptococcus neoformans* ATCC 32264. Strains were grown on Sabouraud-chloramphenicol agar slants for 24 h at 35 °C, maintained on slopes of Sabouraud-dextrose agar (SDA, Oxoid). Inocula of cell suspensions were obtained according to reported procedures and adjusted to 1-5 x10^3 cells with colony forming units (CFU) /mL (Pfaller 2002a).

3.4.3 Antifungal evaluation

The test was performed in 96 wells-microplates. Peptide test wells (PTW) were prepared with stock solutions of each peptide in DMSO (maximum concentration ≤2%), diluted with RPMI-1640 to final concentrations 200 and 100 µM. Inoculum suspension (100 µl) was added to each well (final volume in the well = 200 µL). A growth control well (GCW) (containing medium, inoculum, the same amount of DMSO used in PTW, but compound-free) and a sterility control well (SCW) (sample, medium and sterile water instead of inoculum) were included for each strain tested. Microtiter trays were incubated in a moist, dark chamber at 35 °C, 24 or 48 h for *Candida* spp. or *Cryptococcus* sp., respectively. Microplates were read in a VERSA Max microplate reader (Molecular Devices, Sunnyvale, CA, USA). Amphotericin B (Sigma Chemical Co, St

Louis, MO, USA) was used as positive control (100 % inhibition). Tests were performed by duplicate. Reduction of growth for each peptide concentration was calculated as follows: % of inhibition: 100- (OD_{405} PTW- OD_{405} SCW) / OD_{405} GCW - OD_{405} SCW.

3.4.4 Statistical analysis

Data were statistical analyzed by both, one-way analysis of variance and Student's test. A $p< 0.05$ was considered significant.

3.4.5 Computational methods

3.4.5.1 EDMC calculations

The conformational space of each peptide was explored using the method previously employed by Liwo *et al.* (Liwo et al. 1996b) that included the Electrostatically Driven Monte Carlo (EDMC) method (Ripoll and Scheraga 1988, 1990). The conformational energy was evaluated using the ECEPP/3 force field (Némethy et al. 1992). This force field employs rigid valence geometry. The hydration energy was evaluated using a hydration-shell model with a solvent sphere radius of 1.4 Å and atomic hydration parameters that have been optimized using nonpeptide data (SRFOPT) (Vila et al. 1991; Williams et al. 1992). In this model in addition to a sum of electrostatic, non-bonding, hydrogen-bond and torsional energy terms, the total conformational energy includes terms accounting for loop closing and peptide solvation. The conformation with minimized energy was subsequently perturbed by changing its torsional φ and ψ angles using the Monte Carlo method (Li and Scheraga 1987). Piela's algorithm (Piela and Scheraga 1987), which was also applied at this stage, greatly improves the acceptance coefficient. In this algorithm φ and ψ angles are changed in a manner which allows the corresponding peptide group to find the most proper orientation in the electrostatic field of the rest of the peptide chain. The energy of the new conformation is minimized, compared to the previous one and can be accepted or discarded on the basis of energy and/or geometry. If the new energy-minimized conformation is similar in shape and in energy to the starting conformation, it is discarded. Otherwise, the energy of the new conformation is compared with the energy of the parent conformation. If the new energy is lower, the new conformation is accepted unconditionally, otherwise the Metropolis criterion (Metropolis et al. 1953) is applied in order to accept or reject the new conformation. If the new conformation is accepted, it replaces the starting one; otherwise another perturbation of the parent conformation is tried. A temperature jump may be included if the perturbation is not successful for an arbitrarily chosen number of iterations. The process is iterated, until a sufficient number of conformations have been accepted. Sidor et al. give a more detailed description of this procedure (Sidor et al. 1999).

In order to do an extensive exploration of the conformational space, we have been carried out 10 different runs, each of them with a different random number, for each peptide studied. Since the EDMC procedure uses random numbers, there is a need to initialize the random number generator by providing an integer. Therefore, we collected a total of 5000 accepted conformation for each peptide studied. Each EDMC run was terminated after 500 energy-minimized conformations had been accepted. The parameters controlling the runs were the following: a temperature of 298.15 K had been used for the simulations. A temperature jump of 50000 K had been used; the maximum number of allowed repetitions of the same minimum was 50; the maximum number of electrostatically-predicted conformations per iteration was 400; the maximum number of random-generated conformations per iteration was 100; the fraction of random/electrostically-predicted conformations was 0.30; the maximum number of steps at one increased temperature was 20; and the maximum number of rejected conformations until a temperature jump is executed was 100. Only trans peptide bonds ($\omega \approx 180°$) had been considered.

The ensemble of obtained conforma-

tions was then clustered into families using the program ANALYZE (Meadows et al. 1994b; Post et al. 1990; Scheraga et al. 1983), which applies the minimal-tree clustering algorithm for separation, using backbone atoms, energy threshold of 30 kcal mol^{-1} and R.M.S.D. of 0.75 Å as separation criteria. This procedure allows for substantial reduction of the number of conformations and eliminates repetitions.

3.4.5.2 Molecular electrostatic potentials and molecular interaction calculations

Quantum mechanics calculations were carried out using the Gaussian 03 program (Frisch et al. 2003). We use low-energy conformations of peptide **1-11** obtained from EDMC calculations. Subsequently, single point DFT (RB3LYP/6-31G(d,p)) calculations were carried out. The electronic study was carried out using molecular electrostatic potentials (MEP) (Politzer and Truhlar 1981). These MEP were calculated using RB3LYP/6-31G(d,p) wave functions and MEP graphical presentations were created using the MOLEKEL program (Flükiger et al. 2000).

Molecular graphics images were produced using the UCSF Chimera package from the Resource for Biocomputing, Visualization, and Informatics at the University of California, San Francisco (supported by NIH P41 RR-01081) (Pettersen et al. 2004b). ▪

Acknowledgements

This work is part of the Hungarian-Argentine Intergovernmental S&T Cooperation Programme and was supported by the Research and Technological Innovation Foundation as well as by grants from Universidad Nacional de San Luis and grants to S.A.Z. and R.D.E. from the Agencia de Promoción Científica y Tecnológica de la Argentina (ANPCyT) PICT R 260. It is part of the Iberoamerican Program of Science and Technology for the Development (CYTED, Network RIBIOFAR). F.M.G. is a fellow of ANPCyT, PICT R 260. R.D.E. is member of the CONICET (Argentina) staff. M.F.M is a fellow of CONICET (Argentina).

"I pack my suit in a bag. I'm all dressed up for Prague.
I'm all dressed up with you, all dressed up for him too...
Prepare myself for a war, before I even open up my door, before I even look out, I'm pissing all of my bullets about..."
(D. Rice)

04

"Infectious"

oil on paper (320x450 mm)

M.F. Masman 2010

Chapter 4

C4

Penetratin & derivatives acting as antifungal agents

Marcelo F. Masman, Ana M. Rodríguez, Marcela Raimondi, Susana A. Zacchino, Paul G. M. Luiten, Csaba Somlai, Tamas Kortvelyesi, Botond Penke & Ricardo D. Enriz

European Journal of Medicinal Chemistry (2009) 44:212-228.

Abstract

The synthesis, *in vitro* evaluation, and conformational study of RQIKIWFQNRRMKWKK-NH_2 (penetratin) and related derivatives acting as antifungal agents are reported. Penetratin and some of its derivatives displayed antifungal activity against the human opportunistic pathogenic standardized ATCC strains *Candida albicans* and *Cryptococcus neoformans* as well as clinical isolates of *C. neoformans*. Among the compounds tested, penetratin, along with the nonapeptide RKWRRKWKK-NH_2 and the tetrapeptide RQKK-NH_2 exhibited significant antifungal activities against the *Cryptococcus* sp. A comprehensive conformational analysis on the peptides reported here using three different approaches, Molecular Mechanics, Simulated Annealing and Molecular Dynamics simulations, was carried out. The experimental and theoretical results allow us to identify a topographical template which may provide a guide for the design of new compounds with antifungal characteristics against *C. neoformans*.

4.1 Introduction

Fungal infections are a persistent major health problem which especially affects and threatens immunocompromised patients (Georgopapadakou and Tkacz 1995; McNeil et al. 2001; Pfaller and Diekema 2007; Walsh et al. 2004). Invasive fungal infections as well as dermatomycoses produced by fungal organisms with even low virulence can be life-threatening (Nagiec et al. 1997) for individuals with increased vulnerability such as neonates, cancer patients receiving chemoteraphy, organ transplant patients, and burns patients, apart from those with acquired immunodeficiency syndrome (AIDS). Other risk factors include corticosteroid and antibiotic treatments, diabetes, lesions of epidermis and dermis, malnutrition, neutropenia and surgery (Georgopapadakou and Tkacz 1995). Many fungal infections are caused by opportunistic pathogens that may be endogenous or acquired from the environment (*Candida, Cryptococcus, Aspergillus* infections). Patients with significant immunosuppresion frequently develop *Candida* esophaguitis. *Cryptococcosis*, caused by the encapsulated yeast *Cryptococcus neoformans*, has been the cause of fungal mortality among HIV-infected patients. This organism has a predilection for the central nervous system and leads to severe, life-threatening meningitis. In addition, an increasing number of normal individuals, including children in third-world nations (Ablordeppey et al. 1999; Freixa et al. 1998) that suffer deficient sanitation and education, are prone to fungal infections, specially those involving the skin and mucosal surfaces.

Although it appears that many drugs are available for the treatment of systemic and superficial mycoses, there are in fact only a limited number of effective antifungal drugs (Walsh et al. 2004). Many of the antifungal compounds currently available have undesirable effects or are very toxic (amphotericin B); are fungistatic and not fungicidal (azoles), or lead to the development of resistance, as with 5-fluorocytosine (White et al. 1998). Amphotericin B, developed in the 1950's, still remains a widely used antifungal drug, most recently gaining renewed applications through lipid based formulations. According to Polak ideal drugs to cure fungal infections have not been discovered yet (Polak 1999). In the meantime, resistance to currently available antifungal agents continues to grow (Bartroli et al. 1998a). Although combination therapy has emerged as a good alternative to bypass these disadvantages (Bartroli et al. 1998a, b; Polak 1999), there is an urgent need for a next generation of safer and more potent antifungal agents (Bartroli et al. 1998b; Walsh et al. 2004). These explorations have resulted in the identification of novel molecules, which could prove promising for further future development. Among them, some natural peptides were recently described as antifungal compounds, inhibiting a broad spectrum of fungi (Bulet and Stöcklin 2005; Hancock et al. 1995; Hancock and Lehrer 1998; Lee et al. 2003; Masman et al. 2006). It has also been reported that a group of cationic antimicrobial peptides are major players in the innate immune response (Boman et al. 1993; Ganz and Lehrer 1995; Zasloff 1992). These peptides are very ancient elements of the immune response of all species of animal and plant life, and the induction pathways for these compounds in vertebrates, insects and plants (Boman et al. 1993; Ganz and Lehrer 1995; Hoffmann et al. 1999; Zasloff 1992) are highly conserved. Furthermore, it is becoming increasingly clear that cationic antimicrobial peptides play many potential roles in inflammatory responses, which represent an orchestration of the mechanisms of innate immunity.

Small cationic peptides are abundant in nature and have been described as "nature´s antibiotics" or "cationic antimicrobial peptides" (Hancock 1997; Hancock and Patrzykat 2002). These peptides are 12-50 amino acids long with a net positive charge of +2 or +9, which is due to

an excess of basic arginine and lysine residues, and approximately 50% hydrophobic amino acids (Hancock 1997). These molecules are also folded in three dimensions so that they have both a hydrophobic face comprising non-polar amino acid side-chains, and a hydrophilic face of polar and positively charged residues: these molecules are amphipatic. Despite these two similarities these compounds vary considerably in length, amino acid sequence, and secondary structure. The different spatial orderings include small β-sheets stabilized by disulphide bridges, amphipathic α-helices and, less commonly, extended and loop structures.

Cell-penetrating peptides (CPPs) are defined as peptides with a maximum of 30 amino acids, which are able to enter cells in a seemingly energy-independent manner, thus being able to translocate across membranes in a non-endocytotic fashion (Langel 2002). In 1991 Joliot et al. reported that the 60 amino acid homeodomain of the Antennapedia protein of *Drosophila* was able to translocate over cell membranes (Joliot et al. 1991). In order to understand the driving force for the internalization, the homeodomain was modified by site-directed mutagenesis leading to the discovery that its third helix was necessary and also sufficient for membrane translocation, which resulted in the development of a 16 amino acid-long CPP called penetratin (**1**) (Derossi et al. 1994). Thus, peptide **1**, a synthetic 16-amino acid peptide from the third helix of Antennapedia homeodomain (Derossi et al. 1996; Derossi et al. 1994; Fischer et al. 2000) is a cationic amphipatic peptide which might penetrate cell membranes *via* a proposed "inverted micelle" pathway. However, the mechanism of membrane translocation is not well known. The question is whether the peptide is internalized *via* endocytosis which is energy-dependent or *via* direct transport. While the latter mechanism is scarcely known at present, it is believed that the process is non-receptor-mediated (Derossi et al. 1996; Drin et al. 2001). In addition, we have previously provided evidence on the energy-dependent and lipid raft-mediated endocytic uptake of penetratin (Letoha et al. 2005). Peptide **1** has been proposed as a universal intracellular delivery vehicle (Dupont et al. 2002). Since **1** possesses 16 amino acids and a charge of +8, it might be included in the general classification of "cationic antimicrobial peptide". To the best of our knowledge this is the first study reporting the antifungal activity of **1** and structurally related derivatives.

The aim of the present investigation is exploring the antifungal potential of **1** and its derivatives against *Candida albicans* and *Cryptococcus neoformans*. To better characterize the structure-antifungal activity relationship of peptide **1** and related compounds under study the present analysis explored influences of amino acid substitutions and deletions on its antifungal activity. In addition, an extensive conformational analysis of **1** and its derivatives was carried out using three different approaches: molecular mechanics, simulated annealing (SA) and molecular dynamics (MD) simulations. The ability of each method to obtain the different conformations is tested and compared. Conformational and electronic studies were carried out in order to identify a topographical and/or a sub-structural template, which may be the starting structure for the design of new antifungal compounds.

4.2 Results and discussion

4.2.1 Antifungal activity

To evaluate the antifungal potential, concentrations of peptides up to 200 μM were incorporated in the growth media according to previously reported procedures (Masman et al. 2006; Sortino et al. 2007; Zacchino et al. 2003). Compounds producing no inhibition of fungal growth at 200 μM were considered inactive. TABLE 4.1 gives the antifungal activity obtained

Peptide	Sequence	*Candida albicans*					*Cryptococcus neoformans*				
		% inhib. 200 µM	% inhib. 100 µM	% inhib. 50 µM	% inhib. 25 µM	% inhib. 12,5 µM	% inhib. 200 µM	% inhib. 100 µM	% inhib. 50 µM	% inhib. 25 µM	% inhib. 12,5 µM
1	RQIKIWFQNRRMKWKK-NH_2	**100** ± 0.2	**100** ± 0.6	**95** ± 1.2	**91** ± 1.6	4 ± 0.1	**100** ± 0.1	**100** ± 0	**100** ± 0	**100** ± 0.2	**90** ± 2.3
2	WKQKNIKWRFRQKMIR-NH_2	60 ± 4.2	52 ± 3.0	0	0	0	**96** ± 2.7	**92** ± 5.7	36 ± 3.4	28 ± 2.9	0
3	RKWRRKWKK-NH_2	**100** ± 0.08	**76** ± 0.97	58 ± 0.71	40 ± 1.75	15 ± 1.0	**99** ± 1.68	**68** ± 21.22	14 ± 1.32	16 ± 1.78	0
4	RKFRRKFKK-NH_2	**61** ± 1.16	44 ± 7.00	33 ± 7.42	23 ± 3.79	0	**73** ± 1.51	11 ± 3.92	13 ± 2.32	9 ± 3.80	0
5	RKRRKWKK-NH_2	29 ± 1.05	13 ± 0.55	0	0	0	**100** ± 0.36	33 ± 4.79	11 ± 4.35	6 ± 2.14	0
6	RKRRKKK-NH_2	43 ± 4.96	12 ± 0.4	0	0	0	60 ± 2.94	14 ± 2.09	19 ± 6.73	10 ± 2.89	0
7	KWKK-NH_2	9 ± 2.3	2 ± 1.0	0	0	0	0	0	0	0	0
8	RQKK-NH_2	6 ± 1.2	0	0	0	0	**100** ± 1.2	**100** ± 4.0	**92** ± 3.6	**62** ± 7.4	32 ± 2.3
Amphotericin B		100	100	100	100	100	100	100	100	100	100
Ketoconazole		100	100	100	100	100	100	100	100	100	100

Table 4.1: Antifungal activity (% inhibition) of peptides against *Candida albicans* ATCC 10231 and *Cryptococcus neoformans* ATCC 32264

for peptide **1** against *C. albicans* and *C. neoformans*. Peptide **1** displayed a significant antifungal activity against both fungi being *C. neoformans* the more sensitive sp. It is interesting to note that **1** displayed a significant degree of inhibition against *C. neoformans* even at low concentrations (90 % of inhibition was observed at 12.5 µM and 100% at 25 µM). The inhibitory effect observed against *C. albicans* was slightly lower than that obtained for *C. neoformans* at 12.5 µM but similar at 25-200 µM.

In order to gain insight into the spectrum of activity, peptide **1** was tested against a panel of clinical isolates of *C. neoformans*. The minimum inhibitory concentration (MIC) values of **1** were determined against this new panel by using three endpoints: MIC_{100}, MIC_{80} and MIC_{50} (the minimum concentration of compounds that inhibit 100, 80 and 50 % of growth, respectively). The application of a less stringent end point such as MIC_{80} and MIC_{50} has been shown to consistently represent the *in vitro* activity of compounds and many times provide a better correlation with other measurements of antifungal activity such as the minimum fungicide concentration (MFC) (Ernst et al. 2002; Klepser et al. 1998). In addition to MIC determinations, the evaluation of MFC of **1** against this panel was accomplished by subculturing a sample of media from MIC tubes showing no growth, onto drug-free agar plates. So, peptide **1** was tested against ten clinical isolates of *C. neoformans,* all provided by the Malbrán Institute (Buenos Aires). These results are shown in table 4.2 and the activity was similar to, or lower than, those obtained against the standard strain (ATCC 32264).

Peptide **2** possesses the same amino acids of peptide **1** but located in a completely different sequence. In fact, the sequence of this peptide was randomly generated. This peptide showed no antifungal activity against both fungi tested at 12.5 µM but inhibit 96% and 60 % of the growth of *C. neoformans* and of *C. albicans* at 200 µM, re-

Table 4.2: Minimum inhibitory concentrations (MIC100, MIC80 and MIC50) and minimum fungicidal concentration (MFC) of penetratin (**1**) against clinical isolates of *C. neoformans*.

Voucher specimen	MIC_{100}	MIC_{80}	MIC_{50}	MFC	Amph. B MIC_{100}	Itz. MIC_{100}
IM 983040	31.2	31.2	31.2	31.2	0.13	<0.015
IM 972724	62.5	62.5	31.2	62.5	0.06	0.25
IM 042074	62.5	62.5	31.2	62.5	0.25	<0.015
IM 983036	62.5	62.5	31.2	62.5	0.13	<0.015
IM 00319	62.5	62.5	31.2	62.5	0.25	<0.015
IM 972751	62.5	31.2	31.2	62.5	0.25	<0.015
IM 031631	62.5	31.2	16	62.5	0.13	0.25
IM 031706	125	31.2	16	125	0.25	0.50
IM 961951	125	31.2	16	125	0.06	<0.015
IM 052470	125	31.2	31.2	125	0.50	<0.015

MIC_{100}, MIC_{80} and MIC_{50}: concentration of a compound that caused 100, 80 or 50% reduction of the growth control, respectively. Within Voucher specimen: IM =Malbran Institute (Buenos Aires, Argentina).Amph. B = Amphotericin B; Itz. = Itraconazole

spectively. It is clear that the antifungal activity of **1** and **2** are markedly different; whereas **1** showed a significant antifungal activity against both *C. albicans* and *C. neoformans*; peptide **2** was practically inactive. On the basis of these results it can be concluded that the sequence as well as the different spatial orderings of the cationic, polar and hydrophobic residues are important determinants for the antifungal activity. In contrast, the positive charge (+8) of **1** appears to be a necessary requirement but not by itself sufficient to produce the antifungal response.

To study the structure-antifungal activity relationship on these peptides, the effects of structural changes in the sequence of peptide **1** were considered. Our principal goal was to synthesize shorter derivatives of **1** trying to maintain the antifungal activity as much as possible. In a first step we synthesized compound **3**, a nonapeptide possessing the last four amino acids of **1**. In this peptide we maintain the same numbers of cationic amino acids (Arg and Lys) deleting Gln^2, Ile^3, Ile^5, Phe^7, Gln^8, Asn^9 and Asn^{12}. Peptide **3** displayed a lower antifungal activity with respect to **1**. The antifungal activity against *C. neoformans* and *C. albicans* was moderately effective but still significant. We decided to perform changes on peptide **3** and then we synthesized peptides **4-6**. In peptide **4** we replaced the two Trp residues of peptide **3** (Trp^3 and Trp^7) by Phe. This structural change yielded a reduction of antifungal activity (compare the % of inhibition of **3** and **4** in TABLE 4.1) which is not an unexpected result; a role for Trp as translocation determinant of peptides has been proposed (Schiffer et al. 1992) and mutation of both tryptophans in peptide **1** was found to abolish internalization (Derossi et al. 1994). In addition, it has previously been reported that tryptophans are poorly replaceable by phenylalanine in **1** and derivatives when tested for their penetrating properties (Letoha et al. 2003). Our results lend support to previously reported findings, but in addition demonstrate the antifungal activity of these peptides. Octapeptide **5** was obtained deleting Trp^3 from peptide **3**; in turn heptapeptide **6** was obtained deleting Trp^3 and Trp^7 from peptide **3**. Whereas octapeptide **5** displayed only a marginal antifungal activity, peptide **6** was practically ineffective in comparison to their congeners.

In order to further understand the above experimental results, we performed a conformational study of the peptides reported here using different approaches.

4.2.2 Conformational study of peptide 1 and derivatives

A large number of studies have been performed in order to shed light on the structural aspects and mechanism of action for translocation of **1**. However, compared to these mechanistic properties, the conformational intricacies of this compound have received relatively little attention. It is however obvious that a better understanding of the conformational behavior of peptide **1** is of paramount importance. Linear peptides are highly flexible and therefore to determine the biologically relevant conformations is a matter of high complexity, which requires an exhaustive conformational analysis of these structures. Consequently, we carried out calculations using three different approaches: electrostatically driven Monte Carlo (EDMC) calculations implemented in the ECCEPAK (Ripoll and Scheraga 1988, 1990) package, SA calculations using the Tinker Molecular Modelling package (Ponder 2004) and MD simulations from the GROMACS program (Lindahl et al. 2001; Van Der Spoel et al. 2005).

Table 4.3: Selected conformational search and clustering results for peptides **1-8** optimized at the EDMC/SRFOPT/ECCEP/3 level of theory.

Pep	Generated[a]				Accepted[b]				#F[c]	#F$_{0.20\%}$[d]	%P[e]
	Elec	Rand	Ther	Total	Elec	Rand	Ther	Total			
1	8973	119535	575	129083	1431	3245	324	5000	639	11	82.92
2	9200	120229	493	129922	1349	3373	278	5000	703	19	81.92
3	8050	107710	304	116064	1372	3412	216	5000	270	6	88.94
4	7490	102380	245	110115	1121	3697	182	5000	288	11	88.72
5	7905	106150	294	114349	1176	3606	218	5000	242	11	89.76
6	7191	98483	213	105887	1192	3635	173	5000	137	6	91.02
7	3007	44352	32	47391	508	4466	26	5000	505	74	82.82
8	3939	54133	54	58126	579	4379	42	5000	481	45	83.34

[a] Number of conformations generated electrostatically, randomly and thermally during the conformational search.
[b] Number of conformations accepted from those generated electrostatically, randomly and thermally during the conformational search.
[c] **#F**: Total number of conformational families as result of the clustering run.
[d] **# F$_{0.20\%}$**: Number of conformational families with populations above 0.20%
[e] **% P**: Sum of the per cent relative population of **# F$_{0.20\%}$**

4.2.2.1 EDMC results

EDMC results are summarized in table 4.3 and figure 4.1 and more details are given in tables 4.1S-4.8S in appendix A as supporting information. Calculations yielded a large set of conformational families for each peptide studied. The total number of conformations generated for each peptide varied between 47391 and 129922, and the number of those accepted was 5000 for all the cases. In the clustering procedure, a RMSD (root mean square deviation) of 0.75 Å and a cutoff of 30 kcal mol^{-1} were used. The number of families after clustering varied between 137 and 1001. The total number of families accepted with a relative population higher of 0.20 % varied between 11 and 86. Their populations sum up to ca 80% of all conformations in each case (see table 4.3)

All low-energy conformers of the peptides studied here were then compared to each other. The comparison involved the spatial arrangements, relative energy and populations.

A total of 639 different families were found for peptide **1**. However, 82.92 % of total population of this peptide corresponded to only eleven families (table 4.3). It is interesting to note that the energetically preferred family comprises 70.48 % of the entire population. Thus, this family which adopts an α-helix structure is the most representative form of this molecule. This conformation is characterized by stabilizing hydrogen bonds between the carbonylic oxygen (residue *i*) and the NH group (residue *i*+4). The first and the last residues do not present a stable structure. A spatial view of this conformation is shown in figure 4.1a. The second most populated family (7.46%) corresponds to a structure possessing the first four residues without a stable structure; residues 5 to 7 in a turn structure and residues 10 to 15 with a typical α-helix structure. The residues 8 and 9 present a bend structure connecting the turn moiety with the α-helix portion. The last residue does not display a stable form (figure 4.1b). However, this family has an energy gap of 22.61 kcal mol^{-1} with respect to the global minimum.

For peptide **2** a total of 703 different families were obtained, from which nineteen comprise 81.92 % of the total population. The most populated family (61.06%) presents an α-helix conformation from residues 3 to 15. This conformation has an energy gap of 1.27 kcal mol^{-1} with respect to the global minimum, which has 6.04% of population. The lowest energy conformation possesses the following structure: from residues 2 to 5 in a turn structure; residue 6 in a bend form and from residue 7 to 15 in a typical α-helix struc-

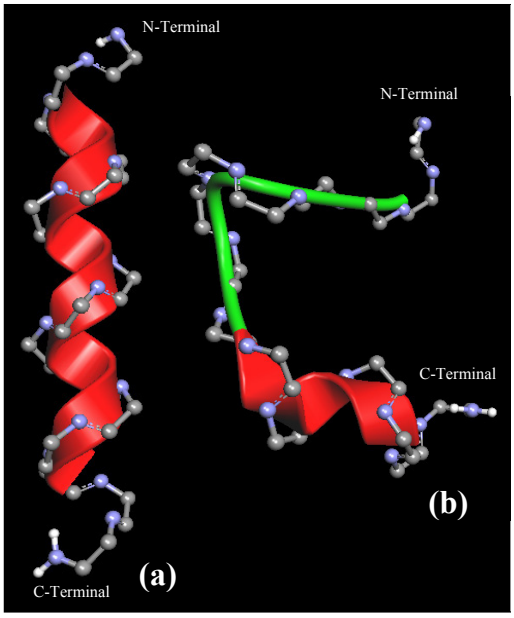

Figure 4.1: Spatial view of the preferred forms obtained for peptide **1**: (**a**) the global minimum (α-helix structure) and (**b**) the second most populated conformation.

ture. Residues 1 and 16 do not show any stable structure. In general the conformational behavior of **1** and **2** is comparable. However, in peptide **1** the most populated family (a typical α- helix structure) is also the energetically preferred one. In contrast, for peptide **2**, the fully α- helix structure is not the most preferred form.

Compounds **3-6** display a closely related conformational behavior preferring a helical structure for the most populated families. Peptides **3-6** are somewhat more rigid with respect to **1**. This fact might be appreciated comparing the total number of conformational families obtained for each compound (TABLE 4.3).

To better characterize the peptide spatial orientations, we plotted Edmundson wheel representations of peptides **1-6** (FIGURE 4.2). The representation obtained for peptide **1** displays two clearly differentiated faces: the "charged face" (denoted in dash blue line in FIGURE 4.2) and a more extended "non-charged face" (denoted in full green line). The first face identifies residues R^{11}, K^4, K^5 and R^1 as those accounting for the mutual coulombic binding. The first three residues are located on the same side of the helical peptide and hence we designated it as the "charged face". These positively charged residues are able to produce salt bridges with the hydrophilic part of the lipids.

The non-charged face is more extensive and is formed by six hydrophobic (M^{12}, I^5, W^6, I^3, W^{14} and F^7) and two polar residues (N^9 and Q^2). However, it should be noted that **1** displays a homogeneously distributed remainder of the positively charged residues. Thus, residue K^{13}, K^{16} and R^{10} are strategically intercalated along the "non-charged face". This is a striking difference with respect to peptide **2** which displays two "charged faces" where all the cationic residues are concentrated. The Edmundson wheel representations obtained for peptides **3** and **4** are very similar displaying a very extensive charged face and a markedly reduced non-charged face. Peptide **5** in turn gives only a minimal non-charged zone corresponding to the W^6 residue and the rest is "charged face". Obviously, peptide **6** displays a completely charged face because only cationic residues form it. Previously Lensink et al. reported that a homogeneous distribution of positively charged residues along the axis of the helical peptide, and especially K^4, R^{11}, and K^{15}, contribute to the association of peptide **1** with lipids (Lensink et al. 2005). Our EDMC results showed some resembling features with those reported by Lensink et al, regarding the conformational preferences of peptide **1**. In addition a very good correlation between the antifungal activities and the potential penetrating properties of these peptides is particularly striking.

4.2.2.2 SA simulation

In order to exhaustively describe the conformational behavior of these peptides, a SA set of simulations was carried out using two different force fields in an implicit solvent model (water). The initial structure of peptides **1-6** was fully extended. The secondary structures of the lowest energy conform-

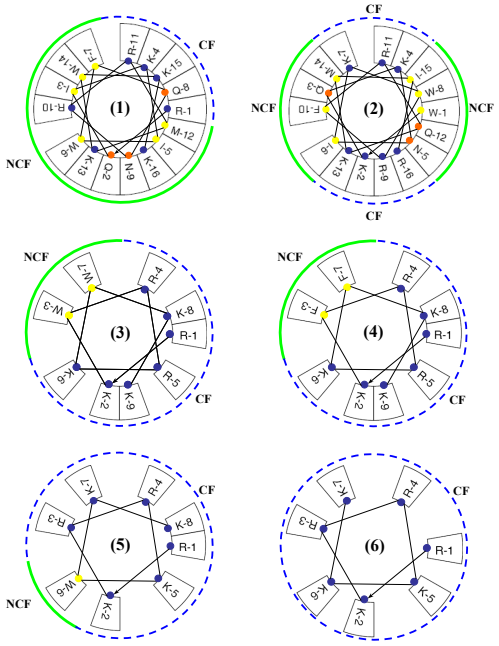

Figure 4.2: Edmundson wheel representations of peptides **1-6**. The number in the center of the wheel corresponds to the peptide number. The "charged" (CF) and "non-charged" (NCF) faces are shown in blue dash lines and full green lines, respectively. Positively charged amino acids are denoted with blue dots, the polar ones with orange, and the hydrophobic ones with yellow.

ers calculated by DSSP program (Kabsch and Sander 1983) are summarized in Table 4.4 The best structure of peptide **1** contains bends (I^3-W^6), 3_{10}-helix (F^7-N^9) and β-turn (R^{10}-R^{11}, K^{13}-K^{15}) and bends (F^7-N^9, R^{11}-K^{13}) in Amber99 and OPLS-AA force field calculations, respectively. Hierarchical clustering shows bending and helical backbone structures for peptide **1** for the most representative clusters. OPLS-AA calculations, as in peptides **2**-**6**, predict H-bonds in other positions than AMBER99. Four H-bonds were formed between O(*i*) and H-N(*j*), two H-bonds between O(*i*) and H-N(*i* +3), one H-bonds between O(*i*) and H-N(*i*+2), and O(*i*) and H-N(*i* +4) (AMBER99 results). The results of OPLS-AA calculations predict eight H-bonds formed between O(*i*) and H-N(*j*), in peptide **1** four H-bonds between O(*i*) and H-N(*i* +2) and two H-bonds between O(*i*) and H-N(*i* +4), one between O(*i*) and H-N(*i* +3). In peptide **2,** bend (Q^3-K^4, I6, Q^{12}-K^{13}) and β-turn (W^8-F^{10}, M^{14}-I^{15}) alternate. Almost all of the bend structures remained (Q^3-N^5, F^{10}, K^{13}) and an α-helix formed (I^6-R^9) which includes H-bonds. Peptides **3**-**6** contain α-helix, 3_{10}-helix and β-turn in the central residues in AMBER99 results. OPLS-AA predicts bend structures almost at the same residues.

Table 4.4: Secondary structures of the best conformation of peptides **1-8** obtained from simulated annealing calculations by using AMBER99 and OPLS-AA force fields (FF).

Pep.[a]	FF	Secundary Structure[b] Residue Number															
		1	2	3	4	5	6	7	8	9	10	11	12	13	14	15	16
1	AMBER99	_	_	S	S	S	S	G	G	G	T	T	_	T	T	T	_
	OPLS-AA	_	_	_	_	_	_	S	S	S	_	S	S	S	_	_	_
2	AMBER99	_	_	S	S	_	S	_	T	T	T	_	S	S	T	T	_
	OPLS-AA	_	_	S	S	S	H	H	H	H	S	_	_	S	_	_	_
3	AMBER99	_	_	G	G	G	T	T	T	_							
	OPLS-AA	_	_	_	S	S	S	_	_	_							
4	AMBER99	_	_	T	T	T	T	T	_	_							
	OPLS-AA	_	_	_	S	S	S	S	_	_							
5	AMBER99	_	_	_	H	H	H	H	_								
	OPLS-AA	_	_	_	S	S	_	_	_								
6	AMBER99	_	_	G	G	G	_	_									
	OPLS-AA	_	_	S	S	S	S	_									
7	AMBER99	_	T	T	_												
	OPLS-AA	_	_	_	_												
8	AMBER99	_	T	T	_												
	OPLS-AA	_	_	_	_												

[a] Peptide codes used in Table 4.1

[b] The secondary structure code obtained from DSSP program. H: 4-helix (α-helix), S: bend, G: 3-helix (3_{10}-helix); T: H-bonded turns, and _: loops or irregular elements.

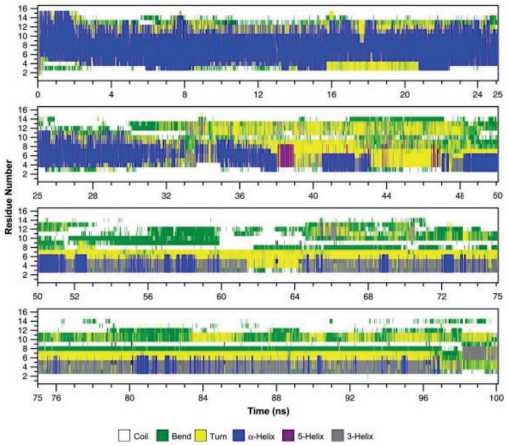

Figure 4.3: Change in the secondary structure during molecular dynamics simulation for pep. **1**.

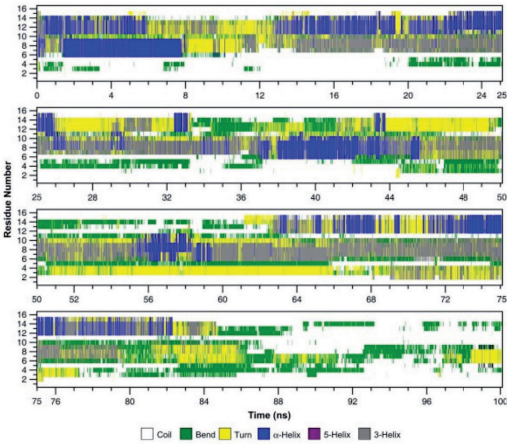

Figure 4.4: Change in the secondary structure during molecular dynamics simulation for pep. **2**.

Due to the different results obtained for these two force fields, no striking conclusions can be made. Thus, less can be said regarding this approach. Although, a consecutive arrangement of bend structures was often observed for peptide **1** and **2**. Such arrangement might confer helical-like features to these peptides. Nevertheless, this fact is not reliable enough to assure that a helical structure is the preferred one. This is a remarkable difference with the EDMC results which showed high preference for helical conformations.

4.2.2.3 MD simulations

To give a deeper look into the conformational preferences of these peptides and also take into account not only the involvement of time but also the influences of an explicit solvent model, we applied here the MD approach.

In the trajectory analysis of peptides **1**-**6**, the total and potential energies, radius of gyration (Rg) and the RMSD of the backbone (N–Cα–C(carbonyl)) atoms related to the structure at the end of equilibration (100 ps) were calculated.(figure 4.1S-4.4S, in appendix A). The root mean square fluctuation (RMSF) of the backbone atoms (figure 4.5S, in appendix A) and the hydrophilic and hydrophobic solvent accessible surface area (SASA) were also calculated. The secondary structures of peptides were analyzed by sampling trajectories every 10 ps with the DSSP program (Kabsch and Sander 1983).

In all peptides simulated here, the initial 3_{10}-helix was destroyed in the first 50–100 ps. The RMSD and the RMSF of the backbone during the simulation characterize this change in their secondary structure. The relatively small change in the RMSD of the peptides in the trajectory is evidence for the stabilization of the backbone structure. RMSD for simulations **1**–**6** are shown in figure 4.4S in appendix A. RMSD increased to 0.2–0.8 nm in all cases and remained almost constant in simulations **3**–**6**. The fluctuation in RMSD is attributed to slight changes in structure. In simulations 1 and **2** the conformations fluctuated between helical and turn/bend structures (figures 4.3 and 4.4).

The *N*- and *C*-terminal residues in all simulations appear to have a large flexibility as indicated by the change of RMSF values during the simulations. The change at central residues is moderate in simulations **1** and **2** (about 0.25 nm). The simulations **3**–**5** have shown a 0.15–0.20 nm change at residues 2–4 and 7. Also, the simulations **3** and **5** in the region which seems to be the most sensitive in the conformational change have a ~0.35 nm change at residues 5 and 4, respectively.

The conformational changes in simulation **1** are shown in figure 4.3. The initial

conformation returned and remained stable in simulation **1**, suggesting that the starting helical structure was destroyed to form a mixture of α-helix, β-turn and bend in the structure at residues 2–15. Such a conformational behavior was observed until the end of the simulation. The residues 4-6 have shown the highest preference for α-helix conformation. The initial and final residues appear to have a random coil structure because of the flexibility of these residues. For the same peptide in water Czajlik et al. (Czajlik et al. 2002) found a significant amount of helix-like conformation, even in a membrane-mimetic solvent system (TFE_{d2}/water = 9 : 1), by ^{1}H-NMR. Thus, our MD simulation is in good agreement with these experimental results. In simulation **2** (FIGURE 4.4), the initial conformation of 3_{10}-helix was destroyed and α-helix, β-turn/bend and random meander structures at the *N*- and *C*-terminal region fluctuated during the whole simulation. The residues 5-10 have shown the highest preference of 3_{10}-helix conformation. Here, in peptide **2**, the β-turn and bend conformations were mainly formed at residues 2–4 and 11-15. Also in this simulation the initial and final residues appear to have random coil structure because of the flexibility of these residues.

In simulations **3-6**, all derivatives adopt a helix-like conformation. However, while peptide **4** displays both *α*-helical and 3_{10}-helical features, the structure of peptide **3** is predominantly a 3_{10}-helix (not shown).

In summary our MD simulations indicate that peptides **1-6** showed a propensity to adopt helix-like conformations. However, whereas peptide **1** displays a marked preference for an α-helix structure, peptide **2** shows a mixture of beta turn, bend and 3_{10}-helix, being the preferred form the 3_{10}-helix features.

4.2.3 Comparison of theoretical results obtained from different approaches

The energetically preferred cluster obtained with EDMC calculations for peptide **1** (70.48% of the total population) contains an α-helix structure, the second most populated cluster (7.46% of the total population) displays α-helix and β-turn structures. On the other hand, the energetically most stable form obtained in SA with minimization showed bend, 3_{10}-helix and β-turn structures using AMBER99 force field, and only bend and coil features using OPLS-AA force fields (see TABLE 4.4). The energetically preferred form of peptide **2** showed bend and β-turn structures for AMBER99 force field, and bend and α-helix structures for OPLS-AA force field. Peptides **3-6** showed structures with helical or consecutive turn secondary structures (AMBER99 force field) and bend with coil features (OPLS-AA force field). These peptides have shown a higher flexibility than peptides **1-2** due to their smaller size. In summary, the AMBER99 force field has shown a slight preference for helical structures. Thus, this force field has a better correlation with ECCEP/3 force field than OPLS-AA force field. The OPLS-AA results differ significantly showing some differences in φ and ψ angles values and H-bond positions. Despite this fact, all force fields used here predict a helix-like structure for peptides **1-6**. The *N*- and *C*-terminal residues have shown a high flexibility, since no regular stable structure could be observed.

These results support the use of the MD simulations for these peptides. It is clear, however that in order to obtain a relatively complete picture about the conformational intricacies of peptide **1** and derivatives at least 100 ns of simulation appears to be necessary. Such simulations can provide useful information about the conformational preferences and molecular flexibility of **1** and derivatives, which might be useful to get a more profound understanding of the biological response of these peptides.

Comparing the results obtained for the conformational analysis using the different approaches, we can conclude that, in general, these methods predict a helix-like structure for peptide **1** and derivatives. These

results are also in agreement with the experimental results obtained from NMR (Czajlik et al. 2002).

4.2.4 MOLECULAR ELECTROSTATIC POTENTIALS

Knowledge of the stereoelectronic attributes and properties of peptide **1** and derivatives will contribute significantly to the elucidation of the molecular mechanism involved in the antifungal activity. Molecular electrostatic fields, and molecular electrostatic potentials (MEPs), which are their visualisation, offer an informative description of the capacity of peptides to generate stereoelectrostatic forces. Thus, the electronic study of peptides was performed using MEPs (Politzer and Truhlar 1981). MEPs have been shown to provide reliable information, both on the interaction sites of molecules with point charges and on the comparative reactivities of those sites (Carrupt et al. 1991; Murray and Politzer 1998; Naray-Szabo and Ferenczy 1995; Politzer and Truhlar 1981). More positive potentials reflect nucleus predominance, while less positive values represent rearrangements of electronic charges and lone pairs of electrons. The fundamental application of this study is the analysis of non-covalent interactions (Naray-Szabo and Ferenczy 1995), mainly by investigating the electronic distribution in the molecule. Thus, this methodology was used to evaluate the electronic distribution around molecular surface for peptides reported here. The MEPs of peptide **1** is shown in FIGURE 4.5 and the MEPs of peptides **3** and **6** are plotted in FIGURE 4.6. We evaluated the MEPs of all peptides tested but we show here only the MEPs obtained for the three peptides which displayed a significant antifungal activity.

To better appreciate the electronic behaviour of 1, and considering that two different faces were denoted in FIGURE 4.2, we present the MEPs of **1**, showing the two faces of this peptide (FIGURE 4.5). FIGURE 4.5a gives the "charged face" (CF) characterised by the presence of four cationic residues (R^1, K^4, R^{11} and K^{15}). Although it is possible to visualise residue K^{16} near to this

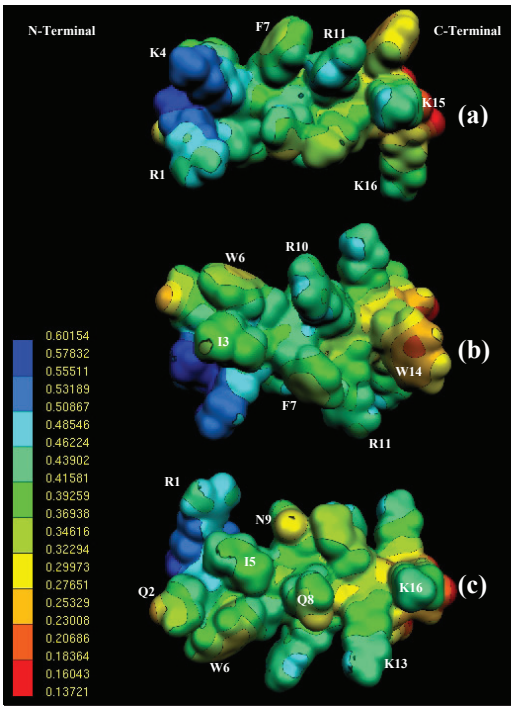

FIGURE 4.5: Electrostatic potential-encoded electron density surfaces of peptide **1**: (**a**) "charged face", (**b**) and (**c**) two different views of the "non-charged face". The surfaces were generated with Gaussian 03 using RHF/6-31G single point calculations. The coloring represents electrostatic potential with red indicating the strongest attraction to a positive point charge and blue indicating the strongest repulsion. The electrostatic potential is the energy of interaction of the positive point charge with the nuclei and electrons of a molecule. It provides a representative measure of overall molecular charge distribution. The color-code is shown at the left.

face, in fact this residue is somewhat shifted in the direction of the non-charged face. It has been previously reported that peptide-lipid association occurs through formation of salt bridges between the positively charged residues K^4, R^{11} and K^{15} and the lipid phosphate groups (Lensink et al. 2005). In addition, tryptophan fluorescence studies previously showed the importance of peptide with positively charged residues for the initial binding to negatively charged vesicles, since double R/K→A mutations involving the residues $K^4/R^{10}/R^{11}/K^{13}/K^{15}$ significantly decreased the binding affinity (Christiaens et al. 2004; Christiaens et al. 2002a, b). The MEPs of **1** suggests that the above mentioned residues

(R[1], K[4], R[11] and K[15]) could be responsible for the initial binding. The previously reported π stacking interaction between F[7] and R[11] residues might be also appreciated on this face (Lensink et al. 2005). Although the main positive potentials ($V_{(r)}$ ranging from 0.60 to 0.43 el.au^{-3}) are concentrated on this face, it should be noted that there is a relatively homogeneous distribution of positively charged residues along the entire structure. Thus, residues R[10], K[16] and K[13] are strategically located in an alternated fashion within the non-charged face. Since the non-charged moiety is too large, two different views of the MEPs were plotted in order to better visualise this face (FIGURES 4.5b and 4.5c). FIGURE 4.5b displays four hydrophobic residues I[3], W[6], F[7] and W[14]. It appears that a kind of π-stacking cluster through W[6]/R[10]/W[14] occurs in this portion of **1**. Lensink et al. reported that these residues could protect the peptide from the water phase (Lensink et al. 2005). A clear hydrophobic interaction between I[3] and W[6] might be also appreciated in this figure. FIGURE 4.5c displays a more polar face in comparison to FIGURE 4.5b, since it possesses the three polar residues of **1** (Q[2], Q[8] and N[9]). Interestingly, I[5] is located in an intercalated position with respect to polar residues and therefore there are no interactions between them. These results suggest that these polar residues could be highly solvated. Mutation of either tryptophan decreases internalization, whereas double substitution completely inhibits peptide internalization (Derossi et al. 1994; Fischer et al. 2000; Letoha et al. 2005; Lindberg et al. 2003). These results indicate that peptide 1 is not sufficiently hydrophobic to insert deeply into phospholipid model membranes (Brattwall et al. 2003; Drin et al. 2001). Therefore charge neutralisation is required for a deeper insertion of the peptide into the hydrophobic core of the membrane. The extended non-charged face alternating cationic residues among the hydrophobic and polar ones observed in the MEPs of **1** appears to be operational in this sense.

FIGURE 4.6a gives the MEPs obtained

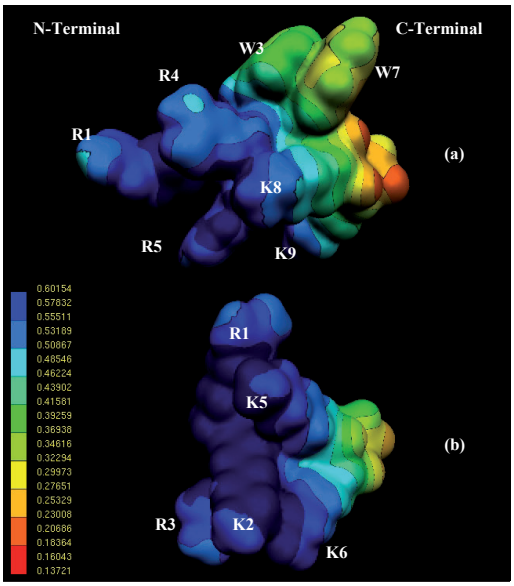

FIGURE 4.6: Electrostatic potential-encoded electron density surfaces of peptides **3** (**a**) and **6** (**b**). The color-code is shown at the left.

for peptide 3. This surface shows a more extended positively charged face with respect to **1**. In this portion are located five cationic residues R[4], K[8], R[1], R[5] and K[9]. The MEPs obtained for peptide 6 is shown in FIGURE 4.6b. A very extensive deep blue zone with potential values in the order of 0.60 el.au^{-3} clearly dominates this surface. Previously reported MD simulations indicated that the aromatic residues do not contribute to the initial binding, but rather to the subsequent insertion of peptide **1** between the bilayer head groups, where they shield the peptide from the aqueous phase (Lensink et al. 2005). The importance of hydrophobic residues seems to be crucial for the antifungal activity as well. Comparing the MEPs obtained for peptides **1**, **3** and **6** it is evident that they correlate very well with their antifungal activities: the most active peptide of this series, intermediate activity and completely inactive molecule, respectively. These results lend additional support for the key role of the hydrophobic residues in these peptides acting as antifungal compounds.

4.2.5 SMALL SIZE ANTIFUNGAL PEPTIDES

The consideration, that a peptide-based

antifungal agent should be as short as possible in order to reduce costs, prompted us to synthesize even shorter derivatives of **1**. Thus, with the aim to predict the potential antifungal effect of small-size peptides, we performed a molecular modeling study in a series of tetrapeptides. Several different tetrapeptides were modeled; however we report here only the results obtained for two of them (KWKK-NH_2 (**7**) and RQKK-NH_2 (**8**)), being representative of the entire series.

Tetrapeptides **7** and **8** displayed a completely different conformational and electronic behavior. EDMC, SA and MD results obtained for these peptides are summarized in TABLES 4.3, 4.4 and TABLES 4.7S-4.8S and FIGURES 4.1S-4.5S in APPENDIX A, respectively. EDMC results obtained for tetrapeptides **7** and **8** predict a higher molecular flexibility in comparison to the longer peptides. Also, considering the length of the backbone of these peptides they cannot achieve a stable structure. Although both tetrapeptides display a statistical-coil (Vila et al. 2002) structure, their conformational preferences are markedly different. Whereas peptide **7** displays a quasi-π-helix form (ψ_1= -62.9, φ_2= -88.1, ψ_2= 81.8, φ_3= -86.4, ψ_3= 72.3 and φ_4= -82.7), peptide 8 prefers a quasi-α-helix structure (ψ_1= -18.7, φ_2= -73.9, ψ_2= -25.5, φ_3= -82.3, ψ_3= -27.6 and φ_4=-78.4). This is a striking difference obtained for these tetrapeptides. SA calculations indicate that these peptides are more flexible than peptides **1-6** (TABLE 4.4). The small size of these peptides could explain the irregular structures obtained for peptides **7-8** (OPLS-AA force field), whereas turn structures were preferred for the central residues of these peptides (AMBER99). MD calculations indicate that peptides **7** and **8** show a statistical coil structure during the whole simulation time because of their high flexibility. However, from MD a clear difference obtained for these tetrapeptides is that peptide 8 displays a tendency to adopt a turn conformation, whereas peptide **7** has the tendency to achieve extended conformations. The spatial ordering adopted by peptide **8** is closely related to

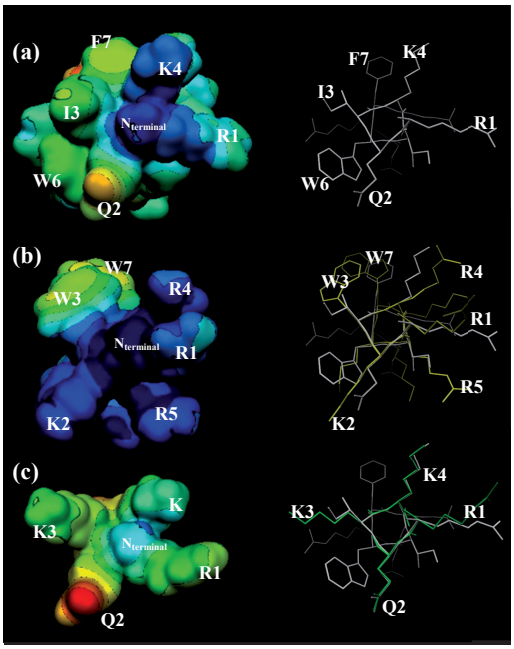

FIGURE 4.7: Electrostatic potential-encoded electron density surfaces obtained for peptides **1** (**a**), **3** (**b**) and **8** (**c**) in a front view of the *N*-terminal portion (left hand). Also this figure sows at the right hand: (**a**) a frontal spatial view of **1**, (**b**) an overlapped stereoview of peptide **1** (white) with peptide **3** (yellow), and (**c**) an overlapped stereoview of peptide **1** (white) with peptide **8** (green).

those obtained for the first four residues of peptide **1** (see FIGURE 4.7c right hand).

FIGURE 4.7 gives the MEPs obtained for compounds **1**, **3** and **8** in a front view. The similar MEPs values obtained for peptides **1** and **8** can be appreciated in this figure. In contrast a more positively charged MEP was obtained for compound **3** as it was previously discussed.

On the basis of the stereoelectronic similarity obtained for peptides **1** and **8**, it is reasonable to think that tetrapeptide **8** could present some antifungal activity, but not peptide **7.** Thus, to confirm our hypothesis, we decide to test the antifungal effects of tetrapeptides **7** and **8.** As expected**,** peptide **7** did not show any antifungal activity with the concentrations reported here. In contrast, peptide **8** displayed a moderate but significant antifungal effect against *C. neoformans* (TABLE 4.1). It must be pointed out that peptide **8**

displays antifungal activity only against *C. neoformans*; in contrast this compound was not active against *C. albicans*. This is a striking difference with respect to **1**. It is clear however, that the antifungal potency found for **8** against *C. neoformans* is very interesting particularly considering its small size.

Inspection of FIGURE 4.7 led us to appreciate that although peptides **1**, **3** and **8** are of different size, they display some stereoelectronic similarities primarily near the *N*-terminal portion, implicating a likely overlap on these moieties. Cellular uptake experiments previously demonstrated the crucial role of arginines in cell-penetrating peptides (Thoren et al. 2003). Also, MD simulations indicated that arginine residues could be responsible for the initial electrostatic binding forming bidentate hydrogen bonds with lipid phosphate groups. It should be noted that the first residue of peptides **1**, **3** and **8** is arginine. In fact there are various ways in which **8** may produce its antifungal activity, on which we can only to speculate. In that respect the similar stereoelectronic behaviors observed between **8** and the *N*-terminal portions of **1** and **3** is particularly noteworthy.

4.3 Conclusions

In the present paper, we report the design, synthesis and antifungal effects of peptide **1** and derivatives, a new series of antifungal peptides. Among the peptides tested, RQIKIWFQNRRMKWKK-NH_2 (**1**), RKWRRKWKK-NH_2 (**3**) and RQKK-NH_2 (**8**) displayed the most powerful inhibitory effect against *C. neoformans*. A detailed conformational and electronic study supported by theoretical calculations helped us to identify a possible "biologically relevant conformation" for these peptides. A particular combination of cationic and hydrophobic residues adopting a definite spatial ordering appears to be the key parameter for the transition from hydrophilic to hydrophobic phase, which could be a necessary step to produce the antifungal activity. We believe that our results could contribute to an understanding of the minimal structural requirements for the antifungal potential of peptides reported here and to the design of novel structurally related agents. These results are very encouraging in that they show a great potential for peptides **1** and **8** as a truly novel class of antifungal compounds particularly against the yeast *C. neoformans*. Thus, the antifungal activity reported in this chapter for peptides **1** and **8** opens promising ways for the development of a new antifungal agent for treatment of cryptococcosis. Since *C. neoformans* remains an important life-threatening complication for immunocompromised hosts, particularly for patients who have undergone transplantation of solid organs and therefore, new compounds effectively acting against this fungus are highly needed (Kontoyiannis et al. 2003; Singh 2003).

Peptide **1** has been used as a nonviral, nontoxic and highly efficient vector for delivering bioactive substances, that by themselves are membrane-impermeable, to the cytoplasm or nucleus of cells (Derossi et al. 1994; Joliot et al. 1991). The antifungal activity found for **1** is very interesting by itself but it is also important considering its potential use as a carrier for other known antifungal drugs. Thus, this system may improve the pharmaceutical properties of the drugs by, for example, improving solubility and bioavailability, or by minimizing toxicity and overcoming drug resistance.

4.4 Experimental section

4.4.1 Synthetic methods

Solid phase synthesis of **1**, RQIKIWFQNRRMKWKK-NH_2, was carried out manually on a *p*-methylbenzhydrylamine resin (MBHA, 0.39 mmol/g) with standard methodology using Boc-strategy. Side chain protecting groups were as follows: Tos for Arg and 2-chloro-Z for Lys. All protected amino acids were coupled in CH_2Cl_2 or CH_2Cl_2/DMF solvent mixture in a ratio of 1:1 (for Gln and Asn) using DCC (2.5 equiv.) and HOBt (2.5 equiv.). Amino acid incorporation was monitored by Kaiser ninhydrin test (Kaiser et al. 1970). After coupling of the amino acid, Boc-deprotection was effected by using TFA/CH_2Cl_2 (1:1) for 5 min first then repeated for 25 min. The completed peptide resin was treated with liquid HF/dimethyl sulfide/anisole/indole (86:6:4:2) at 5°C for 1 h. HF was removed and the resulted free peptide was solubilized in 10% aqueous acetic acid and lyophilized. The crude peptide was purified by semipreparative RP HPLC on a Lichrosorb C-18 column (16 x 250 mm, 7 µm) with a linear gradient of acetonitrile 30-100%, 0.1% TFA in 70 min, 4 ml/min flow. The appropriate fractions were pooled and lyophilized. The purified peptide was characterized by HPLC and mass spectometry using a Finnigan TSQ 7000 tandem quadrupole electrospray mass spectrometer. M+H calc.: 2244.3, found: 2244.5. Analytical HPLC conditions: column: Luna C-18, 5 µm, 4.6 x 250 mm, gradient: 30-50% AcN, 0.1% TFA in 10 min, 1.2 ml/min flow, 220 nm. R_t: 4.280 min. Same synthesis procedures and analytical HPLC conditions were applied for the peptide analogues (**2**-**8**) as shows TABLE 4.5.

Table 4.5: HPLC data of the synthesized peptides.

Compounds	Retention factor (min)	Gradient elution (%)
RQIKIWFQNRRMKWKK-NH_2 (**1**)	4.280	30-50 (10 min)
WKQKNIKWRFRQKMIR-NH_2 (**2**)	11.200	5-80 (25 min)
RKWRRKWKK-NH_2 (**3**)	13.200	5-35 (15 min)
RKFRRKFKK-NH_2 (**4**)	9.387	5-30 (10 min)
RKRRKWKK-NH_2 (**5**)	9.339	5-35 (15 min)
RKRRKKK-NH_2 (**6**)	4.576	5-35 (15 min)
KWKK-NH_2 (**7**)	9.012	5-35 (15 min)
RQKK-NH_2 (**8**)	3.553	5-20 (15 min)

4.4.2 Antifungal evaluation

4.4.2.1 Microorganisms and media

For the antifungal evaluation, standardized strains from the American Type Culture Collection (ATCC), Rockville, MD, USA, were used. *Candida albicans* ATCC 10231, *Cryptococcus neoformans* ATCC 32264. Active compounds were tested against clinical isolates from the Malbrán Institute [(M), Av. Velez Sarsfield 563. Buenos Aires)]. The isolates included 10 strains of *Cryptococcus neoformans* which *voucher specimens* are presented in TABLE 4.2. Strains were grown on Sabouraud-chloramphenicol agar slants for 48 h at 30 °C, maintained on slopes of Sabouraud-dextrose agar (SDA, Oxoid) and subcultured every 15 days to prevent pleomorphic transformations. Inocula of cells were obtained according to reported procedures and adjusted to 1-5 $x10^3$ cells with colony forming units (CFU) / mL (Pfaller 2002a).

4.4.2.2 Antifungal susceptibility testing. MIC determinations

MIC of each extract or compound was determined by using broth microdilution techniques according to the guidelines of the Clinical and Laboratory Standards Institute (CLSI), formerly National Committee for Clinical and Laboratory Standards for yeasts (M27-A2) (Pfaller 2002a). MIC values were determined in RPMI-1640 (Sigma, St Louis, Mo, USA) buffered to pH 7.0 with MOPS. Microtiter trays were incubated at 35 °C in a moist, dark chamber, and MICs were visually recorded at 48 h. For the assay, stock solutions of pure compounds were two-fold diluted with RPMI from 256 - 0.98 µg/mL (final volume = 100 µl) and a final DMSO concentration ≤ 1%. A volume of 100 µl of inoculum suspension was added to each well with the exception of the sterility control where ster-

ile water was added to the well instead. Ketoconazole, Amphotericin B and Itraconazole (all from Sigma Chemical Co, St Louis, MO, USA) were used as positive controls. Endpoints were defined as the lowest concentration of drug resulting in total inhibition (MIC_{100}) of visual growth compared to the growth in the control wells containing no antifungal. MIC_{80} and MIC_{50} were defined as the lowest concentration of a compound that caused 80 % or 50 % reduction of the growth control respectively (culture media with the microorganism but without the addition of any compound) and was determined spectrophotometrically with the aid of a VERSA Max microplate reader (Molecular Devices, USA). The MFC of peptide **1** against each isolate was also determined as follows: after determining the MIC, an aliquot of 5 µL sample was withdrawn from each clear well of the microtiter tray and plated onto a 150-mm RPMI-1640 agar plate buffered with MOPS (Remel, Lenexa, Kans.). Inoculated plates were incubated at 30°C, and MFC were recorded after 48 h. The MFC was defined as the lowest concentration of each compound that resulted in total inhibition of visible growth.

4.4.2.3 Determination of percentage of inhibition

The test was performed in 96 wells-microplates. Peptide test wells (PTW) were prepared with stock solutions of each peptide in DMSO (maximum concentration ≤ 2%), diluted with RPMI-1640 to final concentrations 200 -12.5 µM. Inoculum suspension (100 µl) was added to each well (final volume in the well = 200 µL). A growth control well (GCW) (containing medium, inoculum, the same amount of DMSO used in PTW, but compound-free) and a sterility control well (SCW) (sample, medium and sterile water instead of inoculum) were included for each strain tested. Microtiter trays were incubated in a moist, dark chamber at 35 °C, 24 or 48 h for *Candida* spp. or *Cryptococcus* sp., respectively. Microplates were read in a VERSA Max microplate reader (Molecular Devices, Sunnyvale, CA, USA). Amphotericin B was used as positive control (100 % inhibition). Tests were performed by duplicate. Reduction of growth for each peptide concentration was calculated as follows: % of inhibition: 100- (OD_{405} PTW- OD_{405} SCW) / OD_{405} GCW - OD_{405} SCW.

4.4.2.4 Statistical analysis

Data were statistical analyzed by one-way analysis of variance. A $p< 0.05$ was considered significant.

4.5 Computational methods

4.5.1 EDMC calculations

The conformational space of each peptide was explored using the method previously employed by Liwo et al. (Liwo et al. 1996b) that included the electrostatically driven Monte Carlo (EDMC) method (Ripoll and Scheraga 1988, 1990). Conformational energy was evaluated using the ECEPP/3 force field (Némethy et al. 1992). This force field employs rigid valence geometry. Hydration energy was evaluated using a hydration-shell model with a solvent sphere radius of 1.4 Å and atomic hydration parameters that have been optimized using nonpeptide data (SRFOPT) (Vila et al. 1991; Williams et al. 1992). In this model, in addition to a sum of electrostatic, non-bonding, hydrogen-bond and torsional energy terms, the total conformational energy includes terms accounting for loop closing and peptide solvation. The conformation with minimized energy was subsequently perturbed by changing its torsional φ and ψ angles using the Monte Carlo method (Li and Scheraga 1987). Piela's algorithm (Piela and Scheraga 1987) which was also applied at this stage, greatly improves the acceptance coefficient. In this algorithm φ and ψ angles are changed in a manner which allows the corresponding peptide group to find the most proper orientation in the electrostatic field of the rest of the peptide chain. The energy of the new conformation is minimized, compared to the previous one and may be accepted or discarded on the basis of energy and/or geometry. If the new energy-minimized conformation is similar in shape and in energy to the starting conformation, it is discarded. Otherwise, the energy

of the new conformation is compared to the energy of the parent conformation. If the new energy is lower, the new conformation is accepted unconditionally, otherwise the Metropolis criterion (Metropolis et al. 1953) is applied in order to accept or reject the new conformation. If the new conformation is accepted, it replaces the starting one; otherwise another perturbation of the parent conformation is tried. A temperature jump may be included if the perturbation is not successful for an arbitrarily chosen number of iterations. The process is iterated, until a sufficient number of conformations have been accepted. Sidor et al. give a more detailed description of this procedure (Sidor et al. 1999).

In order to explore the conformational space extensively, we carried out 10 different runs, each of them with a different random number, for each peptide studied. Since the EDMC procedure uses random numbers, there is a need to initialize the random number generator by providing an integer. Therefore, we collected a total of 5000 accepted conformations for each peptide studied. Each EDMC run was terminated after 500 energy-minimized conformations had been accepted. The parameters controlling the runs were the following: a temperature of 298.15 K was used for the simulations. A temperature jump of 50,000 K was used; the maximum number of allowed repetitions of the same minimum was 50. The maximum number of electrostatically predicted conformations per iteration was 400; the maximum number of random-generated conformations per iteration was 100; the fraction of random/electrostically predicted conformations was 0.30. The maximum number of steps at one increased temperature was 20; and the maximum number of rejected conformations until a temperature jump is executed was 100. Only *trans* peptide bonds ($\omega \approx 180°$) were considered.

The ensemble of obtained conformations was then clustered into families using the program ANALYZE (Meadows et al. 1994b; Post et al. 1990; Scheraga et al. 1983), which applies the minimal-tree clustering algorithm for separation, using all heavy atoms, energy threshold of 30 kcal mol^{-1}, and RMSD of 0.75 Å as separation criteria for all peptides here studied. Molecules containing seven, eight and sixteen amino acids residues were clustered using the same method but, instead of using all heavy atoms it used only the backbone atoms (Cα, N and C(carbonyl)). This procedure allows for substantial reduction of the number of conformations and eliminates repetitions.

4.5.2 SA calculations

To find the best structures of peptides studied, 5000 structures were generated by simulated annealing (SA) implemented in Tinker Version 4.2 (Kundrot et al. 1991). Peptides were generated by the software and minimized with a charge and van der Waals cutoff of 1.8 nm and 1.4 nm, respectively, with OPLS-AA and AMBER99 force fields. A taper of 0.8 was applied to smooth the cutoff to zero in the calculations. The solvation was simulated by GB/SA (generalized Born/surface area model). The tolerance of the minimization was 0.001 kcal mol^{-1} $Å^{-1}$. The following protocol was used in the simulated annealing: 5000 times were repeated 2000 steps equilibration in 1000K and 2000 steps cooling to 50K exponentially with 1 fs step-size. After cooling the structures were minimized with the previous method. The minimized structure was applied for the next step. The secondary structures of the peptides were analyzed by DSSP (Kabsch and Sander 1983). The algorithm measures the geometry and the hydrogen bonding in peptides. The secondary structures are assigned by the following way: turns within 3, 4 and 5 residues, respectively, are assigned on the basis of hydrogen bonds between *i* to *i* + 1 (three residue turn), *i* to *i* + 1 or *i* + 2 (four residue turn), *i* to *i* + 1 or *i* + 2 or *i* + 3 (five residue turn). A β-bridge is assigned when two non-overlapping stretches of 3 residues each, *i* - 1, *i*, *i* + 1 and *j* - 1, *j*, *j* + 1 form H-bonding parallel or antiparallel pattern. Two or more consecutive β-bridge structures are assigned as β-sheet structures. A bend is defined as a five residue turn without H-bonds with a curvature of at least 70° between the first 3 residues (*i* - 2, *i* - 1 and *i*) and the last 3 residues (*i*, *i* + 1 and *i* + 2). The position of the bend is marked at *i*. Two consecutive turns at position *i* - 1 and *i* form a helix. 3_{10}-helix is marked a positions *i*, *i* + 1 and *i* + 2. α-helix and π-helix

at *i*, *i* + 1, *i* + 3 and *i*, *i* + 1, *i* + 2, *i* + 3, *i* + 4, respectively. Residues without recognized secondary structures are assigned as irregular or loop (random coil) structure. For clustering 5000 structures a perl script in MMTSB (Feig et al. 2001) was used.

4.5.3 MD simulations

Molecular dynamics (MD) simulations were performed using the GROMACS 3.2.1 package of programs (Lindahl et al. 2001; Van Der Spoel et al. 2005), with the OPLS-AA force field (Jorgensen et al. 1996; Kaminski et al. 2001; McDonald and Jorgensen 1998; Price et al. 2001; Rizzo and Jorgensen 1999; Watkins and Jorgensen 2001). The calculations were carried out using a standard 3_{10}-helix (φ = -49.00°,ψ = -26.00°) as a starting structure. The peptides 1-8 were embedded in a box containing the SPC water model (Berendsen et al. 1981a) that extended to at least 10 Å between the solutes and the edge of the box. The total number of water molecules was between 1389 and 2791. Then Cl^- ions were added to the systems by replacing water molecules in random positions, thus making the whole system neutral. For details see TABLE 4.9S in APPENDIX A. Prior to dynamics simulation, internal constraints were relaxed by energy minimization. Following the minimization, a MD equilibration run was performed under position restraints for 20 ps. An unrestrained run was then initiated. During the MD runs, the LINCS algorithm (Hess et al. 1997) was used to constrain the lengths of hydrogen containing bonds; the waters were restrained using the SETTLE algorithm (Miyamoto and Kollman 1992). The time step for the simulations was 0.002 ps. The simulations were run under NPT conditions, using Berendsen's coupling algorithm (Berendsen et al. 1984) for keeping the temperature and pressure constant (P = 1 bar, τ_p = 0.5 ps; T = 310 K, τ_T = 0.1 ps). The compressibility was 4.8x10-5 bar-1. Van der Waals forces were treated using a 12 Å cutoff. Long-range electrostatic forces were treated using the particle mesh Ewald method (PME) (Darden et al. 1993b). The coordinates were saved every 10 ps. The total simulation time was 100 ns for every peptide. The analysis of the simulations was performed using the analysis tools provided in the Gromacs package.

4.5.4 Molecular electrostatic potentials

Quantum mechanics calculations were carried out using the Gaussian 03 program (Frisch et al. 2003). We use the most populated conformations of peptides **1-8** obtained from EDMC calculations. Subsequently, single point *ab initio* (RHF/6-31G(d)) calculations were carried out. The electronic study was carried out using molecular electrostatic potentials (MEPs) (Politzer and Truhlar 1981). These MEPs were calculated using RHF/6-31G(d) wave functions and MEPs graphical presentations were created using the MOLEKEL program (Flükiger et al. 2000). ▪

Acknowledgements

This work is part of the Hungarian-Argentine Intergovernmental S&T Cooperation Programme and was supported by the Research and Technological Innovation Foundation and by the SECyT, as well as by grants from Universidad Nacional de San Luis and grants to S.A.Z. and R.D.E. from the Agencia de Promoción Científica y Tecnológica de la Argentina (ANPCyT) PICT R 260. It is part of the Iberoamerican Program of Science and Technology for the Development (CYTED, Network RIBIOFAR). T.K. and B.P. thank the Hungarian Research Fund OTKA K61577. R.D.E. is member of the CONICET (Argentina) staff. M.F.M is a fellow of CONICET (Argentina). M.F.M. is a recipient of a Bernouilli Fellowship from the University of Groningen. The authors thank E. Menyhárt for the technical assistance of peptide synthesis.

"Algún día en cualquier parte, en cualquier lugar indefectiblemente te encontrarás a ti mismo, y ésa, sólo ésa, puede ser la más feliz o la más amarga de tus horas"
(P. Neruda)

05

"These memories"

oil on paper (296x420 mm)

M.F. Masman 2010

Chapter 5

In silico study of full length amyloid β 1-42

Tri- & penta-oligomers in solution

Marcelo F. Masman, Ulrich L. M. Eisel, Imre G. Csizmadia, Botond Penke, Ricardo D. Enriz, Siewert Jan Marrink & Paul G.M. Luiten

Journal of Physical Chemistry B (2009) 113:11710-11719.

Abstract

Amyloid oligomers are considered to play causal roles in the pathogenesis of amyloid-related degenerative diseases including Alzheimer's disease. Using MD simulations techniques, we explored the contributions of the different structural elements of trimeric and pentameric full-length $A\beta_{42}$ aggregates in solution to their stability and conformational dynamics. We found that our models are stable at the temperature of 310 K, and converge toward an interdigitated side-chain packing for intermolecular contacts within the two β-sheet regions of the aggregates: β1 (residues 18-26) and β2 (residues 31-42). MD simulations reveal that the β-strand twist is a characteristic element of Aβ aggregates, permitting a compact, interdigitated packing of side chains from neighboring β-sheets. The β2 portion formed a tightly organised β-helix, whereas the β1 portion did not show such a firm structural organization although it maintained its β-sheet conformation. Our simulations indicate that the hydrophobic core comprising the β2 portion of the aggregate is a crucial stabilizing element in the Aβ aggregation process. Based on these structure-stability findings the β2 portion emerges as an optimal target for further anti-amyloid drug-design.

5.1 Introduction

Proteins can adopt an amazing array of sequence-dependent structures that enable them to perform the myriad of chemical functions critical to life. However, over the past decade, it has become clear that many different proteins can also form misfolded structures leading to insoluble aggregates. With respect to human brain functioning protein misfolding can have dramatic consequences and can result in devastating diseases of the brain. There are several known degenerative diseases whose pathogenic mechanism is based on the pathological aggregation of polypeptides. These types of neurodegenerative diseases include Alzheimer's disease (AD), Parkinson's disease, Huntington's disease, prion diseases like Creutzfeldt-Jacob disease, and type II diabetes (Lynn and Meredith 2000; Rochet and Lansbury 2000; Selkoe 2003). It is a common feature to all of the above mentioned diseases that the native structure of the specific peptides has been changed and that during a fast aggregation process, they provide fibrillary products which are toxic to nerve cells or nervous tissue and resistant against enzymatic breakdown. The most extensively studied amyloid-associated disease is AD, which is characterized pathologically by abnormally high numbers of amyloid- or senile plaques in the cerebral cortex and amyloid deposits in the walls of cerebral blood vessels, and by neurofibrillary tangles in dead and dying neurons (Holtzman and Mobley 1991). Amyloid plaques are brain lesions that are composed of amyloid polymers and degenerating neurites accompanied by activated microglia, the inflammatory cells of the brain. The major component of amyloid plaques is a small peptide of 39 to 43 amino acids in length called β-amyloid (Aβ), which is a proteolytic splicing product of the large amyloid precursor protein (APP). Compelling evidence now indicates that factors which increase the production of amyloidogenic variants of Aβ, or which facilitate deposition or inhibit elimination of amyloid deposits, are major risk factors for AD (Selkoe 1999).

Currently, more than 20 different forms of Aβ are known (Westermark 1997), some of which are rare and some of which play central roles in the pathogenesis of diseases affecting millions of patients worldwide. The investigation of amyloid, as a major example of pathology due to protein misfolding, has become a widely studied enterprise (Kisilevsky 2000; Lesne et al. 2006; Sato et al. 2006; Sciarretta et al. 2006b; Soto et al. 2007; Westermark 2005; Zheng et al. 2007). Consequently, the 3D structure of the amyloid polymers and fibrils is a focus of interest both for a molecular understanding of amyloidogenesis and for the development of innovative therapeutic and diagnostic approaches. Solid-state NMR studies have contributed substantially to the understanding of amyloid fibrils (Ritter et al. 2005; Tycko 2004). However, only a few 3D structures of amyloid fibrils have yet been determined (Luhrs et al. 2005; Nelson et al. 2005), owing in part to the fibrils' noncrystalline, insoluble, and mesoscopically heterogeneous nature. This makes these structures difficult to access by established structural techniques such as X-ray crystallography or solution-state NMR (Thompson 2003). Since the 1970's, amyloid has been defined by its main β-sheet fibrillary structure (Eanes and Glenner 1968; Glenner 1980a, b), and by properties associated with this. The unifying structure is an assembled protein fibril in which the sheets are parallel to the fibril direction and where the strands run perpendicular to the fibril. This principal organization is believed to be common to all amyloid fibrils, irrespective of the biochemical nature (Westermark 2005).

The amyloid beta 1-42 peptide ($A\beta_{42}$) fragment is the dominant Aβ species in the amyloid plaques of AD patients, and compared with $A\beta_{40}$ it displays a dramatically increased propensity to form amyloid fibrils *in vitro* (Burdick et al. 1992; Jarrett et al. 1993a, b; Riek et al. 2001). Furthermore, a comparison of the kinetic data

of $A\beta_{40}$ and $A\beta_{42}$ shows that $A\beta_{40}$ adopts more varied conformational structures compared to $A\beta_{42}$, as seen by the fluctuations of the Tyr signal displayed by $A\beta_{40}$ (Vestergaard et al. 2005). A comparative experimental-theoretical conformational study has been carried out by Sgourakis et al. (Sgourakis et al. 2007), which sheds light on the differential conformational behavior of the monomers in aqueous solution of $A\beta_{40}$ and $A\beta_{42}$. The presence of metal ions, in particular copper, zinc, and iron, has been reported to enhance Aβ aggregation (Atwood et al. 1999; Atwood et al. 2004; Huang et al. 2004). Several important structural characteristics of $A\beta_{42}$ fibrils have been determined (Luhrs et al. 2005; Nelson et al. 2005; Ritter et al. 2005; Thompson 2003; Tycko 2004), establishing that $A\beta_{42}$ fibrils form a cross-β structure (Kirschner et al. 1986) that contains parallel, in-register β-sheets (Balbach et al. 2002). Most recently it was found that memory deficits in middle-age transgenic AD model mice are caused by the extracellular accumulation of a dodecameric $A\beta_{42}$ soluble assembly (Lesne et al. 2006). While the major toxic species in AD are probably Aβ-oligomers, thus being a principal target of AD drug development, it remains unclear why Aβ-oligomers should be neurotoxic. Plausible mechanisms of toxicity include links to oxidative stress, metal binding, free radical formation (Chauhan and Chauhan 2006) or ion channel formation (Quist et al. 2005), and therefore it may be possible to interact with these processes by applying reducing agents, metal chelators (Bush 2002) or ion channel inhibitiors. In general terms an ideal approach would be to interfere with the early phases of molecular pathways that lead to the disease. Consequently, one attractive therapeutic strategy for the treatment of AD is to inhibit Aβ peptide aggregation since this appears to be one of the first steps in the pathogenic process of amyloidosis that is not associated with some natural biological function (Lansbury 1997). Breaking these amyloid aggregates down by non-peptide or peptide inhibitors seems to be a promising way to combat AD (Doig 2007). To that aim, it is crucial to understand the conformational and dynamic behavior of the structure of the $A\beta_{42}$ aggregates in order to rationally design a putative AD drug. Moreover, the conformational analysis and the investigation of the structure of $A\beta_{42}$ aggregates might lead to a more profound understanding of the primary pathogenesis of AD and comprehend the development at the molecular level of this dramatic disease.

Most computational investigations of the structure and dynamics of Aβ-peptides have focused on monomers (Baumketner et al. 2006; Buchete et al. 2005; Gordon and Meredith 2003; Lazo et al. 2005; Massi et al. 2001; Petkova et al. 2005; Petkova et al. 2006; Sato et al. 2006; Scheibel et al. 2003; Sciarretta et al. 2006a; Sgourakis et al. 2007; Wei and Shea 2006), dimers (Huet and Derreumaux 2006; Tarus et al. 2005; Urbanc et al. 2004), and other low-order oligomers (Buchete and Hummer 2007; Gnanakaran et al. 2006; Hwang et al. 2004; Klimov and Thirumalai 2003; Ma and Nussinov 2006; Rohrig et al. 2006; Zheng et al. 2007). The idea of considering a full-length molecular model of the Aβ aggregates is worthy of consideration, since the majority of the studies mentioned above have employed models using a truncated-sequence molecular model and/or insoluble fibril state. In our present investigation, profiting from the structural information available from recent solid-state nuclear magnetic resonance (ssNMR) experiments (Balbach et al. 2002; Luhrs et al. 2005; Paravastu et al. 2006; Petkova et al. 2002; Petkova et al. 2005; Petkova et al. 2006) on the parallel cross-β structure of Aβ protofilaments, we perform all-atom/explicit solvent simulations of amyloid aggregates containing three and five peptide units. Every unit with "hairpin" shaped Aβ1–42 peptides was located in a plane roughly perpendicular to the fibril axis as it was observed by using ssNMR (Luhrs et al. 2005). Among the different structural topologies possible depending on experimental growth conditions (Paravastu et al. 2006; Petkova et al. 2005;

Petkova et al. 2006), we focus on Aβ1–42 fibrils grown under the conditions defined as in reference 16. The objectives of our study are twofold: 1) to explore the contributions of the different structural elements to stability of full-length aggregated $A\beta_{42}$ in solution, and 2) to investigate the most promising, potential structural target for further drug-design based on the structure-stability information of our model. Our reasonably long-time simulations (100 ns) of both tri- and pentameric aggregates at 310 K, in which fibrils are experimentally stable (below ~330 K), permit us to draw conclusions on structurally relevant aggregate characteristics such as the secondary-to-quaternary structural elements (e.g., β-strands, intra- and intermolecular contacts), internal salt-bridges, and the interior hydration. In the present study we analyze the evolution of these elements at 310 K, focusing in particular on the structure and dynamics behavior in solution of the full-length $A\beta_{42}$ aggregates.

5.2 Methods

5.2.1 System setup

The human amyloid beta 1-42 peptide ($A\beta_{42}$) (figure 5.1) was taken as a model system. The calculations were carried out using the structure of the $A\beta_{42}$ fibrils (PDB entry 2BEG) determined by Lührs and coworkers (Luhrs et al. 2005) that was downloaded from the Protein Data Bank (Berman et al. 2002). Due to the fact that residues 1-17 are disordered and lacking a unique and stable conformation we only had experimental structural information from residues 18-42 (Luhrs et al. 2005). Therefore, in order to have the completed molecule of $A\beta_{42}$, the sequence for the residues 1-17 was completed using an arbitrary totally extended orientation ($\varphi \approx 180°$ and $\psi \approx 180°$). Both trimeric and pentameric aggregates were investigated. The trimeric system was obtained by deletion of the edging chains of the experimental structure determined by Lührs and coworkers (Luhrs et al. 2005), which is a pentameric aggregate. Protons were added using the program pdb2gmx, in the GROMACS suite of programs, for optimization of the hydrogen bond network.

The peptide aggregates were embedded in a rectangular box containing SPC waters (Berendsen et al.), leaving at least 10 Å between the solutes and the edge of the box. The total number of water molecules varied between 15630 and 25919. Na+ ions were added to the systems by replacing water molecules in random positions, thus making the whole system neutral (table 5.1). In order to equilibrate our systems we carried out an extensive simulating annealing (SA) protocol with repeating heating/cooling cycles covering a broad temperature range (from 310 up to 500 K), in which fibrils are experimentally stable

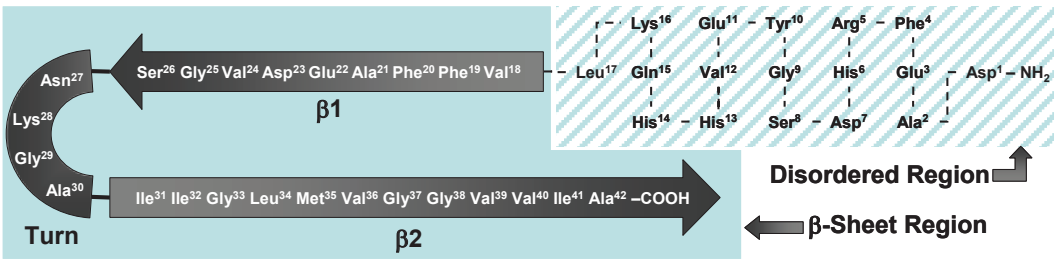

Figure 5.1: Amino acid sequence of human amyloid beta 1-42 peptide ($A\beta_{42}$) and schematic representation of a molecule of $A\beta_{42}$ in a hairpin shape. The residues 1-17 comprise the disordered region. The residues 18-42 comprise the β-sheet region.

Table 5.1: Selected parameters used in simulations A-E. Molecular Dynamics simulation code (MD), number of $A\beta_{42}$ chains per system (#βA), number of Na^+ ions added for neutrality (#Na^+), number of water molecules per simulation (#H2O), total number of atoms per system (#Atoms) and total simulation time (Time, in ns) are shown.

MD	# βA	# Na^+	# H_2O	# Atoms	Time
A3	3	9	17284	53742	20
B3	3	9	17284	53742	20
C3	3	9	17302	53796	20
D3	3	9	15630	48780	20
E3	3	9	17284	53742	100
A5	5	15	25919	80907	20
B5	5	15	21200	66750	20
C5	5	15	20832	65646	20
D5	5	15	20832	65646	20
E5	5	15	20009	63177	100

(below ~330 K) or fully dissociated (above ~373 K) (Meersman and Dobson 2006; Sasahara et al. 2005). During the whole minimization position restraint was applied for the alpha carbons (Cα) of residues 18-42. As a result of the SA runs, the DR residues showed a large range of conformational sampling. Multiple simulations were performed for each system, starting from different initial random velocity distributions, generating five independent strands of simulations (labelled A-E, see TABLE 5.1). Details of the equilibration procedure can be found in the Supp. Information of CHAPTER 5 in APPENDIX A. For each strand between 20-100 ns production runs were obtained and analyzed. The coordinates were saved every 2 ps.

5.2.2 Simulation parameters

All simulated annealing (SA) simulations and molecular dynamics (MD) simulations were performed using the GROMACS 3.3.2 package of programs (Van Der Spoel et al. 2005), with the OPLS-AA force field (Kaminski et al. 2001). The simulations were run under NPT conditions, using Berendsen's coupling algorithm (Berendsen et al. 1984) for keeping the temperature and pressure constant (P = 1 bar, τ_p = 0.5 ps; T = 310 K or 500 K, τ_T = 0.1 ps). The LINCS algorithm (Hess et al. 1997) was used to constrain the lengths of hydrogen containing bonds; the waters were restrained using the SETTLE algorithm (Miyamoto and Kollman 1992). A force constant of 1000 kJ mol^{-1} nm^{-1} was used for position restraints during the SA. For the subsequent unrestrained MD simulations, the same parameters were used as for the restrained MD, except that the temperature was maintained at 310 K and no positional restraints were applied. The time step for the simulations was 0.002 ps and the compressibility $4.8x10^{-5}$ bar^{-1}. Van der Waals forces were treated using a 1.2 nm cutoff. Long-range electrostatic forces were treated using the particle mesh Ewald method (PME) (Darden et al. 1993a).

5.2.3 Analysis

The analysis of the simulations was performed using the analysis tools provided in the Gromacs package. The root mean square deviation (RMSD) of backbone atoms, the total and potential energies were calculated. The root mean square fluctuation (RMSF) of the backbone atoms and the hydrophilic, hydrophobic and total Solvent Accessible Surface Area (SASA) were also determined. The total number of hydrogen bonds in the peptide group were quantified by counting acceptor and donor atom pairs that are not further apart than 0.35 nm (Beke et al. 2006). Secondary structure analysis used DSSP (Kabsch and Sander 1983). All molecular graphical presentations were created by VMD (Humphrey et al. 1996) and/or UCSF Chimera (Pettersen et al. 2004a) packages. The standard deviation of every given value is shown in between brackets.

5.3 Results and discussion

To more clearly present the results obtained with our simulations, we have divided our system into two regions. The first region encompasses the residues 1 to 17, which is very likely to be a region with a large degree of flexibility. We will refer to this region as the "disordered region" (DR). The second region comprises the residues 18 to 42, which is the β-sheet region (βR). The βR presents a β-strand-turn-β-strand motif (hook-like or hairpin shape) that contains two intermolecular, parallel, in-register β-sheets that are formed by residues 18-26 (β1) and 31-42 (β2) connected by a turn formed by residues 27-30(Luhrs et al. 2005) (FIGURE 5.1). FIGURE 5.2 shows the superposition of five structures collected every 2 ns of SA of the pentameric system, which form the starting structures of the five independent simulations performed (denoted strands A-E). In FIGURE 5.2, a high degree of mobility of the DR is clearly visible. A similar result was observed for the trimeric system. Using the final structures obtained by the SA protocol as starting structures for the MD simulations, we initially generated 20 ns trajectories for each of the strands. Although the potential energies of the systems quickly equilibrate over a period of 100 ps (see FIGURE 5.3S in APPENDIX A), it became clear that 20 ns is too short to reach equilibrium in the overall structural properties of the aggregates, e.g.: β-helix formation.

Therefore we extended two of the simulations, for both the trimeric and the pentameric system, to 100 ns. The first 20 ns of these simulations is considered equilibration time. The results described and discussed in the remaining part of this paper are mainly based on the extended simulations, corresponding to string E, nevertheless, strings A-D have shown similar results. FIGURE 5.3 shows snapshots of the trimeric and pentameric aggregates at 0 and 100 ns of simulation. Top and lateral views are shown.

The average values of the properties (e.g. RMSD and angles) are calculated only considering the last 80 ns of the simulations. FIGURE 5.4 displays the evolution of RMSDs and RMSFs for simulations E. As a general feature it can be observed that the trimeric system compared to the pentameric form displays a higher flexibility. FIGURES 5.4A and 5.4C shows the evolution of the RMSD for the DR and the βR (and its subdivisions; β1, Turn and β2) for simulations E3 and E5. The portions β1 and Turn showed the higher

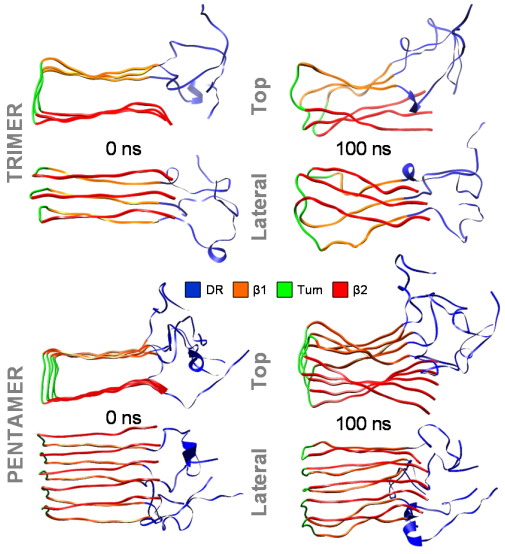

FIGURE 5.3: Snapshots at 0 and 100 ns of simulation of the trimeric and pentameric aggregates. Top and lateral views are shown.

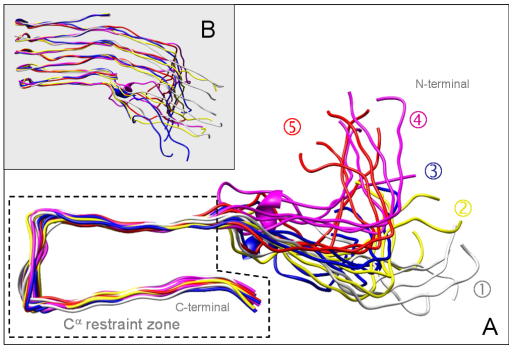

FIGURE 5.2: Overlapped stereoviews of 5 configurations collected every 2 ns of simulation from the SA of the pentameric aggregate. (**A**) Top view indicating the Cα's position restraint zone. (**B**) Lateral view.

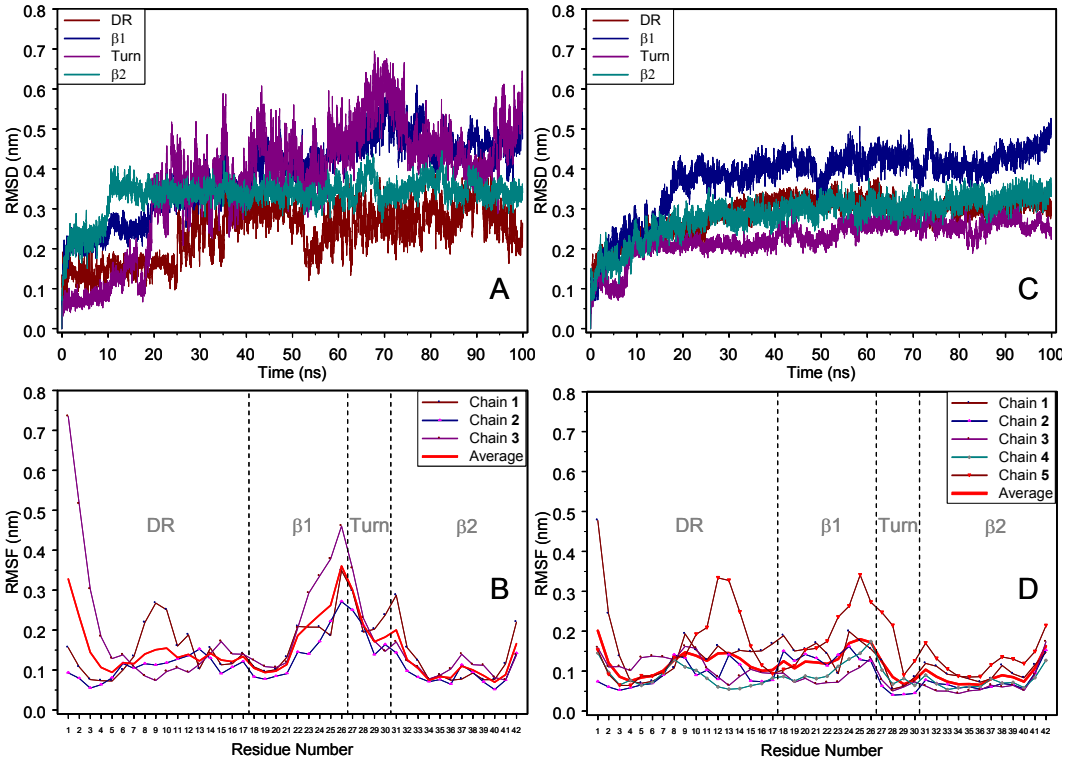

Figure 5.4: C^{α} Root Mean Square Deviation (RMSD) and Root Mean Square Fluctuation as a function of time and (RMSF) plotted against the number of residues for; (**A** and **B**) trimeric aggregate and (**C** and **D**) pentameric aggregate.

fluctuations of RMSD. This flexibility can also be appreciated in figures 5.4B and 5.4D which show the RMSF values per residue per chain. It was observed in all simulations (strings A-E) and as a general feature, that the trimeric aggregate is structurally more flexible than the pentamer.

This fact may be attributed to the higher degree of packing that a pentameric aggregate has in comparison with the trimeric one. Especially in the case of the trimeric aggregate, generally large fluctuations in RMSD occurred for the β1 and Turn portions with an average value of 0.43 (0.06) and 0.44 nm (0.08), respectively. On the other hand, it is interesting to note that the β2 portion reached an average RMSD value of 0.34 nm (0.02) after ~12 ns of simulation (figure 5.4A). This can be correlated with the formation of a β-helix structure in this portion of the aggregate. Nevertheless, in the case of pentameric aggregates generally no large RMSD fluctuations were observed. For pentamers the largest RMSD value was observed for the β1 portion with 0.41 nm (0.03), while the turn portion revealed the smallest RMSD value of 0.24 nm (0.03). The β2 portion showed an average RMSD value of 0.30 nm (0.03) (figure 5.4C) which was smoothly reached after 20 ns of simulation, and which can be attributed to the formation of a β-helix structure in this portion of the aggregate. A good correlation with what was observed for RMSD profiles can be appreciated in figures 5.4B and 5.4D that show the RMSF values for each portion of the trimeric and pentameric aggregate respectively. The highest RMSF values were observed for amino acid residues located in the DR, β1 and turn portions for the trimeric aggregate, while for the pentameric aggregate this was mainly seen in DR and β1 portions (figures 5.4B and 5.4D). Interestingly, in the vicinity of each Gly residue (residues 9, 25, 29, 33, 37 and 38) RMSF values increased due to

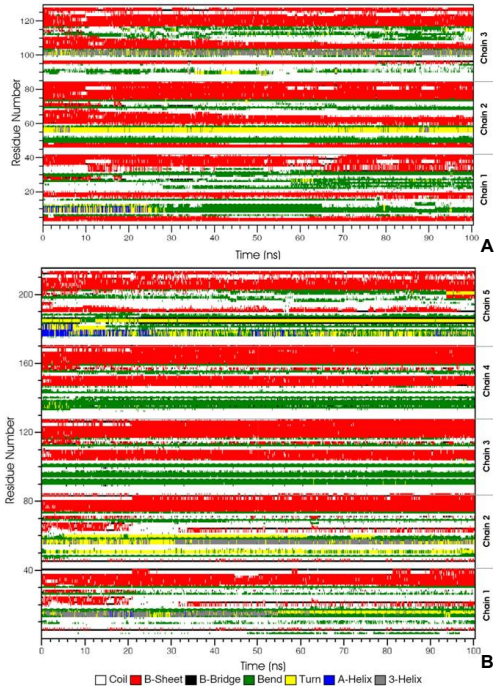

Figure 5.5: Change in the secondary structure during molecular dynamics simulation for both trimeric (**A**) and pentameric (**B**) model systems.

the natural lack of side chains of this amino acid residue. It is worth noting that the lowest RMDF values, in all simulations for both trimeric and pentameric aggregates, were observed for those amino acid residues located in the β2 portion.

figure 5.5A and 5.5B, illustrate the temporal development of the secondary structure content for the trimeric and pentameric aggregates, along the 100 ns trajectory. In table 5.2 the secondary structure content for the DR and βR is summarized. For all simulations, both β1 and β2 portions are stable at room temperature for the duration of the simulations. Even peptides located at the ends of the aggregate present stable β-strand regions, with the occasional loss of β-sheet content in the β1 portion. A small content of α-helix and 3_{10}-helix structures is infrequently observed for the DR. These kinds of helices are notably present with peptides at the edge of the aggregate. As a general phenomenon, the loss of structure is more pronounced in the trimeric aggregates, indicating

Table 5.2: Summarized average percentage of the secondary structural composition of the different regions and portions of the Aβ aggregates in solution. The average values here shown are calculated over the last 80 ns of simulation.

System	Secondary Structure	DR	βR		
			β1	Turn	β2
Trimeric	Extended[a]	15.1(3.1)	24.4(7.0)	0.0	63.1(7.7)
	Helical[b]	4.5(2.9)	0.0	0.0	0.0
	Bend[c]	28.3(4.7)	7.4(4.0)	0.8(3.3)	0.5(1.0)
	Coil[e]	52.4(4.5)	68.2(6.4)	99.2(3.4)	36.4(7.8)
Pentameric	Extended[a]	5.2(1.3)	29.3(5.3)	6.5(5.8)	63.7(4.4)
	Helical[b]	4.4(3.1)	0.00	0.00	0.00
	Bend[c]	36.1(3.6)	0.6(1.1)	0.7(2.3)	0.00
	Coil[e]	54.2(2.1)	70.1(5.5)	92.7(6.1)	36.3(4.4)

[a] Extended = β-Strand + β-Bridge
[b] Helical = α-Helix + 3^{10}-Helix (3-Helix) + π-Helix (5-Helix)
[c] Bend = Turns Type I-IV + Bend
[e] Coil = Unstructured
The standard deviation is given in between brackets

that, at least at the finite lengths studied here, they are more structurally flexible than the pentamers. The loss of structure, especially of the β-strand motifs, of peptides from the aggregate ends seems to start at the β1 and in the turn portions, while the core of the aggregate comprised of the β2 portion remains largely intact. On the other hand, transient helical conformations in the *N*-terminal residues (figure 5.5) were also reported in previous fibril formation experiments and simulations (Baumketner et al. 2006; Kirkitadze et al. 2001; Massi et al. 2002; Tarus et al. 2005).

figure 5.6 shows the average inter-chain distances of the mass center of the C^{α}'s at the various regions of our systems. A large fluctuation can be appreciated for the turn portion in simulation E3, which suggests a great mobility in this portion of the aggregate. The DR showed an average value of 0.77 nm (0.04), which is also slowly reached (after ~40 ns) by the β1 portion with an average of 0.72 nm (0.09) indicating that these two parts of the molecule behave similarly with respect to inter-chain mobility.

It is interesting to note the great influence that the DR has over the β1 portion. The β2 portion showed the lowest fluctuation as compared to the other portions, and also the lowest average value of 0.42 nm (0.03) suggesting a low

inter-chain mobility and a great compactness in this portion (FIGURE 5.6A). A very similar pattern was observed for the pentameric aggregate of the β2 portion with respect to mobility and compactness. In this case an average value of 0.45 nm (0.01) was rapidly and smoothly reached (FIGURE 5.6B). On the other hand, the DR region showed a general trend towards a larger inter-chain distance (1.21 nm (0.02) for simulation E5), while the β1 portion did not follow a same pattern as the DR which we found for the trimeric aggregate. Therefore, the β1 portion in the pentameric configuration appears to be more compact (0.66 nm (0.04)) than the β1 portion of the trimeric aggregate. Interestingly, the turn portion in the pentamers showed a smaller fluctuation than the same portion in the trimers, suggesting that this as well as the β1 portion, has a lower inter-chain mobility and a higher compactness (0.53 nm (0.02)) in the pentameric aggregate. Very similar inter-chain distances in the center of mass were seen for the Ccarbonyl's and Cβ's of each portion in our system (see FIGURE 5.4S in APPENDIX A). These results, especially the behavior of the β2 portion, are in good agreement with the experimental findings of Balbach et al. (Balbach et al. 2002) for a parallel β-sheet organization, who reported the nearest-neighbor intermolecular distances of 4.8±0.5 Å for carbon sites. At this point we emphasize the high stability observed for the β2 portion, which suggests a possible mechanism for fibril elongation as was previously reported (Buchete and Hummer 2007). Hypothetically, in a first step, the initial monomer addition at the end of a growing aggregate would be driven by strong hydrophobic interactions stabilizing the β2 portion. In a second stage, the less stable β1 portion would form, finally followed by the more flexible turn with its relatively hydrophilic residues adopting the fibril conformation. On the other hand, it was also observed for $A\beta_{42}$ monomers in solution that the sequence $I^{31}IGLMVGGVVIA^{42}$ (namely, the β2 portion) may be responsible for the higher propensity of this peptide to form amyloids (Sgourakis et al. 2007).

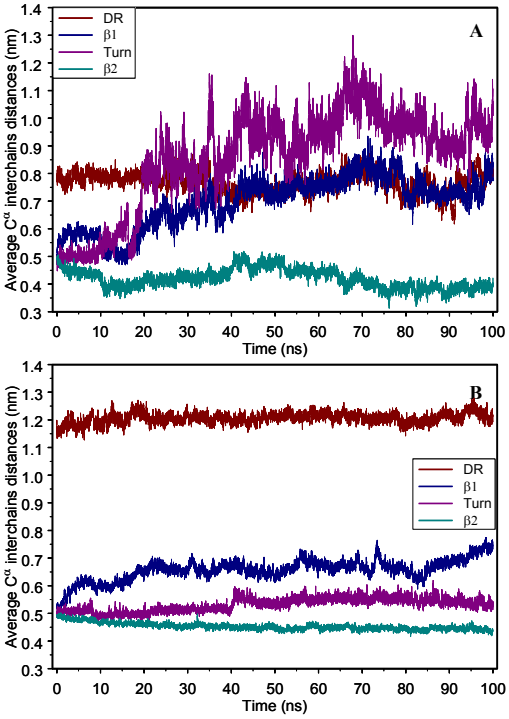

FIGURE 5.6: Average inter-chain distances of the mass center of the Cα's versus time of the different regions and portions of the trimeric (**A**) and pentameric (**B**) system.

Consistent with ssNMR data on amyloid fibrils (Petkova et al. 2002; Petkova et al. 2005; Petkova et al. 2006), all our starting fibril conformations have Asp^{23}/Lys^{28} salt bridge contacts in the loop region. Other studies also showed that charged residues are important for the dynamics of protein aggregation and the stability of β-sheet structures (Dima and Thirumalai 2004; Ma and Nussinov 2006; Massi et al. 2002; Thirumalai et al. 2003). Consistent with previous results (Buchete and Hummer 2007; Buchete et al. 2005), our trajectories of both trimeric and pentameric aggregates reveal that the Asp^{23}/Lys^{28} bridges are maintained at 310 K. FIGURE 5.7 shows the distance between the center of mass of the carboxyl group of Asp^{23} and the center of mass of the NH_3^+ group of Lys^{28}, as well as a simplified image of the starting configuration and the configuration after 100 ns of simulation for the pentameric case.

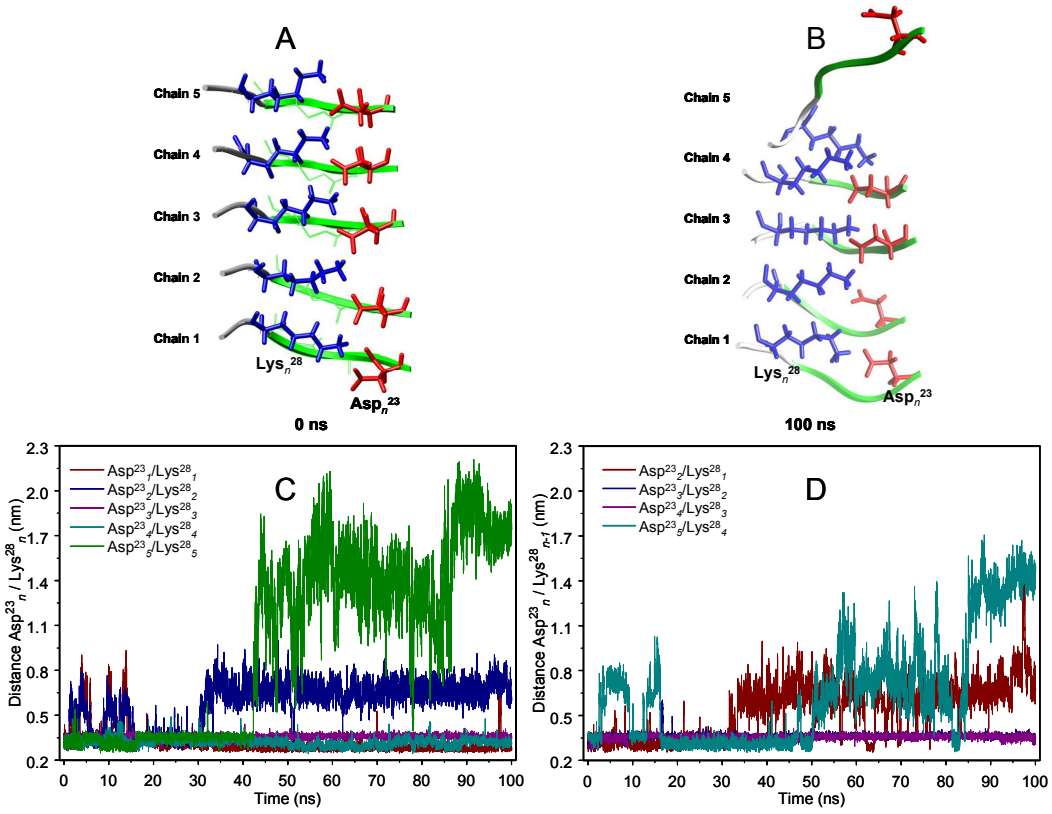

Figure 5.7: A simplified image of the starting configuration (**A**) and the final configuration (**B**) after 100 ns of the interaction Asp^{23}/Lys^{28} for the pentameric system is shown. The distance between the center of mass of the carboxyl group of Asp^{23} and the center of mass of the NH_3^+ group of Lys^{28} versus time for the interactions Asp$^{23}_n$/Lys$^{28}_n$ (**C**; intra-chain salt-bridge) and Asp$^{23}_n$/Lys$^{28}_{n-1}$ (**D**; inter-chain salt-bridge), where *n* stands for the peptide chain number, is also shown.

It can be appreciated that the positive and negative charges alternate along the fibril axis as in a one-dimensional ionic crystal. We observed that both trimeric and pentameric aggregates form intra-chain salt bridges (Asp$_n^{23}$/Lysn^{28}) and inter-chain salt bridges (Asp$_n^{23}$/Lys$_{n-1}^{28}$), where n stands for the chain number. Moreover, the majority of the salt bridges were maintained during the whole simulation time reaching an average distance between the center of mass of the carboxyl group of Asp^{23} and the center of mass of the NH_3^+ group of Lys^{28} of 0.32 nm (0.03) for simulation E5, and of 0.38 nm (0.19) for simulation E3. Also, as illustrated in FIGURE 5.6 it can be concluded that for those salt bridges where Asp$_2^{23}$ took part in, an average distance of 0.58 nm (0.15) was reached after approximately 32 ns, which was kept until the end of the simulation. On the other hand, salt bridges involving Asp$_5^{23}$ were broken (~43 ns, Asp523/Lys528, FIGURE 5.7C) or displayed large fluctuations (~50 ns, Asp$_5^{23}$/Lys$_4^{28}$, FIGURE 5.7D) since after a certain amount of simulation time this negatively charged amino acid residue was totally solvated by molecules of water. FIGURE 5.5S, in APPENDIX A, shows the distance between the center of mass of the carboxyl group of Asp^{23} and the center of mass of the NH_3^+ group of Lys^{28} for the trimeric system. In this case, the intra-chain salt bridges and the inter-chain salt bridges were formed and broken over the entire simulation time. In case of trimeric aggregates large fluctuations occurred, salt bridges being formed and broken over the entire simulation time, which may explain, at least in part, the high-

er flexibility of the trimeric system compared to the pentameric conformation (FIGURE 5.5S in APPENDIX A). Also, as reported before for $A\beta_{40}$ fibrils (Buchete and Hummer 2007; Buchete et al. 2005), we find narrow water channels solvating the Asp[23]/Lys[28] salt bridges within the aggregates. Indirect experimental evidence for interior hydration of Aβ fibrils comes from differential scanning calorimetry (Sasahara et al. 2005), although ssNMR data do not indicate large structural differences between lyophilized and wet fibrils (Paravastu et al. 2006; Petkova et al. 2006). Visual inspection reveals the formation of narrow water channels solvating the interior Asp[23]/Lys[28] salt bridges into the aggregates. Recent simulations of fibrils with up to 32 Aβ16–22 peptides in antiparallel β-strands have also shown similar water channels hydrating the Lys[16]/Glu[22] side chains (Rohrig et al. 2006). In several instances we noted an exchange in the salt bridge partners from the initial Asp[23]/Lys[28] pair to Glu[22]/Lys[28] as the end peptides begin to dissociate from the aggregates (FIGURE 5.6S). FIGURE 5.6S in APPENDIX A displays the distance between the center of mass of the carboxyl group of Glu[22] and the center of mass of the NH_3^+ group of Lys[28] for the intra-chain salt bridges (Glu_n^{22}/Lys_n^{28}) and the inter-chain salt bridges (Glu_n^{22}/Lys_{n-1}^{28}) for the pentameric case. The presence of Glu[22]/Lys[28] salt bridges has been suggested for small Aβ peptide aggregates, Aβ monomers in solution (Baumketner et al. 2006; Borreguero et al. 2005; Cruz et al. 2005; Lazo et al. 2005), and $A\beta_{40}$ fibrils (Buchete and Hummer 2007). The Glu[22]/Lys[28] ion pair might play an important role in the aggregate elongation (Buchete and Hummer 2007). Overall, based on our own and other previous studies the main driving force for fibril elongation appears to be the formation of *C*-terminal β-sheets (our β2 portion). This hypothesis seems to be supported by recent experiments showing that perturbing the hydrogen bonds in the β1 and β2 portions through selective *N*-methylation affects both fibril growth and structure (Sciarretta et al. 2006a). Disrupting the backbone hydrogen bonds of the β1 portion resulted in relatively slow growth of fibrils with a blurred boundary, while derangement of the β2 hydrogen bonds, had less effects on fibril growth and yielded fibrils with a sharply defined surface. These experimental results are consistent with our simulation findings.

FIGURE 5.8 displays the formation of a β-helix structure occurring especially on the β2 portion of the pentamers. In order to quantify the twist of this β-helix motif, two dihedral angles were defined, namely γ and δ. Using as a pivot the amino acid residue Val[36], which encompasses the β2 portion of our model, the definition of the γ angle involves the Cα's of residues Ile_n^{31}, Val_n^{36}, Val_{n-1}^{36} and Ile_{n-1}^{31}, while the definition of the δ angle involves residues Ala_n^{42}, Val_n^{36}, Val_{n-1}^{36} and Ala_{n-1}^{42}. FIGURES 5.8A and 5.8B show a spatial view of the β2 portion at 0 ns and 100 ns of simulation time respectively. Top views (FIGURES 8A1 and 8B1) and lateral views (FIGURES 8A2 and 8B2) are also shown. FIGURES 8C and 8D illustrate the temporal development of the γ and δ angles, respectively.

The β-helix is a plausible structural motif for amyloid fibrils, since it is primarily a β-sheet structure with the proper cross-β orientation(Esposito et al. 2006; Ferguson et al. 2006; Zheng et al. 2006a; Zheng et al. 2006b) and known to occur in bona fide proteins. As described above, in our model of $A\beta_{42}$ aggregates in solution the formation of a β-helix structure occurred especially on the β2 portion (FIGURE 5.8). The model used by us is an elaboration of the classical cross-β molecular structure, which permits the incorporation of the favorable twisted β-sheet structures. This kind of helical structures enables the hydrogen bonding between the β-strands to be extended over the total length of the amyloid fibrils, thereby accounting for their characteristic rigidity and stability(Tycko 2004). Increased fibril twisting could be caused by the loss of directional hydrogen bonding, and a gain in packing interactions(Chothia and Janin 1982).

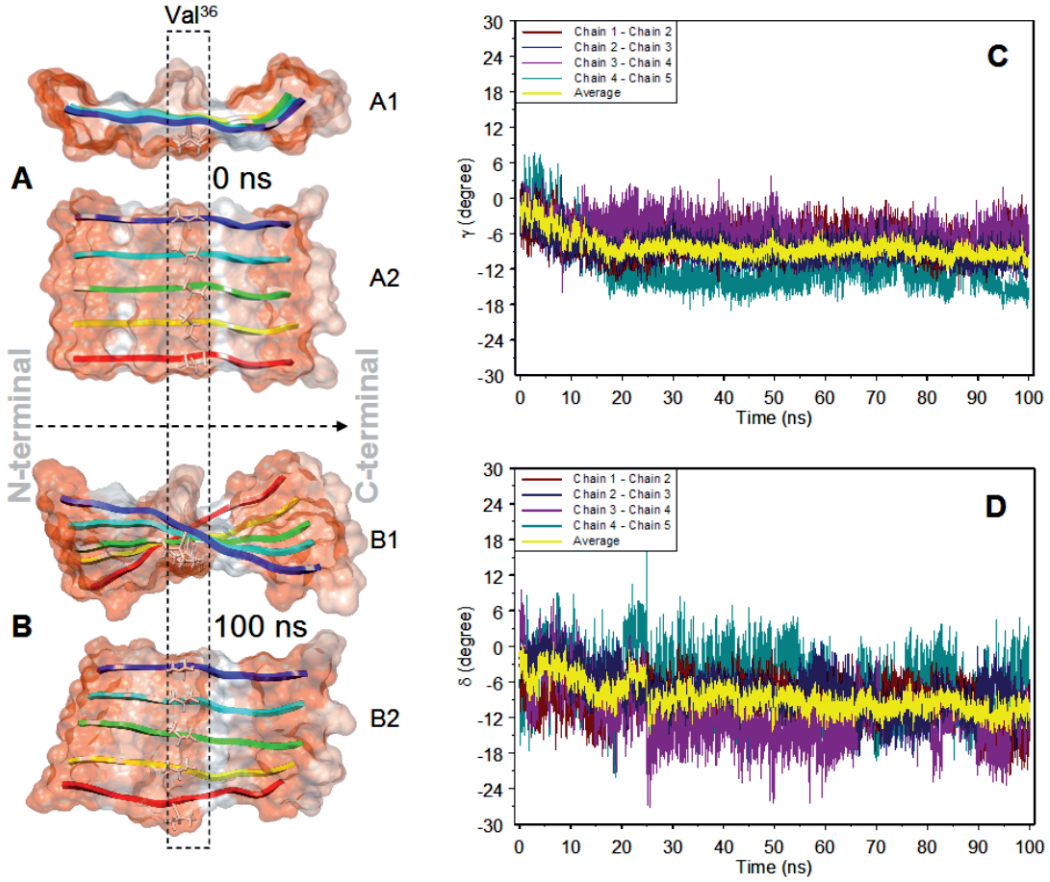

Figure 5.8: Simplified images of the starting configuration (**A1**, top view and **A2** lateral view) and the final configuration (**B1**, top view and **B2** lateral view) after 100 ns of the β2 portion for the pentameric system is shown. The γ (**C**) and δ (**D**) dihedral angles versus time are also shown. The definition of the γ dihedral angle involves the Cα's of residues Ilen^{31}, Valn^{36}, Val$_{n-1}{}^{36}$ and Ile$_{n-1}{}^{31}$, while the definition of the δ dihedral angle involves residues Ala$_n{}^{42}$, Val$_n{}^{36}$, Val$_{n-1}{}^{36}$ and Ala$_{n-1}{}^{42}$, where *n* stands for the number of the peptide chain.

A schematic definition of those angles is shown in figure 5.8A. In general, after approximately 20 ns of simulation an average value of -8.95° (0.97) and -9.40° (1.93) was reached for γ and δ, respectively. In figure 5.8C a great fluctuation for the δ angle can be observed. This may be caused by the fact that the definition of this angle involves the Cα of the terminal residues Ala42, which are in direct contact with the solvent and therefore leading to a greater mobility. Since twisted β-sheets optimize the hydrogen bonds, side-chain stacking, and electrostatic interactions, it is commonly accepted that twisted sheets are more stable than flat ones. This result is in good agreement with those reported by Periole et al. that shows the formation of a cross-β by the peptide GNNQQNY with a twist ranging from 0 to 12 degrees per peptide around its axis when fully solvated (Periole et al. 2009).

Although our model is a full-length model for $A\beta_{42}$ aggregate in solution, it is of interest to compare our results to other proposed truncated and/or full-length models for $A\beta_{40}$ structures. The so called Tycko's model(Petkova et al. 2006), and the LECB model(Ma and Nussinov 2002) are similar to our model, specifically, regarding the hairpin shape of the aggregates. There

is a slight difference between our model, and the Tycko's model. Our model forms a hydrophobic core with Leu[34] facing the interior of the aggregate in the β2 portion, whereas in Tycko's model the Leu[34] faces outside. In our model it was observed that the residues Leu[34] and Val[36] of the portion β2 formed an inner hydrophobic core in the aggregates. Regarding this matter, our model is more similar to the LECB model than Tycko's. The internal Asp[23]/Lys[28] salt bridge interaction is supported by experimental and theoretical data(Luhrs et al. 2005; Ma and Nussinov 2002, 2006; Petkova et al. 2002; Petkova et al. 2006). This interaction has been observed in our model, as well as in the above mentioned models. We note that the position of the turn in our model differs with the position of the same moiety in the LECB model. The turn portion encompasses the residues Asn[27]-Ala[30] in our model, while the same portion encompasses the residues Val[24]-Asn[27] in the LECB model. As a result of this organization the Asp[23]/Lys[28] salt bridge shows a slight difference between the LECB model and our model. In the LECB model the Asp[23] residue is located in one of the β-strands of the peptide, and the Lys28 residue is located in the other β-strand segment, therefore, the Asp[23]/Lys[28] interaction occurs in between the two β-strand portion of this model. In our model, the Asp[23] is located in the β1 portion, while the Lys[28] is located in the turn portion. A closely related structural model for $A\beta_{40}$ fibrils has been proposed by Wetzel et al.(Shivaprasad and Wetzel 2004; Williams et al. 2004). In agreement with our model, the Wetzel's model places the side chains of Phe[19], Ile[32], Leu[34], and Val[36] in the interior of a single molecular layer. In contrast to our model, side chains of Asp[23] and Lys[28] are on the exterior of a single molecular layer. A highly similar molecular organization has been described for another peptide with amyloidogenic properties. The molecular structural organization of the CA150.WW2 protofilament(Ferguson et al. 2006) is stabilized by interdigitated hydrophobic regions, as well as, by the presence of a intra-chain salt bridge between the Glu7 and Arg24 in a parallel β-sheet arrangement. This structural model has similarities to those reported for aggregates of the Aβ1–40(Petkova et al. 2002), Aβ1–42 peptides(Luhrs et al. 2005) and the structure reported for the peptide Sup35(Zheng et al. 2006b). Beyond the stabilization effect due to the long-range interactions (e.g.: salt bridges formation) depending on sequence composition, length, and environmental conditions, the interdigitating hydrophobic side chains interactions of the aggregates seems to be a commonly recurring feature of these aggregates.

In summary, the contributions of the different structural elements of the full-length $A\beta_{42}$ aggregates in solution to their stability and conformational dynamics were explored. Using multiple 20–100 ns long MD simulations of fibril systems of ~60,000 atoms, we studied aggregate models that differ in the quantity of peptide chains, notably pentameric and trimeric aggregates. We found that our models are stable at the temperature of 310 K, and converge towards an interdigitated side-chain packing for intermolecular contacts within the two parallel β-sheet regions of the aggregates, β1 (residues 18-26) and β2 (residues 31-42). In spite of the fact that those chains at the edge of the aggregates showed a higher mobility than those chains near to the aggregate core, the β-sheet region kept its arrangement (β1-turn-β2 / hairpin shape) during the entire simulation time. The β1 portion showed to be more flexible than the β2 portion, which may well be induced by the proximity of the disordered region to the β1 portion. This provides good arguments to study the full-length Aβ models, since the dynamic behavior of a determinate portion of the aggregate can affect the behavior of its surroundings. The Asp[23]/Lys[28] salt bridges maintain a stable and relatively rigid interdigitated structure. However, during the initial stages of fibril dissociation the Asp[23]/Lys[28] contacts in Aβ peptides at the aggregates ends can break to form the competing Glu[22]/Lys[28] interaction. Thus, it suggests

that the loss of Glu^{22}/Lys^{28} contacts could be an important indicator for the transition of the Aβ peptides from their solution structures towards the aggregated conformations (Baumketner et al. 2006; Buchete and Hummer 2007). Our whole molecule simulations reveal that the β-strand twist is a characteristic element of Aβ aggregates, permitting a compact, interdigitated packing of side chains from neighboring β-sheets. The β2 portion formed a very well organised β-helix, whereas the β1 portion did not reach such a high level of organization although it maintained its β-sheet conformation.

5.4 Conclusions

This study demonstrates the importance of studying the full-length Aβ aggregates in solution in order to have a more general view of how each part of the aggregate influences the conformational behavior of the whole system. Moreover, these simulations suggest that the hydrophobic core comprising the β2 portion of the aggregate is a crucial stabilizing element in the process of aggregation and possibly in the elongation of Aβ aggregates. For that reason the β2 portion appears to be a promising target for further drug-design based on the structure-stability information, such as new potential "amyloid inhibitors" capable to interact specifically with this portion of the aggregates. ▪

Acknowledgements

The studies described in this paper were partially performed under the Project HPC-EUROPA (RII3-CT-2003-506079), with financial support of the European Community - Research Infrastructure Action of the FP6 Programme. The authors thank Mrs. Laura Leistikow of HPC-EUROPE for assistance and Ferenc Bogár, Gábor Paragi and Máté Labádi for their technical support and Aldo Rampioni and Xavier Periole for helpful discussions. M.M is recipient of a Fellowship of the University of Groningen. R.D.E. is member of CONICET (Argentina).

"I learn to bribe, I learn to say please.
Oh won't you lick the pavement for me.
I learn to bribe, I learn to say please.
I like you best when you're on your knees."
(Garbage)

06

"Still here"

oil on paper (320x450 mm)

M.F. Masman 2010

Chapter 6

C6

Leu-pro-tyr-phe-asp-NH_2 neutralizes aβ-induced memory impairment & toxicity

Ivica Granic, Marcelo F. Masman, Kees C. Mulder, Ingrid M. Nijholt, Pieter J.W. Naude, Ammerins de Haan, Emőke Borbély, Botond Penke, Paul G.M. Luiten & Ulrich L.M. Eisel

Journal of Alzheimer's Disease (2010), 19:991-1005.

Abstract

Misfolding, oligomerization and aggregation of the amyloid-beta (Aβ) peptide is widely recognized as a central event in the pathogenesis of Alzheimer's disease (AD). Recent studies have identified soluble Aβ oligomers as the main pathogenic agents and provided evidence that such oligomeric Aβ aggregates are neurotoxic, disrupt synaptic plasticity and inhibit long-term potentiation (LTP). A promising therapeutic strategy in the battle against AD is the application of short synthetic peptides which are designed to bind to specific Aβ-regions thereby neutralizing or interfering with the devastating properties of oligomeric Aβ species. In the present study we investigated the neuroprotective properties of the amyloid sequence derived pentapeptide Leu-Pro-Tyr-Phe-Asp-NH_2 (LPYFDa) *in vitro* as well as its memory preserving capacity against $Aβ_{42}$-induced learning deficits *in vivo*. *In vitro* we could show that neurons in culture treated with LPYFDa are protected against $Aβ_{42}$-induced cell death. Moreover, *in vivo* LPYFDa prevented memory impairment tested in a contextual fear conditioning paradigm in mice after bilateral intrahippocampal $Aβ_{42}$ injections. We thus showed for the first time that an anti-amyloid peptide like LPYFDa can preserve memory by reverting $Aβ_{42}$ oligomer induced learning deficits.

6.1 Introduction

Progressive neurodegeneration and cognitive decline are typical features of Alzheimer's disease (AD), the most common form of dementia (Haass and Selkoe 2007). Besides the formation of neurofibrillary tangles, it is widely acknowledged that the aggregation of amyloid β (Aβ) initiates a complex series of events that ultimately results in neuronal cell death particularly in forebrain regions, which is paralleled by the cognitive and behavioral decline that is characteristic for pathogenesis of AD. Aβ is generated by sequential proteolytic cleavage from the amyloid-β precursor protein (APP) by beta-, and gamma-secretases (amyloidogenic processing). Alternatively APP can be cleaved by α-secretase within the Aβ sequence which prevents the generation of Aβ peptide. Once released, Aβ due to its physico-chemical properties has the strong tendency to misfold, oligomerize and to aggregate into fibrils and plaques (Wisniewski et al. 1997).

Although amyloid plaques represent a major hallmark of AD, they correlate poorly with the progression of the disease (Forman et al. 2007). Interestingly, more recent studies have identified soluble Aβ–oligomer assemblies as the main pathogenic agents which, in contrast to plaques, do correlate well with the mental decline observed in AD patients (Haass and Selkoe 2007; Lue et al. 1999; McLean et al. 1999; Naslund et al. 2000; Wang et al. 1999). Furthermore, soluble Aβ oligomers have been shown to be neuro- and synaptotoxic, and to inhibit long-term potentiation (LTP) (Chang et al. 2006; Chapman et al. 1999a; Shankar et al. 2008; Walsh and Selkoe 2007; Wasling et al. 2009). Acute application of oligomeric Aβ leads to internalization of glutamatergic AMPA and NMDA receptors and finally to synaptic downscaling (Hsieh et al. 2006; Shankar et al. 2007a). However, it should be appreciated that next to its pathological properties, Aβ notably in very low physiological concentrations, may have important roles in synaptic plasticity and normal brain functioning (Pearson and Peers 2006; Puzzo et al. 2008; Wasling et al. 2009). The endogenous level of Aβ in the brain is regulated by synaptic activity *in vivo*, suggesting a dynamic feedback loop involving APP metabolism and Aβ that may modulate synaptic activity (Haass and Selkoe 2007). Recently, Garcia-Osta and coworkers showed that depletion of endogenous Aβ by a single intrahippocampal (i.h.) administration of anti- Aβ -antibody leads to disrupted memory retention in rats (Garcia-Osta and Alberini 2009). During the pathogenesis of AD the equilibrium of Aβ generation and Aβ clearance is disturbed, which eventually leads to elevated Aβ levels, increased Aβ aggregation and impaired memory function (Wasling et al. 2009).

Multiple therapeutic strategies have been developed since the second half of the previous century (Harkany et al. 2000). Unfortunately, most of the currently available therapies target only the symptoms since acting on presumed downstream neurotoxic pathogenic mechanisms without tackling the cause and thus hardly able to affect the progression of the disease. Experimental data from animal studies using immunotherapy in order to remove Aβ from the brain were highly promising (Schenk et al. 1999). However, clinical trials with active immunization against Aβ were halted due to severe brain inflammation and premature death of several patients (Hock et al. 2003; Orgogozo et al. 2003b).

Consequently, as a therapeutic strategy compounds were developed that could inhibit or delay the development of Aβ aggregation, fibrillization, and/or plaque formation and were thus potentially capable of protecting neurons from Aβ toxicity. As part of this approach small peptides derived from the Aβ sequence were designed such as the pentapeptide Leu-Pro-Tyr-Phe-Asp-NH_2 (LPYFDa) which seemed to offer a promising starting point to develop potential drugs that can somehow revert the devastating impact of Aβ

aggregates. The advantage of such compounds, in comparison to other putative therapeutic approaches for AD such as vaccination, is that they specifically target the abnormal conformation of Aβ without interfering with any possible physiological function of the soluble, monomeric Aβ peptide.

There have been numerous attempts to develop treatments developed to interfere with various key steps in the amyloidogenic process. Promising putative treatments may be those designed to inhibit steps that precede Aβ peptide aggregation, by blocking production of the toxic soluble Aβ oligomers in the first place, or by reversing, somehow, the toxic effect of these oligomers.

In the present study we established an *in vivo* model in the mouse for Aβ induced memory impairment through a single bilateral injection of oligomeric $A\beta_{42}$ into the hippocampus and explored in this model whether LPYFDa can be beneficial against the Aβ-induced cognitive deficits. Furthermore, we investigated the neuroprotective properties of Aβ-derived synthetic pentapeptide Leu-Pro-Tyr-Phe-Asp-NH_2 (LPYFDa) (Datki et al. 2004; Juhasz et al. 2009; Szegedi et al. 2005) against the neurotoxic effects of soluble $A\beta_{42}$ oligomers in cultured mouse primary cortical neurons (PCN). Finally, we employed molecular modeling and docking experiments to reveal part of the putative mechanism of action of these peptides.

6.2 Material and methods

6.2.1 Compounds

The beta-sheet breaker LPYFDa was synthesized in our laboratories by a solid-phase procedure involving the use of Merrifield resin and Boc chemistry. Purity control and structure verification were carried out by amino acid analysis and mass spectrometry as previously described (Zarandi et al. 2007). The control peptide (scrP), which is a scrambled version of the LPYFD peptide (Pro-Asp-Tyr-Leu-Phe-NH_2), and Aβ1–42 ($A\beta_{42}$) were purchased from EZBiolab Inc. (Carmel, USA). Anti-Aβ antibody (6E10) was obtained from Covance (Emeryville, USA). Other compounds used in this study were purchased from Invitrogen (Carlsbad, USA) or Sigma-Aldrich Corporation (St. Louis, USA).

6.2.2 Preparation of Aβ-oligomers

Oligomeric $A\beta_{42}$ was prepared as was described by Dahlgren and colleagues (Dahlgren et al. 2002). In short, the synthetic $A\beta_{42}$ peptide was initially dissolved in 1,1,1,3,3,3-hexafluoro-2-propanol (HFIP) to a concentration of 1 mM. The peptide solution was divided into aliquots and the HFIP removed by evaporation under vacuum (SpeedVac; Savant Instruments, Hyderabad, India). The dry peptide films were stored at -20°C until further processing. Before use, the dry film $A\beta_{42}$ was dissolved in anhydrous DMSO to 5 mM followed by bath sonication (Decon, Hove Sussex, UK) for 10 min, subsequently diluted in neurobasal medium to a final concentration of 100 μM (stock solution) and incubated at 4°C for 24 h to enable $A\beta_{42}$ oligomerization. The aggregation state and the secondary structure of the oligomeric $A\beta_{42}$ preparation was examined by sodium dodecyl sulfate (SDS) - PAGE Western blotting and Circular Dichroism (CD) spectrometry (FIGURE 6.1).

6.2.3 Gel electrophoresis and western blot analysis

Gel electrophoresis and Western blot analysis were adopted from Stine et al., 2003 (Stine et al. 2003). Briefly, unheated samples in SDS sample buffer were applied to 10-20% tris-tricine gradient gels (Bio-Rad, Munich, Germany), electrophoresed using tricine running buffer and subsequently transferred to 0.45-μm polyvinylidene difluoride membranes (Millipore, Bilerca,

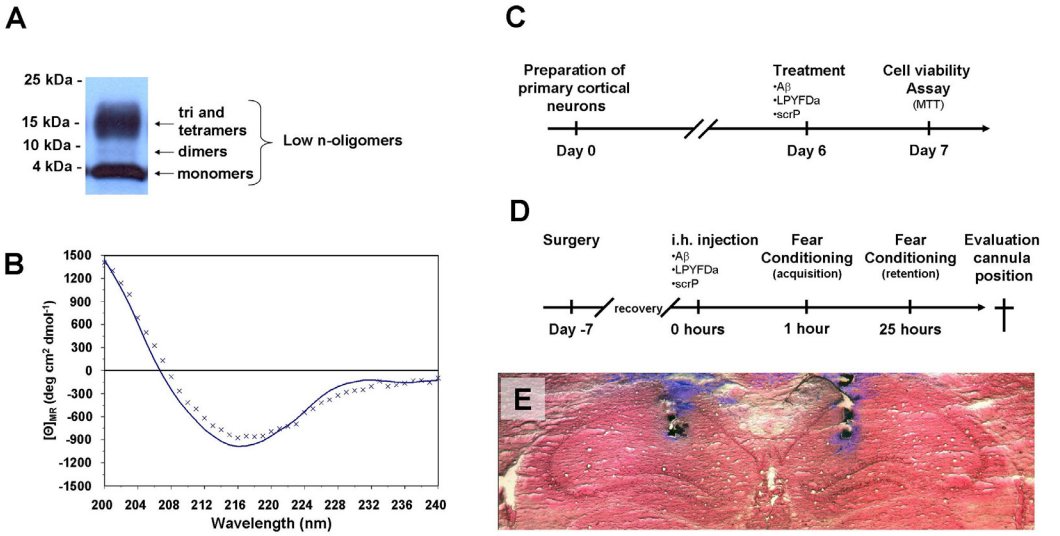

Figure 6.1: (**A**) Oligomeric preparation of $A\beta_{42}$ was examined by Western blot using the anti-Aβ antibody 6E10 (1:2000). Bands correspond to monomeric up to tetrameric forms of $A\beta_{42}$. (**B**) CD spectrum of (×) $A\beta_{42}$ in PBS after 24 hours incubation at 4 °C.(—) fitted line data using K2D2 program. (**C**) Schematic outline of the experimental procedure *in vitro*. PCN from C57BL6 mouse embryos (E14) were cultured for 6 days and then treated for 24 h with different concentrations of oligomerized $A\beta_{42}$, beta-sheet breaker peptides or combinations of both. On day 7 medium was completely exchanged and 24 h later the cell viability was assessed by an MTT reduction assay. (**D**) Schematic outline of the experimental setup *in vivo*. C57BL/6J mice were cannulated 7 days prior i.h. injection with oligomerized $A\beta_{42}$ and/or beta-sheet breaker peptides. One hour after the injection the animals were trained in a contextual fear conditioning paradigm. 24 h after the training session memory performance was assessed. Cannula position was evaluated by methylene blue injection after the behavioural test. (**E**) Representative coronal brain sections of a bilateral dorsal hippocampal (i.h.) injection with methylene blue counterstained with nuclear fast red.

USA). Membranes were blocked with 1% I-Block (Tropix, Bedford, USA) in Trisbuffered saline containing 0.0625% Tween-20. Blots were incubated with primary antibody 6E10 over night (1:2000; mouse monoclonal against Aβ residues 1–16; Covance Emeryville, USA). Immunoreactivity was detected using enhanced chemiluminescence (Pierce Biotechnology, Rockford, USA) and imaged on an Kodak X-Ray film (Eastman Kodak Company, Rochester, USA) (figure 6.1A). Molecular weight values were estimated using the PageRuler (Fermentas International, Ontario, Canada) pre-stained molecular weight marker.

6.2.4 CD spectrometry

CD measurements were performed at 25 °C on a CD Spectrometer Model 62DS (AVIV Associates Inc., Lakewood, USA) using a quartz cell of 0.1-cm pathlength. All spectra were averages of four scans; the resolution was 1 nm. The oligomerized Aβ was diluted in PBS to a concentration of 25 µM. The samples were sonicated for 10 min immediately after dissolution. CD spectra were expressed as mean residue ellipticity [Q]MR in units of deg cm2 $dmol^{-1}$, (figure 6.1B). The percentages of secondary structures were analyzed using the K2D2 program (Perez-Iratxeta and Andrade-Navarro 2008).

6.2.5 Primary cortical neuron culture

Primary cortical neurons were prepared from embryonic brains (E14) of C57Bl/6J mice. The cortices were carefully dissected, meninges were removed and the neurons separated by trituration. Cells were plated on poly-*D*-lysine pre-coated plates at a density of 1.2 x 10^5 cells/well (96 well plates). Neurobasal medium supplemented with 2% (v/v) B27-supplement, 0.5 mM

glutamine and 1% (v/v) penicillin/ streptomycin was used as a culture medium. After 48 h neurons were treated with 10 µM cytosine arabinoside for another 48 h to inhibit non-neuronal cell growth. Subsequently, the medium was completely exchanged and after 6 days of *in vitro* culture, the neurons were used for experiments.

6.2.5.1 Treatment of cells

Possible toxicity of LPYFDa, its control peptide scrP and $A\beta_{42}$ oligomers was determined by incubating neuronal cultures for 24 h with different concentrations of the peptide solutions. The neuroprotective effect of LPYFDa was assessed by incubating neurons (cultured in 96 well plates) for 24 h with 20 mM oligomeric Aβ in the presence or absence of different concentrations of LPYFDa or control peptide. After the treatment, the medium was completely exchanged, and 24 h later, the cell viability was determined by an MTT-assay (figure 6.1C). All treatments were performed in triplicates and the experiments were repeated at least two times.

6.2.5.2 Determination of cell viability by MTT-assay

Neuronal viability was determined by the colorimetric MTT [3-(4,5-dimethylthiazol-2-yl-)2,5-diphenyltetrazolium bromide] assay as described previously (Mosmann 1983). 1.25 mg/ml MTT solution was added to each well of a 96 well plate. After 2 h of incubation, cells were lysed in acidic propan-2-ol solution (37% HCl/ propan-2-ol: 1/166). The absorbance of each well was measured with an automated ELISA plate reader (Bio-Rad, Munich, Germany) at 595 nm with a reference filter at 630 nm.

6.2.6 Animals

Behavioral experiments were performed with 9–12 weeks old male C57Bl/6J mice (Harlan, Horst, The Netherlands). Individually housed mice were maintained on a 12 h light/dark cycle (lights on at 7.00 a.m.) with food (Hopefarms, standard rodent pellets) and water ad libitum. A layer of sawdust served as bedding. The animals were allowed to adapt to the housing conditions for 1–2 weeks before the experiments started. The procedures concerning animal care and treatment were in accordance with the regulations of the Ethical Committee for the use of experimental animals of the University of Groningen (DEC4668C).

6.2.6.1 Animal surgery

Double guide cannulae type C235 (Plastics One, Roanoke, USA) were implanted in the brain using a Kopf stereotactic instrument during Hypnorm/ Midazolam (10 ml/kg, i.p.) anesthesia under aseptic conditions as previously described (Nijholt et al. 2008) with anteroposterior (AP) coordinates zeroed at Bregma directed toward both dorsal hippocampi (i.h.), AP -1.5 mm, lateral 1 mm, depth 2 mm (Franklin and Paxinos 1997). Each double guide cannula with inserted dummy cannula and dust cap was fixed to the skull with dental cement (3M ESPE AG, Seefeld, Germany). Administration of 1 mg/ml finadyne (2.5 mg/kg s.c.) before the surgery served as analgesic. The animals were allowed to recover for 6–7 days before the behavioral measurements started.

6.2.6.2 Intrahippocampal injections

Bilateral i.h. injections were performed under short isofluran anesthesia using a Hamilton microsyringe fitted to a syringe pump unit (TSE systems, Bad Homburg, Germany) at a constant rate of 0.3 µl/min (final volume: 0.3 µl per side). The amount of injected $A\beta_{42}$ was of 15, 30 or 60 pmol and LPYFDa as well as the control peptide scrP in an amount of 150 pmol into the dorsal hippocampus. PBS (pH 7.5) served as vehicle. One hour after the injection the animals were subjected to a training session in a fear conditioning paradigm (figure 6.1D). The number of animals per group varied from 5 to 9.

6.2.6.3 Fear conditioning

Fear conditioning was performed in a plexiglas cage (44 x 22 x 44 cm) with constant illumination (12 V, 10W halogen lamp, 100–500 lux). The training

(conditioning) consisted of a single trial. Before each individual mouse entered the box, the box was cleaned with 70% ethanol. The mouse was exposed to the conditioning context for 180 s followed by a scrambled footshock (0.7 mA, 2 s, constant current) delivered through a stainless steel grid floor. The mouse was removed from the fear conditioning box 30 s after shock termination to avoid an aversive association with the handling procedure. Memory tests were performed 24 h after fear conditioning. Contextual memory was tested in the fear conditioning box for 180 s without footshock presentation. Freezing, defined as the lack of movement except for respiration and heart beat, was assessed as the behavioral parameter of the defensive reaction of mice by a time-sampling procedure every 10 s throughout memory tests. In addition, mean activity of the animal during the training and retention test was measured with the Ethovision system (Noldus, Wageningen, The Netherlands).

6.2.7 Histology

Immediately after the behavioral test mice were injected i.h. with methylene blue solution during sodium-pentobarbital anesthesia (0.1 ml/ 10g, i.p.). Brains were removed and serially sectioned at 50 µm. Sections were stained on glass for 5 min in 0.1% nuclear fast red solution. To identify the location of the injection, sections were analyzed using light microscopy. Only data from animals in which the proper intrahippocampal site of injection was confirmed, were evaluated (figure 6.1E).

6.2.8 Molecular modeling

6.2.8.1 Stochastic conformational search. Edmc calculations

The conformational space was explored using the method previously employed by Liwo et al. (Liwo et al. 1996a) which includes the electrostatically driven Monte Carlo (EDMC) method (Ripoll and Scheraga 1988, 1990) implemented in the ECEPPAK package. Conformational energy was evaluated using the ECEPP/3 force field (Némethy et al. 1992). Hydration energy was evaluated using a hydration-shell model with a solvent sphere radius of 1.4 Å and atomic hydration parameters that have been optimized using nonpeptide data (SRFOPT) (Vila et al. 1991; Williams et al. 1992). In order to explore the conformational space extensively, we carried out 10 different runs, each of them with a different random number. Therefore, we collected a total of 5000 accepted conformations. Each EDMC run was terminated after 500 energy-minimized conformations had been accepted. The parameters controlling the runs were the following: a temperature of 298.15 K was used for the simulations. A temperature jump of 1,000 K was used; the maximum number of allowed repetitions of the same minimum was 50. The maximum number of electrostatically predicted conformations per iteration was 400; the maximum number of random-generated conformations per iteration was 100; the fraction of random/electrostatically predicted conformations was 0.30. The maximum number of steps at one increased temperature was 20; and the maximum number of rejected conformations until a temperature jump is executed was 100. Only *trans* peptide bonds ($\omega \approx 180°$) were considered. All accepted conformations were then clustered into families using the program ANALYZE (Meadows et al. 1994a; Pohorille and Pratt 1990) by applying the minimal-tree clustering algorithm for separation, using all heavy atoms, energy threshold of 30 kcal mol^{-1}, and RMSD of 0.75 Å as separation criteria. This clustering step allows a substantial reduction of the number of conformations and the elimination of repetitions. A more detailed description of the procedure used here is given in section 4.4 Computational methods of (Masman et al. 2009b).

6.2.8.2 Docking studies

Two models for Aβ were used as target systems; the monomeric $A\beta_{42}$ elucidated by Crescenzi et al (monomeric model) (Crescenzi et al. 2002), PDB code 1IYT, and the pentam-

eric aggregate $A\beta_{42}$ developed by Masman et al (pentameric model) (Masman et al. 2009a). The structures were prepared for docking study as follows: for the $A\beta_{42}$ molecules, water molecules were removed from the PDB file and hydrogen atoms were added; Gasteiger charges, atomic solvation parameters and fragmental volumes were merged to the target system. For both LPYFDa and scrP, the structure of the most populated family (results from the *EDMC calculations*) was taken as initial conformation. Gasteiger charges were assigned and non-polar hydrogen atoms were merged. All torsions were allowed to rotate during docking. The docking energy grid was produced with the auxiliary program AutoGrid. The grid dimensions were 60x60x60 for the monomeric model, and 90x60x60 for the pentameric model, points along the x-, y- and z-axes, with points separated by 0.375Å. The grids were chosen to be sufficiently large to cover significant portions of the putative binding sites. The center of the pentapeptide was positioned at the grid center. All graphic manipulations and visualizations were performed by means of the AutoDock Tools (Sanner 1999) and the Chimera (Pettersen et al. 2004a) programs, and ligand docking with AUTODOCK 4 (Morris et al. 2009). The Lamarckian genetic algorithm was utilized and the energy evaluations were set at $2.5x10^6$. A total of 250 accepted conformations were collected. Other parameters were set to default values.

6.2.9 Statistical analysis

Behavioral data were analyzed by analysis of variance (ANOVA) followed by the Bonferroni post-hoc test to determine statistical significance. For statistical analysis of the MTT assays, an unpaired Student's *t* test with unequal variance was used. A p-value < 0.05 was considered to be statistically significant. Data are presented as mean value ± standard error of the mean (SEM).

6.3 Results

6.3.1 Characterization of the oligomeric $A\beta_{42}$

The state of aggregation of the oligomeric $A\beta_{42}$ preparation was determined by Western blot analysis. The results confirmed that the $A\beta_{42}$ preparation consisted of a mixture of small molecular weight $A\beta_{42}$ oligomers from monomeric to tetrameric $A\beta_{42}$ (figure 6.1A). In addition we used CD spectrometry to characterize the secondary structure of $A\beta_{42}$ in solution. We could show that our oligomeric $A\beta_{42}$ preparation consists of 43.02% β-sheets, 5.40% α-helix and 51.58% random-coil conformation (figure 6.1B), which shows a good correlation to the conformation behavior of $A\beta_{42}$ aggregates observed by Masman et al (Masman et al. 2009a).

6.3.2 Molecular modeling and stochastic conformational search. Edmc calculations

To have a better view at the molecular lever, it is crucial to assess the conformational behavior of the pentapeptides in solution. Therefore, LPYFDa and scrP were selected for energy calculations to determine the biologically relevant conformations. The results of the theoretical calculations are summarized in table 6.1.

Calculations yielded a large set of conformational families for each peptide studied. The total number of conformations generated was 62515 and 65056, for LPYFDa and scrP respectively, whereof 5000 conformations for each pentapeptide were accepted. In the clustering procedure, an R.M.S.D (Root Mean Square Deviation) of 0.75 Å and a ΔE of 30 kcal mol^{-1} were used. The number of families after clustering was 220 and 323, for LPYFDa and scrP, resp. The total number of families accepted with a relative population higher than 0.50% was 10 and 25, for LPYFDa and scrP, resp. that sum up to *ca* 90% of

Table 6.1: Conformational search and clustering results for LPYFDa and scrP optimized at the EDMC/SRFOPT/ECCEP/3 level of theory. Total (E_{tot}, kcal mol^{-1}) and relative (ΔE, kcal mol^{-1}) energies are also shown. All conformational families shown here have relative population (%PF) higher than 0.5%.

LPYFDa	Electrostatic	Random	Thermal	Total
Generated[a]	4233	58242	40	62515
Accepted[b]	535	4431	34	**5000**
Family	**NF** [c]	**%PF** [d]	E_{tot}	**ΔE**
1	2502	50.04	-70.79	0.00
2	768	15.36	-70.76	0.03
3	370	7.40	-69.43	1.36
4	262	5.24	-70.12	0.66
5	261	5.22	-69.31	1.47
6	247	4.94	-70.25	0.54
7	62	1.24	-69.37	1.42
8	47	0.94	-70.13	0.66
9	35	0.70	-69.75	1.03
10	30	0.60	-68.45	2.34
scrP	**Electrostatic**	**Random**	**Thermal**	**Total**
Generated[a]	4288	60708	60	65056
Accepted[b]	362	4595	43	**5000**
Family	**NF** [c]	**%PF** [d]	E_{tot}	**ΔE**
1	1146	22.92	-49.71	1.18
2	635	12.70	-50.16	0.73
3	478	9.56	-49.95	0.93
4	329	6.58	-50.88	0.00
5	272	5.44	-49.66	1.22
6	250	5.00	-49.94	0.94
7	190	3.80	-50.19	0.69
8	116	2.32	-49.71	1.17
9	114	2.28	-50.57	0.31
10	101	2.02	-49.44	1.44
11	97	1.94	-49.63	1.26
12	88	1.76	-50.23	0.65
13	60	1.20	-50.25	0.64
14	53	1.06	-49.47	1.41
15	51	1.02	-49.81	1.07
16	48	0.96	-49.39	1.50
17	45	0.90	-48.58	2.30
18	39	0.78	-48.78	2.10
19	39	0.78	-48.22	2.66
20	38	0.76	-48.97	1.91
21	37	0.74	-49.23	1.65
22	32	0.64	-49.74	1.14
23	30	0.60	-48.90	1.98
24	27	0.54	-49.03	1.86
25	26	0.52	-49.07	1.81

[a] Number of conformations generated electrostatically, randomly and thermally during the conformational search.
[b] Number of conformations accepted from those generated electrostatically, randomly and thermally during the conformational search.
[c] *NF* represents the total number of conformational families as result of the clustering run.
[d] *%PF* represents the percent relative population based on a total of 5000 accepted conformations.

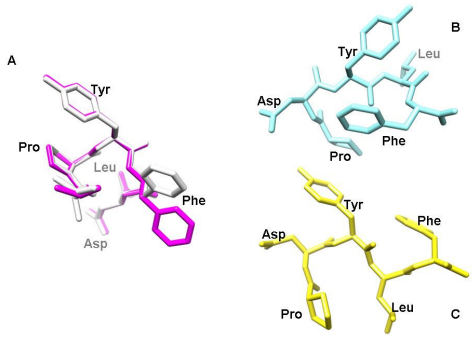

Figure 6.2: Stereoview of selected conformations for LPYFDa and scrP optimized at EDMC/SRFOPT/ECCEP/3 level of theory. (**A**) overlapping of the two most populated and energetically preferred families of LPYFDa, family 1 (ΔE = 0.00 cal.mol^{-1}, white) and family 2 (ΔE = 0.03 kcal mol^{-1}, pink). (**B**) Family 4 with a relative energy (ΔE) of 0.00 kcal mol^{-1} and (**C**) Family 1 with an ΔE = 1.18 kcal mol^{-1} of ScrP. All hydrogen atoms have been deleted for more clarity.

all conformations. All low-energy conformers of pentapeptides studied here were then compared to each other. The comparison involved the spatial arrangements, relative energy and populations. The LPYFDa evaluation showed that the most populated family (50.04%) is also the energetically preferred one, while its second most populated family (15.36%) has a relative energy of 0.03 kcal mol^{-1} above the global minimum. This small energetic difference is due to a slight reorientation of the side-chain of the residue Phe (see FIGURE 6.2A), while the rest of the structure showed approximately the same orientation. On the other hand, the most populated family of scrP (22.92%) showed a relative energy of 1.18 kcal mol^{-1} above the global minimum and a relative population of 6.38%. It was observed that LPYFDa is confrontationally, generally more restricted than scrP, with a preference to form folded structures, while scrP tended to form semi-extended or fully-extended conformations. Spatial views of selected conformations, for LPYFDa and scrP are shown in FIGURE 6.2.

Table 6.2: The two most populated families of LPYFDa and scrP found by docking simulations on the monomeric and pentameric $A\beta_{42}$ peptide and the corresponding binding energies (EB, kcal mol^{-1}) of the complexes. The binding constant (KB, M) and the relative populations (%P) are also shown.

			LPYFDa			scrP		
			E_B	K_B[a]	%P	E_B	K_B[a]	%P
Monomeric $A\beta_{42}$	Site I	1	-4.42	$5.78x10^{-4}$	13.60	-3.67	$2.05x10^{-3}$	4.80
		2	-4.35	$6.49x10^{-4}$	8.00	-3.18	$4.66x10^{-3}$	4.00
	Site II	1	-4.95	$2.35x10^{-4}$	6.40	-4.10	$9.89x10^{-4}$	3.20
		2	-4.66	$3.85x10^{-4}$	3.20	-3.96	$1.24x10^{-3}$	2.00
Pentameric $A\beta_{42}$	TOP	1	-5.67	$6.99x10^{-5}$	5.60	-4.50	$5.03x10^{-4}$	5.20
		2	-5.04	$2.02x10^{-4}$	3.60	-4.73	$3.39x10^{-4}$	3.60
	β1	1	-8.19	$9.88x10^{-7}$	8.80	-6.17	$3.00x10^{-5}$	5.20
		2	-7.05	$6.75x10^{-6}$	6.80	-5.01	$2.11x10^{-4}$	4.40
	β2	1	-4.75	$3.32x10^{-4}$	6.00	-4.68	$3.69x10^{-4}$	2.80
		2	-4.77	$3.20x10^{-4}$	3.20	-4.92	$2.48x10^{-4}$	2.40

[a] K_B is calculated in with the equation $K_B=\exp((\Delta G*1000.)/(Rcal*TK)$, where ΔG is the docking energy, Rcal is 1.98719 and TK is 298.15

6.3.3 Docking studies

6.3.3.1 Monomeric model

Two potential binding sites were found by using a single blind docking run (results not shown) on the monomeric $A\beta_{42}$ molecule (PDB code 1IYT), which comprises two α-helix moieties (residues 8-25 and 29-39) connected by a loop (residues 26-28). Site I encompasses the residues 21-26 containing Glu^{22} and Asp^{23}, which were previously identified as residues for aggregation of the oligomers (Buchete and Hummer 2007; Masman et al. 2009a). Site II includes residues 6-12 located in the portion of the molecule that loses all structural organization after oligomer formation, thus forming the so-called disordered region. In Table 6.2 the two most populated families of the complexes of LPYFDa and scrP with the monomeric $A\beta_{42}$ are summarized. LPYFDa showed lower binding energies, while site II was in general energetically preferred over site I but families on site II poorly populated. In general it can be concluded that LPYFDa binds stronger to the monomeric $A\beta_{42}$ than scrP.

6.3.3.2 Pentameric model

As previously reported by Masman et al. (Masman et al. 2009a), the $A\beta_{42}$ aggregates contain two β-sheet moieties (β1, residues 18-26 and β2, residues 31-42) organized into a parallel interchain orientation, which were proposed as intermolecular binding sites for the pentameric conformation. Moreover, a third possible site for interactions with ligand molecules was postulated, which involves the β1 and β2 portions of the chain located at the edge of the aggregate. This site is orientated into axis of the oligomers, in the same direction where the oligomers grows by aggregation. Table 6.2 shows the two most populated families of the complexes of LPYFDa and ScrP with the pentameric $A\beta_{42}$.

For all the sites proposed, LPYFDa showed lower binding energies than scrP. Interestingly, both pentapeptide LPYFDa and scrP, revealed an energetic preference for site β1. LPYFDa was designed on the basis of Soto's pentapeptide LPFFD, which derives from the amino acid sequence Leu^{17}-Val-Phe-Phe-Ala^{21} of $A\beta_{42}$, being the β1 portion of the aggregate. Figure 6.3 shows the atomic details of the interactions of the best complex (family β1 1, in Table 6.2) found between LPYFDa and the pentameric $A\beta_{42}$. It can be appreciated that the *N*-terminal of LPYFDa formed a double salt bridge with the Glu^{22}'s of the second and third chain of the aggregate. Also, a second salt bridge links the Lys^{16} to the Asp residue of LPYFDa. All salt bridges, indicated with a block-arrow that points to the positive member of the interaction, revealed an interacting distance of approximately 3.5 Å. All the ligand-target contacts are depicted as wireframe spheres. An important hydrophobic pocket was formed between the residues Phe^{20} and Val^{18} of the aggregate, and the residues Leu, Pro and Phe of the pentapeptide LPYFDa. This hydrophobic pocket is indicated with a dashed line.

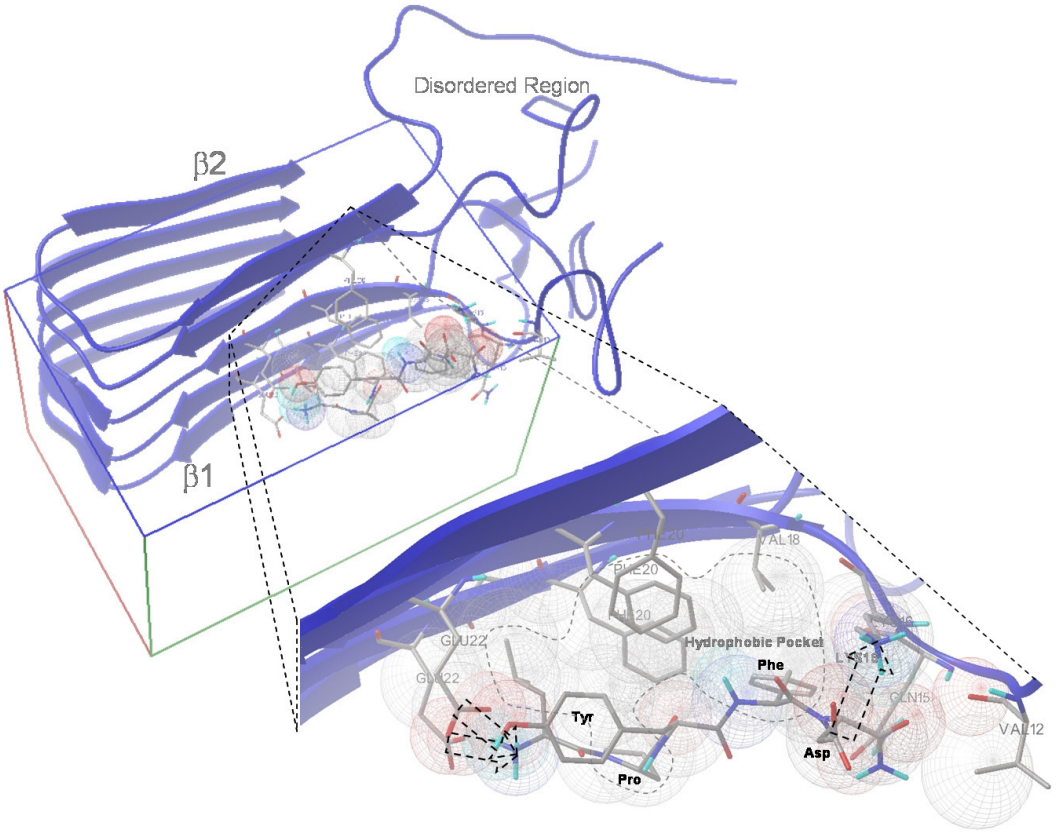

Figure 6.3: A steric view of binding between the pentameric $A\beta_{42}$ model and LPYFDa. Salt bridges are signalized with block-arrows. All the ligand-target contacts are depicted as wireframe spheres.

6.3.4 Leu-pro-tyr-phe-asp-NH_2 is neuroprotective against oligomeric $A\beta_{42}$ *in vitro*

Part of our study was to assess the neuroprotective potential of the beta-sheet breaker LPYFDa against Aβ-induced toxicity. Therefore, we first determined the toxic effect of the $A\beta_{42}$ oligomer preparation *in vitro* on cultured primary cortical neurons (PCN). Neuronal cultures were exposed to increasing concentrations of oligomerized $A\beta_{42}$ for 24 h, followed by an MTT-reduction assay to assess cell viability. The results showed a clear Aβ-induced, dose dependent decrease in cell survival reaching significance at concentrations higher than 10 µM (figure 6.4A). For the subsequent experiments we used oligomeric $A\beta_{42}$ at a concentration of 25 µM as a toxic stimulus.

Second, we investigated if LPYFDa or the control peptide scrP exhibited any toxicity to PCN and whether the beta-sheet breaker peptides were capable to overcome the toxic effect of oligomeric $A\beta_{42}$. For this purpose PCN were exposed to different concentrations of LPYFDa or scrP alone, $A\beta_{42}$ alone (25 µM) or beta-sheet breaker peptides and $A\beta_{42}$ together for 24 h. The results showed that LPYFDa and scrP alone were not toxic to PCN at any tested concentration (figure 6.4B). Furthermore, the control peptide scrP was not able to protect the neurons from Aβ-induced toxicity (figure 6.4C). In contrast, we could demonstrate a dose dependent neuroprotective effect of LPYFDa against Aβ-induced toxicity, reaching significance at 4 µM LPYFDa and higher (figure 6.4D).

6.3.5 A single intrahippocampal injection of oligomeric $A\beta_{42}$ induces cognitive deficits in contextual fear conditioning

One hour prior to the training session in

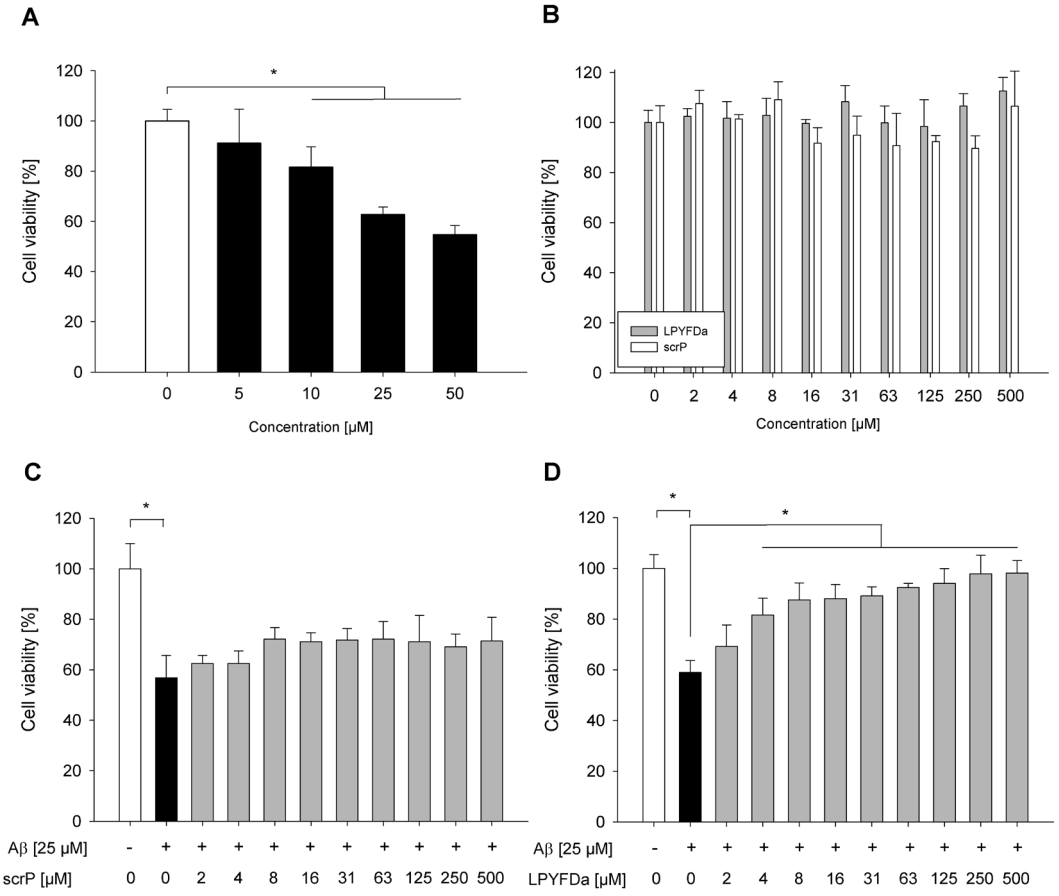

Figure 6.4: Cell viability of PCN as determined by an MTT-assay. Neurons treated with increasing concentrations of (**A**) $A\beta_{42}$ or (**B**) pentapeptides LPYFDa and scrP incubated for 24 h. Neuroprotection by (**C**) scrP or (**D**) LPYFDa was determined by co incubating increasing concentrations of the pentapeptides with 25 μM $A\beta_{42}$ for 24 h. Bars indicate the mean cell viability in % relative to untreated controls ± SEM. (* = significant at $p < 0.05$).

a contextual fear conditioning paradigm C57BL/6J mice received a single injection of oligomeric $A\beta_{42}$ (15, 30 or 60 pmol) or vehicle. Injections did not affect locomotion or the shock reaction during training (data not shown). The vehicle injected animals displayed an average relative freezing behavior of 58.9± 2.9% which did not differ from untreated control animals (61.1± 2.4 %). The mice injected with $A\beta_{42}$ showed a dose dependent decrease in freezing behavior (figure 6.5A). 15 pmol $A\beta_{42}$ caused an average relative freezing of 50.0±4.2 % which was not significantly different from the vehicle-injected animals. However, the mice injected with 30 pmol and 60 pmol of $A\beta_{42}$ had significantly reduced freezing scores compared to the vehicle group (36.2± 4.6%; p=0.024 and 33.3± 5.3%; p=0.037).

Next, we investigated whether LPYFDa is able to revert the Aβ-induced memory deficits. Therefore, we injected mice with 150 pmol LPYFDa or 150 pmol of the non specific control peptide scrP in the presence or absence of 30 pmol oligomerized $A\beta_{42}$ into the hippocampus. The LPYFDa and the scrP injected mice showed an average freezing of 61.1± 5.0% and 63.0± 5.5% which did not significantly differ from the untreated (61.1± 2.4%) or vehicle injected group (58.9± 2.9%).

However, LPYFDa co-injected with $A\beta_{42}$ was able to abolish the $A\beta_{42}$ oligomer-induced

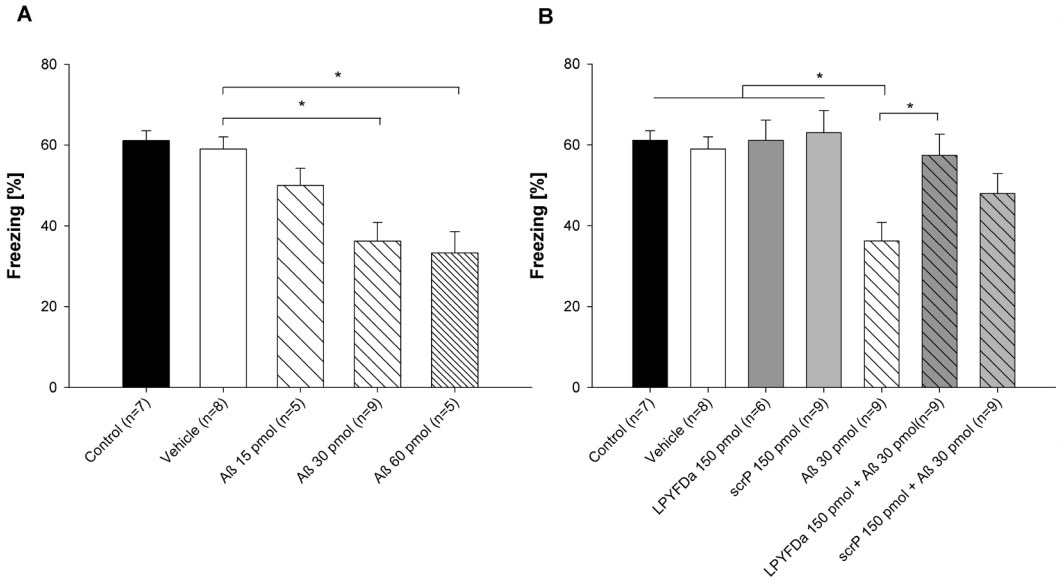

Figure 6.5: Effect of $A\beta_{42}$ and LPYFDa on contextual fear conditioning. (**A**) A single i.h. injection of oligomeric $A\beta_{42}$ led to a dose dependent significant decrease in conditioned fear when compared to a vehicle injection. (**B**) Co-injection of $A\beta_{42}$ with LPYFDa prevented the Aβ-induced memory impairment significantly, whereas the non-specific control peptide scrP failed to revert memory deficits. Bars indicate the mean relative freezing score in % ± SEM. Differences were determined by ANOVA (* = significant at $p < 0.05$).

memory impairment (57.4± 5.2% vs 36.2± 4.46%; p=0.039). Co-injection of Aβ with the control peptide scrP, which resulted in an average freezing score of 48.0± 4.9%, did not significantly reverse the Aβ-induced memory deficits (figure 6.5B). These results indicate that LPYFDa can reverse the detrimental effects of $A\beta_{42}$ oligomers and subsequent impaired memory performance.

6.4 Discussion

In the present study we could show that $A\beta_{42}$ oligomers are toxic to primary cortical neurons in culture in a dose-dependent manner (figure 6.4A). These results are in line with studies by Dahlgren and colleagues, who reported that the oligomeric form of $A\beta_{42}$ is 10 fold more toxic when compared to the fibrillar form (Dahlgren et al. 2002). These and our present findings support the growing general view that in particular oligomeric $A\beta_{42}$ peptides contribute to the progressive neuronal loss and the associated memory impairment observed in AD patients. Indeed, several studies showed that elevated levels of soluble oligomeric Aβ correlate strongly with cognitive decline in AD patients (McLean et al. 1999; Wang et al. 1999). Walsh et al. observed that a low-n oligomeric assembly of naturally secreted human Aβ alters hippocampal synaptic plasticity by inhibiting long-term potentiation (Walsh et al. 2002). Also the number of spines was dramatically decreased when neurons were incubated with Aβ oligomers, but not with monomers (Walsh et al. 2002). However, the loss in dendritic spines could be reverted by treating neurons with an anti-Ab antibody (Shankar et al. 2007a).

A possibility to counteract the injurious effects of oligomeric Aβ is by modulating its aggregation. Crucial for the aggregation process of the Aβ molecule are the hydrophobic residues

(amino acids 17-21: LVFFA) within the internal region of the Aβ peptide. Experiments by Hilbich and colleagues revealed that replacement of those hydrophobic residues by hydrophilic residues results in impaired fibril formation (Hilbich et al. 1992). These and other findings eventually led to the concept of beta-sheet breakers as therapeutic strategy for AD as proposed by Soto et al. (Soto 1999; Soto et al. 1996). The initially synthesized compounds were peptides from 11-5 amino acids targeting the center region of the Aβ peptide and evolved to compounds like LPFFD (iAβ5) and/or LPYFDa, which are partially homologous to this hydrophobic region and bind with a relatively high affinity to Aβ (Hetenyi et al. 2002a; Permanne et al. 2002; van Groen et al. 2009) by similar intermolecular interactions, leading to a competitive replacement of Aβ molecules. A major drawback with peptide drugs for neurological disorders is their rapid degradation *in vivo* by proteolytic enzymes and their poor blood-brain permeability (Adessi and Soto 2002). This issues were overcome by chemical modifications, like *C*-terminal amidation and *N*-terminal carboxylation, which resulted in increased half life *in vivo* and rapid brain up-take (Permanne et al. 2002). Although, we learned a lot about the biochemistry in respect to catabolism and brain uptake of certain aggregation inhibitor peptides, the detailed mechanism of action is still poorly understood. Therefore, it is important to elucidate and to study the three dimensional structure of the Aβ peptide/aggregation inhibiting peptide complex to gain more insight into the molecular dynamics of the Aβ aggregation process.

We used computational modeling and docking experiments to address this question. Interestingly our docking results showed that LPYFDa binds preferably to the β1 portion of the aggregate (TABLE 6.2 and FIGURE 6.3), which has a good correlation with the design of this pentapeptide, since LPYFDa derives from the wild-type sequence Leu17-Val-Phe-Phe-Ala21 of $A\beta_{42}$, which is contained in this portion of the aggregate. Our docking results did not show any binding preference of LPYFDa (nor scrP) for the monomeric or the pentameric Aβ.

In the present study we showed that the pentapeptide LPYFDa can protect cultured neurons from oligomeric Aβ-induced cell death. Datki et al. reported similar results on neuronal-like cell lines, e.g. SHSY-5Y cells. They could show that a 5-fold molar excess of LPYFDa protects these cells from toxic effects of fibrillar Aβ (Datki et al. 2004; Fulop et al. 2004). In our study we could confirm that a molar excess of LPYFDa can protect against $A\beta_{42}$ mediated neurotoxicity. Moreover, we could demonstrate a dose dependent protective effect of LPYFDa and that this pentapeptide already has significant neuroprotective properties even with a 6-fold molar excess of oligomeric $A\beta_{42}$. Our results also in agreement with other studies reporting protection by LPYFDa against the rapid neuromodulatory action of fibrillar $A\beta_{42}$ demonstrated by *in vitro* and *in vivo* electrophysiology (Szegedi et al. 2005).

We found that a single bilateral intrahippocampal injection of oligomeric $A\beta_{42}$ impairs memory formation if applied 1 h before the training session in a contextual fear conditioning paradigm. Our findings are in line with several other studies, which consistently report on memory deficits after intracerebral injections of $A\beta_{42}$ peptides, although the experimental conditions vary in terms of the injected peptide, injection procedure and behavioral tasks employed (Ammassari-Teule et al. 2002; Christensen et al. 2008; Harkany et al. 2001; Malin et al. 2001; Nakamura et al. 2001; O'Hare et al. 1999). It should be noted that these injections obviously lead to Aβ levels beyond the basal levels necessary for proper synaptic functioning. Garcia-Osta showed that neutralization of endogenous Aβ by an anti-Aβ antibody resulted in a memory impairment which implies that physiological soluble Aβ levels are required for proper memory function (Garcia-Osta and Alberini 2009).

The peptide LPFFD, which was designed by the Soto group was able to prevent fibrillogenesis in a rat brain model (Soto et al. 1998) and to reduce Aβ deposition in transgenic mice (Permanne et al. 2002). Most interestingly, iAβ5p was shown to reverse the memory impairment caused by intrahippocampal injections of Aβ fibrills in rats (Chacon et al. 2004). However, these studies did not reveal whether impairment of learning and memory after oligomeric Aβ injections could be counteracted by such compounds. An important novelty of our study is that we used Aβ oligomers instead of the less effective Aβ fibrills. Therefore, an important aim of our study was to establish if a compound like LPYFDa is able to prevent Aβ oligomer–induced learning and memory deficits. We showed that a 5-fold molar excess of LPYFDa to Aβ could overcome the detrimental effects of Aβ oligomers on memory. Thus, we provide evidence that so-called beta-sheet breaker peptides such as LPYFDa bear therapeutic potential against Aβ-induced memory impairment. Moreover, it was recently demonstrated that intraperitoneally administered LPYFDa is able to cross the blood brain barrier and protects synapses against excitatory action of fibrillar Aβ (Juhasz et al. 2009).

The mechanism how these pentapeptides exert their protective effects on cell death and behavior is not yet fully understood. However, it should be noted that the two actions of Aβ reported here, namely, the neuronal degeneration following application of Aβ oligomers *in vitro* and memory loss following injections of Aβ oligomers *in vivo* may be unrelated. In hippocampal tissue extracted one hour after Aβ injection we were unable to detect any caspase-3 cleavage which would indicate apoptotic cell death (data not shown). Furthermore, there are no studies so far that show toxic effects of oligomeric Aβ on neurons *in vivo*. Therefore, the effects on memory following an hour post-injection may not have a direct correlation with neuronal degeneration, but could simply reflect the effects of Aβ on synapses. It is well documented that the main effects of Aβ on synapses are inhibition of LTP (Chapman et al. 1999a; Kamenetz et al. 2003) and elimination of post synaptic glutamate receptors (Almeida et al. 2005; Chang et al. 2006; Ting et al. 2007). Remarkably, the Aβ induced synaptic dysfunction occurs rather rapidly, starting with 20 minutes after application, and does not need chronic exposure (Chen et al. 2000; Chen et al. 2002; Townsend et al. 2006; Wang et al. 2004).

Furthermore, it is likely that the injected oligomeric Aβ does not remain unchanged in terms of its conformation, and the effects on memory may be due to changes of Aβ to other conformations. The importance of the Aβ conformation on memory was demonstrated by Lesne et al (Lesne et al. 2006), who showed that only specific Aβ protein assemblies in the brain are able to impair memory (Lesne et al. 2006).

It remains elusive whether aggregation inhibiting peptides like LPYFDa directly bind to Aβ, and thereby prevent possible interactions between Aβ and neuronal membrane proteins, and in this way neutralize its toxic effect. We could consider two options of interaction with Aβ, 1) the pentapeptides bind to the monomeric Aβ, thus preventing and/or retarding the formation of toxic oligomers, and 2) the pentapeptides bind the Aβ oligomers already formed preventing and/or modulating, somehow, its neurotoxic properties. On the other hand, both above mentioned possibilities might act simultaneously comprising a third possible way of action of this peptide toward its neuroprotective effects.

Being aware of the many possible biological pathways that these peptides might follow while inducing neuroprotection, it is interesting to see whether these peptides show a preference to bind the monomeric Aβ or its soluble oligomers. Previous studies using CD spectrometry and molecular docking studies have been carried out on LPYFDa and other so-called β-sheet breaker

peptides (Datki et al. 2004; Hetenyi et al. 2002a; Hetenyi et al. 2002b; Laczko et al. 2008) but none of them so far have demonstrated proof at the molecular level of the β-sheet breaking properties of these peptides. We also might consider the possibility that these peptides might act as "glue" that promote elongation to biologically inert larger aggregates, or conversely, bind to the monomeric Aβ and this way inhibits oligomer formation. By either of these actions, or both, the neurotoxicity of Aβ is decreased or reverted.

In summary our findings provide evidence on how and where LPYFD interacts with Aβ mono- and oligomers, that LPYFDa neutralizes the neurotoxic activity of soluble Aβ oligomers, and in the present conditions can effectively prevent the oligomer-induced deficits in memory performance. ▪

Acknowledgements

This work was supported by grants from the International Foundation for Alzheimer Research (ISAO), the Netherlands Brain Foundation (Hersenstichting Nederland), the Gratama Stichting, the EU-grant FP6 NeuroprMiSe LSHM-CT-2005-018637 and EC-grant FP-7 201 159 (Memoload). We thank Gea Schuurman-Wolters, Neele Mayer and Sepp R. Jansen for their excellent technical assistance. This work reflects only the author's views. The European Community is not liable for any use that may be made of the information herein.

"Ausencia. Habré de levantar la vasta vida
que aún ahora es tu espejo:
cada mañana habré de reconstruirla.
Desde que te alejaste,
cuántos lugares se han tornado vanos
y sin sentido, iguales
a luces en el día.
Tardes que fueron nichos de tu imagen,
músicas en que siempre me aguardabas;
palabras de aquel tiempo,
yo tendré que quebrarlas con mis manos.
¿En qué hondonada esconderé mi alma
para que no vea tu ausencia
que como un sol terrible, sin ocaso,
brilla definitiva y despiadada?
Tu ausencia me rodea
como la cuerda a la garganta,
el mar al que se hunde."
(J.L. Borges)

07

"Mi Alma"

oil on paper (320x450 mm)

M.F. Masman 2010

Chapter 7

Neuroprotective action & neutralization of $A\beta_{42}$-induced memory impairment by a novel *in silico* designed *N*-methyl amino acids containing peptide

Marcelo F. Masman, Ivica Granic, Sebastian A. Andujar, Pieter J.W. Naude, Ulrich L.M. Eisel, Ricardo D. Enriz, Siewert Jan Marrink & Paul G.M. Luiten

Article in preparation to submission

Abstract

We report the *in silico* design and the neuroprotective properties of $A\beta_{42}$ derived synthetic *N*-methyl amino acids containing penta-peptide Ac-Lys-(Me)Ile-Ile-(Me)Gly-Leu-NH_2. These data demonstrate the ability of this novel peptide to interact with different regions of $A\beta_{42}$ which may be targeted selectively. Furthermore, this study provides proof of principle that this rationally designed peptide has protective properties against the neurotoxic effects of oligomeric $A\beta_{42}$ *in vitro* and *in vivo*. This peptide can serve as a crucial molecular model design for development of therapeutic molecules for treatment of Alzheimer's disease.

7.1 Introduction

Alzheimer's disease (AD) is a complex multifactorial neurodegenerative syndrome characterized by the patient's memory loss and impairment of a wide range of cognitive abilities. This devastating disease affects more than 20 million people worldwide and, as a consequence of the worlds aging population, the prevalence of AD is expected to increase to endemic dimensions both in developed and developing nations (Blennow et al. 2006; Pratico and Delanty 2000). AD is the most extensively studied amyloid-based disease, whose main hallmarks are characterized by pathological high levels of amyloid deposits in frontal brain regions (senile or amyloid or neuritic plaques) and neurofibrillary tangles (Haass and Selkoe 2007; Holtzman and Mobley 1991). The major components of senile plaques are small peptides of 39-43 amino acids called β-amyloid (Aβ) which are produced through endoproteolysis of the amyloid precursor protein (APP). During the pathogenesis of AD the equilibrium of Aβ production and Aβ clearance is disturbed, which eventually leads to elevated Aβ levels, increased Aβ aggregation and consequently impaired memory function (Wasling et al. 2009). Recent evidence now indicates that particularly soluble oligomeric forms of $A\beta_{42}$ are to be considered as the most toxic form of this peptide, and correlate well with the progression and cognitive decline of the disease (Lesne et al. 2006; Wasling et al. 2009)

Due to the high incidence that AD has in the human aging population, there is an evident need of therapeutic agents that could at least significantly delay the course of the disease (Hardy and Selkoe 2002; Wolfe 2002). Several research strategies currently attempt to develop therapies and therapeutic agents that aim to reduce Aβ production, enhancing its clearance and/or preventing or retarding the amyloidogenic processes. Amongst them, the use of peptides or peptidomimetic molecules derived from the Aβ sequence is particularly appealing (Granic et al. 2009; Soto et al. 1998; Tjernberg et al. 1996; Wolfe 2002). Promising putative treatments may be those designed to inhibit steps that *precede* Aβ peptide aggregation, by blocking the production of toxic soluble Aβ oligomers in the first place, or by reversing, somehow, the toxic effect of these soluble oligomers (figure 7.1).

In fact, some short peptides that are derived from the Aβ sequence have already been reported to specifically interact with Aβ and cause interferences with its neurotoxic effects. LPFFD (Soto et al. 1996; Soto et al. 1998), KLVFF (Hetenyi et al. 2002b; Tjernberg et al. 1997; Tjernberg et al. 1996), RIIGLa (Fulop et al. 2004) and LPYFDa (Datki et al. 2003; Datki et al. 2004; Granic et al. 2009; Juhasz et al. 2009; Szegedi et al. 2005) are some of the promising starting points to develop potential drugs that can somehow reverse the negative impacts of soluble Aβ aggregates, although their underlying molecular mechanisms remain partly elusive. In order to increase the anti-amyloidogenic properties of these peptides, a new strategy was recently explored with the introduction of *N*-methyl amino acids in these sequences (Cruz et al. 2004; Gordon et al. 2001; Gordon et al. 2002). *N*-Methyl amino acids have been used in several systems to control, or prevent the aggregation of β-sheet and β-strand peptides (Chitnumsub et al. 1999; Clark et al. 1998; Doig 1997; Hughes et al. 2000; Nesloney and Kelly 1996; Rajarathnam et al. 1994). The goal of this modification is to block the hydrogen bond network that stabilizes the β-sheet amyloid structure and this way to inhibit the formation of toxic oligomers and/or amyloid aggregates.

In the present study, we report the *in silico* design of a new Aβ-derived synthetic penta-peptide Ac-Lys-Ile-Ile-Gly-Leu-NH_2 (PN20) and its chemically modified version; Ac-Lys-(Me)Ile-Ile-(Me)Gly-Leu-NH_2 (PN22), which contains alternated *N*-methyl amino acids (scheme 7.1). The protective property of these

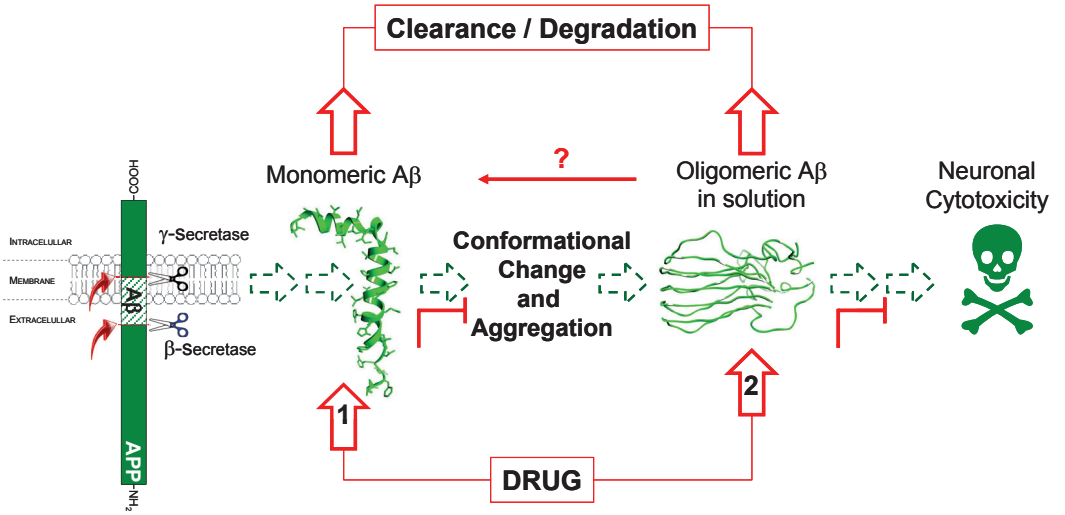

Figure 7.1: Simplified schematic representation of the up-stream amyloid assembly process that leads to neuronal cytotoxicity. In disease states, the mechanisms of Aβ production and it clearance is unbalance causing that soluble Aβ monomers undergo aggregation to form various intermediates consisting of different forms of multimeric Aβ oligomers that, somehow, performers negative effect on brain cells. Aβ oligomers subsequently assemble to generate insoluble fibrils that accumulate in the affected tissues or organs (pathway no shown). Compounds that inhibit formation of these undesirable species may, therefore, be capable of protecting tissues or organs from their toxic effects. Two possible inhibition pathways are depicted. Pathway 1 shows an up-stream intervention of a putative drug. Thus, this drug may stop or retard the amyloigenic process by preventing the conformational change of the Aβ monomers that leads to toxic Aβ aggregates. Pathway 2 shows the intervention of a putative drug that, somehow, blocks the toxic effects of Aβ oligomers and might also reverse the amyloidic assembly process.

peptides against the neurotoxic effects of soluble $A\beta_{42}$ oligomers was investigated in cultured mouse primary cortical neurons (PCN). Furthermore, we explored in a previously established *in vivo* model of Aβ injections directly into the hippocampus of mice whether PN22 exerts beneficial action against the Aβ-induced cognitive deficits (Granic et al. 2009). Ultimately, we intended to reveal some of the putative mechanism of action of these chemically modified peptides by employing molecular modeling techniques.

These peptides were designed based on the observations of the conformational behavior of the $A\beta_{42}$ aggregates *in silico* previously reported by Masman and coworkers (Masman et al. 2009a). The portion β2 of these aggregates, specifically the highly hydrophobic sequence Ala^{30}-Ile^{31}-Ile^{32}-Gly^{33}-Leu^{34}, was the starting point of the present design.

7.1.1 Rational *in silico* design of PN20 and PN22

In this study we rationally designed two novel aggregation modulating peptides (PN20 and PN22). Their *in silico* design was based on the conformational behavior of $A\beta_{42}$ aggregates, which was previously reported by Masman and coworkers (Masman et al. 2009a). The so-called β2 portion of these aggregates, specifically the highly hydrophobic sequence Ala^{30}-Ile^{31}-Ile^{32}-Gly^{33}-Leu^{34}, was the starting point of this design. Due to its hydrophobic nature some chemical modifications were applied to the peptides in order to increase the solubility of the final peptides. Thus, the first modification was the change of the Ala residue to Lys. A positively charged residue not only increases the water solubility of the peptides but also offers the possibility of targeting important negatively charged residues that play a crucial role in the stabilization of the aggregated $A\beta_{42}$ oligomers, e.g. Glu^{22} and Asp^{23}. *A posteriori*, the *N*- and *C*-terminal were blocked by acetylation and amidation respectively. This provides some advantages: (*i*) peptide ends are uncharged (no zwitterionic), thus we have a better control on the charges that take place in a biological medium; (*ii*) increased biological membrane permeability and cell penetration; (*iii*) the stability and resistance towards digestion

by aminopeptidases is enhanced; and (*iv*) peptide ends are blocked against synthetase activities. Moreover, *C*-terminal amidation is essential to the biological activity of many neuropeptides and hormones (Fricker 2005; Kim and Seong 2001). These two modifications were our guiding principle to the design of PN20.

In fact, a possibility to counteract the detrimental effects of oligomeric Aβ is by modulating its aggregation process. A very appealing strategy to endow peptides with aggregation modulating properties is the incorporation of non-natural amino acids to their sequence. Such is the case of *N*-methyl amino acids containing peptides. When the *N*-methyl amino acids residues are located in an alternated fashion into the peptide sequence, and the peptide has the possibility to form extended conformations, e.g. β-sheets, two different "faces" are expressed. On the one hand, one of the faces has all the normal H-bonding possibilities that a natural peptide has (the so-called "rich H-bonding face"). On the other hand, the other face is limited on H-bonding possibilities due to the presence of the *N*-methyl groups (SCHEME 7.1). Thus, the incorporation of *N*-methyl-*L*-isoleusine and *N*-methyl-glycine (or sarcosine) in position 2 and 4 respectively, by replacement of their natural analogs, led us to PN22.

7.2 Material and methods

7.2.1 Molecular modeling

7.2.1.1 Stochastic conformational search. EDMC calculations

The conformational space of the pentapeptides PN20 and PN22 was explored using the method previously employed by Liwo et al. (Liwo et al. 1996a) which includes the electrostatically driven Monte Carlo (EDMC) method (Ripoll and Scheraga 1988, 1990) implemented in the ECEPPAK package. Conformational energy was evaluated using the ECEPP/3 force field (Némethy et al. 1992). Hydration energy was evaluated using a hydration-shell model with a solvent sphere radius of 1.4 Å and atomic hydration parameters that have been optimized using nonpeptide data

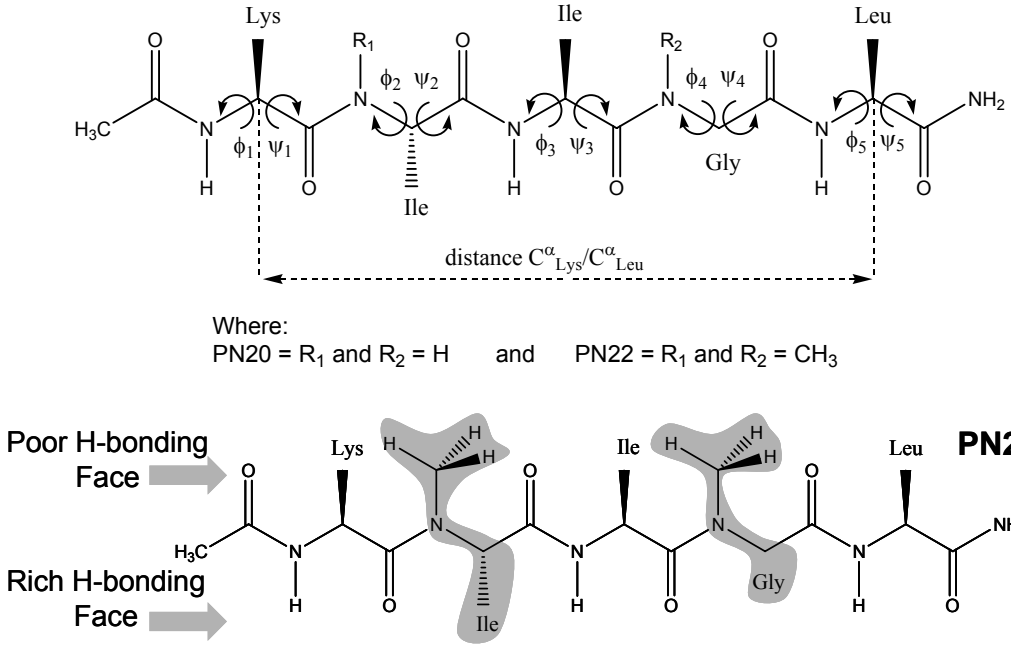

SCHEME 7.1: Schematic representation of the chemical structure of PN20 and PN22. Backbone torsional angles and the distance $C^{\alpha}_{Lys}/C^{\alpha}_{Leu}$ are also shown. For the case of PN22 the "poor and rich H-bonding faces" are shown.

(SRFOPT) (Vila et al. 1991; Williams et al. 1992). In order to explore the conformational space extensively, we carried out 20 different runs, each of them with a different random number. Therefore, we collected a total of 5000 accepted conformations. Each EDMC run was terminated after 250 energy-minimized conformations had been accepted. The parameters controlling the runs were the following: a temperature of 298.15 K was chosen for the simulations. A temperature jump of 50,000 K was used; the maximum number of allowed repetitions of the same minimum was 50. The maximum number of electrostatically predicted conformations per iteration was 400; the maximum number of random-generated conformations per iteration was 100; the fraction of random/electrostically predicted conformations was 0.30. The maximum number of steps at one increased temperature was 20; and the maximum number of rejected conformations until a temperature jump was executed was 100. Only *trans* peptide bonds ($\omega \approx 180°$) were considered. All accepted conformations were then clustered into families using the program ANALYZE (Meadows et al. 1994a; Pohorille and Pratt 1990) by applying the minimal-tree clustering algorithm for separation, using all heavy atoms, energy threshold of 30 kcal mol^{-1}, and RMSD of 0.75 Å as separation criteria. This clustering step allows a substantial reduction of the number of conformations and the elimination of repetitions. A more detailed description of the procedure used here is given in section 4.4 Computational methods of (Masman et al. 2009b).

7.2.1.2 Molecular dynamics simulations

The most populated conformation of PN20 and PN22 obtained from the EDMC were embedded in a cubic box containing SPC waters, (Berendsen et al. 1981b) leaving at least 10 Å between the solutes and the edge of the box. The total number of water molecules varied between 15630 and 25919. Cl^- ions were added to the systems by replacing water molecules in random positions, thus making the whole system neutral. Multiple simulations were performed for each system, starting from different initial random velocity distributions. Details of the equilibration procedure can be found in the Suppl. Information. For each system 10 ns production runs were obtained and analyzed. The coordinates were saved every 2 ps. Molecular dynamics (MD) simulations were performed using the GROMACS 3.3.2 package of programs (Van Der Spoel et al. 2005), with the OPLS-AA force field (Kaminski et al. 2001). The simulations were run under NPT conditions, using Berendsen's coupling algorithm (Berendsen et al. 1984) for keeping the temperature and pressure constant (P = 1 bar, τP = 0.5 ps; T = 310 K, τT = 0.1 ps). The LINCS algorithm (Hess et al. 1997) was used to constrain the lengths of hydrogen containing bonds; the waters were restrained using the SETTLE algorithm (Miyamoto and Kollman 1992). The time step for the simulations was 0.002 ps and the compressibility 4.8×10^{-5} bar^{-1}. Van der Waals forces were treated using a 1.2 nm cutoff. Long-range electrostatic forces were treated using the particle mesh Ewald method (PME) (Darden et al. 1993a). The analysis of the simulations was performed using the analysis tools provided in the Gromacs package. The root mean square deviation (RMSD) of backbone atoms, the total and potential energies were calculated. The root mean square fluctuation (RMSF) of the backbone atoms and the hydrophilic, hydrophobic and total Solvent Accessible Surface Area (SASA) were also determined. The total number of hydrogen bonds in the peptide group were quantified by counting acceptor and donor atom pairs that are not further apart than 0.35 nm. All molecular graphical presentations were created by VMD (Humphrey et al. 1996) and/or UCSF Chimera (Pettersen et al. 2004a) packages. The standard deviation of every given value is shown in between brackets.

7.2.1.3 Docking studies

Two models for Aβ were used as target systems; the monomeric $A\beta_{42}$ elucidated by

Crescenzi et al (monomeric model) (Crescenzi et al. 2002), PDB code 1IYT, and the pentameric aggregate $A\beta_{42}$ developed by Masman et al (pentameric model) (Masman et al. 2009a). The structures were prepared for docking study as follows: for the $A\beta_{42}$ molecules, water molecules were removed from the PDB file and hydrogen atoms were added; Gasteiger charges, atomic solvation parameters and fragmental volumes were merged to the target system. For all peptides, the structure of the most populated family (results from the *EDMC calculations*) was taken as initial conformation. Gasteiger charges were assigned and non-polar hydrogen atoms were merged. All torsions were allowed to rotate during docking. The docking energy grid was produced with the auxiliary program AutoGrid. The grid dimensions were 61x61x61 for the monomeric model, and 90x60x60 for the pentameric model, points along the x-, y- and z-axes, with points separated by 0.375Å. The grids were chosen to be sufficiently large to cover significant portions of the putative binding sites. The center of the pentapeptide was positioned at the grid center. All graphic manipulations and visualizations were performed by means of the AutoDock Tools (Sanner 1999) and the Chimera (Pettersen et al. 2004a) programs, and ligand docking with AUTODOCK 4 (Morris et al. 2009). The Lamarckian genetic algorithm was utilized and the energy evaluations were set at $2.5x10^6$. A total of 250 accepted conformations were collected. Other parameters were set to default values.

7.2.2 Experimental section

7.2.2.1 Compounds

The peptides Ac-Lys-Ile-Ile-Gly-Leu-NH_2 (PN20), Pro-Asp-Tyr-Leu-Phe-NH_2 (scrP) and Amyloid β peptide 1–42 ($A\beta_{42}$) were purchased from EZBiolab Inc.(Carmel, USA). Anti-Aβ antibody (6E10) was obtained from Covance (Emeryville, USA). The peptide Ac-Lys-(Me)Ile-Ile-(Me)Gly-Leu-NH_2 (PN22) was purchased from AnaSpec Inc (San Jose, CA, USA). HPLC purity higher than 95% was described for all peptides used here. Other compounds used in this study were purchased from Invitrogen (Carlsbad, USA) or Sigma-Aldrich Corporation (St. Louis, USA).

7.2.2.2 Preparation of $A\beta_{42}$-oligomers

Oligomeric $A\beta_{42}$ was prepared as described by Granic and colleagues (Granic et al. 2009). Also, the aggregational state and the secondary structure of the oligomeric $A\beta_{42}$ preparation were examined by sodium dodecyl sulfate (SDS)-PAGE Western blotting and Circular Dichroism (CD) spectrometry. For a more detailed description of the methodology used here, see Granic et al. (2009).

7.2.3 *In vitro* testing

7.2.3.1 Primary cortical neuron culture

Primary cortical neurons were prepared from embryonic brains (E14) of C57Bl/6J mice. The cortices were carefully dissected, meninges were removed and the neurons separated by trituration. Cells were plated on poly-*D*-lysine precoated plates at a density of 1.2×10^5 cells/well (96 well plates). Neurobasal medium supplemented with 2% (v/v) B27-supplement, 0.5 mM glutamine and 1% (v/v) penicillin/streptomycin was used as a culture medium. After 48 h neurons were treated with 10 µM cytosine arabinoside for another 48 h to inhibit non-neuronal cell growth. Subsequently, the medium was completely exchanged and after 6 days of *in vitro* culture, the neurons were used for experiments.

7.2.3.2 Treatment of cells

Possible toxicity of the penta-peptides used here and $A\beta_{42}$ oligomers was determined by incubating neuronal cultures for 24 h with different concentrations of the peptide solutions. The neuroprotective effect of PN20 and PN22 was assessed by incubating neurons (cultured in 96 well plates) for 24 h with 25 µM oligomeric Aβ in the presence or absence of different concentrations of

PN20 or PN22 peptides. After treatments, the medium was completely exchanged, and 24 h later, the cell viability determined by an MTT-assay. All treatments were performed in triplicates and the experiments were repeated at least two times.

7.2.3.3 Determination of cell viability by MTT-assay

Neuronal viability was determined by the colorimetric MTT [3-(4,5-dimethylthiazol-2-yl-)2,5-diphenyltetrazolium bromide] assay as described previously (Mosmann 1983). 1.25 mg/ml MTT solution was added to each well of a 96 well plate. After 2 h of incubation, cells were lysed in acidic propan-2-ol solution (37% HCl/ propan-2-ol: 1/166). The absorbance of each well was measured with an automated ELISA plate reader (Bio-Rad, Munich, Germany) at 595 nm with a reference filter at 630 nm.

7.2.4 *In vivo* testing

7.2.4.1 Animals

Behavioral experiments were performed with 9–12 weeks old male C57Bl/6J mice (Harlan, Horst, The Netherlands). Individually housed mice were maintained on a 12 h light/dark cycle (lights on at 7.00 a.m.) with food (Hopefarms, standard rodent pellets) and water ad libitum. A layer of sawdust served as bedding. The animals were allowed to adapt to the housing conditions for 1–2 weeks before the experiments started. The procedures concerning animal care and treatment were in accordance with the regulations of the Ethical Committee for the use of experimental animals of the University of Groningen (License number DEC4668D).

7.2.4.2 Animal surgery

Double guide cannulae type C235 (Plastics One, Roanoke, USA) were implanted in the brain using a Kopf stereotactic instrument during Hypnorm/Midazolam (10 ml/kg, i.p.) anesthesia under aseptic conditions as previously described (Nijholt et al. 2008) with anteroposterior (AP) coordinates zeroed at Bregma directed toward both dorsal hippocampi (i.h.), AP -1.5 mm, lateral 1 mm, depth 2 mm (Franklin and Paxinos 1997). Each double guide cannula with inserted dummy cannula and dust cap was fixed to the skull with dental cement (3M ESPE AG, Seefeld, Germany). Administration of 1 mg/ml finadyne (2.5 mg/kg s.c.) before the surgery served as analgesic. The animals were allowed to recover for 6–7 days before the behavioral test.

7.2.4.3 Intrahippocampal injections

Bilateral i.h. injections were performed under short isoflurane anesthesia using a Hamilton microsyringe fitted to a syringe pump unit (TSE systems, Bad Homburg, Germany) at a constant rate of 0.3 µl/min (final volume: 0.3 µl per side). Oligomerized $A\beta_{42}$ was injected in a final concentration of 30 pmol and PN22 or scrP in a final concentration of 150 pmol into the dorsal hippocampus. PBS (pH 7.5) served as vehicle. ScrP was used as a sequence control peptide. One hour after the injection the animals were subjected to a training session in a fear conditioning paradigm (scheme 7.2). The number of animals per group varied from 7 to 10.

7.2.4.4 Fear conditioning

Fear conditioning was performed in a plexiglas cage (44x22x44 cm) with constant illumination (12 V, 10W halogen lamp, 100–500 lux). The training (conditioning) consisted of a single trial. Before each individual mouse entered the box, the box was cleaned with 70% ethanol. The

Scheme 7.2: Schematic outline of the experimental *in vivo* setup. C57BL/6J mice were cannulated 7 days prior i.h. injection with oligomerized $A\beta_{42}$ and/or aggregation inhibiting peptides. One hour after the injection the animals were trained in a contextual fear conditioning paradigm. 24 h after the training session memory performance was assessed.

mouse was exposed to the conditioning context for 180 s followed by a scrambled footshock (0.7 mA, 2 s, constant current) delivered through a stainless steel grid floor. The mouse was removed from the fear conditioning box 30 s after shock termination to avoid an aversive association with the handling procedure. Memory tests were performed 24 h after fear conditioning. Contextual memory was tested in the fear conditioning box for 180 s without footshock presentation. Freezing, defined as the lack of movement except for respiration and heart beat, was assessed as the behavioral parameter of the defensive reaction of mice by a time-sampling procedure every 10 s throughout memory tests. In addition, mean activity of the animal during the training and retention test was measured with the Ethovision system (Noldus, Wageningen, The Netherlands). Immediately after the behavioral test mice were injected i.h. with methylene blue solution during sodium-pentobarbital anesthesia (0.1 ml/ 10g, i.p.). Brains were removed and serially sectioned at 50 µm. Sections were stained on glass for 5 min in 0.1% nuclear fast red solution. To identify the location of the injection, sections were analyzed using light microscopy. Only data from animals in which the proper intrahippocampal site of injection was confirmed, were evaluated.

7.2.5 Statistical analysis

Behavioral data were analyzed by analysis of variance (ANOVA) followed by the Bonferroni post-hoc test to determine statistical significance. For statistical analysis of the MTT assays, an unpaired Student's *t* test with unequal variance was used. A p-value *< 0.05 was considered to be statistically significant. A p-value **< 0.005 was considered to be highly significant. Data are presented as mean value ± standard error of the mean (SEM).

7.3 Results

7.3.1 Molecular modeling

7.3.1.1 Stochastic conformational search in solution. EDMC calculations

In order to have a better view at the molecular level, it is crucial to assess the conformational behavior of PN20 and PN22 in solution. Therefore, all peptides were selected for energy calculations to determine the relevant conformations. The results of the theoretical calculations are summarized in table 7.1S in appendix A. Calculations yielded a large set of conformational families for each peptide studied. The total number of conformations generated was 70236 and 79077, for PN20 and PN22 respectively, whereof 5000 conformations for each pentapeptide were accepted. In the clustering procedure, an R.M.S.D (Root Mean Square Deviation) of 0.75 Å and a ΔE of 30 kcal mol^{-1} were used. The number of families after clustering was 703 and 409, for PN20 and PN22, respectively. The total number of families accepted with a relative population higher than

Table 7.1: Backbone tortional angles of the three most populated families for PN20 and PN22 found at the EDMC/SRFOPT/ECCEP/3 level of theory. All angles values are given in degrees. The distance (d C^{α}_{Lys}/ C^{α}_{Leu}, Å) between the C^{α} atoms of residue Lys^{1} and residue Leu^{5} is also shown.

		Lys		Ile/(Me)Ile		Ile		Gly/(Me)Gly		Leu		d $C^{\alpha}_{Lys}/C^{\alpha}_{Leu}$
		ϕ_1	ψ_1	ϕ_2	ψ_2	ϕ_3	ψ_3	ϕ_4	ψ_4	ϕ_5	ψ_5	
PN20	1	-77.93	-26.75	-77.76	-36.70	-76.80	-39.50	95.11	49.13	-76.76	-34.73	6.39
	2	-89.21	-48.10	-92.61	-50.83	-154.25	138.47	-83.89	67.60	-78.96	-41.85	9.91
	3	-74.25	-24.36	-79.41	-32.43	-76.68	-54.86	150.07	70.85	-71.13	-41.12	4.83
PN22	1	-150.42	75.40	-120.16	79.15	-140.85	73.54	-80.59	71.04	-82.85	-33.07	11.20
	2	-150.36	75.98	-117.73	83.13	-151.48	75.78	-100.57	47.66	-77.99	-34.30	11.47
	3	-150.42	76.58	-116.92	81.14	55.16	68.55	-93.90	58.60	-81.90	-32.94	9.62

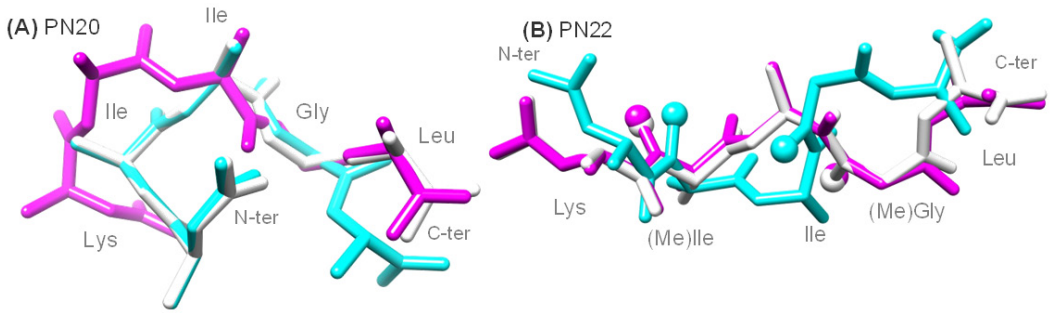

Figure 7.2: Stereoview of the three most populated families for PN20 and PN22 optimized at EDMC/SRFOPT/ECCEP/3 level of theory. (**A**) Overlapped geometries of family 1 (ΔE = 0.00 cal mol^{-1}, white), family 2 (ΔE = 2.55 kcal mol^{-1}, magenta) and family 3 (ΔE= 1.66 kcal mol^{-1}, cyan) for PN20. (**B**) Overlapped geometries of family 1 (ΔE = 0.00 kcal mol^{-1}, white), family 2 (ΔE= 0.57 kcal mol^{-1}, magenta) and family 3 (ΔE= 0.61 kcal mol^{-1}, cyan) for PN22. All hydrogen atoms and side-chains have been deleted for more clarity. *N*-Methyl groups are depicted in ball-and-stick model.

0.50% was 30 and 11, for PN20 and PN22, resp. that sum up to ca 85% of all conformations. All low-energy conformers of pentapeptides studied here were then compared to each other. The comparison involved the spatial arrangements, relative energy and populations. The PN20 evaluation showed that the most populated family (24.20%) is also the energetically preferred one, while its second most populated family (5.52%) has a relative energy of 2.55 kcal mol^{-1} above the global minimum. The third most populated family (3.76%) shows a relative energy of 1.66 kcal mol^{-1} above the global minimum. On the other hand, the most populated family of PN22 (62.38%) is also the global minimum, while its second most populated family showed a relative energy of 0.57 kcal mol^{-1} above the global minimum and a relative population of 8.50%. The third most populated family (5.20%) has a relative energy of 0.61 kcal mol^{-1} above the global minimum. It was observed that PN20 possesses a marked tendency to form folded conformations while PN22 shows high preference to form semi-extended or fully-extended conformations. Table 7.1 shows the values of f and y torsional angles for the three most populated families of PN20 and PN22. Spatial overlapped stereoviews of selected conformations, for PN20 and PN22 are shown in figure 7.2.

7.3.1.2 Molecular dynamics

PN20 and PN22 were examined by MD due to the need of exploring their conformational behavior in a more realistic system by means of an explicit solvent. Figure 7.3 shows the distance between the C^{α} atoms of residues Lys^{1} and Leu^{5} (d C^{α}_{Lys}/ C^{α}_{Leu}) as a function of the simulation time for PN20 and PN22. This parameter is a clear and easy way of depicting the conformational preferences of these peptides. In this figure, it is observed that PN20 prefers folded conformation with a d C^{α}_{Lys}/ C^{α}_{Leu}= 4.22(0.49) Å while PN22 showed a marked preference to extended conformations (d C^{α}_{Lys}/ C^{α}_{Leu}= 12.25(1.08) Å).

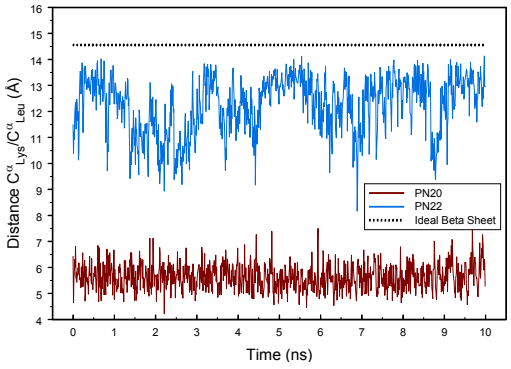

Figure 7.3: Distance between C^{α} atoms of residues Lys^{1} and Leu^{5} as a function of simulation time. The maximum ideal (for a fully extended conformation, where all φ and ψ ≈ 180°) distance between the above mentioned atoms is also shown.

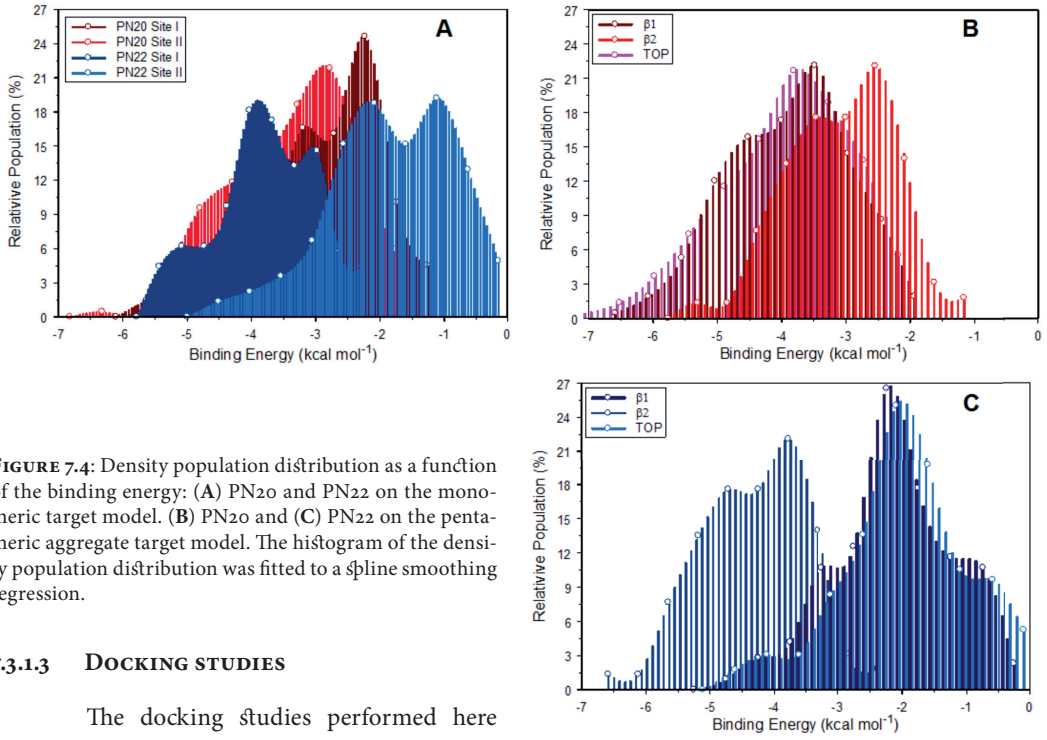

Figure 7.4: Density population distribution as a function of the binding energy: (**A**) PN20 and PN22 on the monomeric target model. (**B**) PN20 and (**C**) PN22 on the pentameric aggregate target model. The histogram of the density population distribution was fitted to a spline smoothing regression.

7.3.1.3 Docking studies

The docking studies performed here have been analyzed on the basis of their conformational population distribution as a function of the binding energy. The clusterization procedure was run with a cut-off of 2.00 Å RMSD. Figure 7.4 shows the density population distribution for PN20 and PN22 on the two target system-models used here.

Monomeric Model. Two potential binding sites were found by using a single blind docking run (results not shown) on the monomeric $A\beta_{42}$ molecule (PDB code 1IYT). Figure 7.5A depicts the location of these potential binding sites. Site I encompasses the residues 21-26 containing Glu^{22} and Asp^{23}, which were previously identified as residues for aggregation of the oligomers (Buchete and Hummer 2007; Masman et al. 2009a). Site II includes residues 6-12 located in the portion of the molecule that loses all structural organization after oligomerization, thus forming part of the so-called disordered region. The docked-conformational population for PN20 and PN22 is shown in figure 7.4, panel A. It can be observed that PN20 does not show a preference to bind either Site I or Site II. PN20 obviously binds both sites unselectively and with more or less the same intensity. On the other hand, the most populated conformations of PN22 show a binding preference for Site I. Thus, the binding of

Table 7.2: The two most populated families of PN20 and PN22 found by docking simulations on the monomeric and pentameric $A\beta_{42}$ peptide and the corresponding binding energy (EB, kcal mol^{-1}) of the complexes. The binding constant (KB, M) and the relative populations (%P) are also shown.

			PN20			PN22		
			E_B	K_B	%P	E_B	K_B[a]	%P
Monomeric $A\beta_{42}$	Site I	1	-2.23	$2.29x10^{-2}$	24.62	-4.03	$1.09x10^{-3}$	18.14
		2	-3.17	$4.72x10^{-3}$	16.58	-3.67	$2.04x10^{-3}$	17.25
	Site II	1	-2.77	$9.13x10^{-3}$	21.82	-1.11	$1.58x10^{-1}$	19.20
		2	-3.28	$3.88x10^{-3}$	18.64	-2.08	$2.98x10^{-2}$	18.75
Pentameric $A\beta_{42}$	TOP	1	-3.81	$1.56x10^{-3}$	21.66	-2.10	$2.88x10^{-2}$	25.00
		2	-3.26	$4.23x10^{-3}$	18.89	-1.60	$6.84x10^{-2}$	19.74
	β1	1	-3.48	$2.73x10^{-3}$	22.12	-2.24	$2.23x10^{-2}$	26.51
		2	-4.00	$1.17x10^{-3}$	17.31	-1.74	$5.23x10^{-2}$	17.67
	β2	1	-2.54	$1.38x10^{-2}$	22.07	-4.24	$7.48x10^{-4}$	20.34
		2	-3.46	$2.90x10^{-3}$	17.57	-4.71	$3.25x10^{-4}$	19.49

[a] K_B is calculated in with the equation $K_B=\exp((\Delta G*1000.)/(Rcal*TK)$, where ΔG is the docking energy, R_{cal} is 1.98719 and TK is 298.15

PN22 on Site II is energetically weaker than the one observed on Site I. In TABLE 7.2 the two most populated families of the complexes of PN20 and PN22 with the monomeric $A\beta_{42}$ are summarized. PN22 showed lower binding energies, while site I was in general energetically preferred over site II. FIGURE 7.5B shows the interacting complex of PN22 on Site I. Amongst all the interaction observed here, it is important to highlight that the NH_3^+ group of residue Lys forms a strong salt-bridge interaction with residue Asp^{23}.

Pentameric Model. The target model used here was previously reported by Masman and coworkers (Masman et al. 2009a). This $A\beta_{42}$ aggregates model contains two β-sheet moieties (β1, residues 18-26 and β2, residues 31-42), which are proposed as putative binding sites. Moreover, a third possible site for interactions with ligand molecules is postulated, which involves both above mentioned sites (β1 and β2) at the edge of the aggregate. This site, here called the TOP site, is orientated into the oligomeric axis, in the same direction where the oligomers grows by aggregation. TABLE 7.2 shows the two most populated families of the complexes of PN20 and PN22 with the pentameric $A\beta_{42}$. It is observed in FIGURE 7.4B that PN20, in contrast with our expectation, has no preference to bind any of the sites targeted here. PN20 unselectively binds to β1, β2 and TOP sites. On the other hand, PN22 displayed a preference to bind the β2 site compared to the other two proposed sites. FIGURE 7.4C shows that the most populated conformations are energetically preferred when PN22 binds to site β2, while this peptide binds nonspecifically to β1 and TOP sites. FIGURE 7.6A illustrates an ideal H-bonding arrangement for TOP interaction of PN22 with an Aβ aggregate. It is depicted that PN22 may expose a "rich H-bonding face" to interact with the target molecule while exposing a "poor H-bonding face" that may stop the aggregation process. FIGURE 7.6B shows the atomic details of the interactions of the most populated complex (family 1 TOP, in TABLE 7.2). This interacting complex is the most similar arrangement to the ideal case. Even though the quantity of H-bonds was less numerous than in the ideal case, the orientation of the "poor and rich" H-bonding faces appear similar. FIGURE 7.7 reveals the atomic details of the interactions of the second most populated complex (family 2 β2, in TABLE 7.2) found between PN22 and the pentameric $A\beta_{42}$. All the ligand-target contacts are depicted as wireframe spheres. PN22 is located in a transversal direction to the Aβ chains, and inside an important channel-like hydrophobic pocket formed between the residues Ile31 and Met35 of the aggregate. The side-chains of PN22 are localized parallel to the Aβ backbone. Thus, the side-chains act as hydrophobic anchors. Obviously, due to the highly hydrophobic nature of both, target and drug molecules, the predominant interaction type is the hydrophobic contact. Also, it is interesting to mention that the *N*-methyl groups face the Aβ aggregate, this way increasing the hydrophobic contact between drug and receptor. Accordingly, the "rich H-bonding face" is exposed to the surrounding space, where the solvent (water) should be.

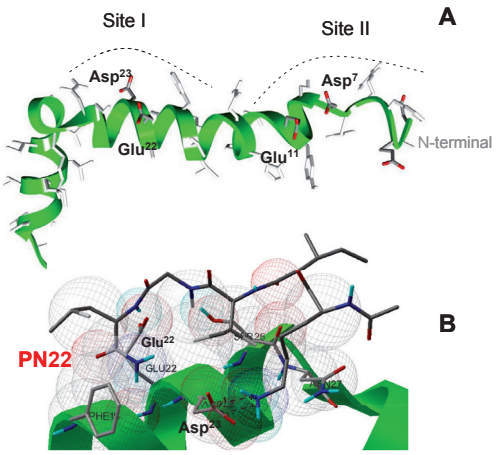

FIGURE 7.5: (**A**) Location of site I and site II on the monomeric $A\beta_{42}$ model. (**B**) Stereoview of the populated complex PN22/$A\beta_{42}$ monomeric on site I. All ligand-target contact are depicted as wireframe spheres. Salt-bridge Lys-NH_3^+/Asp^{23} is marked with a block-arrow.

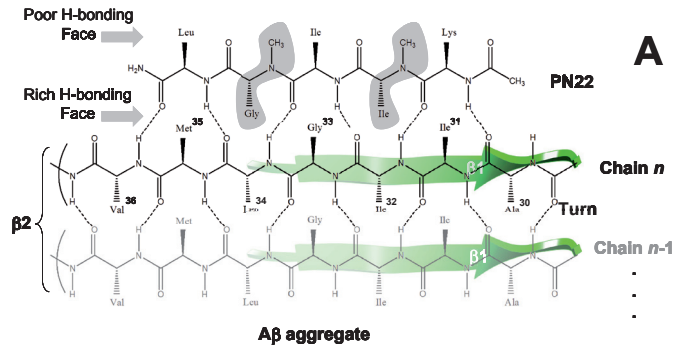

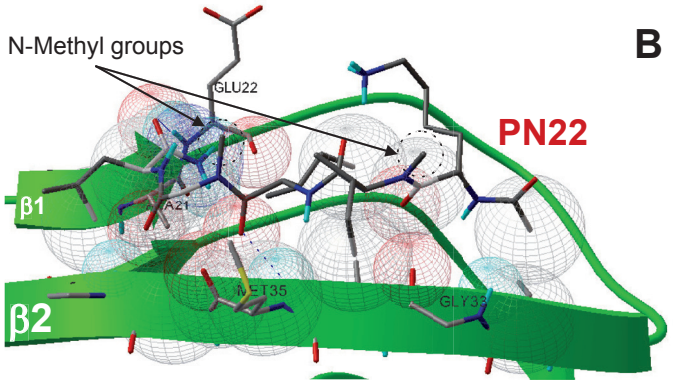

Figure 7.6: (*left*) (**A**) An ideal TOP interaction of PN22 with an $A\beta_{42}$ aggregate. The *N*-methyl amino acid residues are shaded in grey. Hydrogen bonds are represented as slashed lines (---). (**B**) A stereoview of most populated complex PN22/$A\beta_{42}$ pentameric model on site TOP. All ligand-target contact are depicted as wireframe spheres.

Figure 7.7: (*down*) A stereoview of the second most populated complex PN22/$A\beta_{42}$ pentameric on site β2. Different views are shown: lateral (**A**), frontal (**B**), zoomed in (**C** and **D**). Panel C shows the ligand-target contact which are depicted as wireframe spheres. Panel **D** shows a stereo-view of PN22 in the channel-like hydrophobic pocket formed, mainly by residues Ile31 and Met35.

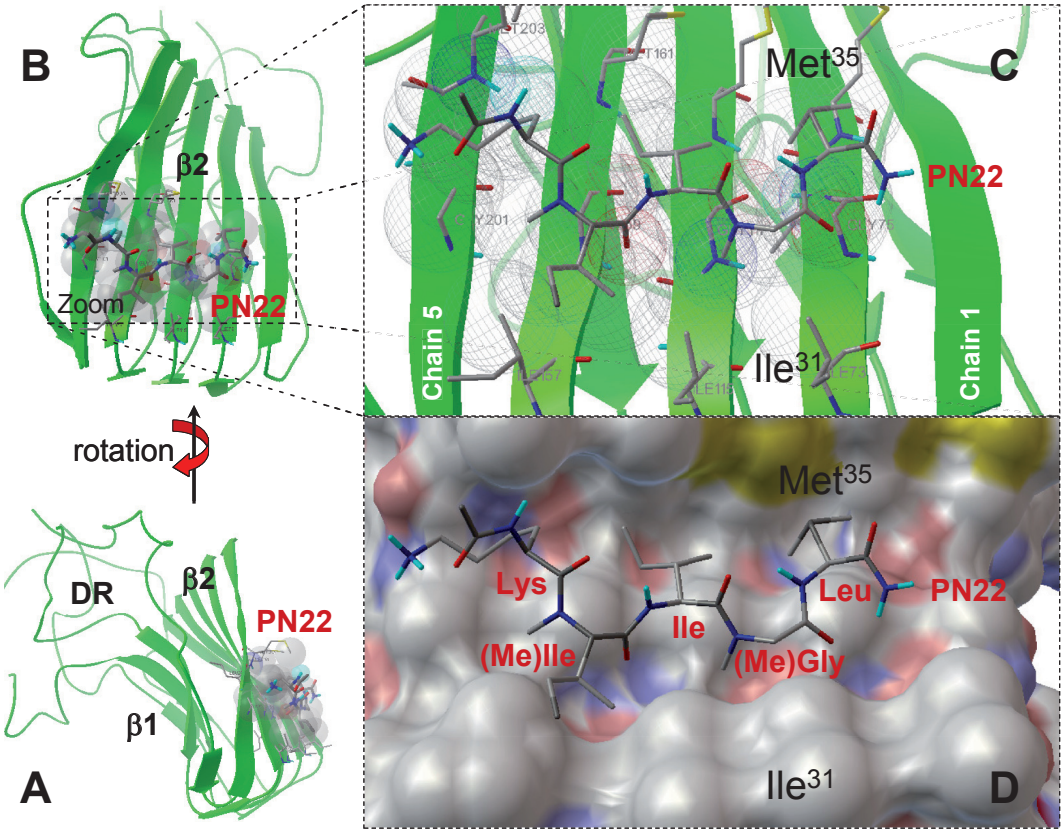

7.3.2 Experimental testing

7.3.2.1 PN22 is neuroprotective against oligomeric $A\beta_{42}$ *in vitro*

Part of this study was to provide proof of principle that the newly designed aggregation modulator peptides have the potential to protect nerve cells against Aβ-induced toxicity. Thus, we tested firstly whether these novel peptides exhibited any toxicity to neuronal cultures by themselves, and secondly whether PN20 and PN22 were capable to neutralize the toxic effect of oligomeric $A\beta_{42}$. To this purpose primary cortical neurons in culture were exposed to different concentrations of PN20 or PN22 alone, to $A\beta_{42}$ alone (25 µM) or to pentapeptides and $A\beta_{42}$ together for 24 h. Neither PN20 nor PN22 alone was toxic to neurons at any tested concentration (figure 7.8). When exposed to 25 µM oligomeric $A\beta_{42}$ only 30-40 % of the cultured neurons survived a 24 h incubation. Furthermore, both PN20 and PN22 were able to protect the neurons from $A\beta_{42}$-induced toxicity in a dose dependent manner (figure 7.8). The methylated PN22 (figure 7.8B) in that respect proved to be more effective reaching significance at 8 µM; P=0.02 when compared to the non-methylated PN20 (figure 7.8A) (reaching significance at 32 µM; P=0.01). With the highest concentration (250 µM) of PN20 up to 62.3± 12.9% of the neurons survived the Aβ treatment. 250 µM of PN22 was even more protective against the $A\beta_{42}$ challenge with up to 86.3± 3.7% cell survival.

7.3.2.2 Cognitive deficits induced by oligomeric $A\beta_{42}$ can be neutralized by PN22

Based on the *in vitro* data we selected the most effective peptide PN22 and tested whether PN22 is able to reverse the Aβ-induced memory deficits. We further included a scrambled peptide (scrP) as a control for sequence specificity of the peptides. To that purpose we used an animal model in which we injected mice with oligomeric $A\beta_{42}$ into the hippocampus to induce memory deficits (Granic et al., 2009).

One hour prior to the training session in a contextual fear conditioning paradigm C57BL/6J mice received a single injection of oligomeric $A\beta_{42}$ (30 pmol) or vehicle with PN22 (150 pmol) or scrP (150 pmol). In general the injections did not affect locomotion or the shock reaction during training

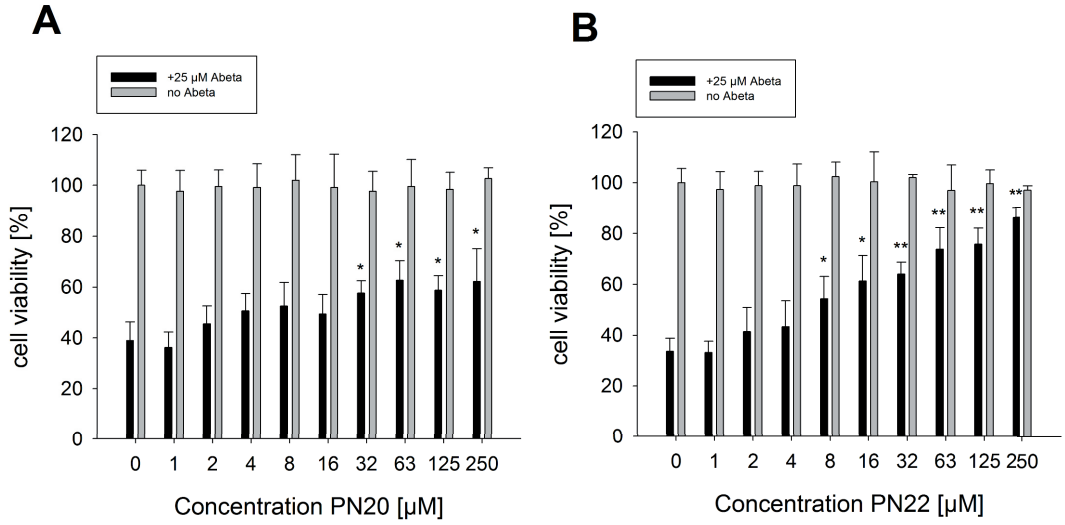

Figure 7.8: Cell viability of primary cortical neurons determined by an MTT-assay. Neuronal survival was determined after incubating increasing concentrations of the pentapeptides (**A**) PN20 and (**B**) PN22 with or without 25 µM $A\beta_{42}$ for 24 h. Bars indicate the mean cell viability in % relative to untreated controls ± SEM. (* = significant at $p < 0.05$; ** = highly significant at $p<0.005$).

(data not shown). The vehicle injected animals displayed an average relative freezing behavior, as a measure of memory score of 57.1± 2.2%, which did not differ from untreated control animals (58.1± 3.6 %). The injection of 30 pmol oligomerized $A\beta_{42}$ led to a significant decrease in freezing behavior compared to the vehicle group (33.7± 6.5% vs 57.1± 2.2; p=0.002) (FIGURE 7.9) indicative of impaired memory storage.

The PN22 and the scrP injected mice showed an average freezing of 54.9± 5.0% and 63.0± 5.5% respectively, which did not significantly differ from the untreated control (61.1± 2.4%) or vehicle injected group (58.9± 2.9%).

However, PN22 co-injected with $A\beta_{42}$ was able to abolish the $A\beta_{42}$ oligomer-induced memory impairment (53.7± 2.8% vs 33.7± 6.5%; p=0.01). Co-injection of Aβ with scrP resulted in an average freezing score of 48.0± 4.9%, which did not significantly reverse the Aβ-induced memory deficits. These results provide evidence that PN22 is capable to neutralize the negative effects induced by $A\beta_{42}$ oligomers on memory performance in an *in vivo* test paradigm.

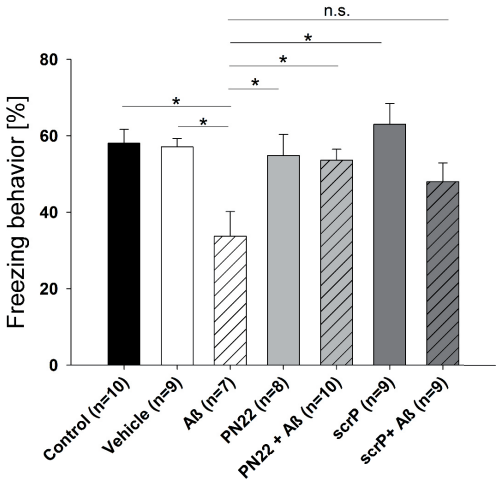

FIGURE 7.9: Effect of $A\beta_{42}$ and PN22 on contextual fear conditioning. Co-injection of $A\beta_{42}$ with PN22 prevented the Aβ-induced memory impairment significantly, whereas the non-specific control peptide scrP failed to revert memory deficits. Bars indicate the mean relative freezing score in % ± SEM. Differences were determined by ANOVA (* = significant at $p < 0.05$).

7.4 Discussion

Crucial for the aggregation process of the Aβ molecule are the hydrophobic residues that encompass the β2 region (amino acids 30-42). Thus, it was also observed for $A\beta_{42}$ monomers in solution that the sequence $I^{31}IGLMVGGVVIA^{42}$ (namely, the β2 portion) may be responsible for the higher propensity of this peptide to form amyloid aggregates (Sgourakis et al. 2007). Therefore, small peptides like PN20 and PN22, which are partially homologous to this hydrophobic region, bind with a relatively high affinity to Aβ by similar intermolecular interactions, leading to a competitive replacement of Aβ molecules. Interestingly our docking results showed that PN22 binds preferably to the β2 portion of the aggregate (TABLE 7.2 and FIGURE 7.4C), which has a good correlation with the design of this pentapeptide. However, in contrast with our expectations, PN20 did not show such a binding profile. This may be explained by the fact that PN20 displayed a complete different conformational behavior in solution than PN22 as shown by EDMC and MD simulations. PN22 had a strong preference for extended conformations, while PN20 showed a strong affinity to folded conformations. This was not only observed in solution but also in our docking results. Thus, an extended or semi-extended conformation was observed for the majority of the most populated complexes that PN22 formed, whereas the opposite was the case for

PN20. It appears to be that an extended or semi-extended conformation is the possible "biologically relevant conformation" or "pharmacophoric patron" for these peptides.

On the other hand, all the docked preferred conformations showed a tendency to extended or semi-extended ligand's orientation. Moreover, the docking studies could predict that a modification of PN20 by alternated *N*-methylation, thereby moderately increasing its hydrophobicity, improves the interaction to the β2 portion of the $A\beta_{42}$.aggregates. Thus, PN22 shows a selective binging to the portion β2. Neither PN20 nor PN22 showed a preference to bind the monomeric or the pentameric $A\beta_{42}$ model, which suggests us that the peptides may bind to both forms of $A\beta_{42}$.

We hypothesize that Site I-bound-PN22, especially on Asp[23], causes impediment or slowing down of the conformational change that precedes the aggregation. Consequently, PN22 binding increases the possibilities of degradation or clearance of Aβ monomers (see FIGURE 7.1), since, Asp[23] plays a crucial role in the stabilization of the Aβ aggregates. In general it can be observed that PN22 binds stronger and selectively to Site I, to the monomeric $A\beta_{42}$ than PN20.

The present results indicated that pentapeptides PN20 and PN22 can significantly preserve cultured neurons from Aβ-induced cell death in a dose dependent manner. Moreover, the methylated pentapeptide PN22 protected the cells more effectively than the non-methylated PN20. Similar results on PC12 cells by using different single *N*-methyl amino acid containing peptides were previously reported (Cruz et al. 2004; Hughes et al. 2000). Peptides endowed with *N*-methyl amino acids have some clear advantages with respect to their potential as a therapeutic agent. These peptides remain remarkably stable to changes in solvent conditions and resist denaturation by heating, changes in pH (from 2.5 to 10.5), and addition of denaturants. Furthermore, this kind of peptides despite their hydrophobic composition is highly water soluble. A water soluble but hydrophobic nature suggest that these peptides might be able to pass spontaneously through biological cell membranes (Gordon et al. 2002).

An important aim of our study was to establish if a compound like PN22 is able to prevent Aβ–induced learning and memory deficits in a mammalian animal model. We showed that a 5-fold molar excess of PN22 to Aβ could overcome the detrimental effects of Aβ oligomers on memory when injected into the hippocampal region. Thus, we provide evidence that *N*-methyl containing peptides such as PN22 bear therapeutic potential against Aβ-induced memory impairment.

The mechanism how these pentapeptides exert their protective effects on cell death and behavior is not yet fully understood. However, these peptides directly bind to Aβ and thereby may prevent possible interactions between Aβ and neuronal membrane proteins and in this way neutralize the toxic effect of Aβ oligomers. We hypothesize two options of interaction notably of PN22 with Aβ that are depicted in figure 1. Pathway 1 proposes that PN22 binds to the monomeric Aβ thus preventing and/or retarding the formation of toxic oligomers, by interfering with the conformational change that precedes the oligomer formation. Pathway 2 suggests that PN22 binds to the already formed Aβ oligomers thereby preventing and/or modulating, somehow, its neurotoxic properties. By either of these actions, or both, the neurotoxicity of Aβ is decreased or reverted and the Aβ clearance/degradation processes be reactivated.

We may conclude that this novel *in silico* designed *N*-methyl amino acid containing peptide interacts with $A\beta_{42}$ and that different regions of Aβ may be selectively targeted by this peptide. Our findings provide evidence on how and where PN22 interacts with $A\beta_{42}$ mono- and oligomers, that PN22 can neutralize the neurotoxic effects

of soluble $A\beta_{42}$ oligomers *in vitro* and *in vivo*. In the latter condition we obtained proof of principle that this pentapeptide can effectively prevent the Aβ oligomer-induced deficits in memory performance. More structural evidence is required to consolidate the proposed mechanism and to further improve our peptide designs. Nevertheless, it is clear that these peptides can serve as promising molecular designs that hold promise as therapeutic molecules for treatment of AD. ▪

Acknowledgements

This work was supported by grants from the International Foundation for Alzheimer Research (ISAO), the Netherlands Brain Foundation (Hersenstichting Nederland), the Gratama Stichting, and EU-grant FP6 NeuroprMiSe LSHM-CT-2005-018637. This work reflects only the author's views. The European Community is not liable for any use that may be made of the information herein.

"The brain may take advice, but not the heart, and love, having no geography, knows no boundaries: weight and sink it deep, no matter, it will rise and find the surface: and why not? any love is natural and beautiful that lies within a person's nature; only hypocrites would hold a man responsible for what he loves, emotional illiterates and those of righteous envy, who, in their agitated concern, mistake so frequently the arrow pointing to heaven for the one that leads to hell'
(T. Capote)

08

"Rescued"

oil on paper (320x450 mm)

M.F. Masman 2010


USED

Chapter 8

C8

General discussion & future perspectives

Marcelo F. Masman

8.1 The role of computational medicinal chemistry in today's drug discovery

It is well known that the ultimate goal of the medicinal chemist is to develop, by rational design, a molecule which will produce a desired biological activity without producing undesirable collateral effects. To be able to achieve such an objective a complete description of the pharmacophore (box 8.1) is extremely important. Although the presently available techniques of molecular modeling have allowed more "rational" and planned investigation with respect to those developed in the last century, they are still far from perfect. However, computational chemical techniques are used routinely to identify underlying reasons and explanations for observed chemical reactivity, or to assess the probability of a molecule to exhibit certain desired properties. Thus, *in silico* (box 8.2) techniques reduce the human effort, the time consumed in bioassays, and the number of experimental animal laboratory studies necessary to provide the first steps towards developing a new drug. In order to achieve the above mentioned goals, compromises in view of the complexity of the biological system and individual variations must be taken into account. Otherwise, a realistic approach of a given system may be put at risk.

Box 8.1: Pharmacophore definitions
- P. Ehrlich, (1909); "a molecular framework that carries (phoros) the essential features responsible for a drug's (pharmacon) biological activity".
- P. Gund, (1977); "a set of structural features in a molecule that is recognized at a receptor site and is responsible for that molecule's biological activity"
- IUPAC (1998); "an ensemble of steric and electronic features that is necessary to ensure the optimal supramolecular interactions with a specific biological target and to trigger or block its biological response".

Besides being a very interesting source of new potential drugs, peptides are still relatively large sized systems which seriously limit the complexity of the level of theory that is going to be used to attack the problem from the point of view of the computational technique. Normally, a hybrid methodology that combines molecular dynamics with quantum mechanical geometry optimization is nowadays used. Complex molecular systems can be approached by using this methodology in a relatively realistic fashion. Also, a reduced model may be generated from the former one in order to perform more exact energetic determinations by using quantum calculations. Thus, the "whole" system can be studied by splitting it into several reduced models. It is for this reason that this reductionist approach is generally called a "divide and conquer" challenge.

On the other hand, the rapidly evolving and improving cost-performance relationship is placing high-tech computers on the desktop of today's medicinal chemist. Access to high resolution interactive computer graphics, conformational energy minimization of relatively larger biological systems, classical and quantum molecular dynamics, geometrical optimizations, homologous protein structure generation and sequence database searching are examples of some tools which can routinely accessed through commercial molecular modeling software packages. All in all, these improvements allow us to perform more realistic simulations of the biological system under study.

The application of molecular modeling techniques in any area of medicinal chemistry have been shown to be convenient and necessary in order to determine the potential compounds to be synthesized and tested. Some great findings have been accomplished regarding drug design based on molecular modeling. For instance, Agouron Pharmaceutical designed Viracept, an HIV-1 protease inhibitor, using structure-based design tools (Babine et al. 1995). Crixivan (Dorsey et al. 1994), another HIV-1 protease inhibitor received FDA approval in record time, and is now used by over 300,000 patients worldwide. Also, by means of structure-based methods, Merck developed a glaucoma therapeutic agent called Trusopt (Greer et al. 1994). Without such calculations, neither structure based approaches nor *de novo* drug design would be at the stage that they are at present. In addition, these techniques helped to design several new candidate drugs as mentioned above.

I personally consider from a scientific point of view that the use of molecular modeling supporting experimental bioassays is not only preferable, but also necessary. It has been recognized that scientific knowledge has advanced far enough to permit a focus on molecular mechanisms with atomistic details. In today's drug discovery *in silico* molecular modeling studies are now developed and fully accepted, not as a supplement to a checklist procedure, but rather as integral part of medicinal chemistry.

Box 8.2: *In silico* is an expression used to mean "performed on computer or via computer simulation." The phrase is coined in analogy to the latin phrases *in vivo* and *in vitro* which are commonly used in biology and refer to experiments done in living organisms and outside of living organisms, respectively. The term *in silico* does not mean anything in latin. The proper latin phrase would likely be in simulacro to describe experiments done on the likeness (simulacrum) or model of a phenomenon.

8.2 cAMP signaling pathways as a putative new target of antifungal drugs

Amongst the fungi tested as part of the present thesis, *Cryptococcus neoformans* (box 8.3) and *Candida albicans* (box 8.4) were the most sensitive to the antifungal peptides designed in this thesis. It is important to highlight that the mechanism of action of these peptides has not been determined yet. Nevertheless, as a general feature, antimicrobial cationic peptides possess a relatively non-specific mechanism of action by either acting through a detergent-like disruption of the bacterial or fungal cell membrane or by the formation of transient transmembrane pores (Huang 2000; Shai 2002). The former mechanisms are the ones proposed especially for cell-penetrating peptides studied in chapter 4, since these peptides are long enough to form α-helix conformations that may lead to cell membrane pore formation. However, peptides derived from the α-MSH studied in chapters 2-3 may be too short to form cell membrane pores. Nevertheless, there is now evidence that the antimicrobial activity of α-MSH and derivative peptides is exerted through a unique mechanism substantially different from that of other natural antimicrobial peptides, at least in the case of *C. albicans* (Grieco et al. 2003).

Previous investigations have yielded evidence that the candidacidal effect of α-MSH is linked to mechanism of cAMP-inducing activity. α-MSH seems to increase cAMP production in *C. albicans* and the adenylyl cyclase inhibitor ddAdo (dideoxyadenosine) partly reversed the candidacidal effect of the peptide (Cutuli et al. 2000; Grieco et al. 2003). It is remarkable, however when we carefully look at it, this mechanism of action in *C. albicans* mimics the influence of α-MSH in mammalian cells in which the peptide binds to G-protein-linked melanocortin receptors, activates adenylyl cyclase, and increases cAMP. In support of this, Singh and coworkers reported that, by using phosphodiesterase inhibitors, the alteration in the cAMP signaling pathway affects the cell cycle progression in *Candida albicans* (Singh et al. 2007). Therefore, implication of cAMP signaling in both the cell cycle and morphogenesis seems to be a potential target for the development of new antifungal drugs. However, due to the overall implications that cAMP signaling pathways have in humans, one may ask; how selective the designed drugs using this target would be? Since, fungal cells seem to have similar cAMP signaling pathways as human cells, a compound that targets this pathway would not be, at least in principle, a selective enough candidate.

Box 8.3: *Cryptococcus neoformans* is an encapsulated yeast-like fungus that can live in both plants and animals. This species belongs to the broad class of organisms called "club fungi" or division basidiomycota, which is one the five major types of fungi. *C. neoformans* usually grows as a yeast (unicellular) and replicates by budding. Under certain conditions, both in nature and in the laboratory, *C. neoformans* can grow as a filamentous fungus. When grown as a yeast, *C. neoformans* has a prominent capsule composed mostly of polysaccharides. Infection with *C. neoformans* is termed cryptococcosis. Most infections with *C. neoformans* consist of a lung infection. However, fungal meningitis, especially as a secondary infection for AIDS patients, is often caused by *C. neoformans* making it a particularly dangerous fungus. Infections with this fungus are rare in those with fully functioning immune systems. For this reason, *C. neoformans* is sometimes referred to as an opportunistic fungus.

Box 8.4: *Candida albicans* is a yeast fungus and a causal agent of opportunistic oral and genital infections in humans. Systemic fungal infections, especially candidiasis, have emerged as important causes of morbidity and mortality in immunocompromised patients (e.g., AIDS, cancer chemotherapy and organ or bone marrow transplantation). *C. albicans* is among the many organisms that live in the human mouth and gastrointestinal tract. Under normal circumstances, *C. albicans* lives in *ca* 80% of the human population with no harmful effects, although overgrowth results in candidiasis.

8.3 Targeting the amyloid hypothesis with Aβ-toxicity offsetting peptides

It is controversially discussed whether the amyloid fibrils are an epiphenomenon linked to Alzheimer's disease (AD) or whether fibril formation causes AD (Forman et al. 2007; Wisniewski et al. 1997). There is now more consensus, however, based on *in vitro* and *in vivo* evidence that soluble oligomeric forms of Aβ have potent neurotoxic activity and are the primary causes of neuronal injury and cell death occurring in AD (Lesne et al. 2006; Lue et al. 1999; Naslund et al. 2000; Wasling et al. 2009). On the other hand, there is a relatively weak correlation between the severity of dementia and the density of fibrillar amyloid plaques (Dickson et al. 1995; Katzman 1986; Terry et al. 1991) and indeed this has been frequently cited as a critical flaw in the Aβ hypothesis. However, several studies have shown a robust correlation between soluble Aβ levels and the extent of synaptic loss and severity of cognitive impairment (Chang et al. 2006; Chapman et al. 1999b; Dineley et al. 2002; Dodart et al. 2002; Haass and Selkoe 2007; Jacobsen et al. 2006; Lesne et al. 2006; Lue et al. 1999; McLean et al. 1999; Naslund et al. 2000; Shankar et al. 2008; Shankar et al. 2007b; Walsh and Selkoe 2007; Wang et al. 1999; Wasling et al. 2009).

It is important to mention that the production of Aβ is a normal process (Haass et al. 1992a; Seubert et al. 1992; Shoji et al. 1992), but in a small number of individuals, the overproduction of all Aβ species, or an increased proportion of the 42 amino acids form, appears sufficient to cause early onset AD (Bentahir et al. 2006; Cai et al. 1993; Citron et al. 1992; Haass et al. 1992b; Kumar-Singh et al. 2006; Roveletlecrux et al. 2006; Seubert et al. 1992; Suzuki et al. 1994). Therefore, the mere presence of Aβ does not cause neurodegeneration; rather neuronal injury appears to ensue as a result of the ordered self-association of Aβ molecules (Busciglio et al. 1992; Geula et al. 1998; Pike et al. 1991). However, it should be appreciated that besides its pathological properties, Aβ may have important roles in synaptic plasticity and normal brain functioning (Pearson and Peers 2006; Puzzo et al. 2008; Wasling et al. 2009). The endogenous level of Aβ in the brain is regulated by synaptic activity *in vivo*, suggesting a dynamic feedback loop involving APP metabolism and Aβ that may modulate synaptic activity (Haass and Selkoe 2007). Thus, it has been shown that the depletion of endogenous Aβ, by a single intrahippocampal administration of anti-Aβ-antibody, leads to disrupted memory retention in rats (Garcia-Osta and Alberini 2009).

The advantage of targeting the amyloid hypothesis with Aβ-toxicity offsetting peptides (BOX 8.5), in comparison to other putative therapeutic approaches for AD such as vaccination, is that they specifically target the abnormal conformation of Aβ without interfering with any possible physiological function of the soluble monomeric Aβ peptide. Moreover, this type of compounds may not interfere with the metabolism of APP, and this is an advantage in comparison with the secretase inhibitors (e.g.: β-secretase and g-secretase inhibitors). Blocking this secretase system can cause failures of very important metabolic pathways. Thus, blocking γ-secretase complex, besides lowering Aβ formation in experimental systems, interferes with receptor/signalling system of the protein Notch. The reduction of Notch activity could interfere with important cellular proliferation and differentiation pathways (Pollack and Lewis 2005).

Box 8.5: The term Aβ-toxicity offsetting peptides is used in this thesis to refer to those peptides that somehow, neutralize the toxic effect of Aβ on neurons. The term "*β-sheet breakers*", introduced by C. Soto in 1998, have been widely used to refer to this kind of peptides, even when the peptides did not show any β-sheet breaking properties. For this reason, I propose to use this new terminology to refer to this novel class of compounds, in which the effect of the peptide is mentioned but not necessarily its way of action.

On the other hand, it was shown that Leu-Pro-Tyr-Phe-Asp-NH_2 and PN22 peptides, in respectively CHAPTERS 6 and 7, may bind the monomeric form of $A\beta_{42}$. Nevertheless, this binding property may interfere with the conformational changes that precede the aggregation process and not with the normal physiological functions of the soluble monomeric Aβ peptide.

8.4 May anti-amyloid properties lead to antifungal activity?

Some of the Aβ-toxicity offsetting peptides studied here were designed on the basis of their capabilities to bind Aβ aggregates by "mimicking" Aβ properties and conformational behavior (CHAPTERS 6 and 7), which might endow them anti-amyloid properties. On the other hand, the antifungal peptides ported in CHAPTERS 2-4 share some structural similarities with these Aβ-offsetting peptides. For instance, both types of peptides are positively charged and have a compromising relationship between hydrophobic/aromatic residues and charged residues. However, they do not necessarily share the same conformational preferences. In general, cell-penetrating peptides with antifungal properties (CHAPTER 4) showed a preference to form folded conformations (a-helix-like conformations), while α-MSH derived antifungal peptides (CHAPTERS 2-3) preferred extended conformations (β-sheet-like conformations). The latter one is another similarity shared with the Aβ-toxicity offsetting peptides reported in CHAPTER 7. Regarding the above mentioned, one may wonder whether anti-amyloid properties can lead to antifungal activity?

Within the past two decades, several proteins that do not necessarily have similar amino-acid sequences have been reported to form amyloid-like aggregates on the surfaces of some fungi and bacteria (Claessen et al. 2003; Claessen et al. 2002; Gebbink et al. 2005). The functions that these aggregated proteins seem to play on the surfaces of these microorganisms are multifold. For instances, these amyloids play an important role in the invasion of abiotic and biotic substrates, reduce the water surface tension allowing hyphae to escape aqueous environments, and enable hyphae to penetrate solid surfaces (e.g.: host cuticle) amongst others. There is also experimental evidence that the amyloid layer forms a protective "coat" to allow microorganisms to evade the immune system of the host (Wosten and De Vocht 2000). Currently, hydrophobins are the only proteins known to form amyloids on fungal surfaces (Linder 2009). Other proteins may fulfill this role in fungi that do not express hydrophobins (e.g.: *Candida albicans*) (Gebbink et al. 2005). Bacteria have been shown to form cell-surface-located amyloids of two classes of proteins; chaplins and curli/tafi (Claessen et al. 2003; Gebbink et al. 2005). Thus, it seems that the presence of amyloid structures on the cell surface of microorganisms is widespread. Therefore, these amyloid-like arrangements seem to be a promising novel target to design compounds capable of disrupting the structure of these aggregates and through this action to expert their anti-microbial properties. In that respect, *C. neoformans* seems to be highly affected by the peptides reported in this thesis (CHAPTERS 2-4). May be this due to an existing amyloid "coat" on the surface of this fungus, which may be disrupted by these peptides? Whether this is the case of *C. neoformans* or not, the finding of such structures on the surface of pathogenic microorganisms that cause life-threatening infections, is a novel target to develop selective therapeutic agents.

8.5 Overall conclusions and perspectives

The work described in this thesis is a step forward towards a protein based drug design in which methods of rational drug design and dynamical features of the target have been taken into account. Clearly, the *in silico* design is a method that can be used to study complex biological systems. However, the results of the simulations should be interpreted with caution.

Several new targets to develop putative drugs have been mentioned in this thesis, which may give the possibility to project future investigation programs, some of them are already being in a developing phase. With regards to antifungal peptides, new families, based on our results reported in CHAPTER 4, are being designed, synthesized and tested. Regarding the Aβ-toxicity offsetting peptides, new structures have been proposed as well as peptidomimetic structures currently under investigation in our labs. We may conclude with the statement that the findings presented in this thesis hold great potential for further development of a strategy towards therapeutic applications in two major human health conditions. ▪

REFERENCES

A

Ablordeppey SY, Fan P, Ablordeppey JH and Mardenborough L (1999) Systemic antifungal agents against AIDS-related opportunistic infections: Current status and emerging drugs in development. Current Medicinal Chemistry 6:1151-1195.

Adessi C and Soto C (2002) Converting a peptide into a drug: strategies to improve stability and bioavailability. Curr Med Chem 9:963-978.

Aisen PS (2005) The development of anti-amyloid therapy for Alzheimer's disease: From secretase modulators to polymerisation inhibitors. CNS Drugs 19:989-996.

Almeida CG, Tampellini D, Takahashi RH, Greengard P, Lin MT, Snyder EM and Gouras GK (2005) Beta-amyloid accumulation in APP mutant neurons reduces PSD-95 and GluR1 in synapses. Neurobiol Dis 20:187-198.

Ammassari-Teule M, Middei S, Passino E and Restivo L (2002) Enhanced procedural learning following beta-amyloid protein (1-42) infusion in the rat. Neuroreport 13:1679-1682.

Atkinson AB and Robertson JIS (1979) Captopril in the treatment of clinical hypertension and cardiac failure. Lancet 2:836-839.

Atwood CS, Huang X, Moir RD, Tanzi RE and Bush AI (1999) Role of free radicals and metal ions in the pathogenesis of Alzheimer's disease. Met Ions Biol Syst 36:309-364.

Atwood CS, Perry G, Zeng H, Kato Y, Jones WD, Ling KQ, Huang X, Moir RD, Wang D, Sayre LM, Smith MA, Chen SG and Bush AI (2004) Copper mediates dityrosine cross-linking of Alzheimer's amyloid-beta. Biochemistry 43:560-568.

B

Babine RE, Bleckman TM, Kissinger CR, Showalter R, Pelletier LA, Lewis C, Tucker K, Moomaw E, Parge HE and Villafranca JE (1995) Design, synthesis and X-ray crystallographic studies of novel FKBP-12 ligands. Bioorganic and Medicinal Chemistry Letters 5:1719-1724.

Bakhle YS, Reynard AM and Vane JR (1969) Metabolism of the angiotensins in isolated perfused tissues. Nature 222:956-959.

Balbach JJ, Petkova AT, Oyler NA, Antzutkin ON, Gordon DJ, Meredith SC and Tycko R (2002) Supramolecular structure in full-length Alzheimer's beta-amyloid fibrils: evidence for a parallel beta-sheet organization from solid-state nuclear magnetic resonance. Biophys J 83:1205-1216.

Bartroli J, Turmo E, Alguero M, Boncompte E, Vericat ML, Conte L, Ramis J, Merlos M, Garcia-Rafanell J and Forn J (1998a) New azole antifungals. 2. Synthesis and antifungal activity of heterocyclecarboxamide derivatives of 3-amino-2-aryl-1-azolyl-2-butanol. Journal of Medicinal Chemistry 41:1855-1868.

Bartroli J, Turmo E, Alguero M, Boncompte E, Vericat ML, Conte L, Ramis J, Merlos M, Garcia-Rafanell J and Forn J (1998b) New azole antifungals. 3. Synthesis and antifungal activity of 3- substituted-4(3H)-quinazolinones. Journal of Medicinal Chemistry 41:1869-1882.

Bartus RT (2000) On neurodegenerative diseases, models, and treatment strategies: Lessons learned and lessons forgotten a generation following the cholinergic hypothesis. Experimental Neurology 163:495-529.

Bartus RT, Dean Iii RL, Beer B and Lippa AS (1982) The cholinergic hypothesis of geriatric memory dysfunction. Science 217:408-417.

Baumketner A, Bernstein SL, Wyttenbach T, Lazo ND, Teplow DB, Bowers MT and Shea JE (2006) Structure of the 21-30 fragment of amyloid beta-protein. Protein Sci 15:1239-1247.

Beke T, Csizmadia IG and Perczel A (2006) Theoretical Study on Tertiary Structural Elements of beta-peptides: Nanotubes Formed from Parallel-Sheet-Derived Assemblies of beta-Peptides. Journal of the American Chemical Society 128:5158-5167.

Bentahir M, Nyabi O, Verhamme J, Tolia A, Horre K, Wiltfang J, Esselmann H and De Strooper B (2006) Presenilin clinical mutations can affect β-secretase activity by different mechanisms. Journal of Neurochemistry 96:732-742.

Berendsen HJC, Postma JPM, van Gunsteren WF, DiNola A and Haak JR (1984) Molecular dynamics with coupling to an external bath. The Journal of Chemical Physics 81:3684-3690.

Berendsen HJC, Postma JPM, Van Gunsteren WF and Hermans J (1981a) Interaction models for water in relation to protein hydration. Intermolecular Forces:331-342.

Berendsen HJC, Postma JPM, von Gunstaren WF and Hermans J in Intermolecular Forces. edited by B Pullman (Reidel, Dordrecht, Holland, 1981):331.

Berendsen HJC, Postma JPM, von Gunstaren WF and Hermans J (1981b) in Intermolecular Forces. edited by B Pullman (Reidel, Dordrecht, Holland):331.

Berman HM, Battistuz T, Bhat TN, Bluhm WF, Bourne PE, Burkhardt K, Feng Z, Gilliland GL, Iype L, Jain S, Fagan P, Marvin J, Padilla D, Ravichandran V, Schneider B, Thanki N, Weissig H, Westbrook JD and Zardecki C (2002) The Protein Data Bank. Acta Crystallogr D Biol Crystallogr 58:899-907.

Bhakdi S, Muhly M and Roth M (1983) Preparation and isolation of specific antibodies to complement components. Methods in Enzymology Vol. 93:409-420.

Bhakdi S and Tranum Jensen J (1983) Membrane damage by complement. Biochimica et Biophysica Acta - Reviews on Biomembranes 737:343-372.

Billings LM, Oddo S, Green KN, McGaugh JL and LaFerla FM (2005) Intraneuronal Aβ causes the onset of early Alzheimer's disease-related cognitive deficits in transgenic mice. Neuron 45:675-688.

Bisogno F, Mascoti L, Sanchez C, Garibotto F, Giannini F, Kurina-Sanz M and Enriz R (2007) Structure-antifungal activity relationship of cinnamic acid derivatives. Journal of Agricultural and Food Chemistry 55:10635-10640.

Black SE, Wilcock G and Haworth J (2005) A placebo-controlled, double-blind trial of the selective $A\beta_{42}$-lowering agent, Flurizan in patients with mild to moderate Alzheimer's disease: Efficacy, safety, and follow-up study results.

Blennow K, de Leon MJ and Zetterberg H (2006) Alzheimer's disease. Lancet 368:387-403.

Boman HG, Agerberth B and Boman A (1993) Mechanisms of action on Escherichia coli of cecropin P1 and PR-39, two antibacterial peptides from pig intestine. Infection and Immunity 61:2978-2984.

Borel JF (1989a) The cyclosporins. Transplantation Proceedings 21:810-815.

Borel JF (1989b) Pharmacology of cyclosporine (sandimmune). IV. Pharmacological properties *in vivo*. Pharmacological Reviews 41:259-371.

Borel JF, Di Padova F, Mason J, Quesniaux V, Ryffel B and Wenger R (1989) Pharmacology of cyclosporine (sandimmune). I. Introduction. Pharmacological Reviews 41:239-242.

Borreguero JM, Urbanc B, Lazo ND, Buldyrev SV, Teplow DB and Stanley HE (2005) Folding events in the 21-30 region of amyloid beta-protein (Abeta) studied *in silico*. Proc Natl Acad Sci U S A 102:6015-6020.

Bowdish DME and Hancock REW (2005) Anti-endotoxin properties of cationic host defence peptides and proteins. Journal of Endotoxin Research 11:230-236.

Brattwall CEB, Lincoln P and Norden B (2003) Orientation and Conformation of Cell-Penetrating Peptide Penetratin in Phospholipid Vesicle Membranes Determined by Polarized-Light Spectroscopy. Journal of the American Chemical Society 125:14214-14215.

Brown KL and Hancock REW (2006) Cationic host defense (antimicrobial) peptides. Current Opinion in Immunology 18:24-30.

Brunkan AL and Goate AM (2005) Presenilin function and β-secretase activity. Journal of Neurochemistry 93:769-792.

Buchete NV and Hummer G (2007) Structure and dynamics of parallel beta-sheets, hydrophobic core, and loops in Alzheimer's A beta fibrils. Biophys J 92:3032-3039.

Buchete NV, Tycko R and Hummer G (2005) Molecular dynamics simulations of Alzheimer's beta-amyloid protofilaments. J Mol Biol 353:804-821.

Bulet P and Stöcklin R (2005) Insect antimicrobial peptides: Structures, properties and gene regulation. Protein and Peptide Letters 12:3-11.

Bull HG, Thornberry NA and Cordes MHJ (1985) Inhibition of rabbit lung angiotensin-converting enzyme by N(a)-[(S)-1-carboxy-3-phenylpropyl]*L*-alanyl-*L*-proline and N(a)-[(S)-1-carboxy-3-phenylpropyl]*L*-lysyl-*L*-proline. Journal of Biological Chemistry 260:2952-2962.

Burdick D, Soreghan B, Kwon M, Kosmoski J, Knauer M, Henschen A, Yates J, Cotman C and Glabe C (1992) Assembly and aggregation properties of synthetic Alzheimer's A4/beta amyloid peptide analogs. J Biol Chem 267:546-554.

Busciglio J, Lorenzo A and Yankner BA (1992) Methodological variables in the assessment of beta amyloid neurotoxicity. Neurobiology of Aging 13:609-612.

Bush AI (2002) Metal complexing agents as therapies for Alzheimer's disease. Neurobiol Aging 23:1031-1038.

C

Cabiaux V, Agerberth B, Johansson J, Homble F, Goormaghtigh E and Ruysschaert JM (1994) Secondary structure and membrane interaction of PR-39, a Pro+Arg-rich antibacterial peptide. European Journal of Biochemistry 224:1019-1027.

Cai XD, Golde TE and Younkin SG (1993) Release of excess amyloid b protein from a mutant amyloid b protein precursor. Science 259:514-516.

Carotenuto A, Saviello MR, Auriemma L, Campiglia P, Catania A, Novellino E and Grieco P (2007) Structure-function relationships and conformational properties of α-MSH(6-13) analogues with candidacidal activity. Chemical Biology and Drug Design 69:68-74.

Carrupt PA, El Tayar N, Karlen A and Testa B (1991) Molecular electrostatic potentials for characterizing drug-biosystem interactions. Methods in Enzymology 203:638-677.

Chacon MA, Barria MI, Soto C and Inestrosa NC (2004) Beta-sheet breaker peptide prevents Abeta-induced spatial memory impairments with partial reduction of amyloid deposits. Mol Psychiatry 9:953-961.

Chang EH, Savage MJ, Flood DG, Thomas JM, Levy RB, Mahadomrongkul V, Shirao T, Aoki C and Huerta PT (2006) AMPA receptor downscaling at the onset of Alzheimer's disease pathology in double knockin mice. Proc Natl Acad Sci U S A 103:3410-3415.

Chapman PF, White GL, Jones MW, Cooper-Blacketer D, Marshall VJ, Irizarry M, Younkin L, Good MA, Bliss TV, Hyman BT, Younkin SG and Hsiao KK (1999a) Impaired synaptic plasticity and learning in aged amyloid precursor protein transgenic mice. Nat Neurosci 2:271-276.

Chapman PF, White GL, Jones MW, Cooper-Blacketer D, Marshall VJ, Irizarry M, Younkin L, Good MA, Bliss TVP, Hyman BT, Younkin SG and Hsiao KK (1999b) Impaired synaptic plasticity and learning in aged amyloid precursor protein transgenic mice. Nature Neuroscience 2:271-276.

Chasse GA, Rodriguez AM, Mak ML, Deretey E, Perczel A, Sosa CP, Enriz RD and Csizmadia IG (2001) Peptide and protein folding. Journal of Molecular Structure: THEOCHEM 537:319-361.

Chauhan V and Chauhan A (2006) Oxidative stress in Alzheimer's disease. Pathophysiology 13:195-208.

Chen QS, Kagan BL, Hirakura Y and Xie CW (2000) Impairment of hippocampal long-term potentiation by Alzheimer amyloid beta-peptides. J Neurosci Res 60:65-72.

Chen QS, Wei WZ, Shimahara T and Xie CW (2002) Alzheimer amyloid beta-peptide inhibits the late phase of long-term potentiation through calcineurin-dependent mechanisms in the hippocampal dentate gyrus. Neurobiol Learn Mem 77:354-371.

Chitnumsub P, Fiori WR, Lashuel HA, Diaz H and Kelly JW (1999) The nucleation of monomeric parallel β-sheet-like structures and their self-assembly in aqueous solution. Bioorganic and Medicinal Chemistry 7:39-59.

Chothia C and Janin J (1982) Orthogonal packing of beta-pleated sheets in proteins. Biochemistry 21:3955-3965.

Christensen R, Marcussen AB, Wortwein G, Knudsen GM and Aznar S (2008) Abeta(1-42) injection causes memory impairment, lowered cortical and serum BDNF levels, and decreased hippocampal 5-HT(2A) levels. Exp Neurol 210:164-171.

Christiaens B, Grooten J, Reusens M, Joliot A, Goethals M, Vandekerckhove J, Prochiantz A and Rosseneu M (2004) Membrane interaction and cellular internalization of penetratin peptides. European Journal of Biochemistry 271:1187-1197.

Christiaens B, Symoens S, Vanderheyden S, Engelborghs Y, Joliot A, Prochiantz A, Vandekerckhove J, Rosseneu M and Vanloo B (2002a) Erratum: Tryptophan flourescene study of the interaction of penetratin peptides with model membranes (European Journal of Biochemistry (2002) 269 (2918-2962)). European Journal of Biochemistry 269:5101.

Christiaens B, Symoens S, Vanderheyden S, Engelborghs Y, Joliot A, Prochiantz A, Vandekerckhove J, Rosseneu M and Vanloo B (2002b) Tryptophan fluorescence study of the interaction of penetratin peptides with model membranes. European Journal of Biochemistry 269:2918-2926.

Cirrito JR, Deane R, Fagan AM, Spinner ML, Parsadanian M, Finn MB, Jiang H, Prior JL, Sagare A, Bales KR, Paul SM, Zlokovic BV, Piwnica-Worrns D and Holtzman DM (2005) P-glycoprotein deficiency at the blood-brain barrier increases amyloid-b deposition in an Alzheimer disease mouse model. Journal of Clinical Investigation 115:3285-3290.

Citron M (2004) Strategies for disease modification in Alzheimer's disease. Nature Reviews Neuroscience 5:677-685.

Citron M, Oltersdorf T, Haass C, McConlogue L, Hung AY, Seubert P, Vigo-Pelfrey C, Lieberburg I and Selkoe DJ (1992) Mutation of the β-amyloid precursor protein in familial Alzheimer's disease increases β-protein production. Nature 360:672-674.

Claessen D, Rink R, De Jong W, Siebring J, De Vreugd P, Boersma FGH, Dijkhuizen L and Wosten HAB (2003) A novel class of secreted hydrophobic proteins is involved in aerial hyphae formation in Streptomyces coelicolor by forming amyloid-like fibrils. Genes and Development 17:1714-1726.

Claessen D, Wosten HAB, Van Keulen G, Faber OG, Alves AMCR, Meijer WG and Dijkhuizen L (2002) Two novel homologous proteins of Streptomyces coelicolor and Streptomyces lividans are involved in the formation of the rodlet layer and mediate attachment to a hydrophobic surface. Molecular Microbiology 44:1483-1492.

Clark TD, Buriak JM, Kobayashi K, Isler MP, McRee DE and Reza Ghadiri M (1998) Cylindrical β-sheet peptide assemblies. Journal of the American Chemical Society 120:8949-8962.

Crescenzi O, Tomaselli S, Guerrini R, Salvadori S, D'Ursi AM, Temussi PA and Picone D (2002) Solution structure of the Alzheimer amyloid beta-peptide (1-42) in an apolar microenvironment. Similarity with a virus fusion domain. Eur J Biochem 269:5642-5648.

Cruz L, Urbanc B, Borreguero JM, Lazo ND, Teplow DB and Stanley HE (2005) Solvent and mutation effects on the nucleation of amyloid beta-protein folding. Proc Natl Acad Sci U S A 102:18258-18263.

Cruz M, Tusell JM, Grillo-Bosch D, Albericio F, Serratosa J, Rabanal F and Giralt E (2004) Inhibition of β-amyloid toxicity by short peptides containing *N*-methyl amino acids. Journal of Peptide Research 63:324-328.

Cutuli M, Cristiani S, Lipton JM and Catania A (2000) Antimicrobial effects of α-MSH peptides. Journal of Leukocyte Biology 67:233-239.

Czajlik A, Mesko E, Penke B and Perczel A (2002) Investigation of penetratin peptides. Part 1. The environment dependent conformational properties of penetratin and two of its derivatives. Journal of Peptide Science 8:151-171.

D

Dahlgren KN, Manelli AM, Stine WB, Jr., Baker LK, Krafft GA and LaDu MJ (2002) Oligomeric and fibrillar species of amyloid-beta peptides differentially affect neuronal viability. J Biol Chem 277:32046-32053.

Darden T, York D and Pedersen L (1993a) Particle mesh Ewald: An N [center-dot] log(N) method for Ewald sums in large systems. The Journal of Chemical Physics 98:10089-10092.

Darden T, York D and Pedersen L (1993b) Particle mesh Ewald: An N • log(N) method for Ewald sums in large systems. The Journal of Chemical Physics 98:10089-10092.

Datki Z, Juhasz A, Galfi M, Soos K, Papp R, Zadori D and Penke B (2003) Method for measuring neurotoxicity of aggregating polypeptides with the MTT assay on differentiated neuroblastoma cells. Brain Res Bull 62:223-229.

Datki Z, Papp R, Zadori D, Soos K, Fulop L, Juhasz A, Laskay G, Hetenyi C, Mihalik E, Zarandi M and Penke B (2004) *In vitro* model of neurotoxicity of Abeta 1-42 and neuroprotection by a pentapeptide: irreversible events during the first hour. Neurobiol Dis 17:507-515.

Demuro A, Mina E, Kayed R, Milton SC, Parker I and Glabe CG (2005) Calcium dysregulation and membrane disruption as a ubiquitous neurotoxic mechanism of soluble amyloid oligomers. Journal of Biological Chemistry 280:17294-17300.

Derossi D, Calvet S, Trembleau A, Brunissen A, Chassaing G and Prochiantz A (1996) Cell internalization of the third helix of the antennapedia homeodomain is receptor-independent. Journal of Biological Chemistry 271:18188-18193.

Derossi D, Joliot AH, Chassaing G and Prochiantz A (1994) The third helix of the Antennapedia homeodomain translocates through biological membranes. Journal of Biological Chemistry 269:10444-10450.

Deshpande A, Mina E, Glabe C and Busciglio J (2006) Different conformations of amyloid b induce neurotoxicity by distinct mechanisms in human cortical neurons. Journal of Neuroscience 26:6011-6018.

Dickson DW, Crystal HA, Bevona C, Honer W, Vincent I and Davies P (1995) Correlations of synaptic and pathological markers with cognition of the elderly. Neurobiology of Aging 16:285-298.

Didomenico B (1999) Novel antifungal drugs. Current Opinion in Microbiology 2:509-515.

Dima RI and Thirumalai D (2004) Proteins associated with diseases show enhanced sequence correlation between charged residues. Bioinformatics 20:2345-2354.

Dineley KT, Xia X, Bui D, David Sweatt J and Zheng H (2002) Accelerated plaque accumulation, associative learning deficits, and up-regulation of a7 nicotinic receptor protein in transgenic mice co-expressing mutant human presenilin 1 and amyloid precursor proteins. Journal of Biological Chemistry 277:22768-22780.

Diot P, Gagnadoux F, Martin C, Ellataoui H, Furet Y, Breteau M, Boissinot E and Lemarie E (1997) Nebulization and anti-Pseudomonas aeruginosa activity of colistin. Eur Respir J 10:1995-1998.

Dodart JC, Bales KR, Gannon KS, Greene SJ, DeMattos RB, Mathis C, DeLong CA, Wu S, Wu X, Holtzman DM and Paul SM (2002) Immunization reverses memory deficits without reducing brain Aβ burden in Alzheimer's disease model. Nature Neuroscience 5:452-457.

Doig AJ (1997) A three stranded β-sheet peptide in aqueous solution containing *N*-methyl amino acids to prevent aggregation. Chemical Communications:2153-2154.

Doig AJ (2007) Peptide inhibitors of beta-amyloid aggregation. Curr Opin Drug Discov Devel 10:533-539.

Dorsey BD, Levin RB, McDaniel SL, Vacca JP, Guare JP, Darke PL, Zugay JA, Emini EA, Schleif WA, Quintero JC, Lin JH, Chen IW, Holloway MK, Fitzgerald PMD, Axel MG, Ostovic D, Anderson PS and Huff JR (1994) L-735,524: The design of a potent and orally bioavailable HIV protease inhibitor. Journal of Medicinal Chemistry 37:3443-3451.

Drin G, Mazel M, Clair P, Mathieu D, Kaczorek M and Temsamani J (2001) Physico-chemical requirements for cellular uptake of pAntp peptide: Role of lipid-binding affinity. European Journal of Biochemistry 268:1304-1314.

Dupont E, Joliot AH and Prochiantz A (2002) Cell Penetrating Peptides: Processes and Applications. CRC Press, Boca Raton, FL:23-51.

E

Eanes ED and Glenner GG (1968) X-ray diffraction studies on amyloid filaments. J Histochem Cytochem 16:673-677.

Eberle A, Fauchere JL, Tesser GI and Schwyzer R (1975) Hormone receptor interactions. Syntheses of a melanotropin and of informational sequences thereof with the aid of alkali labile protecting groups. Helvetica Chimica Acta 58:2106-2129.

Eberle A and Schwyzer R (1975) Hormone receptor interactions. Demonstration of two message sequences (active sites) in a melanotropin. Helvetica Chimica Acta 58:1528-1535.

Eberle A and Schwyzer R (1976) Surface Membrane Receptors:291-304.

Eberle AN (1988) The Melanotropins: Chemistry, Physiology and Mechanisms of Action. Karger, Basel: Switzerland:393-394.

Edwards CM, Cohen MA and Bloom SR (1999) Peptides as drugs. QJM 92:1-4.

Enriz RD (2005) The legacy of the past, the reality of the present and the hopes of the future. Journal of Molecular Structure: THEOCHEM 731:163-172.

Epand RM, Shai Y, Segrest JP and Anantharamaiah GM (1995) Mechanisms for the modulation of membrane bilayer properties by amphipathic helical peptides. Biopolymers - Peptide Science Section 37:319-338.

Epand RM and Vogel HJ (1999) Diversity of antimicrobial peptides and their mechanisms of action. Biochimica et Biophysica Acta - Biomembranes 1462:11-28.

Eriksen JL, Sagi SA, Smith TE, Weggen S, Das P, McLendon DC, Ozols VV, Jessing KW, Zavitz KH, Koo EH and Golde TE (2003) NSAIDs and enantiomers of flurbiprofen target β-secretase and lower $A\beta_{42}$ *in vivo*. Journal of Clinical Investigation 112:440-449.

Ernst EJ, Roling EE, Petzold CR, Keele DJ and Klepser ME (2002) *In vitro* activity of micafungin (FK-463) against Candida spp.: Microdilution, time-kill, and postantifungal-effect studies. Antimicrobial Agents and Chemotherapy 46:3846-3853.

Esposito L, Pedone C and Vitagliano L (2006) Molecular dynamics analyses of cross-beta-spine steric zipper models: beta-sheet twisting and aggregation. Proc Natl Acad Sci U S A 103:11533-11538.

F

Feig M, Karanicolas J and Brooks Iii CL (2001)

MMTSB Tool Set. MMTSB NIH Research Resource, The Scripps Research Institute.

Ferguson N, Becker J, Tidow H, Tremmel S, Sharpe TD, Krause G, Flinders J, Petrovich M, Berriman J, Oschkinat H and Fersht AR (2006) General structural motifs of amyloid protofilaments. Proc Natl Acad Sci U S A 103:16248-16253.

Ferreira SH, Bartelt DC and Greene LJ (1970a) Isolation of bradykinin-potentiating peptides from bothrops jararaca venom. Biochemistry 9:2583-2593.

Ferreira SH, Greene LJ, Alabaster VA, Bakhle YS and Vane JR (1970b) Activity of Various Fractions of Bradykinin Potentiating Factor against Angiotensin i Converting Enzyme. Nature 225:379-380.

Ferreira SH and Rocha e Silva M (1965) Potentiation of bradykinin and eledoisin by BPF (bradykinin potentiating factor) from Bothrops jararaca venom. Experientia 21:347-349.

Fischer PM, Zhelev NZ, Wang S, Melville JE, Fahraeus R and Lane DP (2000) Structure-activity relationship of truncated and substituted analogues of the intracellular delivery vector Penetratin. Journal of Peptide Research 55:163-172.

Flükiger P, Lüthi HP, Portmann S and Weber J (2000) MOLEKEL 4.0. Swiss Center for Scientific Computing: Manno, Switzerland, 2000

Forman MS, Mufson EJ, Leurgans S, Pratico D, Joyce S, Leight S, Lee VM and Trojanowski JQ (2007) Cortical biochemistry in MCI and Alzheimer disease: lack of correlation with clinical diagnosis. Neurology 68:757-763.

Franklin K and Paxinos G (1997) The Mouse Brain in Stereotaxic Coordinates. Academic Press,San Diego.

Freile ML, Giannini F, Pucci G, Sturniolo A, Rodero L, Pucci O, Balzareti V and Enriz RD (2003) Antimicrobial activity of aqueous extracts and of berberine isolated from Berberis heterophylla. Fitoterapia 74:702-705.

Freixa B, Vila R, Vargas L, Lozano N, Adzet T and Cañigueral S (1998) Screening for antifungal activity of nineteen Latin American plants. Phytotherapy Research 12:427-430.

Fricker LD (2005) Neuropeptide-processing enzymes: Applications for drug discovery. AAPS Journal 7.

Frisch MJ, Trucks GW, Schlegel HB, Scuseria GE, Robb MA, Cheeseman JR, Montgomery Jr JA, Vreven T, Kudin KN, Burant JC, Millam JM, Iyengar SS, Tomasi J, Barone V, Mennucci B, Cossi M, Scalmani G, Rega N, Petersson GA, Nakatsuji H, Hada M, Ehara M, Toyota K, Fukuda R, Hasegawa J, Ishida M, Nakajima T, Honda Y, Kitao O, Nakai H, Klene M, Li X, Knox JE, Hratchian HP, Cross JB, Adamo C, Jaramillo J, Gomperts R, Stratmann RE, Yazyev O, Austin AJ, Cammi R, Pomelli C, Ochterski JW, Ayala PY, Morokuma K, Voth GA, Salvador P, Dannenberg JJ, Zakrzewski VG, Dapprich S, Daniels AD, Strain MC, Farkas O, Malick DK, Rabuck AD, Raghavachari K, Foresman JB, Ortiz JV, Cui Q, Baboul AG, Clifford S, Cioslowski J, Stefanov BB, Liu G, Liashenko A, Piskorz P, Komaromi I, Martin RL, Fox DJ, Keith T, Al-Laham MA, Peng CY, Nanayakkara A, Challacombe M, Gill PMW, Johnson B, Chen W, Wong MW, Gonzalez C and Pople JA (2003) Gaussian 03, Revision B.05. Gaussian, Inc, Pittsburgh PA.

Fromtling RA (1999) Progress in antifungal chemotherapy. Drug News and Perspectives 12:557-569.

Fulop L, Zarandi M, Datki Z, Soos K and Penke B (2004) Beta-amyloid-derived pentapeptide RIIGLa inhibits Abeta(1-42) aggregation and toxicity. Biochem Biophys Res Commun 324:64-69.

G

Ganz T and Lehrer RI (1995) Defensins. Pharmacology and Therapeutics 66:191-205.

Garber G (2001) An overview of fungal infections. Drugs 61:1-12.

Garcia-Osta A and Alberini CM (2009) Amyloid beta mediates memory formation. Learn Mem 16:267-272.

Gebbink MFBG, Claessen D, Bouma B, Dijkhuizen L and Wosten HAB (2005) Amyloids - A functional coat for microorganisms. Nature Reviews Microbiology 3:333-341.

Georgopapadakou NH and Tkacz JS (1995) The fungal cell wall as a drug target. Trends in Microbiology 3:98-104.

Geula C, Wu CK, Saroff D, Lorenzo A, Yuan M and Yankner BA (1998) Aging renders the brain vulnerable to 26 β-protein neurotoxicity. Nature Medicine 4:827-831.

Geysen HM (1985) Antigen-antibody interactions at the molecular level: adventures in peptide synthesis. Immunology Today 6:364-369.

Geysen HM, Meloen RH and Barteling SJ (1984) Use of peptide synthesis to probe viral antigens for epitopes to a resolution of a single amino acid. Proceedings of the National Academy of Sciences of the United States of America 81:3998-4002.

Geysen HM, Rodda SJ and Mason TJ (1987) Strategies for epitope analysis using peptide synthesis. Journal of Immunological Methods 102:259-274.

Ghannoum MA and Rice LB (1999) Antifungal agents: Mode of action, mechanisms of resistance, and correlation of these mechanisms with bacterial resistance. Clinical Microbiology Reviews 12:501-517.

Giannini FA, Aimar ML, Sortino M, Gomez R, Sturniollo A, Juarez A, Zacchino S, De Rossi RH and Enriz RD (2004) *In vitro-in vivo* antifungal evaluation and structure-activity relationships of 3H-1,2-dithiole-3-thione derivatives. Farmaco 59:245-254.

Gilman S, Koller M, Black RS, Jenkins L, Griffith SG, Fox NC, Eisner L, Kirby L, Boada Rovira M, Forette F and Orgogozo JM (2005) Clinical effects of

Aβ immunization (AN1792) in patients with AD in an interrupted trial. Neurology 64:1553-1562.

Glenner GG (1980a) Amyloid deposits and amyloidosis. The beta-fibrilloses (first of two parts). N Engl J Med 302:1283-1292.

Glenner GG (1980b) Amyloid deposits and amyloidosis: the beta-fibrilloses (second of two parts). N Engl J Med 302:1333-1343.

Glenner GG and Wong CW (1984) Alzheimer's disease: Initial report of the purification and characterization of a novel cerebrovascular amyloid protein. Biochemical and Biophysical Research Communications 120:885-890.

Gnanakaran S, Nussinov R and Garcia AE (2006) Atomic-level description of amyloid beta-dimer formation. J Am Chem Soc 128:2158-2159.

Gordon DJ and Meredith SC (2003) Probing the role of backbone hydrogen bonding in beta-amyloid fibrils with inhibitor peptides containing ester bonds at alternate positions. Biochemistry 42:475-485.

Gordon DJ, Sciarretta KL and Meredith SC (2001) Inhibition of β-amyloid(40) fibrillogenesis and disassembly of β-amyloid(40) fibrils by short β-amyloid congeners containing *N*-methyl amino acids at alternate residues. Biochemistry 40:8237-8245.

Gordon DJ, Tappe R and Meredith SC (2002) Design and characterization of a membrane permeable *N*-methyl amino acid-containing peptide that inhibits Aβ1-40 fibrillogenesis. Journal of Peptide Research 60:37-55.

Granic I, Masman MF, Mulder KC, Nijholt IM, Naude PJW, de Haan A, Borbély E, Penke B, Luiten PGM and Eisel ULM (2009) LPYFDa neutralizes Aβ-induced memory impairment and toxicity. J Alzheimers Dis In Press.

Greeling P, Langenaeker W, De Proft F and Baeten A (1996) Molecular Electrostatic Potentials: Concepts and Applications. Theoretical and Computational Chemistry. Elsevier Science BV, Amsterdam 3:587-617.

Greer J, Erickson JW, Baldwin JJ and Varney MD (1994) Application of the three-dimensional structures of protein target molecules in structure-based drug design. Journal of Medicinal Chemistry 37:1035-1054.

Grieco P, Rossi C, Colombo G, Gatti S, Novellino E, Lipton JM and Catania A (2003) Novel α-melanocyte stimulating hormone peptide analogues with high candidacidal activity. Journal of Medicinal Chemistry 46:850-855.

Grieco P, Rossi C, Gatti S, Colombo G, Carlin A, Novellino E, Lama T, Lipton JM and Catania A (2005) Design and synthesis of melanocortin peptides with candidacidal and anti-TNF-a properties. Journal of Medicinal Chemistry 48:1384-1388.

H

Haass C, Schlossmacher MG, Hung AY, Vigo-Pelfrey C, Mellon A, Ostaszewski BL, Lieberburg I, Koo EH, Schenk D, Teplow DB and et al. (1992a) Amyloid beta-peptide is produced by cultured cells during normal metabolism. Nature 359:322-325.

Haass C, Schlossmacher MG, Hung AY, Vigo-Pelfrey C, Mellon A, Ostaszewski BL, Lieberburg I, Koo EH, Schenk D, Teplow DB and Selkoe DJ (1992b) Amyloid β-peptide is produced by cultured cells during normal metabolism. Nature 359:322-325.

Haass C and Selkoe DJ (2007) Soluble protein oligomers in neurodegeneration: lessons from the Alzheimer's amyloid beta-peptide. Nat Rev Mol Cell Biol 8:101-112.

Hancock RE (2001) Cationic peptides: Effectors in innate immunity and novel antimicrobials. Lancet Infectious Diseases 1:156-164.

Hancock RE, Falla T and Brown M (1995) Cationic bactericidal peptides. Adv Microb Physiol 37:135-175.

Hancock REW (1997) Peptide antibiotics. Lancet 349:418-422.

Hancock REW and Lehrer R (1998) Cationic peptides: A new source of antibiotics. Trends in Biotechnology 16:82-88.

Hancock REW and Patrzykat A (2002) Clinical development of cationic antimicrobial peptides: From natural to novel antibiotics. Current Drug Targets - Infectious Disorders 2:79-83.

Hardy J and Allsop D (1991) Amyloid deposition as the central event in the aetiology of Alzheimer's disease. Trends in Pharmacological Sciences 12:383-388.

Hardy J and Selkoe DJ (2002) The amyloid hypothesis of Alzheimer's disease: Progress and problems on the road to therapeutics. Science 297:353-356.

Harkany T, Abraham I, Konya C, Nyakas C, Zarandi M, Penke B and Luiten PG (2000) Mechanisms of beta-amyloid neurotoxicity: perspectives of pharmacotherapy. Rev Neurosci 11:329-382.

Harkany T, O'Mahony S, Keijser J, Kelly JP, Konya C, Borostyankoi ZA, Gorcs TJ, Zarandi M, Penke B, Leonard BE and Luiten PG (2001) Beta-amyloid(1-42)-induced cholinergic lesions in rat nucleus basalis bidirectionally modulate serotonergic innervation of the basal forebrain and cerebral cortex. Neurobiol Dis 8:667-678.

Hartley DM, Walsh DM, Ye CP, Diehl T, Vasquez S, Vassilev PM, Teplow DB and Selkoe DJ (1999) Protofibrillar intermediates of amyloid Î²-protein induce acute electrophysiological changes and progressive neurotoxicity in cortical neurons. Journal of Neuroscience 19:8876-8884.

Hashimoto M, Kazui H, Matsumoto K, Nakano Y, Yasuda M and Mori E (2005) Does donepezil treatment slow the progression of hippocampal atrophy in patients with Alzheimer's disease? American Journal of Psychiatry 162:676-682.

Hess B, Bekker H, Berendsen HJC and Fraaije JGEM (1997) LINCS: A linear constraint solver

for molecular simulations. Journal of Computational Chemistry 18:1463-1472.

Hetenyi C, Kortvelyesi T and Penke B (2002a) Mapping of possible binding sequences of two beta-sheet breaker peptides on beta amyloid peptide of Alzheimer's disease. Bioorg Med Chem 10:1587-1593.

Hetenyi C, Szabo Z, Klement E, Datki Z, Kortvelyesi T, Zarandi M and Penke B (2002b) Pentapeptide amides interfere with the aggregation of beta-amyloid peptide of Alzheimer's disease. Biochem Biophys Res Commun 292:931-936.

Hilbich C, Kisters-Woike B, Reed J, Masters CL and Beyreuther K (1992) Substitutions of hydrophobic amino acids reduce the amyloidogenicity of Alzheimer's disease beta A4 peptides. J Mol Biol 228:460-473.

Hiltz ME, Catania A and Lipton JM (1991) Anti-inflammatory activity of α-MSH(11-13) analogs: Influences of alteration in stereochemistry. Peptides 12:767-771.

Hock C, Konietzko U, Streffer JR, Tracy J, Signorell A, Muller-Tillmanns B, Lemke U, Henke K, Moritz E, Garcia E, Wollmer MA, Umbricht D, de Quervain DJ, Hofmann M, Maddalena A, Papassotiropoulos A and Nitsch RM (2003) Antibodies against beta-amyloid slow cognitive decline in Alzheimer's disease. Neuron 38:547-554.

Hoffmann JA, Kafatos FC, Janeway Jr CA and Ezekowitz RAB (1999) Phylogenetic perspectives in innate immunity. Science 284:1313-1318.

Holder JR and Haskell-Luevano C (2004) Melanocortin Ligands: 30 Years of Structure-Activity Relationship (SAR) Studies. Medicinal Research Reviews 24:325-356.

Holtzman DM and Mobley WC (1991) Molecular studies in Alzheimer's disease. Trends Biochem Sci 16:140-144.

Hoshi M, Sato M, Matsumoto S, Noguchi A, Yasutake K, Yoshida N and Sato K (2003) Spherical aggregates of β-amyloid (amylospheroid) show high neurotoxicity and activate tau protein kinase I/glycogen synthase kinase-3b. Proceedings of the National Academy of Sciences of the United States of America 100:6370-6375.

Houghten RA (1985) General method for the rapid solid-phase synthesis of large numbers of peptides: Specificity of antigen-antibody interaction at the level of individual amino acids. Proceedings of the National Academy of Sciences of the United States of America 82:5131-5135.

Hruby VJ, Wilkes BC, Hadley ME, Al-Obeidi F, Sawyer TK, Staples DJ, De Vaux AE, Dym O, Castrucci AMDL, Hintz MF, Riehm JP and Rao KR (1987) α-Melanotropin: The minimal active sequence in the frog skin bioassay. Journal of Medicinal Chemistry 30:2126-2130.

Hsieh H, Boehm J, Sato C, Iwatsubo T, Tomita T, Sisodia S and Malinow R (2006) AMPAR removal underlies Abeta-induced synaptic depression and dendritic spine loss. Neuron 52:831-843.

Huang HW (2000) Action of antimicrobial peptides: Two-state model. Biochemistry 39:8347-8352.

Huang X, Atwood CS, Moir RD, Hartshorn MA, Tanzi RE and Bush AI (2004) Trace metal contamination initiates the apparent auto-aggregation, amyloidosis, and oligomerization of Alzheimer's Abeta peptides. J Biol Inorg Chem 9:954-960.

Huet A and Derreumaux P (2006) Impact of the mutation A21G (Flemish variant) on Alzheimer's beta-amyloid dimers by molecular dynamics simulations. Biophys J 91:3829-3840.

Hughes E, Burke RM and Doig AJ (2000) Inhibition of toxicity in the β-amyloid peptide fragment β-(25-35) using *N*-methylated derivatives. A general strategy to prevent amyloid formation. Journal of Biological Chemistry 275:25109-25115.

Humphrey W, Dalke A and Schulten K (1996) VMD: visual molecular dynamics. J Mol Graph 14:33-38, 27-38.

Hwang W, Zhang S, Kamm RD and Karplus M (2004) Kinetic control of dimer structure formation in amyloid fibrillogenesis. Proc Natl Acad Sci U S A 101:12916-12921.

I

Ida N, Hartmann T, Pantel J, Schröder J, Zerfass R, Förstl H, Sandbrink R, Masters CL and Beyreuther K (1996) Analysis of heterogeneous βA4 peptides in human cerebrospinal fluid and blood by a newly developed sensitive western blot assay. Journal of Biological Chemistry 271:22908-22914.

J

Jacobsen JS, Wu CC, Redwine JM, Comery TA, Arias R, Bowlby M, Martone R, Morrison JH, Pangalos MM, Reinhart PH and Bloom FE (2006) Early-onset behavioral and synaptic deficits in a mouse model of Alzheimer's disease. Proceedings of the National Academy of Sciences of the United States of America 103:5161-5166.

Jarrett JT, Berger EP and Lansbury PT, Jr. (1993a) The *C*-terminus of the beta protein is critical in amyloidogenesis. Ann N Y Acad Sci 695:144-148.

Jarrett JT, Berger EP and Lansbury PT, Jr. (1993b) The carboxy terminus of the beta amyloid protein is critical for the seeding of amyloid formation: implications for the pathogenesis of Alzheimer's disease. Biochemistry 32:4693-4697.

Joliot A, Pernelle C, Deagostini-Bazin H and Prochiantz A (1991) Antennapedia homeobox peptide regulates neural morphogenesis. Proceedings of the National Academy of Sciences of the United States of America 88:1864-1868.

Jorgensen WL, Maxwell DS and Tirado-Rives J (1996) Development and Testing of the OPLS All-Atom Force Field on Conformational Energetics and Properties of Organic Liquids. Journal of the American Chemical Society 118:11225-11236.

Juhasz G, Marki A, Vass G, Fulop L, Budai D, Penke B, Falkay G and Szegedi V (2009) An intraperitoneally administered pentapeptide protects

against Abeta (1-42) induced neuronal excitation *in vivo*. J Alzheimers Dis 16:189-196.

K

Kabsch W and Sander C (1983) Dictionary of protein secondary structure: pattern recognition of hydrogen-bonded and geometrical features. Biopolymers 22:2577-2637.

Kaiser E, Colescott RL, Bossinger CD and Cook PI (1970) Color test for detection of free terminal amino groups in the solid-phase synthesis of peptides. Analytical Biochemistry 34:595-598.

Kamenetz F, Tomita T, Hsieh H, Seabrook G, Borchelt D, Iwatsubo T, Sisodia S and Malinow R (2003) APP processing and synaptic function. Neuron 37:925-937.

Kaminski GA, Friesner RA, Tirado-Rives J and Jorgensen WL (2001) Evaluation and Reparametrization of the OPLS-AA Force Field for Proteins via Comparison with Accurate Quantum Chemical Calculations on Peptides. Journal of Physical Chemistry B 105:6474-6487.

Karolyhazy L, Freile ML, Anwair M, Beke G, Giannini F, Sortino M, Ribas JC, Zacchino S, Matyus P and Enriz RD (2003) Synthesis, *in vitro/in vivo* antifungal evaluation and structure-activity relationship study of 3(2H)-pyridazinones. Arzneimittel-Forsch 53:738-743.

Katzman R (1986) Alzheimer's disease. New England Journal of Medicine 314:964-973.

Kim KH and Seong BL (2001) Peptide amidation: Production of peptide hormones *in vivo* and *in vitro*. Biotechnology and Bioprocess Engineering 6:244-251.

Kirkitadze MD, Condron MM and Teplow DB (2001) Identification and characterization of key kinetic intermediates in amyloid beta-protein fibrillogenesis. J Mol Biol 312:1103-1119.

Kirschner DA, Abraham C and Selkoe DJ (1986) X-ray diffraction from intraneuronal paired helical filaments and extraneuronal amyloid fibers in Alzheimer disease indicates cross-beta conformation. Proc Natl Acad Sci U S A 83:503-507.

Kisilevsky R (2000) Review: amyloidogenesis-unquestioned answers and unanswered questions. J Struct Biol 130:99-108.

Klepser ME, Ernst EJ, Ernst ME, Messer SA and Pfaller MA (1998) Evaluation of endpoints for antifungal susceptibility determinations with LY303366. Antimicrobial Agents and Chemotherapy 42:1387-1391.

Klimov DK and Thirumalai D (2003) Dissecting the assembly of Abeta16-22 amyloid peptides into antiparallel beta sheets. Structure 11:295-307.

Kmietowicz Z (2005a) Erratum: NICE proposes to withdraw Alzheimer's drugs from NHS (British Medical Journal (March 5, 2005) 330 (495)). British Medical Journal 330:759.

Kmietowicz Z (2005b) NICE proposes to withdraw Alzheimer's drugs from NHS. BMJ (Clinical research ed) 330:495.

Koch HJ, Uyanik G and Fischer-Barnicol D (2005) Memantine: A therapeutic approach in treating Alzheimer's and vascular dementia. Current Drug Targets: CNS and Neurological Disorders 4:499-506.

Kontoyiannis DP, Mantadakis E and Samonis G (2003) Systemic mycoses in the immunocompromised host: An update in antifungal therapy. Journal of Hospital Infection 53:243-258.

Kornacker MG, Lai Z, Witmer M, Ma J, Hendrick J, Lee VG, Riexinger DJ, Mapelli C, Metzler W and Copeland RA (2005) An inhibitor binding pocket distinct from the catalytic active site on human β-APP cleaving enzyme. Biochemistry 44:11567-11573.

Kotelchuck D, Scheraga HA and Walter R (1972) Conformational energy studies of oxytocin and its cyclic moiety. Proc Natl Acad Sci U S A 69:3629-3633.

Kouznetsov V, Urbina J, Palma A, Lopez S, Devia C, Enriz R and Zacchino S (2000) Synthesis and *in vitro* antifungal properties of 4-aryl-4-N-arylamine-1-butenes and related compounds. Molecules 5:428-430.

Kouznetsov VV, Vargas Mendez LY, Sortino M, Vasquez Y, Gupta MP, Freile M, Enriz RD and Zacchino SA (2008) Antifungal and cytotoxic activities of some *N*-substituted aniline derivatives bearing a hetaryl fragment. Bioorganic and Medicinal Chemistry 16:794-809.

Kumar-Singh S, Theuns J, Van Broeck B, Pirici D, Vennekens K, Corsmit E, Cruts M, Dermaut B, Wang R and Van Broeckhoven C (2006) Mean age-of-onset of familial Alzheimer disease caused by presenilin mutations correlates with both increased Aî²42 and decreased Aî²40. Human Mutation 27:686-695.

Kundrot CE, Ponder JW and Richards FM (1991) Algorithms for calculating excluded volume and its derivatives as a function of molecular conformation and their use in energy minimization. J Comput Chem 12:402-409.

Kuo WL, Gehm BD and Rich Rosner M (1990) Cloning and expression of the cDNA for a Drosophila insulin-degrading enzyme. Molecular Endocrinology 4:1580-1591.

L

Laczko I, Vass E, Soos K, Fulop L, Zarandi M and Penke B (2008) Aggregation of Abeta(1-42) in the presence of short peptides: conformational studies. J Pept Sci 14:731-741.

Lam FC, Liu R, Lu P, Shapiro AB, Renoir JM, Sharom FJ and Reiner PB (2001) β-Amyloid efflux mediated by p-glycoprotein. Journal of Neurochemistry 76:1121-1128.

Lambert MP, Barlow AK, Chromy BA, Edwards C, Freed R, Liosatos M, Morgan TE, Rozovsky I, Trommer B, Viola KL, Wals P, Zhang C, Finch CE, Krafft GA and Klein WL (1998) Diffusible, nonfibrillar ligands derived from Aî²1-42 are potent central nervous system neurotoxins. Proceedings of the National Academy of Sciences of the United States of America 95:6448-6453.

Langel U (2002) Cell-Penetrating Peptides: Processes and Applications. CRC Press: Boca Raton, FL.

Lansbury PT, Jr. (1997) Inhibition of amyloid formation: a strategy to delay the onset of Alzheimer's disease. Curr Opin Chem Biol 1:260-267.

Lanz TA, Fici GJ and Merchant KM (2005) Lack of specific amyloid-b(1-42) suppression by nonsteroidal anti-inflammatory drugs in young, plaque-free Tg2576 mice and in guinea pig neuronal cultures. Journal of Pharmacology and Experimental Therapeutics 312:399-406.

Lazo ND, Grant MA, Condron MC, Rigby AC and Teplow DB (2005) On the nucleation of amyloid beta-protein monomer folding. Protein Sci 14:1581-1596.

Lee DG, Kim HK, Kim SA, Park Y, Park SC, Jang SH and Hahm KS (2003) Fungicidal effect of indolicidin and its interaction with phospholipid membranes. Biochemical and Biophysical Research Communications 305:305-310.

Lee JP, Dunlap B and Rich DH (1990) Synthesis and immunosuppressive activities of conformationally restricted cyclosporin lactam analogues. International Journal of Peptide and Protein Research 35:481-494.

Leissring MA, Farris W, Chang AY, Walsh DM, Wu X, Sun X, Frosch MP and Selkoe DJ (2003) Enhanced proteolysis of β-amyloid in APP transgenic mice prevents plaque formation, secondary pathology, and premature death. Neuron 40:1087-1093.

Lensink MF, Christiaens B, Vandekerckhove J, Prochiantz A and Rosseneu M (2005) Penetratin-membrane association: W48/R52/W56 shield the peptide from the aqueous phase. Biophysical Journal 88:939-952.

Lesne S, Koh MT, Kotilinek L, Kayed R, Glabe CG, Yang A, Gallagher M and Ashe KH (2006) A specific amyloid-beta protein assembly in the brain impairs memory. Nature 440:352-357.

Letoha T, Gaal S, Somlai C, Czajlik A, Perczel A and Penke B (2003) Membrane translocation of penetratin and its derivatives in different cell lines. Journal of Molecular Recognition 16:272-279.

Letoha T, Gaal S, Somlai C, Venkei Z, Glavinas H, Kusz E, Duda E, Czajlik A, Petak F and Penke B (2005) Investigation of penetratin peptides. Part 2. *In vitro* uptake of penetratin and two of its derivatives. Journal of Peptide Science 11:805-811.

Li Z and Scheraga HA (1987) Monte Carlo-minimization approach to the multiple-minima problem in protein folding. Proceedings of the National Academy of Sciences of the United States of America 84:6611-6615.

Lichtenthaler SF and Haass C (2004) Amyloid at the cutting edge: Activation of α-secretase prevents amyloidogenesis in an Alzheimer disease mouse model. Journal of Clinical Investigation 113:1384-1387.

Lindahl E, Hess B and van der Spoel D (2001) GROMACS 3.0: a package for molecular simulation and trajectory analysis. Journal of Molecular Modeling 7:306-317.

Lindberg M, Biverstahl H, Graslund A and Maler L (2003) Structure and positioning comparison of two variants of penetratin in two different membrane mimicking systems by NMR. European Journal of Biochemistry 270:3055-3063.

Linder MB (2009) Hydrophobins: Proteins that self assemble at interfaces. Current Opinion in Colloid and Interface Science 14:356-363.

Liwo A, Tempczyk A, Oldziej S, Shenderovich MD, Hruby VJ, Talluri S, Ciarkowski J, Kasprzykowski F, Lankiewicz L and Grzonka Z (1996a) Exploration of the conformational space of oxytocin and arginine-vasopressin using the electrostatically driven Monte Carlo and molecular dynamics methods. Biopolymers 38:157-175.

Liwo A, Tempczyk A, Oldziej S, Shenderovich MD, Hruby VJ, Talluri S, Ciarkowski J, Kasprzykowski F, Lankiewicz L and Grzonka Z (1996b) Exploration of the conformational space of oxytocin and arginine-vasopressin using the electrostatically driven monte carlo and molecular dynamics methods. Biopolymers 38:157-175.

Lopez SN, Castelli MV, Rogerio Correa F, Cechinel Filho V, Yunes RA, Zamora MA, Enriz RD, Ribas JC and Zacchino SA (2005) *In vitro* antifungal properties structure-activity relationships and studies on the mode of action of *N*-phenyl, *N*-aryl, *N*-phenylalkyl maleimides and related compounds. Arzneimittel-Forsch 55:123-132.

Lopez SN, Castelli MV, Zacchino SA, Dominguez JN, Lobo G, Charris-Charris J, Cortes JCG, Ribas JC, Devia C, Rodriguez AM and Enriz RD (2001) *In vitro* antifungal evaluation and structure-activity relationships of a new series of chalcone derivatives and synthetic analogues, with inhibitory properties against polymers of the fungal cell wall. Bioorganic and Medicinal Chemistry 9:1999-2013.

Lue LF, Kuo YM, Roher AE, Brachova L, Shen Y, Sue L, Beach T, Kurth JH, Rydel RE and Rogers J (1999) Soluble amyloid b peptide concentration as a predictor of synaptic change in Alzheimer's disease. American Journal of Pathology 155:853-862.

Luhrs T, Ritter C, Adrian M, Riek-Loher D, Bohrmann B, Dobeli H, Schubert D and Riek R (2005) 3D structure of Alzheimer's amyloid-beta(1-42) fibrils. Proc Natl Acad Sci U S A 102:17342-17347.

Lynn DG and Meredith SC (2000) Review: model peptides and the physicochemical approach to beta-amyloids. J Struct Biol 130:153-173.

M

Ma B and Nussinov R (2002) Stabilities and conformations of Alzheimer's beta -amyloid peptide oligomers (Abeta 16-22, Abeta 16-35, and Abeta 10-35): Sequence effects. Proc Natl Acad Sci U S A 99:14126-14131.

Ma B and Nussinov R (2006) The stability of monomeric intermediates controls amyloid formation: Abeta25-35 and its N27Q mutant. Biophys J 90:3365-3374.

Maiorini AF, Gaunt MJ, Jacobsen TM, McKay AE, Waldman LD and Raffa RB (2002) Potential novel targets for Alzheimer pharmacotherapy: I. Secretases. Journal of Clinical Pharmacy and Therapeutics 27:169-183.

Malin DH, Crothers MK, Lake JR, Goyarzu P, Plotner RE, Garcia SA, Spell SH, Tomsic BJ, Giordano T and Kowall NW (2001) Hippocampal injections of amyloid beta-peptide 1-40 impair subsequent one-trial/day reward learning. Neurobiol Learn Mem 76:125-137.

Maloy WL and Kari UP (1995) Structure-activity studies on magainins and other host defense peptides. Biopolymers - Peptide Science Section 37:105-122.

Marks N and Walter R (1972) MSH-release-inhibiting factor: inactivation by proteolytic enzymes. Proc Soc Exp Biol Med 140:673-676.

Marshall GR (1996) Burguer`s Medicinal Chemistry and Drug Discovery. 5th ed, Wiley, New York 1:373-659.

Masman MF, Eisel ULM, Csizmadia IG, Penke B, Enriz RD, Marrink SJ and Luiten PGM (2009a) In silico study of full-length amyloid b 1-42 Tri- and penta-oligomers in solution. Journal of Physical Chemistry B 113:11710-11719.

Masman MF, Rodriguez AM, Raimondi M, Zacchino SA, Luiten PG, Somlai C, Kortvelyesi T, Penke B and Enriz RD (2009b) Penetratin and derivatives acting as antifungal agents. Eur J Med Chem 44:212-228.

Masman MF, Rodríguez AM, Svetaz L, Zacchino SA, Somlai C, Csizmadia IG, Penke B and Enriz RD (2006) Synthesis and conformational analysis of His-Phe-Arg-Trp-NH_2 and analogues with antifungal properties. Bioorganic and Medicinal Chemistry 14:7604-7614.

Masman MF, Somlai C, Garibotto FM, Rodriguez AM, de la Iglesia A, Zacchino SA, Penke B and Enriz RD (2008) Structure-antifungal activity relationship of His-Phe-Arg-Trp-Gly-Lys-Pro-Val-NH_2 and analogues. Bioorganic and Medicinal Chemistry 16:4347-4358.

Mason JM, Kokkoni N, Stott K and Doig AJ (2003) Design strategies for anti-amyloid agents. Current Opinion in Structural Biology 13:526-532.

Massi F, Klimov D, Thirumalai D and Straub JE (2002) Charge states rather than propensity for beta-structure determine enhanced fibrillogenesis in wild-type Alzheimer's beta-amyloid peptide compared to E22Q Dutch mutant. Protein Sci 11:1639-1647.

Massi F, Peng JW, Lee JP and Straub JE (2001) Simulation study of the structure and dynamics of the Alzheimer's amyloid peptide congener in solution. Biophys J 80:31-44.

Mayor S (2006) NICE recommends drugs for moderate Alzheimer's disease. BMJ (Clinical research ed) 332:195.

McDonald NA and Jorgensen WL (1998) Development of an All-Atom Force Field for Heterocycles. Properties of Liquid Pyrrole, Furan, Diazoles, and Oxazoles. Journal of Physical Chemistry B 102:8049-8059.

McLean CA, Cherny RA, Fraser FW, Fuller SJ, Smith MJ, Beyreuther K, Bush AI and Masters CL (1999) Soluble pool of Aβ amyloid as a determinant of severity of neurodegeneration in Alzheimer's disease. Annals of Neurology 46:860-866.

McNeil MM, Nash SL, Hajjeh RA, Phelan MA, Conn LA, Plikaytis BD and Warnock DW (2001) Trends in mortality due to invasive mycotic diseases in the United States, 1980-1997. Clinical Infectious Diseases 33:641-647.

Meadows RP, Olejniczak ET and Fesik SW (1994a) A computer-based protocol for semiautomated assignments and 3D structure determination of proteins. J Biomol NMR 4:79-96.

Meadows RP, Post CB, Luxon BA and Gorenstein DG (1994b) MORASS 2.1.

Meersman F and Dobson CM (2006) Probing the pressure-temperature stability of amyloid fibrils provides new insights into their molecular properties. Biochim Biophys Acta 1764:452-460.

Melnikova I (2007) Therapies for Alzheimer's disease. Nature Reviews Drug Discovery 6:341-342.

Merrifield B (1986) Solid phase synthesis. Science 232:341-347.

Merrifield RB (1963) Solid phase peptide synthesis. I. The synthesis of a tetrapeptide. Journal of the American Chemical Society 85:2149-2154.

Metropolis N, Rosenbluth AW, Rosenbluth MN, Teller AH and Teller E (1953) Equation of state calculations by fast computing machines. The Journal of Chemical Physics 21:1087-1092.

Miyamoto S and Kollman PA (1992) Settle: An analytical version of the SHAKE and RATTLE algorithm for rigid water models. Journal of Computational Chemistry 13:952-962.

Morris GM, Huey R, Lindstrom W, Sanner MF, Belew RK, Goodsell DS and Olson AJ (2009) AutoDock4 and AutoDockTools4: Automated docking with selective receptor flexibility. J Comput Chem.

Mosmann T (1983) Rapid colorimetric assay for cellular growth and survival: application to proliferation and cytotoxicity assays. J Immunol Methods 65:55-63.

Muller-Hill B and Beyreuther K (1989) Molecular biology of Alzheimer's disease. Annual Review of Biochemistry 58:287-307.

Murray JS and Politzer P (1998) The molecular electrostatic potential: A tool for understanding and predicting molecular interactions. Molecular Orbital Calculations for Biological Systems:49-84.

N

Nagiec MM, Nagiec EE, Baltisberger JA, Wells GB, Lester RL and Dickson RC (1997) Sphingolipid synthesis as a target for antifungal drugs. Complementation of the inositol phosphorylceramide synthase defect in a mutant strain of Saccharomyces cerevisiae by the AUR1 gene. Journal of Biological Chemistry 272:9809-9817.

Nakamura S, Murayama N, Noshita T, Annoura H and Ohno T (2001) Progressive brain dysfunction following intracerebroventricular infusion of beta(1-42)-amyloid peptide. Brain Res 912:128-136.

Naray-Szabo G and Ferenczy GG (1995) Molecular electrostatics. Chemical Reviews 95:829-847.

Naslund J, Haroutunian V, Mohs R, Davis KL, Davies P, Greengard P and Buxbaum JD (2000) Correlation between elevated levels of amyloid beta-peptide in the brain and cognitive decline. JAMA 283:1571-1577.

Nelson R, Sawaya MR, Balbirnie M, Madsen AO, Riekel C, Grothe R and Eisenberg D (2005) Structure of the cross-beta spine of amyloid-like fibrils. Nature 435:773-778.

Némethy G, Gibson KD, Palmer KA, Yoon CN, Paterlini G, Zagari A, Rumsey S and Scheraga HA (1992) Energy parameters in polypeptides. 10. Improved geometrical parameters and nonbonded interactions for use in the ECEPP/3 algorithm, with application to proline-containing peptides. Journal of Physical Chemistry 96:6472-6484.

Nesloney CL and Kelly JW (1996) A 2,3'-substituted biphenyl-based amino acid facilitates the formation of a monomeric β-hairpin-like structure in aqueous solution at elevated temperature. Journal of the American Chemical Society 118:5836-5845.

Nijholt IM, Ostroveanu A, Scheper WA, Penke B, Luiten PG, Van der Zee EA and Eisel UL (2008) Inhibition of PKA anchoring to A-kinase anchoring proteins impairs consolidation and facilitates extinction of contextual fear memories. Neurobiol Learn Mem 90:223-229.

North ACT (1989) Applications of molecular graphics for the study of recognition. Journal of Molecular Graphics 7:67-70.

O

O'Hare E, Weldon DT, Mantyh PW, Ghilardi JR, Finke MP, Kuskowski MA, Maggio JE, Shephard RA and Cleary J (1999) Delayed behavioral effects following intrahippocampal injection of aggregated A beta (1-42). Brain Res 815:1-10.

Ondetti MA, Cushman DW, Sabo EF and Cheung HS (1979) Drug Action and Design: Mechanism-Based Enzyme Inhibitors. Elsevier/North-Holland, New York (Kalman, T.I ed):271.

Ondetti MA, Williams NJ, Sabo EF, Pluščec J, Weaver ER and Kocy O (1971) Angiotensin-converting enzyme inhibitors from the venom of Bothrops jararaca. Isolation, elucidation of structure, and synthesis. Biochemistry 10:4033-4039.

Orgogozo JM, Gilman S, Dartigues JF, Laurent B, Puel M, Kirby LC, Jouanny P, Dubois B, Eisner L, Flitman S, Michel BF, Boada M, Frank A and Hock C (2003a) Subacute meningoencephalitis in a subset of patients with AD after $A\beta_{42}$ immunization. Neurology 61:46-54.

Orgogozo JM, Gilman S, Dartigues JF, Laurent B, Puel M, Kirby LC, Jouanny P, Dubois B, Eisner L, Flitman S, Michel BF, Boada M, Frank A and Hock C (2003b) Subacute meningoencephalitis in a subset of patients with AD after Abeta42 immunization. Neurology 61:46-54.

Otsyka H and Inouye K (1964) The synthesis of an MSH-active tetrapeptide *L*-histidyl-*L*-phenylalanyl-*L*-arginyl-*L*-triptophan. Bull Chem Soc Jap 37:289-290.

P

Paravastu AK, Petkova AT and Tycko R (2006) Polymorphic fibril formation by residues 10-40 of the Alzheimer's beta-amyloid peptide. Biophys J 90:4618-4629.

Park CB, Kim HS and Kim SC (1998) Mechanism of action of the antimicrobial peptide buforin II: Buforin II kills microorganisms by penetrating the cell membrane and inhibiting cellular functions. Biochemical and Biophysical Research Communications 244:253-257.

Parvathy S, Ehrlich M, Pedrini S, Diaz N, Refolo L, Buxbaum JD, Bogush A, Petanceska S and Gandy S (2004) Atorvastatin-induced activation of Alzheimer's a secretase is resistant to standard inhibitors of protein phosphorylation-regulated ectodomain shedding. Journal of Neurochemistry 90:1005-1010.

Patchett AA, Harris E and Tristram EW (1980) A new class of angiotensin converting enzyme inhibitors. Nature 288:280-283.

Pearson HA and Peers C (2006) Physiological roles for amyloid beta peptides. J Physiol 575:5-10.

Peng PJ, Sahm UG, Doherty RVM, Kinsman RG, Moss SH and Pouton CW (1997) Binding and biological activity of *C*-terminally modified melanocortin peptides: A comparison between their actions at rodent MC_1 and MC_3 receptors. Peptides 18:1001-1008.

Perez-Iratxeta C and Andrade-Navarro MA (2008) K2D2: estimation of protein secondary structure from circular dichroism spectra. BMC Struct Biol 8:25.

Periole X, Rampioni A, Vendruscolo M and Mark AE (2009) Factors that affect the degree of twist in beta-sheet structures: a molecular dynamics simulation study of a cross-beta filament of the GNNQQNY peptide. J Phys Chem B 113:1728-1737.

Permanne B, Adessi C, Saborio GP, Fraga S, Frossard MJ, Van Dorpe J, Dewachter I, Banks WA, Van Leuven F and Soto C (2002) Reduction of amyloid load and cerebral damage in a transgenic mouse model of Alzheimer's disease by treatment with a beta-sheet breaker peptide. FASEB J 16:860-862.

Petkova AT, Ishii Y, Balbach JJ, Antzutkin ON, Leapman RD, Delaglio F and Tycko R (2002) A structural model for Alzheimer's beta -amyloid fibrils based on experimental constraints from solid state NMR. Proc Natl Acad Sci U S A 99:16742-16747.

Petkova AT, Leapman RD, Guo Z, Yau WM, Mattson MP and Tycko R (2005) Self-propagating, molecular-level polymorphism in Alzheimer's beta-amyloid fibrils. Science 307:262-265.

Petkova AT, Yau WM and Tycko R (2006) Experimental constraints on quaternary structure in Alzheimer's beta-amyloid fibrils. Biochemistry 45:498-512.

Pettersen EF, Goddard TD, Huang CC, Couch GS, Greenblatt DM, Meng EC and Ferrin TE (2004a) UCSF Chimera--a visualization system for exploratory

research and analysis. J Comput Chem 25:1605-1612.

Pettersen EF, Goddard TD, Huang CC, Couch GS, Greenblatt DM, Meng EC and Ferrin TE (2004b) UCSF Chimera - A visualization system for exploratory research and analysis. Journal of Computational Chemistry 25:1605-1612.

Pfaller MA (2002a) CLSI/NCCLS M27A2: Reference Method for Broth Dilution Antifungal Susceptibility Testing of Yeasts; Approved Standard, M27-A2, Second Edition. Clinical and Laboratory Standards Institute / National Committee for Clinical and Laboratory Standards Wayne, Ed 22:1-29.

Pfaller MA (2002b) CLSI/NCCLS M38A: Reference Method for Broth Dilution Antifungal Susceptilibity Testing of Filamentous Fungi; Approved Standard, M38-A. First Edition. Clinical and Laboratory Standards Institute / National Committee for Clinical and Laboratory Standards Wayne, Ed 22:1-27.

Pfaller MA and Diekema DJ (2004) Rare and emerging opportunistic fungal pathogens: Concern for resistance beyond *Candida albicans* and *Aspergillus fumigatus*. Journal of Clinical Microbiology 42:4419-4431.

Pfaller MA and Diekema DJ (2007) Epidemiology of invasive candidiasis: A persistent public health problem. Clinical Microbiology Reviews 20:133-163.

Piela L and Scheraga HA (1987) On the multiple-minima problem in the conformational analysis of polypeptides. I. Backbone degrees of freedom for a perturbed alpha-helix. Biopolymers - Peptide Science Section 26 Suppl.

Pike CJ, Walencewicz AJ, Glabe CG and Cotman CW (1991) *In vitro* aging of β-amyloid protein causes peptide aggregation and neurotoxicity. Brain Research 563:311-314.

Pliska V, Barth T and Rychlik I (1967) Effect of human serum oxytocinase on the antidiuretic action of lysine vasopressin and oxytocin in the rat. Experientia 23:196-197.

Pohorille A and Pratt LR (1990) Cavities in molecular liquids and the theory of hydrophobic solubilities. J Am Chem Soc 112:5066-5074.

Polak A (1999) The past, present and future of antimycotic combination therapy. Mycoses 42:355-370.

Politzer P and Truhlar DG (1981) Chemical Applications of Atomic and Molecular Electrostatic Potentials. Plenum Publishing, New York.

Pollack SJ and Lewis H (2005) β-Secretase inhibitors for Alzheimer's disease: Challenges of a promiscuous protease. Current Opinion in Investigational Drugs 6:35-47.

Ponder JW (2004) TINKER: Software Tools for Molecular Design. User's Guide for Version 42 Washington University School of Medicine.

Post CB, Meadows RP and Gorenstein DG (1990) On the evaluation of interproton distances for three-dimensional structure determination by NMR using a relaxation rate matrix analysis. Journal of the American Chemical Society 112:6796-6803.

Powers JPS and Hancock REW (2003) The relationship between peptide structure and antibacterial activity. Peptides 24:1681-1691.

Pratico D and Delanty N (2000) Oxidative injury in diseases of the central nervous system: Focus on Alzheimer's disease. American Journal of Medicine 109:577-585.

Price MLP, Ostrovsky D and Jorgensen WL (2001) Gas-phase and liquid-state properties of esters, nitriles, and nitro compounds with the OPLS-AA force field. Journal of Computational Chemistry 22:1340-1352.

Puttagunta AL and Toth EL (1998) Insulin lispro (Humalog), the first marketed insulin analogue: indications, contraindications and need for further study. CMAJ 158:506-511.

Puzzo D, Privitera L, Leznik E, Fa M, Staniszewski A, Palmeri A and Arancio O (2008) Picomolar amyloid-beta positively modulates synaptic plasticity and memory in hippocampus. J Neurosci 28:14537-14545.

Q

Quist A, Doudevski I, Lin H, Azimova R, Ng D, Frangione B, Kagan B, Ghiso J and Lal R (2005) Amyloid ion channels: a common structural link for protein-misfolding disease. Proc Natl Acad Sci U S A 102:10427-10432.

R

Rajarathnam K, Sykes BD, Kay CM, Dewald B, Geiser T, Baggiolini M and Clark-Lewis I (1994) Neutrophil activation by monomeric interleukin-8. Science 264:90-92.

Riek R, Guntert P, Dobeli H, Wipf B and Wuthrich K (2001) NMR studies in aqueous solution fail to identify significant conformational differences between the monomeric forms of two Alzheimer peptides with widely different plaque-competence, A beta(1-40)(ox) and A beta(1-42)(ox). Eur J Biochem 268:5930-5936.

Ripoll DR and Scheraga HA (1988) On the multiple-minima problem in the conformational analysis of polypeptides. II. An electrostatically driven Monte Carlo method--tests on poly(*L*-alanine). Biopolymers - Peptide Science Section 27:1283-1303.

Ripoll DR and Scheraga HA (1990) On the multiple-minima problem in the conformational analysis of polypeptides. IV. Application of the electrostatically driven Monte Carlo method to the 20-residue membrane-bound portion of melittin. Biopolymers 30:165-176.

Ritter C, Maddelein ML, Siemer AB, Luhrs T, Ernst M, Meier BH, Saupe SJ and Riek R (2005) Correlation of structural elements and infectivity of the HET-s prion. Nature 435:844-848.

Rizzo RC and Jorgensen WL (1999) OPLS All-Atom Model for Amines: Resolution of the Amine Hydration Problem. Journal of the American Chemical Society 121:4827-4836.

Rochet JC and Lansbury PT, Jr. (2000) Amyloid

fibrillogenesis: themes and variations. Curr Opin Struct Biol 10:60-68.

Rohrig UF, Laio A, Tantalo N, Parrinello M and Petronzio R (2006) Stability and structure of oligomers of the Alzheimer peptide Abeta16-22: from the dimer to the 32-mer. Biophys J 91:3217-3229.

Rovelet-Lecrux A, Hannequin D, Raux G, Le Meur N, LaquerriÃ¨re A, Vital A, Dumanchin C, Feuillette S, Brice A, Vercelletto M, Dubas F, Frebourg T and Campion D (2006) APP locus duplication causes autosomal dominant early-onset Alzheimer disease with cerebral amyloid angiopathy. Nature Genetics 38:24-26.

S

Sabesan NM and Harper ET (1983) Are aromatic residues essential at the "active sites" of peptide hormones? J Theor Biol 83:457-467.

Sahm UG (1994) Synthesis and biological evaluation of α-MSH analogues substituted with alanine. Peptides 15:1297-1302.

Sanner MF (1999) Python: a programming language for software integration and development. J Mol Graph Model 17:57-61.

Sarai A (1989) Molecular recognition and information gain. Journal of Theoretical Biology 140:137-143.

Sasahara K, Naiki H and Goto Y (2005) Kinetically controlled thermal response of beta2-microglobulin amyloid fibrils. J Mol Biol 352:700-711.

Sato T, Kienlen-Campard P, Ahmed M, Liu W, Li H, Elliott JI, Aimoto S, Constantinescu SN, Octave JN and Smith SO (2006) Inhibitors of amyloid toxicity based on beta-sheet packing of Abeta40 and Abeta42. Biochemistry 45:5503-5516.

Scarpini E and Cogiamanian F (2003) Alzheimer's disease: From molecular pathogenesis to innovative therapies. Expert Review of Neurotherapeutics 3:619-630.

Scarpini E, Scheltens P and Feldman H (2003) Treatment of Alzheimer's disease: Current status and new perspectives. Lancet Neurology 2:539-547.

Scheibel T, Parthasarathy R, Sawicki G, Lin XM, Jaeger H and Lindquist SL (2003) Conducting nanowires built by controlled self-assembly of amyloid fibers and selective metal deposition. Proc Natl Acad Sci U S A 100:4527-4532.

Schenk D, Barbour R, Dunn W, Gordon G, Grajeda H, Guido T, Hu K, Huang J, Johnson-Wood K, Khan K, Kholodenko D, Lee M, Liao Z, Lieberburg I, Motter R, Mutter L, Soriano F, Shopp G, Vasquez N, Vandevert C, Walker S, Wogulis M, Yednock T, Games D and Seubert P (1999) Immunization with amyloid-beta attenuates Alzheimer-disease-like pathology in the PDAPP mouse. Nature 400:173-177.

Scheraga HA, Ripoll DR, Liwo A and Czaplewski C (1983) User Guide ECEPPAK and ANALYZE Programs.

Schiffer M, Chang CH and Stevens FJ (1992) The functions of tryptophan residues in membrane proteins. Protein Engineering 5:213-214.

Sciarretta KL, Boire A, Gordon DJ and Meredith SC (2006a) Spatial separation of beta-sheet domains of beta-amyloid: disruption of each beta-sheet by *N*-methyl amino acids. Biochemistry 45:9485-9495.

Sciarretta KL, Gordon DJ and Meredith SC (2006b) Peptide-based inhibitors of amyloid assembly. Methods Enzymol 413:273-312.

Selkoe DJ (1999) Translating cell biology into therapeutic advances in Alzheimer's disease. Nature 399:A23-31.

Selkoe DJ (2003) Folding proteins in fatal ways. Nature 426:900-904.

Seubert P, Vigo-Pelfrey C, Esch F, Lee M, Dovey H, Davis D, Sinha S, Schlossmacher M, Whaley J, Swindlehurst C, McCormack R, Wolfert R, Selkoe D, Lieberburg I and Schenk D (1992) Isolation and quantification of soluble Alzheimer's β-peptide from biological fluids. Nature 359:325-327.

Sgourakis NG, Yan Y, McCallum SA, Wang C and Garcia AE (2007) The Alzheimer's peptides Abeta40 and 42 adopt distinct conformations in water: a combined MD / NMR study. J Mol Biol 368:1448-1457.

Shai Y (2002) Mode of action of membrane active antimicrobial peptides. Biopolymers - Peptide Science Section 66:236-248.

Shankar GM, Bloodgood BL, Townsend M, Walsh DM, Selkoe DJ and Sabatini BL (2007a) Natural oligomers of the Alzheimer amyloid-beta protein induce reversible synapse loss by modulating an NMDA-type glutamate receptor-dependent signaling pathway. J Neurosci 27:2866-2875.

Shankar GM, Li S, Mehta TH, Garcia-Munoz A, Shepardson NE, Smith I, Brett FM, Farrell MA, Rowan MJ, Lemere CA, Regan CM, Walsh DM, Sabatini BL and Selkoe DJ (2008) Amyloid-beta protein dimers isolated directly from Alzheimer's brains impair synaptic plasticity and memory. Nat Med 14:837-842.

Shankar GM, Townsend M, Walsh DM, Selkoe DJ and Sabatini BL (2007b) Natural oligomers of the Alzheimer amyloid beta-protein induce hippocampal synapse loss but can be neutralized by antibodies and small molecules. J Neurosci.

Shivaprasad S and Wetzel R (2004) An intersheet packing interaction in A beta fibrils mapped by disulfide cross-linking. Biochemistry 43:15310-15317.

Shoji M, Golde TE, Ghiso J, Cheung TT, Estus S, Shaffer LM, Cai XD, McKay DM, Tintner R, Frangione B and et al. (1992) Production of the Alzheimer amyloid beta protein by normal proteolytic processing. Science 258:126-129.

Sidor M, Wojcik J, Pawlak D and Izdebski J (1999) Conformational analysis of a novel cyclic enkephalin analogue using NMR and EDMC calculations. Acta Biochimica Polonica 46:641-650.

Silvestri R (2009) Boom in the development of non-peptidic Î²-secretase (BACE1) inhibitors for the treatment of Alzheimer's disease. Medicinal Research Reviews 29:295-338.

Singer O, Marr RA, Rockenstein E, Crews L, Coufal NG, Gage FH, Verma IM and Masliah E (2005) Targeting BACE1 with siRNAs ameliorates Alzheimer disease neuropathology in a transgenic model. Nature Neuroscience 8:1343-1349.

Singh A, Sharma S and Khuller GK (2007) cAMP regulates vegetative growth and cell cycle in *Candida albicans*. Molecular and Cellular Biochemistry 304:331-341.

Singh N (2003) Treatment of opportunistic mycoses: How long is long enough? Lancet Infectious Diseases 3:703-708.

Sortino M, Delgado P, Juarez S, Quiroga J, Abonia R, Insuasty B, Nogueras M, Rodero L, Garibotto FM, Enriz RD and Zacchino SA (2007) Synthesis and antifungal activity of (Z)-5-arylidenerhodanines. Bioorganic and Medicinal Chemistry 15:484-494.

Soto C (1999) Plaque busters: strategies to inhibit amyloid formation in Alzheimer's disease. Mol Med Today 5:343-350.

Soto C, Kindy MS, Baumann M and Frangione B (1996) Inhibition of Alzheimer's amyloidosis by peptides that prevent beta-sheet conformation. Biochem Biophys Res Commun 226:672-680.

Soto C, Sigurdsson EM, Morelli L, Kumar RA, Castaño EM and Frangione B (1998) β-sheet breaker peptides inhibit fibrillogenesis in a rat brain model of amyloidosis: Implications for Alzheimer's therapy. Nature Medicine 4:822-826.

Soto P, Griffin MA and Shea JE (2007) New insights into the mechanism of Alzheimer amyloid-beta fibrillogenesis inhibition by *N*-methylated peptides. Biophys J 93:3015-3025.

Stewart JM, Ferreira SH and Greene LJ (1971) Bradykinin potentiating peptide PCA-Lys-Trp-Ala-Pro. An inhibitor of the pulmonary inactivation of Bradykinin and conversion of angiotensin I to II. Biochemical Pharmacology 20.

Stine WB, Jr., Dahlgren KN, Krafft GA and LaDu MJ (2003) *In vitro* characterization of conditions for amyloid-beta peptide oligomerization and fibrillogenesis. J Biol Chem 278:11612-11622.

Sugg EE, Cody WL and Abdel-Malek Z (1986) *D*-isomeric replacements within the 6-9 core sequence of Ac-[Nle4]-a-MSH4-11-NH_2: A topological model for the solution conformation of α-melanotropin. Biopolymers 25:2029-2042.

Suvire FD, Rodriguez AM, Mak ML, Papp JG and Enriz RD (2001) Molecular dynamics studies on the interaction of 4-acetylamino-5-hydroxynapthalene-2,7-disulfonic acid with catalytic domain of avian sarcoma virus integrase dimer. Journal of Molecular Structure: THEOCHEM 540:35-46.

Suvire FD, Sortino M, Kouznetsov VV, Vargas M LY, Zacchino SA, Cruz UM and Enriz RD (2006) Structure-activity relationship study of homoallylamines and related derivatives acting as antifungal agents. Bioorganic and Medicinal Chemistry 14:1851-1862.

Suzuki N, Cheung TT, Cai XD, Odaka A, Otvos Jr L, Eckman C, Golde TE and Younkin SG (1994) An increased percentage of long amyloid b protein secreted by familial amyloid b protein precursor (bAPP717) mutants. Science 264:1336-1340.

Szegedi V, Fulop L, Farkas T, Rozsa E, Robotka H, Kis Z, Penke Z, Horvath S, Molnar Z, Datki Z, Soos K, Toldi J, Budai D, Zarandi M and Penke B (2005) Pentapeptides derived from Abeta 1-42 protect neurons from the modulatory effect of Abeta fibrils--an *in vitro* and *in vivo* electrophysiological study. Neurobiol Dis 18:499-508.

T

Tanzi RE, Moir RD and Wagner SL (2004) Clearance of Alzheimer's Aβ peptide: The many roads to perdition. Neuron 43:605-608.

Tarus B, Straub JE and Thirumalai D (2005) Probing the initial stage of aggregation of the Abeta(10-35)-protein: assessing the propensity for peptide dimerization. J Mol Biol 345:1141-1156.

Terry RD, Masliah E, Salmon DP, Butters N, DeTeresa R, Hill R, Hansen LA and Katzman R (1991) Physical basis of cognitive alterations in Alzheimer's disease: Synapse loss is the major correlate of cognitive impairment. Annals of Neurology 30:572-580.

Thirumalai D, Klimov DK and Dima RI (2003) Emerging ideas on the molecular basis of protein and peptide aggregation. Curr Opin Struct Biol 13:146-159.

Thompson LK (2003) Unraveling the secrets of Alzheimer's beta-amyloid fibrils. Proc Natl Acad Sci U S A 100:383-385.

Thoren PEG, Persson D, Isakson P, Goksor M, Onfelt A and Norden B (2003) Uptake of analogs of penetratin, Tat(48-60) and oligoarginine in live cells. Biochemical and Biophysical Research Communications 307:100-107.

Ting JT, Kelley BG, Lambert TJ, Cook DG and Sullivan JM (2007) Amyloid precursor protein overexpression depresses excitatory transmission through both presynaptic and postsynaptic mechanisms. Proc Natl Acad Sci U S A 104:353-358.

Tjernberg LO, Lilliehook C, Callaway DJE, Naslund J, Hahne S, Thyberg J, Terenius L and Nordstedt C (1997) Controlling amyloid β-peptide fibril formation with protease-stable ligand. Journal of Biological Chemistry 272:12601-12605.

Tjernberg LO, Naslundt J, Lindqvist F, Johansson J, Karlstrom AR, Thyberg J, Tereniust L and Nordstedt C (1996) Arrest of β-amyloid fibril formation by a pentapeptide ligand. Journal of Biological Chemistry 271:8545-8548.

Tossi A, Sandri L and Giangaspero A (2000) Amphipathic, α-helical antimicrobial peptides. Biopolymers 55:4-30.

Townsend M, Shankar GM, Mehta T, Walsh DM and Selkoe DJ (2006) Effects of secreted oligomers of amyloid beta-protein on hippocampal synaptic plasticity: a potent role for trimers. J Physiol 572:477-492.

Tycko R (2004) Progress towards a molecular-level structural understanding of amyloid fibrils. Curr Opin Struct Biol 14:96-103.

U

Urbanc B, Cruz L, Ding F, Sammond D, Khare S, Buldyrev SV, Stanley HE and Dokholyan NV (2004) Molecular dynamics simulation of amyloid beta dimer formation. Biophys J 87:2310-2321.

Urbina JM, Cortes JC, Palma A, Lopez SN, Zacchino SA, Enriz RD, Ribas JC and Kouznetzov VV (2000) Inhibitors of the fungal cell wall. Synthesis of 4-aryl-4-N-arylamine-1- butenes and related compounds with inhibitory activities on b(1-3) glucan and chitin synthases. Bioorganic and Medicinal Chemistry 8:691-698.

Urry DW and Walter R (1971) Proposed conformation of oxytocin in solution. Proc Natl Acad Sci U S A 68:956-958.

V

Van Der Spoel D, Lindahl E, Hess B, Groenhof G, Mark AE and Berendsen HJ (2005) GROMACS: fast, flexible, and free. J Comput Chem 26:1701-1718.

van Groen T, Kadish I, Wiesehan K, Funke SA and Willbold D (2009) *In vitro* and *in vivo* staining characteristics of small, fluorescent, Abeta42-binding *D*-enantiomeric peptides in transgenic AD mouse models. ChemMedChem 4:276-282.

Vargas M LY, Castelli MV, Kouznetsov VV, Urbina G JM, Lopez SN, Sortino M, Enriz RD, Ribas JC and Zacchino S (2003) *In vitro* antifungal activity of new series of homoallylamines and related compounds with inhibitory properties of the synthesis of fungal cell wall polymers. Bioorganic and Medicinal Chemistry 11:1531-1550.

Verdon CM, Fossati P, Verny M, DieudonnÃ© B, Teillet L and Nadel J (2007) Social cognition: An early impairment in dementia of the Alzheimer type. Alzheimer Disease and Associated Disorders 21:25-30.

Vestergaard M, Kerman K, Saito M, Nagatani N, Takamura Y and Tamiya E (2005) A rapid label-free electrochemical detection and kinetic study of Alzheimer's amyloid beta aggregation. J Am Chem Soc 127:11892-11893.

Vicente MF, Basilio A, Cabello A and Pelaez F (2003) Microbial natural products as a source of antifungals. Clinical Microbiology and Infection 9:15-32.

Vigo-Pelfrey C, Lee D, Keim P, Lieberburg I and Schenk DB (1993) Characterization of β-amyloid peptide from human cerebrospinal fluid. Journal of Neurochemistry 61:1965-1968.

Vila J, Williams RL, Vasquez M and Scheraga HA (1991) Empirical solvation models can be used to differentiate native from near-native conformations of bovine pancreatic trypsin inhibitor. Proteins: Structure, Function and Genetics 10:199-218.

Vila JA, Ripoll DR, Baldoni HA and Scheraga HA (2002) Unblocked statistical-coil tetrapeptides and pentapeptides in aqueous solution: A theoretical study. Journal of Biomolecular NMR 24:245-262.

Villagra SE, Bernini MC, Rodriguez AM, Zacchino SA, Kouznetsov VV and Enriz RD (2003) Conformational and electronic study of homoallylamines with inhibitory properties against polymers of fungal cell wall. Journal of Molecular Structure: THEOCHEM 666-667:587-598.

Vogelgesang S, Warzok RW, Cascorbi I, Kunert-Keil C, Schroeder E, Kroemer HK, Siegmund W, Walker LC and Pahnke J (2004) The role of P-glycoprotein in cerebral amyloid angiopathy; implications for the early pathogenesis of Alzheimer's disease. Curr Alzheimer Res 1:121-125.

W

Walker LC and LeVine Iii H (2002) Proteopathy: The next therapeutic frontier? Current Opinion in Investigational Drugs 3:782-787.

Walsh DM, Klyubin I, Fadeeva JV, Cullen WK, Anwyl R, Wolfe MS, Rowan MJ and Selkoe DJ (2002) Naturally secreted oligomers of amyloid beta protein potently inhibit hippocampal long-term potentiation *in vivo*. Nature 416:535-539.

Walsh DM and Selkoe DJ (2007) A beta oligomers - a decade of discovery. J Neurochem 101:1172-1184.

Walsh DM, Tseng BP, Rydel RE, Podlisny MB and Selkoe DJ (2000) The oligomerization of amyloid β-protein begins intracellularly in cells derived from human brain. Biochemistry 39:10831-10839.

Walsh TJ, Groll A, Hiemenz J, Fleming R, Roilides E and Anaissie E (2004) Infections due to emerging and uncommon medically important fungal pathogens. Clinical Microbiology and Infection 10:48-66.

Walter R, Glickson JD, Schwartz IL, Havran RT, Meienhofer J and Urry DW (1972) Conformation of lysine vasopressin: a comparison with oxytocin. Proc Natl Acad Sci U S A 69:1920-1924.

Walter R, Schwartz IL, Darnell JH and Urry DW (1971) Relation of the conformation of oxytocin to the biology of neurohypophyseal hormones. Proc Natl Acad Sci U S A 68:1355-1359.

Walter R and Shlank H (1971) *In vivo* inactivation of oxytocin. Endocrinology 89:990-995.

Walter R, Yamanaka T and Sakakibara S (1974) A neurohypophyseal hormone analog with selective oxytocin-like activities and resistance to enzymatic inactivation: an approach to the design of peptide drugs. Proc Natl Acad Sci U S A 71:1901-1905.

Wang J, Dickson DW, Trojanowski JQ and Lee VMY (1999) The levels of soluble versus insoluble brain aÎ² distinguish Alzheimer's disease from normal and pathologic aging. Experimental Neurology 158:328-337.

Wang Q, Rowan MJ and Anwyl R (2004) Beta-amyloid-mediated inhibition of NMDA receptor-dependent long-term potentiation induction involves activation of microglia and stimulation of inducible nitric oxide synthase and superoxide. J Neurosci 24:6049-6056.

Wasling P, Daborg J, Riebe I, Andersson M, Portelius E, Blennow K, Hanse E and Zetterberg H (2009) Synaptic retrogenesis and amyloid-beta in Alzheimer's disease. J Alzheimers Dis 16:1-14.

Watkins EK and Jorgensen WL (2001) Perfluoroalkanes: Conformational Analysis and Liquid-State Properties from ab Initio and Monte Carlo Calculations. Journal of Physical Chemistry A 105:4118-4125.

Wei G and Shea JE (2006) Effects of solvent on the structure of the Alzheimer amyloid-beta(25-35) peptide. Biophys J 91:1638-1647.

Weinberg A, Krisanaprakornkit S and Dale BA (1998) Epithelial antimicrobial peptides: Review and significance for oral applications. Critical Reviews in Oral Biology and Medicine 9:399-414.

Westermark P (1997) Classification of amyloid fibril proteins and their precursors: an ongoing discussion. Amyloid 4:216-218.

Westermark P (2005) Aspects on human amyloid forms and their fibril polypeptides. Febs J 272:5942-5949.

White TC, Marr KA and Bowden RA (1998) Clinical, cellular, and molecular factors that contribute to antifungal drug resistance. Clinical Microbiology Reviews 11:382-402.

WHO-WebSite (2009) Alzheimer's Disease. http://wwwwhoint/en/.

Williams AD, Portelius E, Kheterpal I, Guo JT, Cook KD, Xu Y and Wetzel R (2004) Mapping abeta amyloid fibril secondary structure using scanning proline mutagenesis. J Mol Biol 335:833-842.

Williams RL, Vila J, Perrot G and Scheraga HA (1992) Empirical solvation models in the context of conformational energy searches: Application to bovine pancreatic trypsin inhibitor. Proteins: Structure, Function and Genetics 14:110-119.

Wisniewski T, Ghiso J and Frangione B (1997) Biology of A beta amyloid in Alzheimer's disease. Neurobiol Dis 4:313-328.

Wolfe MS (2002) Therapeutic strategies for Alzheimer's disease. Nature Reviews Drug Discovery 1:859-866.

Wosten HAB and De Vocht ML (2000) Hydrophobins, the fungal coat unravelled. Biochimica et Biophysica Acta - Reviews on Biomembranes 1469:79-86.

Wright LR, Scott EM and Gorman SP (1983) The sensitivity of mycelium, arthrospores and microconidia of *Trichophyton mentagrophytes* to imidazoles determined by *in vitro* tests. Journal of Antimicrobial Chemotherapy 12:317-327.

Wyvratt MJ and Patchett AA (1985) Recent developments in the design of angiotensin-converting enzyme inhibitors. Medicinal Research Reviews 5:483-531.

Z

Zacchino S, Lopez S, Pezzenati G, Furlan R, Santecchia C, Muñoz L, Giannini F, Rodriguez AM and Enriz RD (1999) *In Vitro* Evaluation of Antifungal Properties of Phenylpropanoids and Related Compounds Acting Against Dermatophytes. J Nat Prod 62 1353–1357.

Zacchino S, Rodriguez G, Pezzenati G, Orellana G, Enriz RD and Gonzalez-Sierra M (1997) *In vitro* evaluation of antifungal properties of 8.O.4'-neolignans. J Nat Prod 60:659-662

Zacchino S, Rodriguez G, Santecchia C, Pezzenati G, Giannini F and Enriz R (1998) *In vitro* studies on mode of action of antifungal 8.O.4'-neolignans occurring in certain species of Virola and related genera of Myristicaceae. Journal of Ethnopharmacology 62:35-41.

Zacchino S, Yunes R, Cechinel Filho V, Enriz RD, Kouznetsov V and Ribas JC (2003) Plant-Derived Antimycotics. Current Trends and Future Prospects. Rai M, and Mares D (Eds), Haworth Press, New York:1-47.

Zamora MA, Masman MF, Bombasaro JA, Freile ML, Filho VC, Lopez SN, Zacchino SA and Enriz RD (2003) Conformational and electronic study ofphenylalkyl-3,4-dichloromaleimides: Aβ initio and DFT study. International Journal of Quantum Chemistry 93:32-46.

Zarandi M, Soos K, Fulop L, Bozso Z, Datki Z, Toth GK and Penke B (2007) Synthesis of Abeta[1-42] and its derivatives with improved efficiency. J Pept Sci 13:94-99.

Zasloff M (1992) Antibiotic peptides as mediators of innate immunity. Current Opinion in Immunology 4:3-7.

Zasloff M (2002) Antimicrobial peptides of multicellular organisms. Nature 415:389-395.

Zerbinatti CV and Bu G (2005) LRP and Alzheimer's disease. Reviews in the Neurosciences 16:123-135.

Zheng J, Jang H, Ma B, Tsai CJ and Nussinov R (2007) Modeling the Alzheimer Abeta17-42 fibril architecture: tight intermolecular sheet-sheet association and intramolecular hydrated cavities. Biophys J 93:3046-3057.

Zheng J, Ma B and Nussinov R (2006a) Consensus features in amyloid fibrils: sheet-sheet recognition via a (polar or nonpolar) zipper structure. Phys Biol 3:P1-4.

Zheng J, Ma B, Tsai CJ and Nussinov R (2006b) Structural stability and dynamics of an amyloid-forming peptide GNNQQNY from the yeast prion sup-35. Biophys J 91:824-833.

Summary

Development of Novel Small-Size Peptides as Putative Therapeutic Drugs

Rational design of peptide drugs using computational techniques. This thesis focuses on the development of small peptide molecules with putative therapeutic applications. In particular, our research has been focused on peptides with either antifungal properties (chapters 2-4) or with the ability to control protein deposits that cause the characteristic brain damage in Alzheimer's disease (chapters 5-7). In modern medicinal chemistry research, the use of computational techniques has become an important and almost inevitable step towards the development of new drugs. With these techniques it is possible, with certain accuracy, to simulate what happens between a newly developed drug and its target molecule(s), e.g. protein, DNA, cell-membranes, etc. Molecular dynamics is one of the computational techniques used in this thesis, and perhaps the one most frequently applied in modern medicinal chemistry. Based on the results of these types of calculations, new potential drugs were designed to achieve the optimum desired effects.

New Peptide Drugs for the treatment of fungal infections. Fungal infections in humans are common and may affect skin, intestines, heart, and brain, amongst other organs. Fungi are difficult to combat and can be life threatening, especially in AIDS patients, cancer patients after chemotherapy, organ transplanted patients, diabetes, burns, malnutrition, etc. This is due to the fact that their immune system is remarkably weak, creating an ideal situation for fungi to attack. Fungal infections are difficult to suppress and a really selective, safe and effective drug to treat this type of infections is not yet available. Thus, there is a great need of producing innovative and selective antifungal drugs. Small peptides derived from naturally occurring compounds have been taking under study in this thesis. The antifungal activities of these peptides have been tested in culture for several common pathogenic fungi. These antifungal peptides showed a promising profile to become a selective drug that might exert their effect through interaction with the cell-membrane of the fungal cells.

Novel peptides to protect against Alzheimer's Disease. Alzheimer's disease is a very complex disease where brain damage is associated with an increased degradation of the human mind and memory. Multiple factors play a role in causing the disease, but researchers agree that the production of a specific toxic form of the beta-amyloid peptide plays a key role. This peptide is not toxic by itself but it becomes toxic when several beta-amyloid molecules clump together forming what is called soluble aggregates. In this form the beta-amyloid become

toxic to nerve cells and a slow but unstoppable degradation process begins in brain regions that are essential for learning and memory, which in the course of years leads to the characteristic dementia. The currently available drugs for treating Alzheimer's disease have little impact and may, at best, delay the loss of memory, but do not stop the degradation process of the nerve cells. The severity of the disease and the enormous increase in the number of patients suffering from it, are the driving force of a worldwide search for new and more effective drugs. In our own research we focus on the development of new peptide compounds that prevent or slow down the formation of the toxic beta-amyloid soluble aggregates. By the use of computational techniques, we have been able to explore the self-bound beta-amyloid molecules, as well as their interaction with new potential drugs. With this important information we have designed small peptide drugs aimed at disrupting the toxic form of amyloid. The anti-amyloid potential of these peptides has been tested, in the first place, by cultured brain cells which have been exposed to toxic beta-amyloid forms. Secondly, we have tested these anti-amyloid peptides in the 'hippocampus' of mouse brain, a typical brain area affected in the Alzheimer's patient and which is the key structure for the formation of memory. Both testing experiments have produced not only positive but promising results indicating the potential therapeutic application of these anti-amyloid peptides.▪

Samenvatting

Ontwikkeling van Innovatieve Kleine Eiwitten voor Therapeutische Toepassingen

Rationele ontwerpen van peptide medicijnen met behulp van moleculaire dynamica. Dit proefschrift richt zich op de ontwikkeling van kleine moleculen voor medicinale en therapeutische toepassingen. Met name richt het onderzoek zich op dergelijke kleine eiwit moleculen voor de bestrijding van een tweetal ziekte veroorzakers: 1. Schimmelinfecties (hoofdstukken 2-4), en 2. Eiwitklontering die de oorzaak is van de ziekte van Alzheimer (hoofdstukken 5-7).

In het moderne onderzoek naar nieuwe medicijnen wordt gebruik gemaakt van technieken van de moleculaire dynamica. Met deze technieken is het mogelijk om exact te berekenen wat er gebeurt tussen een nieuw ontwikkeld medicijn en het doeleiwit waar het medicijn op aangrijpt. Op grond van de uitkomsten van deze berekeningen kan het ontwerp van het nieuwe medicijn worden aangepast zodat een optimale werking wordt bereikt. Moleculaire dynamica is een van de berekeningsmethoden die zijn toegepast in dit proefschrift. In het moderne onderzoek van de medicinale chemie is dit waarschijnlijk de meest gebruikte methode voor het ontwerpen en berkenen van nieuwe medicijnen.

Nieuwe Peptide Medicijnen voor Schimmelinfecties. Schimmelinfecties bij de mens komen veelvuldig voor en kunnen een bedreiging vormen voor huid, darmen, inwendige organen, hart en hersenen. Schimmels vormen moeilijk te bestrijden infecties en kunnen levensbedreigend zijn met name in omstandigheden waarbij de weerstand van het individu is aangetast zoals bij HIV besmetting, bij chemotherapie van kankerpatienten, na orgaantransplantaties, bij diabetes, brandwonden, ondervoeding of gebrekkige hygiëne in het algemeen. In dergelijke omstandigheden is het immuunsysteem ernstig verzwakt en krijgen schimmels de kans om het organisme te besmetten. Inwendige of uitwendige schimmelinfecties zijn moeilijk te behandelen en er is grote behoefte aan nieuwe innnovatieve farmaca met afdoende anti-schimmelwerking. Kleine peptiden die zijn afgeleid van in de natuur voorkomende verbindingen vormen daarbij een veelbelovend perspectief. In het proefschrift zijn een aantal van deze kleine peptiden ontworpen en onderzocht op hun vermogen om veel voorkomende schimmels te vernietigen. Een aantal van deze peptiden waren daarbij zeer succesvol door hun antibiotische effect op de celwanden van de schimmelcellen, en hebben de potentie

zich verder te ontwikkelen tot schimmelbestrijdende medicijnen.

Innovatieve Kleine Peptiden voor Bestrijding van Alzheimer Eiwitten. De ziekte van Alzheimer is een zeer ingewikkeld ziektebeeld waarbij beschadiging van het hersenweefsel gepaard gaat met een toenemende afbraak van het menselijk denkvermogen en het geheugen. Uiteindelijk gaan alle ervaringen en herinneringen die gedurende een leven lang zijn opgeslagen in onze hersenen verloren. Meerdere factoren spelen een rol bij het veroorzaken van deze ziekte, maar onderzoekers zijn het erover eens dat de vorming van een eiwit in de grote hersenen beta-amyloid genaamd hierin een sleutelrol speelt. Als afzonderlijk molecuul is beta-amyloid niet toxisch, maar als beta-amyloid moleculen onderling gaan samenklonteren tot meervoudige amyloid moleculen worden ze gifig voor de hersencellen en komt een langzaam maar niet te stoppen afbraakproces in het brein op gang, dat in de loop van jaren tot de kenmerkende en steeds verder toenemende dementie leidt.

Nu beschikbare medicijnen voor behandeling van de ziekte van Alzheimer hebben maar een gering effect en kunnen in het beste geval de achteruitgang van het geheugen enigszins vertragen maar stoppen het afbraakproces niet. De ernst van de ziekte en de enorme toename van het aantal patiënten lijdende aan deze ziekte in de komende jaren zijn een drijvende kracht achter een wereldwijde zoektocht naar nieuwe en meer effectieve medicijnen.

In ons eigen onderzoek richten wij ons op de ontwikkeling van nieuwe peptide medicijnen die de vorming van de beta-amyloid klontering kunnen voorkomen, en daarmee de giftige werking van meervoudig amyloid kunnen bestrijden. Met behulp van moleculaire dynamica technieken hebben we het proces van amyloid klontering nagebootst. Op basis van deze belangrijke informatie hebben we kleine peptide medicijnen ontworpen die erop gericht zijn de amyloid-verbindingen te verbreken en die we anti-amyloid peptiden hebben genoemd.

Enkele van deze peptiden hebben we in het laboratorium getest op hun effectiviteit om hersenen te beschermen tegen de gifitige amyloid klontering. Dit hebben we op verschillende manieren onderzocht. In de eerste plaats door gekweekte hersencellen bloot te stellen aan geklonterde amyloidmoleculen. Hierop sterven de hersencellen, maar toevoeging van onze anti-amyloid peptiden gaf een effectieve bescherming tegen het gifige amyloid. In de tweede plaats hebben we in de hersenen van muizen geklonterd amyloid aangebracht in de 'hippocampus', een hersengebied dat kenmerkend is aangetast in de Alzheimerpatiënt. Hierdoor trad in deze dieren geheugenverlies op dat werd voorkomen door toepassing van de nieuwe anti-amyloid medicijnen. We kunnen concluderen dat we er in zijn geslaagd om nieuwe moleculen te ontwerpen die potentieel in staat zijn om de giftige eigenschappen van beta-amyloid te bestrijden en de gevolgen hiervan voor de aantasting van het geheugen te voorkomen. Deze innovatieve peptide ontwerpen zijn veelbelovend voor een effectieve behandeling van de ziekte van Alzheimer. ▪

Resumen

Desarrollo de Nuevos Péptidos de Pequeño Tamaño como Drogas Terapéuticas Putativas

El diseño racional de drogas peptídicas mediado por técnicas computacionales. Este trabajo de tesis se focaliza en el desarrollo de pequeños péptidos con aplicaciones terapéuticas putativas. En particular, hemos focalizado nuestros esfuerzos en el diseño de estructuras peptídicas que posean, ya sea, actividad antifúngica (capítulos 2-4) o capacidad de controlar las deposiciones proteicas que causan las lesiones cerebrales características del mal de Alzheimer (capítulos 5-7). En el campo de la química medicinal de hoy el uso de técnicas computacionales es una importante y casi inevitable etapa en el desarrollo de nuevas drogas. Con el uso de estas técnicas es posible, con cierta exactitud, simular lo que sucede a nivel molecular entre una nueva droga y su(s) molécula(s) target(s), por ejemplo: proteínas, ADN, membranas celulares, etc. Simulaciones de la dinámica molecular es una de las técnicas utilizadas en este trabajo de tesis y quizás es la técnica más frecuentemente aplicada en la química medicinal actual. Novedosas estructuras peptídicas han sido diseñadas basándonos en los resultados obtenidos con este tipo de técnicas. Estas nuevas drogas putativas han sido desarrolladas con el objetivo de lograr los óptimos efectos deseados.

Nuevas dogas peptídicas para el tratamiento de infecciones fúngicas. Las infecciones fúngicas en humanos son de común ocurrencia y pueden afectar piel, intestinos y cerebro entre otros órganos. Estos patógenos fúngicos son difíciles de combatir y amenazan contra la vida de las personas afectadas, especialmente en pacientes con SIDA, cáncer, que hayan recientemente recibido un órgano trasplantado, sufrido quemaduras, malnutrición, etc. Esto es debido a que estos pacientes poseen un sistema inmunológico marcadamente debilitado, creando así una situación ideal de ataque para este tipo de microorganismos patógenos. Esta infecciones fúngicas son difíciles de suprimir y actualmente no disponemos de una droga que sea realmente selectiva, segura y efectiva para su tratamiento. Es por esto que hay una gran necesidad de producir drogas anti-fúngicas que sean innovadoras y sobre todo selectivas. En este trabajo de tesis se han estudiado pequeños péptidos de ocurrencia natural con potencial actividad anti-fúngica. Esta actividad ha sido testeada en cultivos celulares de diversos patógenos fúngicos comunes. Algunos de los péptidos anti-fúngicos reportados aquí mostraron una prometedora tendencia a convertirse en drogas selectivas que podrían ejercer sus

efectos anti-fúngicos mediante la interacción con la membrana celular fúngica.

Nuevos péptidos que nos protejan contra el mal de Alzheimer. El mal de Alzheimer es una enfermedad extremadamente compleja en la cual el daño cerebral está asociado con una incrementada deterioración de la mente y memoria. Múltiples son los factores que juegan un rol importante en esta enfermedad, sin embargo es de común acuerdo entre los científicos que el rol principal lo juega la presencia de específicas formas del péptido beta-amiloideo en el cerebro de las personas afectadas. Este péptido no es toxico por sí mismo, pero su toxicidad es expresada cuando varias moléculas del péptido en cuestión se aglomeran para formar los llamados agregados en solución. En esta forma el péptido beta-amiloideo se torna neuro-toxico desatando un lento pero imparable proceso de degradación cerebral, afectando principalmente regiones esenciales relacionadas al aprendizaje y a la memoria que con el curso de los años lleva a la demencia característica de esta enfermedad. Las drogas actualmente disponibles para su tratamiento tienen un impacto muy limitado y a lo sumo sólo retardan la pérdida de memoria, pero no detienen la degradación neuronal. La severidad de esta enfermedad y el creciente número de pacientes que la padece son la fuerza impulsora, a nivel mundial, del desarrollo de una droga más efectiva para su tratamiento. En nuestro proyecto de investigación nos hemos focalizado en el desarrollo de nuevos compuestos peptídicos que prevengan o retarden la formación de agregados tóxicos del péptido beta-amiloideo. Basándonos en técnicas computacional hemos podido explorar los asociados moleculares del péptido beta-amiloideo, como así también las interacciones de estos con nuevas potenciales drogas. Con esta importante información hemos diseñado pequeños péptidos que poseen tendencia a perturbar las formas toxicas del péptido beta-amiloideo. Su potencial anti-amiloideo ha sido testeado, en primer lugar, en cultivos celulares de neuronas las cuales fueron expuestas a las especies toxicas del péptido beta-amiloideo. Luego, su actividad anti-amiloidea fue probada *in vivo* en el hipocampo de ratones. Ambos experimentos no sólo han producido resultados positivos, sino que también muestran resultados prometedores indicando las potenciales aplicaciones terapéuticas de estos nuevos péptidos anti-amiloideos.▪

Appendix A

Supplementary Material

Chapter 2

Supplementary materials associated with this chapter can be found, in the online version, at doi:10.1016/j.bmc.2006.07.007.

Chapter 3

Supplementary materials associated with this chapter can be found, in the online version, at doi:10.1016/j.bmc.2008.02.072.

Chapter 4

Supplementary materials associated with this article can be found in the online version, at doi:10.1016/j.ejmech.2008.02.019.

Chapter 5

Supplementary materials associated with this article can be found in the online version, at doi:10.1021/jp901057w

Chapter 7

Table 7.1S: conformational search and clustering results for PN20 and PN22 optimized at the EDMC/SRFOPT/ECCEP/3 level of theory. Total (E_{tot}, kcal.mol^{-1}) and relative (ΔE, kcal.mol^{-1}) energies are also shown. All conformational families shown here have relative population (%PF) higher than 0.5%.

PN20	**Elect.**	**Rand.**	**Ther.**	**Tot.**
Generated [a]	4566	65514	156	70236
Accepted [b]	459	4419	122	**5000**

Family	**NF** [c]	**%PF** [d]	**E_{tot}**	**ΔE**
1	1210	24.2	-36.89	0.00
2	276	5.52	-34.33	2.55
3	188	3.76	-35.22	1.66
4	185	3.7	-33.26	3.62
5	134	2.68	-33.21	3.68
6	121	2.42	-34.08	2.81
7	113	2.26	-31.40	5.48
8	99	1.98	-34.03	2.85
9	97	1.94	-33.93	2.95
10	83	1.66	-33.33	3.56
11	74	1.48	-29.38	7.50
12	70	1.4	-34.31	2.58
13	69	1.38	-33.70	3.19
14	68	1.36	-33.60	3.29
15	55	1.1	-32.82	4.07
16	48	0.96	-32.67	4.22
17	45	0.9	-33.51	3.38
18	43	0.86	-33.24	3.64
19	41	0.82	-31.20	5.69
20	36	0.72	-32.54	4.34
21	34	0.68	-34.15	2.73
22	33	0.66	-32.60	4.29
23	32	0.64	-32.87	4.02
24	32	0.64	-32.51	4.38
25	31	0.62	-32.32	4.57
26	30	0.6	-31.76	5.13
27	30	0.6	-29.97	6.92
28	28	0.56	-33.70	3.19
29	26	0.52	-32.77	4.12
30	26	0.52	-32.06	4.82

PN22	**Elect.**	**Rand.**	**Ther.**	**Tot.**
Generated [a]	5185	73574	318	79077
Accepted [b]	542	4332	126	**5000**

Family	**NF** [c]	**%PF** [d]	**E_{tot}**	**ΔE**
1	3119	62.38	-6.76	0.00
2	425	8.5	-6.19	0.57
3	260	5.2	-6.15	0.61
4	107	2.14	-4.39	2.37
5	93	1.86	-3.97	2.79
6	69	1.38	-2.18	4.58
7	43	0.86	-4.42	2.34
8	40	0.8	-3.41	3.36
9	35	0.7	-4.28	2.49
10	33	0.66	-3.12	3.64
11	31	0.62	-1.20	5.56

[a] Number of conformations generated electrostatically, randomly and thermally during the conformational search.
[b] Number of conformations accepted from those generated electrostatically, randomly and thermally during the conformational search.
[c] *NF* represents the total number of conformational families as result of the clustering run.
[d] *%PF* represents the percent relative population based on a total of 5000 accepted conformations.

Acknowledgements

Here we are again at another turning point in my life and career. This has been an exciting and fulfilling process of attaining acknowledge, artistic creation and, as well as, self-discovery. Undoubtedly, all this could not have been possible to achieve without the invaluable help of many people. Most of them who collaborated to get this enterprise come to an end are formally mentioned at the end of each chapter. However, this is of course not enough.

First of all, I would like to express my gratitude to all my promotors and supervisors (in Groningen and San Luis), who supported me, guided my projects and respected my ideas from the very beginning. I especially want to thank Paul and Daniel for believing in my "crazy computational" approaches, giving me the time and place to carry them out, and always making sure that I stay busy no matter what. Also, I thank Uli and Siewert-Jan because without their guidance and continuous support none of this would have been possible. Your long hours and dedication are greatly appreciated.

The whole staff of the Molecular Neurobiology group has, somehow and at the right time, given its contribution which is also valid for the entire Department of Animal Physiology. Secretaries, technicians, Master students, PhD students and Professors must know that I am fully grateful for your help. Moreover, it's very gratifying to realize that my cultural and scientific background has been substantially enlarged by working with such a nice group of people. Thank you to the entire department.

Special thanks to Ivi, Niki and Pieter for the great time at work and also for the unforgettable "Nirvana, Salsa, Merengue" moments.

I want to give a big thank you to Paulien for those great moments that we shared from the very beginning.

I would also like to express my gratitude to the people who warmly welcomed me in Hungary. I really appreciate the support that the groups of Prof. Penke and Prof. Viskolcz have offered me during my stay in Szeged. Also, I am very grateful to Csaba who did not only guide me in my first steps into peptide synthesis, but also received me as a member of his family.

My deepest appreciation to Prof. Csizmadia, aka IGC. You have been not only my mentor, but also a source of inspiration.

During my first visit to Szeged I was very lucky to meet a formidable person, Mr. Izsák, who soon became one of my dearest friends since then. Robi, I don't know if I would be able to show my appreciation by writing or saying these simple words. However, if something is sure it's that your scientific, artistic, and personal inputs are invaluable to me. Köszönöm szépen!

I would like to extend my sincere appreciation and thanks to the always active community of dancers and dance-related people of Groningen who contributed to the success and failure of my inner and outer artistic being. I can't avoid the need of expressing my most sincere gratitude to Random Collision, especially

to Kirsten and Edan. Thank you guys. From this tiny, but yet rich dance world, I want to especially thank to Helena, aka Ms. Volkov. More than expressing my gratitude I should apologize for using, and sometimes abusing Ms. Volkov's intellectual, physical, and spiritual beauty as an infinite source of inspiration. I deeply appreciate your presence in my life.

Jose, Jacek, Vincent, Wojtek, Anthony, Tomek, Caroline and Glenn are the people who created a fun and very enjoyable ambience not only in Groningen but also in every city of Europe where we have expended some time together. Thanks guys!

En cuanto a la gente que deje en Argentina, lo mínimo que puedo hacer es agradecerles toda la ayuda prestada desde mis primeros pasos en investigación en el gropu de Modelado Molecular hasta mis primeras experiencias docente en la cátedra de Química General. Así es que quiero agradecer a todos mis colegas de la UNSL. Especialmente quiero agradecer a Miguel, Ana y Sebastián. La verdad es que sin Uds. todo esto habría sido imposible de realizar.

Por allí en Mendoza, Dora, Mabel, Edith y Miguel son y siempre lo fueron mi primera y principal plataforma de despegue. Sin Uds. yo hoy no estaría escribiendo estas palabras. Gracias por todo!

Gerardo, Vero y Alma. Les agradezco infinitamente por todo el amor y cariño dado. Por cuidar a Thorio, por haberme convertido en el tío más feliz del mundo y sobre todo por ser mi plataforma de aterrizaje cuando el volar se me hace pesado. Miles de gracias por estar siempre ahí.

Mamá, vos sos la fuerza hecha mujer, tantas cosas que has tenido que hacer por mí, te estoy infinitamente agradecido. Si algo aprendí de vos y el Papá es que debo luchar y trabajar duro por lo que quiera hacer de mi vida, por mis sueños. Y acá estoy terminando otra etapa en mi vida gracias a vos. Esta tesis también va dedicada a vos.

Claro está que no puedo dejar de agradecer a todos los *Argentos* que han hecho de Groningen una "klein Argentinië". Euge, Maxi, Juan, Casper (por adopción) y Marina son mi cable a tierra, o mejor dicho el cable a mi tierra. En cuanto a Marina, que te puedo decir?!, sos lo más piba. No sé como agradecerte todo lo que me has ayudado y bancado desde que estoy en Holanda. Desde la bici de la prehistoria que me prestante cuando vine por primera vez, los mates compartidos, las tardes de gym, los asados y hasta las noches en vela por tus (benditos) experimentos. La verdad es un gustazo haberte conocido.

Ik wil graag mijn dank uitspreken aan Maarten en zijn familie (de hele Wieringa en Zijlstra families), die al snel mijn Nederlandse familie zijn geworden. Jullie hebben een extra gezellig Groningen voor me gecreëerd. Hartelijk bedankt voor jullie steun.

Finally, because it's nearly impossible to mention here everyone who has in one way or another helped me during my PhD adventure, I give you my most sincere THANK Y'ALL! ▪